# Functional analysis of structurally diverged and reduced organelles in *Giardia lamblia*

---

**Dissertation**
**zur**
**Erlangung der naturwissenschaftlichen Doktorwürde**
**(Dr. sc. nat.)**

**vorgelegt der**
**Mathematisch-Naturwissenschaftlichen Fakultät**
**der**
**Universität Zürich**

**von**

**Samuel Rout**
**aus**
**Bhubaneswar / India**

**Promotionskomitee**

Prof. Dr. Adrian B. Hehl
(Vorsitz und Leitung der Dissertation)

Prof. Dr. Cornel Fraefel
Prof. Dr. Norbert Müller
Prof. Dr. Ueli Grossniklaus

**Zürich, 2015**

# Functional analysis of structurally diverged and reduced organelles in *Giardia lamblia*

---

**Faculty of Science University of Zurich**

**Life Science Graduate School – Microbiology and Immunology PhD Program**
**University of Zurich**

PhD Thesis

Submitted by

**Samuel Rout**

from Bhubaneswar, India

**Thesis Supervisor:**
Prof. Dr. Adrian B. Hehl

**Thesis Co-supervisor:**
Dr. Carmen Faso
Institute of Parasitology

**Thesis Committee Members:**

Prof. Dr. Cornel Fraefel
Prof. Dr. Norbert Müller
Prof. Dr. Ueli Grossniklaus

**Zürich, 2015**

# Table of contents:


Part I SUMMARY 1

1. Summary 1-2

2. Zusammenfassung 3-5

Part II AIM OF THE THESIS 6

Part III INTRODUCTION 7

1. *Giardia lamblia* 7

1.1: Giardiasis and *Giardia's* life cycle 7-8

1.2: Evolutionary background 8-9

1.3: Organelle system 9

1.3.1 Endoplasmic reticulum 10

1.3.2 Peripheral vesicles 10

1.3.3 Encystation specific vesicles (ESVs) 11

1.3.4 Mitosomes 12

1.4 Constitutive and regulated protein secretion 12-13

1.4.1 Molecular machinery for regulated protein secretion

2. Mitochondria and mitochondrion-related organelles (MROs) 14

2.1 Mitochondria: evolution and classification 14-15

2.2 MROs: Hydrogenosomes and mitosomes (background and identification) 15-16

2.3 Apoptosis 16-17

3. Mitosomes 18

3.1 Mitosomes (morphology, distribution and function) 18-19

3.2 Mitosomal protein targeting and processing 19

3.2.1 Mitosomal protein targeting sequences (MTS) 19-20

3.2.2 Mitosomal processing peptidase (MPP) 20

3.3 Mitochondrial/mitosomal protein import machinery 21

3.3.1 Translocase of the Outer Membrane (TOM) 22

3.3.2 Structure and Assembly Machinery (SAM) 22-23

3.3.3 Mitochondrial Intermembrane Space Import and Assembly (MIA) 23-24

3.3.4 Translocase of the Inner Membrane 22 (TIM22) 24-25

3.3.5 Translocase of the Inner Membrane 23 (TIM23) 25-26

4. Goals of the thesis 27

4.1 Investigating the role of Arf and Arl small GTPases during encystation in *Giardia lamblia* 27

4.2 Induction of apoptosis in *Giardia lamblia* 28

4.3 Optimization of a co-immunoprecipitation assay to identify organelle specific sub proteomes 29

5. Bibliography 30-37

Part IV RESULTS

Characterization of ARF and ARL homologs in *Giardia lamblia* 38-44

Part V RESULTS

Induction of apoptosis-like cell death in *Giardia lamblia* 45-51

Part VI RESULTS/MANUSCRIPT

1. Development of an *ad hoc* co-immunoprecipitation protocol for efficient pull down of protein complexes from *Giardia lamblia* 52-55

2. MANUSCRIPT I 56-63

3. MANUSCRIPT II 64-102

Part VII DISCUSSION AND FUTURE DIRECTIONS 103

1. Discusison 103

1.1 General 103

1.2 Project 1: Arf and Arls 104

1.2.1 Aside from *Gl*Arf1, none of the additional Arf and Arl homologues tested effect ESV genesis or cyst maturation. 104-105

1.2.2 A case of redundancy or a scope for novelty for small GTPases in *Giardia*? 105

1.2.3 Are small GTPases in *Giardia* involved in additional functions beyond their involvement in the secretory system? 106-107

1.3 Project 2: Apoptosis in *Giardia lamblia* 107

1.3.1 Apoptotic-like cell death can be induced in *Giardia* by altering its physiological conditions. 107-110

1.4 Project 3: Optimization of a co-immunoprecipitation assay to identify organelle specific sub- proteomes. 110

1.4.1 A minimized mitosomal import machinery in *Giardia*: reductionism at its best? 110-114

1.4.2 Diverged mitosome-ER contacts sites in *Giardia*? 115-116

1.4.3 Mitosome dynamics and a novel role for *Giardia* dynamin related protein in mitosome morphogenesis. 116-119

2. Bibliography 119-123

PART VIII CONCLUSION 124-125

Acknowledgement 126

Curriculum Vitae 127-128

# PART I: SUMMARY

## 1. Summary

The proliferating trophozoite stage of the non-invasive protozoan parasite *Giardia lamblia* (syn. *G. intestinalis* and *G. duodenalis*) is a highly polarized motile cell and a tractable laboratory model organism to investigate fundamental cell biological questions. *G. lamblia* belongs to the phylum Diplomonadida (kingdom Excavata), which was, until recently one of the most extant branches of eukaryotic evolution. *G. lamblia* is the leading causative agent for water borne parasite induced diarrheal disease worldwide. It not only affects humans and animals but also causes significant morbidity and economic loss in the livestock industry. *Giardia* has a two stage asexual life cycle comprising of a proliferating binucelate tropozoite stage and an environmentally resistant cyst stage. Proliferating trophozoites actively attach to gut epithelia with the help of a specialized ventral suction disc to avoid elimination via peristalsis. Moreover, cells exhibit antigenic variation of their protein surface coat to evade immuno-mediated clearing by the host, leading to chronicization of *Giardia* infections. However, upon encountering changes in lipid concentration and increase in pH, resident trophozoites undergo complex stage differentiation and transform into an environmentally resistant cyst form which is shed with the feces. This process is defined as "encystation".

The simplification in cellular complexity observed in *Giardia* can be interpreted as a result of massive reductive evolution as an adaptation to its ecological niche and parasitic lifestyle. The endomembrane system in *G. lamblia* is of prime example and may serve as a model to study protein trafficking. Transmission to a new host demands stage conversion from trophozoite to cyst form. The encystation process requires transport of cyst wall proteins (CWPs) from the endoplasmic reticulum (ER) to the plasma membrane (PM) to form the protective extracellular matrix. Despite clear evidence for secretory activity, *Giardia* lacks a canonical steady state Golgi apparatus. However, upon the triggering of encystation, *de novo* generated encystation specific vesicles (ESVs) act as Golgi analogs by accumulating, processing and sorting CWPs prior to regulated secretion. ESV neogenesis and maturation depends on small GTPases such as *Gl*Sar1 and *Gl*Arf1. Over-expression of mutated *Gl*Sar1 and *Gl*Arf1 variants eliciting dominant negative effects impaired ESV genesis and maturation, respectively. In the first part of my doctoral thesis, I investigated the role of 5 additional Arf and Arl homologues by defining their cellular localization and possible function during encystation. Our data confirms that Arf1 is likely the only family member involved in encystation. The other homologues may either be redundant in relation to Arf1 or be involved in other as-yet unidentified cellular process. New insights and/or novel tools are required to obtain a more comprehensive view of Arf and Arl functions in *G. lamblia*.

Encystation is a necessary mechanism for parasite transmission and may be viewed as an escape route for *Giardia* when faced with unfavorable conditions within the host. However, during infection, *Giardia* trophozoites reside at high densities in the host's small intestine. Surprisingly little inflammation and/or damage to epithelial cells is observed. One explanation could reside in a form of programmed cell death (PCD) which limits the stimulation of the immune system by deteriorating parasites. Therefore, in the second part of my doctoral thesis, I investigated PCD-related events in *Giardia* using nutrient starvation and heat shock treatment as physiological triggers. Exposure of phosphatidylserine (PS), ER disintegration, nuclear condensation and DNA damage are hallmarks of *Giardia's* form of PCD, suggesting that this parasite harbors machinery for an apoptotic like cell death. Since apoptosis in more complex eukaryotes is linked to mitochondrial function, we speculated that *Giardia's* mitosomes may be involved. These organelles, similarly to mitochondria, might function as a highly sensitive central switch for monitoring cell health and integrating possible death signals from within and without, beyond their established role in iron-sulfur (Fe-S) protein maturation. However, to address this fundamental biological question and to dissect the full range of mitosomal function, a comprehensive mitosomal proteome is essential.

Despite indications of roles for giardial mitosomes beyond Fe-S maturation, little is known regarding the protein repertoire of of these organelles, primarily due to 1) significant genomic sequence divergence and 2) challenges in organelle purification. A case in point is the organelle's protein import machinery where only a poorly conserved translocon of the outer membrane (*Gl*Tom40) has been identified to date. Therefore, during the last part of my doctoral thesis I developed a customized co-immunoprecipitation (co-IP) assay to pull down organelle-specific protein complexes with high efficiency. Using *Gl*Tom40 as bait protein, this strategy led to the identification of 10 novel mitosomal localized proteins of unknown function. Furthermore, reverse co-IP strategies using five novel mitosome-localized bait proteins allowed for the building of a core membrane interactome and a complex interactome network extending inwards to the organelle matrix as well as outwards to components of the ER membrane and the cytoplasm. Our findings point towards a simplified outer membrane import machinery in giardial mitosomes involving the translocon (*Gl*Tom40), a *Giardia*-specific receptor (*Gl*29147) and a membrane anchored protein (*Gl*14939). In addition, we propose the presence of a diverged mitosome-ER contact site based on the identification of 5 novel hypothetical proteins with dual localization at the ER and mitosomes. Furthermore, we show for the first time association of the single giardial dynamin related protein with mitosomes and provide direct evidence for its involvement in organelle morphogenesis and homeostasis.

## 2. Zusammenfassung

Das proliferative Trophozoiten-Stadium des nicht-invasiven, einzelligen Parasiten *Giardia lamblia* (syn. *G. intestinalis* und *G. duodenalis*) ist eine stark polarisierte, motile Zelle und ein geeigneter Modellorganismus zur Erforschung von zellbiologischen Grundlagen. *G. lamblia* gehört zum Stamm der Diplomonadida (Excavata), welche bis vor kurzem eine der einfachsten Gruppen der eukaryotischen Evolution darstellten. *G. lamblia* ist weltweit der Hauptverursacher für Parasiten-induzierte Durchfallerkrankungen durch verunreinigtes Wasser. Dies führt nicht nur zur gesundheitlichen Beeinträchtigung von Mensch und Tier, sondern hat auch signifikante Morbidität und wirtschaftliche Verluste in der landwirtschaftlichen Tierhaltung zur Folge. Der zwei Stadien umfassende asexuelle Lebenszyklus von *Giardia* besteht aus einem sich vermehrenden zweikernigen Trophozoiten- und einem gegen Umwelteinflüssen resistenten Zysten-Stadium. Erstere heften sich aktiv an Dünndarmepithelzellen des Wirtes mit Hilfe einer spezialisierten Bauchhaftscheibe, um ihrer Beseitigung durch peristaltische Bewegungen entgegenzuwirken. Darüber hinaus erlaubt die Fähigkeit des Parasiten, seine Oberflächenantigene kontinuierlich zu verändern, sich der Immunabwehr des Wirtes zu entziehen. Dies hat eine erfolgreiche Persistenz der Krankheit zur Folge. Trotz der umfassenden Möglichkeiten von *Giardia*, sich dem Abwehrmechanismus des Wirtes zu entziehen, ist der Einzeller nicht immun gegen Erhöhung von pH und Gallenkonzentration. Unter solch ungünstigen Veränderung unterzieht sich der Parasit einer Stadiums-Differenzierung und transformiert sich in die umweltresistente Zystenform, welche mit dem Stuhl ausgeschieden wird. Dieser Prozess nennt sich „Enzystierung“.

Die Vereinfachung der zellulären Komplexität, welche bei *Giardia* beobachtet wird, kann als Resultat von massiv reduktiver Evolution als Folge von Adaptation an seine ökologische Nische und seine parasitische Lebensweise interpretiert werden. Das Endomembransystem in *G. lamblia* ist ein erstklassiges Beispiel und dient als Model zur Erforschung von intrazellulärem Proteintransport. Die Übertragung des Parasiten von einem Wirt zum nächsten erfordert die oben genannte Stadiumskonversion von Trophozoit zur Zyste, die Enzystierung. Dieser Prozess benötigt den Transport von Zystenwand-Material (CWM) vom endoplasmatischen Retikulum (ER) zur Plasmamembran (PM), um die schützende extrazelluläre Matrix zu bilden. Obwohl klare Beweise für eine gewisse sekretorische Aktivität vorliegen, hat *Giardia* keinen klassischen Golgi-Apparat. Wie dem auch sei, während der Einleitung der Enzystierung fungieren *de novo* generierte, enzystierungsspezifische Vesikel (ESV) als Golgi-Analoge aufgrund ihrer Funktion zur Akkumulierung, Prozessierung und Sortierung von CWM vor der regulierten Sekretion. Neogenese und Maturation von ESV sind abhängig von kleinen GTPasen wie *Gl*Sar1 und *Gl*Arf1. Überexpression von mutiertem *Gl*Sar1 und *Gl*Arf1 resultieren in dominant negativen Effekten, wie beeinträchtigte Neogenese resp. Reifung von ESV. Im ersten Teil meiner Doktorarbeit erforschte ich die Funktion von fünf

zusätzlichen Arf und Arl Homologen, indem ich ihre zelluläre Lokalisation und mögliche Rolle während der Enzystierung untersuchte. Unsere Daten bestätigen, dass Arf1 sehr wahrscheinlich das einzige Mitglied der Arf-Familie ist, welches bei dem Prozess eine Funktion innehat. Die anderen Homologen sind möglicherweise redundant in Bezug zu Arf1, oder sie sind in einem bisher unbekannten zellulären Prozess involviert. Weitere Erkenntnisse und/oder neue Instrumente sind vonnöten, um eine umfassendere Einsicht in die Funktion von Arf und Arl in *Giardia lamblia* zu erlangen.

Enzystierung ist ein notwendiger Mechanismus für die Transmission von Parasiten, und kann im Falle von ungünstigen Bedingungen im Wirt als Fluchtroute von *Giardia* betrachtet werden. Während einer Infektion besiedeln *Giardia* Trophozoiten den Dünndarm in hoher Konzentration, obwohl nur schwache Inflammationsanzeichen und/oder Schäden an Zellen des Darmepithels beobachtet werden. Eine Erklärung hierfür könnte eine Form von programmiertem Zelltod (PCD) sein, welche eine Immunantwort gegen die Parasiten dämpft. Um diese These zu prüfen, untersuchte ich im zweiten Teil meiner Doktorarbeit PCD-bezogene Ereignisse in *Giardia*. Hierfür benutzte ich Nährstofflimitation und Hitzeschock als physiologische Auslöser. Externalisierung von Phosphatidylserin (PS), ER-Zerfall, Kernkondensation und DNA-Schäden sind Kennzeichen der PCD-Form von *Giardia*, was auf eine Maschinerie des Parasiten hinweist, die für eine Apoptose-ähnliche Form von Zelltod verantwortlich ist. Die Tatsache, dass Apoptose in komplexeren Eukaryoten mitochondriale Funktionen beinhaltet, lässt uns vermuten, dass auch Mitosomen von *Giardia* in diesen Prozess involviert sind. Diese Organellen, die Ähnlichkeiten zu Mitochondrien aufweisen, könnten nebst ihrer Rolle in der Fe-S Proteinreifung als hochsensitiven, zentralen Schalter zur Überwachung vom Gesundheitszustand der Zelle und von möglichen Zelltod-Auslöser intra- oder extrazellulären Ursprungs fungieren. Um diese fundamentale biologische Frage zu untersuchen und somit sämtliche Funktionen von Mitosomen aufzudecken, ist ein umfassendes mitosomales Proteom notwendig.

Nebst ihrer Rolle in der Fe-S Proteinmaturation ist wenig bekannt über das Proteinrepertoire in Mitosomen. Dies hat einerseits zu tun mit signifikanter Divergenz genomischer Sequenzen, andererseits mit Schwierigkeiten bezüglich der Aufreinigung von Organellen. Ein Beispiel hierfür ist die mitosomale Proteinimport-Maschinerie, bei welcher bisher erst ein schwach konserviertes Translocon der äusseren Membran (*Gl*Tom40) identifiziert werden konnte. Aufgrund dessen entwickelte ich im letzten Teil meiner Doktorarbeit ein auf *Giardia* angepasstes co-Immunpräzipitations (co-IP) Assay, um organellenspezifische Proteinkomplexe mit hoher Effizienz zu isolieren. Durch die Verwendung von *Gl*Tom40 als *bait*-Protein konnten dadurch zehn neue mitosomale Proteine identifiziert werden, deren Funktion noch unbekannt ist. Zusätzlich wurden fünf neue mitosomale *bait*-Proteine für eine inverse co-IP-Strategie verwendet, was einerseits zu einem Membran-Interaktom und

andererseits zu einem complexen Interaktom führte, welches sich zusätzlich nach innen zur Organellenmatrix als auch nach aussen zu Teilen der ER-Membran und zum Cytoplama erstreckt. Unsere Resultate führen zu einer vereinfachten Proteinimport-Maschinerie der äusseren Mitosomenmembran in *Giardia*, welche das Translocon (*Gl*Tom40), einen *Giardia*-spezifischen Rezeptor (*Gl*29147) und ein membranverankertes Protein (*Gl*14939) enthält. Zusätzlich stellen wir aufgrund fünf neu identifizierter, hypothetischer Proteine mit dualer Lokalisation in ER und Mitosomen die Hypothese auf, dass eine divergierende Mitosom-ER-Kontaktseite existiert. Wir konnten auch das erste Mal die Verbindung zwischen dem einzigen Protein in *Giardia*, welches mit Dynamin verwandt ist, und Mitosomen zeigen. Dies stellt einen direkten wissenschaftlichen Beweis für die Beteiligung des Proteins in Morphogenese und Homöostase von Organellen dar.

# Part II: AIM OF THE THESIS

*Giardia lamblia* has a very simple life cycle comprising of a motile trophozoite stage that colonizes the host's small intestine leading to the manifestation of the disease and an environmentally resistant cyst form. The stage conversion is crucial for parasite survival outside the host. *Giardia* trophozoites display a highly minimized compartment organization which is not only functionally but also structurally reduced.

In absence of a steady state Golgi apparatus, *de novo* generated specialized organelles, encystation specific vesicles (ESVs) function as a Golgi body analog where the cyst wall material is sorted and matured prior to sequential deposition on the parasite surface forming the resistant cyst wall. Regulated CWP trafficking is essential for the formation of the cyst wall and in turn survival of the parasite, hence it is an essential stage in parasite transmission. Additionally, *Giardia* lacks canonical mitochondria and possesses mitochondrion-related organelles (mitosomes) which are implicated in iron-sulfur protein maturation. Despite unambiguous evidence for functionally conserved protein import machinery, there is massive divergence in the structural components involved in the machinery.

The minimized organism, *G. lamblia*, because of its simple organization, provides a platform for investigation of basic cellular functions and pathways which are difficult to study in complex eukaryotes. Furthermore, it is also a useful model system to investigate principles of reductive evolution, i.e. why and how adoption of a parasitic life-style leads to the loss of even archetypical sub-cellular organelles, and which minimal machinery is necessary for maintenance of fundamental cellular functions.

Therefore, the aims of my doctoral thesis were to investigate the membrane associated factors involved in ESV maintenance and to identify the repertoire of mitosomal proteins involved in the import machinery and facilitating inter-organellar communications which would help us to unravel the functional range of these highly diverged organelles.

# Part III: INTRODUCTION

## 1 *Giardia lamblia*

### 1.1 Giardiasis and *Giardia's* life cycle

*Giardia lamblia* (syn. *G. intestinalis* and *G. duodenalis*) is a protozoan parasite and is the leading causative agent for non-bacterial water borne diarrhea worldwide. The discovery of this non-invasive intestinal parasite dates back to 1681 by Dutch microscopist Anthony Van Leeuwenhoek while he was analyzing his own stool samples. The parasite has a broad vertebrate host range and causes significant morbidity and economic loss [1, 2]. Despite this impact, giardiasis is a poorly understood disease and was included in the "WHO neglected disease initiative" in 2004 [3]. Giardiasis is highly prevalent in developing countries ranging from 20-30% as compared to developed countries, 2-7% [4]. The etiology of diarrhea in giardiasis is thought to be a leak flux mechanism as a result of compromised epithelial barrier function. The flagellated parasite causes acute and chronic diarrhea accompanied by nausea, abdominal pain, weight loss and malabsorption. Although 5- nitroimidazole compounds are used for treatment of giardiasis, treatment failures have been documented resulting in chronic diarrhea in immunocompromised individuals and children [5, 6].

The life cycle of *G. lamblia* consists of 2 stages, the non- infectious, motile, flagellated trophozoite and the environmentally resistant infectious cyst form, Fig. 1 [7]. Common modes of transmission are either from host to host or through fecal- oral routes. The transmission of the parasite commences when the cysts are shed in the feces and contaminate the water. After ingestion by a host, the giardial cyst undergoes excystation upon encountering acidic conditions in the stomach [2].

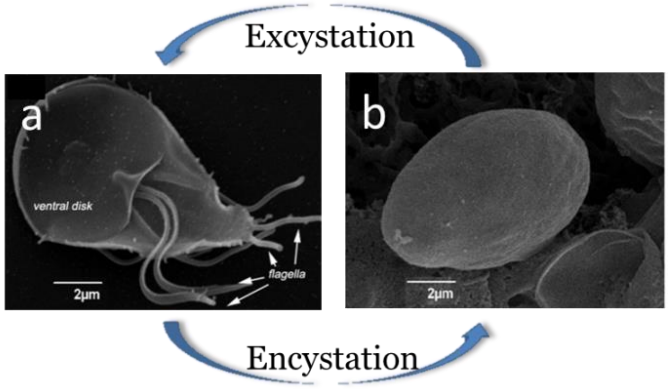


**Figure 1**: **The two stages of giardial life cycle**. **(a)** Non-infectious trophozoite form. **(b)** Infectious cyst form. Adapted from Touz, M.C 2012.

The excystation step is assisted by parasite and host proteases that help to digest the impenetrable cyst wall [8]. Emerging trophozoites attach to the small intestine with the help of an adhesive/ventral disc. The trophozoites divide by binary fission colonizing the small intestine, which eventually leads to the manifestation of the disease. For prolonged survival

within the host the trophozoites exhibit antigenic variation of their protein surface coat to evade clearing by the immune system.

Upon encountering changes in lipid concentration and increase in pH, trophozoites undergo a complex stage differentiation process (encystation) to cysts which are then shed in the environment by the host. However, the exact stimulus/stimuli that trigger encystation are still unknown. The infection cycle is completed when the cysts are ingested by another host. The complete life-cycle including cyst formation and excystation (mimicking infection of a new host after peroral uptake of cysts) can be reproduced in vitro [9].

### 1.2 Evolutionary background

Unicellular parasites such as *Giardia, Entamoeba, Trypanosoma* and *Plasmodium* cause severe health hazard worldwide. Classification of these parasites in the larger context of eukaryotic diversity enables us to learn how these parasites have evolved. Phylogenetic characterization performed in the mid- 1990s based on analyses of 1) SSU rDNA and 2) single protein encoding genes, showed significant divergence of these prominent parasites from the base of the tree [10, 11]. Furthermore, *Giardia* was considered as one of the earliest branching eukaryotes. The absence of several cytoskeletal organelles and most importantly mitochondria led to the hypothesis that the basal lineage which included *Giardia* comprised of amitochondriate protists which diverged before establishment of the an endosymbiont ancestral to mitochindria [12]. This is the basis for the Archezoa hypothesis [13] .

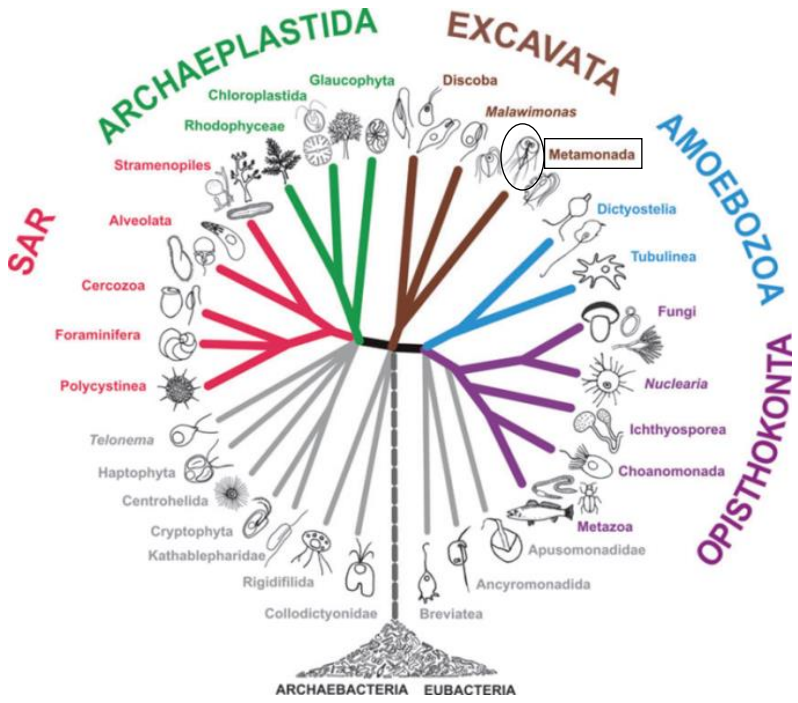


**Figure 2: Five different eukaryotic super groups.** *Giardia* belongs to the phylum Metamonada and the Excavate super group and clusters alongside genera *Trichomonas* and *Trypanosoma* (Discoba). Adapted from Adl *et. al* 2012.

However, since the discovery of mitochondrion-related organelles (mitosomes and hydrogenosomes) in all previously known amitochondriate organisms, the Archezoa hypothesis for phylogeny has been nullified [14]. Availability of whole genome sequences

from diverged eukaryotes and phylogenetic analyses combined with comparative ultrastructural data in the last decade has revolutionized our view of eukaryotic evolution, leading to the clustering of organisms in 5 major phylogenetic groups, Fig. 2 [15]. *G. lamblia* belongs to the Excavata super group and clusters along with genera *Trichomonas* and *Trypanosoma*. The new phylogenetic tree clusters protozoan parasites in three eukaryotic super groups; Excavate, Amoebozoa and SAR which are separated by 2 non- parasitic super groups, Archaeplastida and Ophisthokonta, This suggests that the parasitic life style evolved independently on separate occasions. Therefore, the presence of diverged parasitic life style and analogous structures having similar function in organisms in different parasitic taxa are a result of convergent evolution.

Interestingly, the modern era un-rooted phylogenetic tree reveals that the last eukaryotic common ancestor (LECA) was likely a eukaryote harboring all essential organelles (including mitochondria and stacked Golgi). Therefore the secondary loss of such organelles via reductive evolution in basal eukaryotes is a consequence of parasitic life style.

### 1.3 Organelle system

Consistent with the notion that *G. lamblia* has undergone strong reductive evolution, the compartmental organization of *Giardia* is extraordinarily simple on a morphological level. These minimized cellular sub-compartments consist of two equivalent nuclei, surrounded by a nuclear envelope which is continuous with a horse shoe-shaped endoplasmic reticulum, peripheral vesicles and mitochondrion-related organelles (mitosomes), Fig. 3. Unlike a typical eukaryotic cell, *Giardia* lacks peroxisomes, a typical Golgi complex and mitochondria [16, 17].

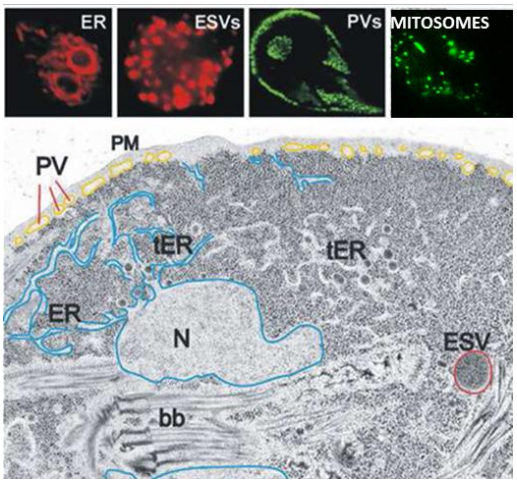


**Figure3: Compartmental organization in *Giardia*.** Steady state organelles include the endoplasmic reticulum, peripheral vesicles and mitosomes. On the other hand, encystation specific vesicles are generated *de novo* during stage differentiation. Adapted from Marti *et. al* 2004

In addition, trophozoites undergoing stage differentiation harbor additional organelles called as encystation specific vesicles (ESVs) that are generated *de novo*. ESVs process the secretory cargo required for regulated export to the cyst wall [18, 19]. The organelles present in *Giardia* are discussed below in more detail.

### 1.3.1 Endoplasmic reticulum

In a eukaryotic cell the secretory system comprises of the ER, Golgi apparatus and the secretory vesicles. *Giardia* harbors a labyrinthine tubular vesicular network (TVN), studded with ribosomes, reminiscent of the rough ER. *Giardia's* ER extends from the peri nuclear region towards the cell periphery, spanning the entire cell body [20]. Despite the omnipresence of ER in the cytoplasmic space, the ER does not permeate the space occupied by PVs [21]. *Giardia* ER was identified by localization studies using 3 known ER markers: 1) immunoglobulin heavy chain-binding protein (BiP), 2) the 3 protein disulphide isomerases (PDI) and 3) acid phosphatase [20, 22-25]. Furthermore, giardial ER possesses conserved machinery for co-translational import of secreted proteins into the organelle's lumen and necessary chaperones such as PDIs, heat shock protein 70 (Hsp70) Binding Protein BiP, and peptidyl-prolyl cis-trans isomerases to facilitate proper protein folding [26]. However, *Giardia* lacks the machinery for the addition of N-linked glycans to secreted proteins. Enzymes that add mannose and glucose to a dolichol precursor are also absent. Therefore, N-glycosylation of proteins is restricted to the addition of 1 or 2 GlcNAc to asparagine which are not further modified during secretory transport [27]. In line with this, *Giardia* lacks an ER based N-glycan dependent quality control machinery for protein folding and degradation [28]. However *Giardia* ER in the absence of a steady state Golgi apparatus is the cornerstone organelle for both exocytosis and endocytosis. It has been regarded as a pluripotent compartment either facilitating direct secretion of proteins to destination organelles/plasma membrane (exocytosis) or helping in catalysis/processing of endocytosed material from the extracellular milieu by peripheral vesicles [18, 29].

### 1.3.2 Peripheral vesicles

Peripheral vesicles (PVs) are small, oval shaped 150nm-sized organelles present below the plasma membrane on the entire dorsal side and at the center of the ventral disk [25]. These specialized organelles provide an all –in- one solution for endocytosis, fluid phase uptake, digestion and retrograde transport of material to the interior of the cell [25]. To date, PVs are the only endocytic organelle in *Giardia* mediating endocytosis of soluble and membrane bound molecules [25, 29-31]. These organelles open to the environment randomly by direct fusion with the PM and take up fluid phase material non-selectively before closing again [32]. Furthermore, due to the presence of lysosomal enzymes (hydrolases and cathepsins) these organelles mature into digestive compartments, facilitating degradation of bulk endocytosed material before their selective trafficking to the ER [29]. Although there is no lateral exchange of fluid phase markers between PVs, these organelles are implicated in a discriminatory sorting function allowing certain markers (e.g. casein) to be rapidly transported to the cell interior (ER) [32]. In addition, detection of cyst wall protein in the lumen of PVs and secretion of acid phosphatases also points towards their probable role in regulated protein secretion and excystation, respectively [33, 34].

### 1.3.3 Encystation specific vesicles (ESVs)

The construction and deposition of the extracellular cyst wall (CW) which renders *Giardia* the ability to survive outside the host is a vital step in the transmission of the disease. The cyst is encased in a biopolymer composed of 3 paralogous cyst wall proteins (CWPs 1-3) [35-37] and a glycopolymer (β-(1-3)-GalNAc) [38, 39]. This glycan is unique to *Giardia* and amounts to 60% of the cyst wall [40]. The 3 CWPs are between 241 and 362 residues long. These 3 proteins are characterized by a hydrophobic amino terminal signal peptide, followed by a stretch of 5 tandem leucine rich repeat domains and a cysteine rich carboxy terminal domain as shown in Fig. 4. However, CWP2 harbors an additional 121 residue long carboxy terminal extension composed of basic amino acids. The C-terminal extension of CWP2 is proteolytically cleaved during ESV maturation [35].

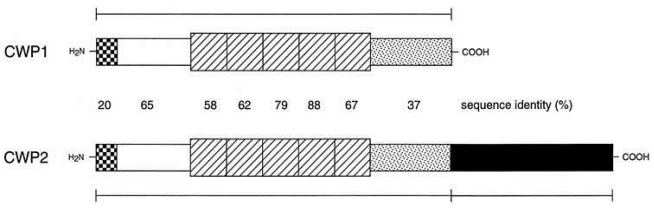


**Figure 4: Schematic representation of cyst wall proteins 1 and 2 in *Giardia*.** CWP1 contains a hydrophobic amino terminal, followed by a stretch of 5 tandem leucine rich repeat domains and a cysteine rich carboxy terminal domain whereas CWP2 contains an additional C-terminal tail which is proteolytically cleaved. CWP3 is similar to CWP1. Adapted from Lujan *et. al* 1995.

The presence of a prominent cyst wall ensures the very existence of a functional and regulated protein secretory system in *Giardia* (discussed later in section 1.4), albeit the absence of a steady state Golgi apparatus. In differentiating trophozoites, ESVs are the only Golgi-like late ER compartments generated *de novo* from ER exit sites [41, 42]. ESVs delay the export of cyst wall material (CWM) for post- translational modification and sequential partitioning before regulated CWM secretion [43], thus functioning as Golgi analogs in *Giardia*. This information is further supported by circumstantial evidence, such as; 1) association of coat protein I (COP I) to ESVs [44], 2) ESV sensitivity to Brefeldin A (fungal metabolite causing Golgi disassembly) [18, 19], 3) dependence of ESV genesis and maturation on small GTPases such as Sar1, Rab1 and Arf1 [42], and 4) recruitment of giardial dynamin to ESVs [32]. Our understanding of ESV genesis and maturation is based on the analogies with the cisternal progression model described by Losev. *et.al* [45] with the important difference that ESVs are not steady-state organelles but arise in response to a pulse of CWM exported from the ER [18, 46]. However, ESVs lack classical markers for the Golgi such as GM130, galactosyl transferases or the trans-Golgi network marker Rab6 and contain only one type of cargo. Therefore, despite increasing evidence that suggest ESVs to be Golgi analogs in *Giardia*, they lack some morphological characteristics that define the very organelle.

### 1.3.4 Mitosomes

Mitosomes are mitochondrion-related organelles (MROs) and are the simplest form of mitochondria. These organelles are devoid of organellar genome and are incapable of generating ATP via oxidative phosphorylation. Consequently, iron- sulfur protein maturation in the only metabolic pathway currently associated to these organelles. Since mitosomes are the main focus of my doctoral thesis, these reduced organelles are discussed in more detail in the next chapter.

## 1.4 Constitutive and regulated protein secretion

Until now two export pathways (constitutive and regulated) have been identified in *Giardia* responsible for trafficking proteins directly from ER either to the PM or to the ESVs [18, 47, 48].

The constitutive protein secretory pathway is mainly responsible for secretion of 3 kinds of proteins in trophozoites 1) proteins harboring a predicted signal sequence, 2) cysteine rich non-variable proteins and 3) variant surface membrane proteins (VSPs) [21]. VSPs are transmembrane anchored surface proteins that cover the whole trophozoite, providing a protective layer [49, 50]. VSPs are targeted to the PM via the conserved C-terminal CRGKA tail [18]. Although VSPs are trafficked directly from the ER to the PM [21, 47, 48], VSP trafficking is sensitive to brefeldin A [19] indicating that VSP trafficking could be via COP I derived vesicles. However such vesicles are not yet identified in *Giardia* trophozoites. Only one out of the predicted 235- 275 VSPs coats the parasite membrane at a time [51]. VSPs are composed of cysteine rich exo-domains which are released as soluble antigens into the environment (VSP switching) facilitating antigenic variation of the surface coat thereby helping the parasite evade the host immune system [52-54]. VSP switching/turnover happens on average every 6-13 generations [55] and is regulated by RNA interference [56, 57]. Furthermore, apart from the approximately 300 VSPs, another 500 cysteine rich non-variable proteins and proteins with a predicted signal sequence are targeted to the PM via the constitutive secretory pathway [58].

The most distinctive secretion process is *Giardia* is however during encystation where the CWM is packed in *de novo* generated ESVs, sorted, partitioned and deposited on the plasma membrane [18, 19, 42]. CWPs are initially sorted from constitutively secreted proteins already at ER exit sites [18, 41] and packed into ESVs prior to their regulated secretion. The encystation process can be studied *in vitro* via several methods; however the two-step encystation protocol is mostly preferred amongst all. This method is based on bile deprivation for 48 hours followed by subsequent increase in pH and porcine bile [59, 60] . The expression of CWM is stage specifically induced and the mRNA levels peak at 7 hours post induction of encystation (hpie) [43]. The whole process of encystation lasts approximately 20- 24 hours [46]. Briefly, at 2 hpie, CWM starts to appear at the ER, followed

by the first round of sorting at the transitional ER where CWM is sorted from the constitutive cargo. The CWM leaves the ER in a COP II dependent manner [41]. Subsequently the *de novo* generated ESVs accumulate CWM and increase in size. CWM is delayed in ESVs allowing for post translational modification of CWPs [43]. Specifically the 121 residue long carboxy terminal extension of CWP2 undergoes proteolytic cleavage generating CWP2 (ΔN) and CWP2 (ΔC) fragments. Around 8-12 hpie the CWM undergoes selective condensation where the CWP3 and the C-terminal portion of CWP2 (ΔC) form the condensed core in the ESV while CWP1 and the N-terminal portion of CWP2 (ΔN) form an outer fluid phase. The fluid phase circulates between ESVs most likely via the ER [42]. 16-20 hpie marks the second sorting event where the fluid phase is sorted away from the condensed core near the cell periphery forming 2 different compartments. Subsequently the fluid phase is secreted first, forming the outer layer of the cyst wall. The condensed core undergoes de-condensation and is secreted slowly over hours, forming the inner layer [42].

### 1.4.1 Molecular machinery for regulated protein secretion

Due to reductive evolution *Giardia* has lost most of the molecular machinery required for protein secretion including the Golgi apparatus which is considered the hub of the secretory pathway. As mentioned above, ESVs act as Golgi analogs although they differ substantially both structurally and biochemically when compared to a canonical Golgi.

Despite these differences, ESVs are sensitive to brefeldin A (a fungal metabolite that inhibits Arf 1 and in turn causes Golgi disassembly in higher eukaryotes). Furthermore, proteins and/ or factors required for budding and fusion of transport vesicles such as coatomer proteins (COP I, COP II), clathrin heavy chain, two adaptor proteins (AP1 and AP2/3) and small GTPases such as Arf1 which are involved in COP I coated vesicles, Rabs and Sar1 have been identified in the *Giardia* genome [61, 62].

In addition, 7 SNARE (soluble N-ethylmalemide- sensitive factor attachment protein receptors) proteins have been also identified [44, 63]. Interestingly, it was demonstrated that the ER resident chaperone Hsp70/Bip was retrieved back to the ER from ESV via KDEL sequence suggesting COP I based retrograde protein trafficking. Furthermore identification of proteasomal components during the early stages on encystation on ESV membranes points towards a quality control step associated with a degradation process [64]. Taken together, identification of all these proteins associated with ESVs makes these organelles stage specifically regulated Golgi analogs and hints towards minimum machinery capable of regulated secretion in *Giardia lamblia*.

# 2: Mitochondria and mitochondrion-related organelles (MROs)

## 2.1 Mitochondria: evolution and classification

Mitochondria are organelles found in virtually all eukaryotic cells and function at the crossroads of life and cell death. These organelles are not only the energy source of the cell capable of performing a myriad of essential biochemical reactions but are also the key triggers for apoptosis [65-69]. Based on the well-established endosymbiotic theory, the mitochondrion was once a free-living prokaryote which was maintained as an organelle after being engulfed by a eukaryotic cell [70-74]. This theory is corroborated by the level of biochemical and physiological similarity of mitochondria to prokaryotic cells [13, 75-77]. Martin *et. al* proposed that the ability of the α-proteobacterium to generate free energy in form of ATP and the inability of the host (eukaryotic ancestor) to do so might have been the reason that drove the endosymbiosis event [78]. However phylogenetic analysis of the mitochondrial ADP/ATP transporter does not support this hypothesis by placing the origin of the transporter post endosymbiosis [79]. Therefore, alternative theories on the nature of the driving force for the endosymbiosis event were proposed such as 1) the hydrogen hypothesis [78], 2) The syntrophic hypothesis [80] and 3) The ox-tox hypothesis [72]. Van der Giezen *et. al* have well documented the biochemical drivers for the above proposed hypotheses [81]. Regardless, the presence of mitochondrial DNA substantiates the endosymbiosis theory. Phylogenetic analysis of mt-DNA and mt-rRNA sequences links the origin of mitochondria to α-proteobacteria, more specifically to the order *Rickettsiales* [82, 83].

Following the endosymbiosis event, evolution of the eukaryotic lineage has led to 5 super-groups based on phylogenetic analyses [15]. The presence of mitochondria or MROs is ubiquitous in all [15]. Several studies provide evidence that the diversified MROs evolved from the mitochondrial ancestor under selection by environmental habitats of the host organisms [84]. Previously, eukaryotes were mostly classified into 3 categories, based on the Archezoa hypothesis: Type 1: Primitive amitochondriate (no endosymbiosis) or secondarily amitochondriate (loss of mitochondria), Type 2: Mitochondrial descendants having compartmentalized energy metabolism (mitochondria/hydrogenosomes) and Type 3: Mitochondrial descendants without compartmentalized energy metabolism (mitosomes) [84, 85]. However, given that the archezoal hypothesis has been nullified, eukaryotes belonging to type 1 class have never been identified until now. More recently, Muller *et. al* differentiated mitochondria in 5 different categories based on organelle biochemistry, energy metabolism and functions, Table 1 [86]. Briefly, classes 1, 2 and 3 generate energy via the electron transport chain (ETC), whereas class 4 and 5 lack such machinery for energy production.

Table 1: Classification of mitochondria

| | | |
|---|---|---|
| Class 1 | Aerobic Mitochondria | Generates ATP and exclusively utilizes O2 at the terminal electron acceptor |
| Class 2 | Anaerobic Mitochondria | Generates ATP and utilizes compounds other than O2 (such as fumarate) as the terminal electron acceptor but does not produce H2 |
| Class 3 | H2-producing Mitochondria | Generates ATP and uses proton as the terminal electron acceptor to produce H2 |
| Class 4 | Hydrogenosomes | Generates ATP and produces H2 |
| Class 5 | Mitosomes | Do not generate ATP |

(Modified from Müller *et. al* 2012)

### 2.2 MROs: Hydrogenosomes and mitosomes (background and identification)

The identification of MROs such as hydrogenosomes and mitosomes in eukaryotes lacking "typical mitochondria" has sparked interest in the origin and evolution of endosymbiosis-derived organelles in eukaryotes [84, 87-90]. It is now well-known that the basal placement of MRO containing organisms is rather an artefact of phylogenetic analyses [91]. Indeed, MROs are not only found in primitive lineages but are also found in diverse group of protists, fungi and ciliates [92-94].

Hydrogenosomes were first discovered in the parabasalid parasite *Tritrichomonas foetus* as early as 1973 [88, 95]. Hydrogenosomes house a unique cellular machinery which produces molecular hydrogen through the oxidation of pyruvate. Hydrogenosomes were initially thought to have originated from a separate endosymbiotic event of *Clostridium* with the primitive eukaryote [96]. However, definitive evidence for the mitochondrial origin of hydrogenosomes comes from phylogenetic analyses of the hydrogenosomal genome of the ciliate *Nyctotherus ovalis* [97]. Hydrogenosomes are present in four supergroups (Chromalveolates, Excavata, Amoebozoa and Opisthokonta) of the eukaryotic lineage [98].

On the other hand, mitosomes were first discovered in *Entamoeba histolytica* [89, 90] by using antisera against chaperonin 60 (Cpn60), a chaperone of mitochondrial ancestry widely used for phylogenetic analysis. Subsequently, mitosomes were also discovered in many other organisms such as the microsporidia *Trachipliestophora hominis* and *Encephalitozoon cuniculi* [99, 100], the apicomplexan *Cryptosporidium parvum* [94] and the diplomonad *Giardia lamblia* [101]. First evidence for mitochondrial ancestry for diplomonad mitosomes came from the phylogenetic analysis of valyl –tRNA synthetase [102, 103]. Direct evidence for mitochondrial ancestry of giardial mitosomes came from localization studies of mitochondrial chaperonin 60, mitochondrial heat shock protein 70 (mt Hsp70), cysteine desulphurase (*Gi*IscS) and members of the Fe-S protein maturation machinery [104-106].

Therefore, the absence of canonical mitochondria in *Giardia* can be explained by a secondary loss due to parasitic adaptation to an anaerobic environment. Interestingly, the *Spironucleus* genus (closest relatives to the *Giardia* genus known and investigated) harbors hydrogenosomes [107, 108]. Based on phylogenetic data, Jerlstrom-Hultqvist, J *et. al* proposed that within the diplomonad kingdom, mitosomes might have evolved from hydrogenosomes and not from mitochondria directly due to the presence of hydrogenosome components in the diplomonad ancestor [109, 110].

### 2.3 Apoptosis

Cell death plays a complementary but opposite role to mitosis in maintaining a cell population, eliminating damaged cells and giving shape to an organism [111]. The term apoptosis (a-po-toe-sis) was first used to describe a morphologically distinct form of cell death [112]. Studies regarding apoptosis have boomed ever since the discovery of programmed cell death (PCD) in *Caenorhabditis elegans* [113]. Cell deletion at specific stages leading to development of organs and digits outlines the precision and importance of this process. Apoptosis therefore has been accepted as the most distinctive form of PCD in metazoans because of its obvious benefits towards multicellular life forms [114]. This however doesn't exclude the existence of other forms of cell death such as necrosis and autophagy [115, 116]. Depending on the type of stimuli and/or degree of exposure to stimuli, cells could either die by apoptosis or necrosis [117]. Apoptosis is accompanied by various physiological and morphological changes in the cell. For instance, cell shrinkage (reduced size, condensed cytoplasm and tightly packed organelles) and pyknosis (condensed chromatin) are early symptoms of apoptosis and are visible by light microscopy. In metazoan cells undergoing apoptosis, pyknosis is accompanied by fragmentation of genomic material into oligonucleosomal fragments of 200bps leading to a characteristic DNA laddering pattern [118]. Other morphological features include excessive plasma membrane blebbing and separation of small cellular fragments generating "apoptotic bodies". These apoptotic bodies are then scavenged by macrophages or parenchymal cells and are degraded within phagolysosomes [119]. Hallmark biochemical changes include phosphatidylserine (PS) externalization, increase in intra-cellular $Ca^{2+}$ levels, breakdown of PARP (DNA repair enzyme) and mitochondrial dysfunction [120]. It is noteworthy that neither apoptosis nor removal of apoptotic cells elicits any inflammatory response due to several reasons: 1) cells do not burst, hence they do not release their cellular content into the environment; 2) they are phagocytosed by macrophages, hence preventing secondary necrosis; 3) the scavenging cells do not release/produce pro-inflammatory cytokines [119].

Apoptosis is a highly complex, sophisticated and energy demanding process. Current research suggests the presence of 2 main apoptotic pathways: the extrinsic (via death receptor) and the intrinsic route (via mitochondria). In fact, these two pathways could be

interconnected. These different routes are activated by specific triggering signals in order to begin a highly complex cascade of molecular events resulting in the characteristic cyto-morphological apoptotic features leading to the demise of the cell (execution pathway). Since MROs and, specifically, mitosomes are the organelles of interest during my doctoral thesis, I briefly summarize the events in the intrinsic death pathway, with mitochondria (cell's Pandora's Box [121],) being the cornerstone organelle [122]. Briefly, specific death stimuli result in loss of mitochondrial membrane potential, opening of the mitochondrial transition pore with release of pro-apoptotic proteins (cytochrome c and Smac/DIABLO) from the inner membrane space into the cytosol. These factors then activate the caspase dependent mitochondrial cell death pathway. Tight regulation of the intrinsic death pathway is carried out by Bcl-2 family proteins [122, 123].

Several groups around the world in the past decade have performed numerous experiments to show the presence of a caspase like execution pathway for cell death in MRO harboring parasites such as *Trichomonas* and *Giardia* [124, 125]. A form of cell death with most if not all features of canonical apoptotic death has been documented, for e.g. chromatin condensation, PS externalization, TUNEL positive DNA fragmentation without any DNA laddering. Furthermore, involvement of caspase like activity has also been reported by the authors [126]. In 2009, Ghosh *et. al* demonstrated that *Giardia* trophozoites underwent a form of PCD when subjected to $H_2O_2$, metronidazole, and upon exposure to a media devoid of cysteine and ascorbic acid [127]. PS externalization and DNA degradation without a typical electrophoretic laddering were observed as read outs for apoptotic like cell death. Interestingly dying cells were negative for caspase activity and other proteases which could be involved in the death machinery. In another study, when giardial trophozoites were treated with the drug beta-lapachone (topoisomerase inhibitor); dying cells exhibited many if not all features of apoptosis, such as cell shrinkage, chromatin condensation, membrane blebbing and vacuolization. In addition, authors have also described autophagic cell death in *Giardia* upon treatment with the drug beta-lapachone based on the appearance of large vacuoles and LC3 staining (hallmark of autophagy) [128]. Similar results were replicated by Bagchi *et. al* in 2012, where the authors could demonstrate apoptotic like morphological changes in giardial trophozoites upon exposure to $H_2O_2$. Interestingly, using *in silico* homology searches, authors could also identify 3 three key players of autophagic cell death (TOR, ATG1 and ATG16) [129].

# 3 Mitosomes

## 3.1 Mitosomes (morphology, distribution and function)

Mitosomes are small spherical 100-150 nm, double membrane bounded organelles and harbor nuclear encoded proteins of mitochondrial origin [130]. Based on confocal and electron microscopy, the number of mitosomes per giardial cell ranges from 25-50 [101, 131, 132]. *Giardia* mitosomes have distinct sub-cellular localizations; 1) peripheral mitosomes, which are distributed in the cytoplasm as single organelles, and 2) central mitosome complex, which is present as a rod like structure between the two nuclei, Fig. 5a. Electron microscopy and current data obtained in our laboratory using high resolution light microscopy (stimulated emission depletion, STED) (Rout, Hehl unpublished data) suggest that the central mitosome complex is a cluster of individual organelles present in a staggered formation buried under the bundle sheaths, Fig. 5 b-c. However, unlike bona fide mitochondria, *Giardia* mitosomes are devoid of an organellar genome and are not involved in energy metabolism. Because organellar genome has been detected in mitosomes of *Blastocystis hominis* [133] and absent in mitosomes of *Giardia*, giardial mitosomes are placed at the furthest extreme on the spectrum of reductive evolution.

Importantly, availability of the mitosomal genome of *Blastocystis* should now allow for genetic probing of the evolutionary history of mitosomes.

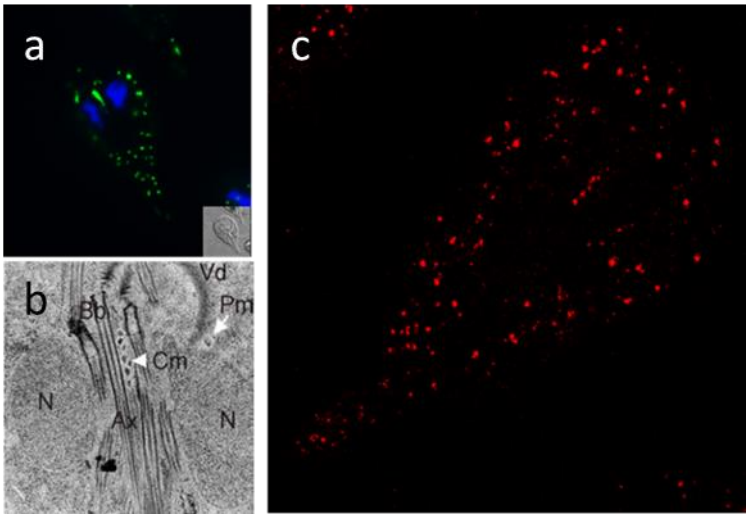


**Figure 5: Sub- cellular distribution of giardial mitosomes. (a)** Immuno-fluorescence microscopy: C-terminally triple HA-tagged *Gl*Tom40 (*Tom40::3xHA*), a marker for mitosomes. Central mitosome complex (CMC) and numerous peripheral mitosomes (green). Nuclear DNA is stained with DAPI (blue). Inset: DIC image. **(b)** tEM showing the CMC is composed of individual organelles[134]. **(c)** Mitosomes (red) as visualized in high resolution STED microscopy (Rout, Hehl unpublished data).

Nevertheless, *Giardia* mitosomes despite being highly reduced/modified are able to import nuclear encoded proteins via conserved protein import pathways (discussed later) [90, 101, 131]. However, iron- sulfur protein (Fe-S) maturation is the only known function ascribed to these organelles and has been shown to be indispensable for mitochondria and conserved throughout evolution [135]. This could be a probable explanation for the retention of mitosomes in *Giardia*. In fact, *Giardia* genome database searches and high throughout proteomics studies revealed that *Giardia* harbors key components for the Fe-S protein maturation machinery such as IscU (*Gl50803_15196*), cysteine desulphurase (*Gl50803_14519*), mtHsp70 (*Gl50803_14581*), IscA2 (*Gl50803_14821*), ferredoxin (*Gl50803_27266*), Nfu *(EAA38809*), DnaJ protein Jac1 (*Gl50803_17030*), Glutaredoxin 5 (*Gl50803_2013*) and GrpE (*Gl50803_1376*) [86, 136]. Surprisingly, frataxin is missing in the *Giardia* genome. Frataxin is a Fe-binding protein that donates Fe to the IscU/IscS complex and is invariably present in all eukaryotes including mitosome harboring *E. cuniculi* [17] and *C. parvum* [137]. Furthermore, an ADP/ATP transporter or any machinery for ATP synthesis has not been identified in *Giardia* mitosomes, despite the presence of 2 mitosomal proteins (Cpn60 and mt Hsp70) having ATP-dependent activity [26, 136, 138]. Therefore, the source of energy in *Giardia* mitosomes for: 1) import of nuclear encoded proteins into mitosomes, 2) transfer of Fe-S cluster, remains elusive till date. Interestingly, a unique ADP/ATP transporter which does not require membrane potential has been identified in *E. histolytica* mitosomes [139].

## 3.2 Mitosomal protein targeting and processing

### 3.2.1 Mitosomal protein targeting sequences (MTS)

In all species known so far harboring a mitochondrion with an organellar genome, 98% of the organellar protein repertoire is nuclear encoded and must be targeted to the organelle and its compartments precisely with the help of specific targeting signals [140, 141]. The nuclear encoded mitochondrial matrix proteins are synthesized with a N-terminal mitochondrial targeting sequence (MTS) which is recognized by the receptors on the mitochondrial surface (Tom20), subsequently transporting the preproteins to their final destination via translocases of the outer and inner membranes [142, 143]. Some carrier proteins however lack the N-terminal MTS and instead possess several internal mitochondrial targeting signals distributed throughout the entire length of the protein which are recognized by the Tom70 receptor [142, 144].

Typical MTSs are composed of approximately 10-80 positively charged, hydrophobic and hydroxylated amino acids [140, 145-147]. Apart from these characteristics MTSs have very little primary sequence conservation amongst different phylogenetic groups [148]. In fact, the MTS present in organisms harboring mitosomes and hydrogenosomes are comparatively shorter than their eukaryotic homologs. Smid *et. al* have shown that the length of the MTS in

these relic mitochondria containing organisms varies from 4-21 amino acids [149, 150]. Experimental evidence in the literature suggests that the MTS of mitosomal proteins in *Giardia*, *Entamoeba* and of hydrogenosomal proteins in *Trichomonas* contains an arginine residue which is located 2 residues upstream of the cleavage site, thus facilitating recognition of the cleavage site [151, 152]. Surprisingly, in 2 independent studies performed in *Giardia* and *Saccharomyces cerevisiae*, it was demonstrated that IscU protein was delivered to mitosomes and mitochondria respectively regardless of the MTS, albeit with reduced efficiency in its absence [132, 153]. These experiments suggested that the internal signals present in mitochondrial proteins are sufficient for proper delivery; however a MTS increases the efficiency of transport.

Matrix proteins harboring positively charged MTS are inserted via membrane potential dependent Tim 23 translocon after which the MTS is cleaved by the mitochondrial processing peptidases marking the final step of the import process. This processing step is important as it ensures proper protein function and/or protein stability [154]. Subsequently the unfolded protein is refolded in the matrix to its native structure with the help of the cpn60/cpn10 chaperone complex.

### 3.2.2 Mitosomal processing peptidase

Canonical mitochondrial processing peptidases (MPPs) comprise of 2-α and 2-β subunits and work as a heterodimer and remain non-functional individually [148, 155]. Kitada *et. al* in 2007 proposed that the modern day MPP's ancestor was probably a monomeric α-proteobacterial peptidase because of high sequence similarity with *Rickettsia prowazekii* peptidase [156]. During evolution, gene duplication events led to formation of α/β subunits resulting in a heterodimeric MPP. Both subunits are responsible for different function; the α-subunit infers substrate binding and release whereas the β-subunit is responsible for catalysis process [149, 155]. The two subunits form a negatively charged cavity where the MTS is processed by electrostatic interaction. Out of the few mitosomal and hydrogenosomal proteins known/identified so far, a subset of the proteins are shown to possess a N-terminal MTS responsible for proper targeting to the organelle [101, 131, 152]. In fact, *Giardia* harbors a gene encoding a β-MPP and the product is localized to mitosomes [26, 132]. *Giardia* MPP is unique in itself as it lacks the α-subunit and functions as a β-monomeric enzyme [149]. Furthermore, the recombinant *Giardia* β-MPP can process MTS harboring *Giardia* proteins *in vitro*. Likewise a protein with limited similarity with *S. cereviseae* β-MPP has been identified in genome of hydrogenosome containing *Trichomonas vaginalis* [157]. However, the *T. vaginalis* MPP functions as a β-homodimer enzyme. Therefore, the presence of the monomeric subunit β-peptidase in *Giardia* and homodimer β-peptidase in *Trichomonas* points towards either a consequence of secondary reduction or retention of the ancestral MPP [156].

### 3.3 Mitochondrial/mitosomal protein import machinery

The mitochondrion of *Saccharomyces cereviseae* harbors around 1000 proteins out of which over 98% are encoded on the nuclear genome and are synthesized as precursor proteins on the cytosolic ribosomes [158]. As mentioned above precursor proteins either carry a MTS or internal signal in the mature protein that guides them to their correct sub-cellular destination within mitochondria. Because mitochondria are double membrane bound organelles, the protein translocation into mitochondria is more complex than in single-membrane bound compartments. Proteins need to be directed to four different compartments within the organelle, the outer membrane (OM), inner membrane space (IMS), inner membrane (IM) and the mitochondrial matrix.

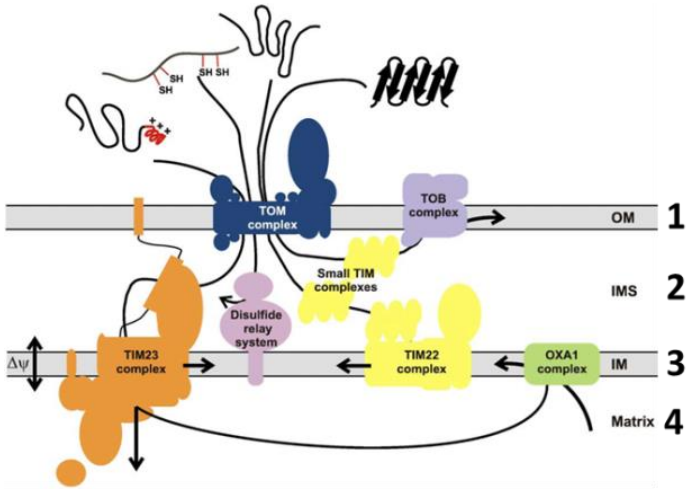


**Figure 6: Mitochondrial protein translocation to 4 distinct sub-cellular compartments across two membranes.**[159]. 1: Outer membrane (OM), 2: Inner membrane space (IMS), 3: Inner membrane (IM) and 4: Matrix. Adapted from Mokranjac *et. al* 2009. Details of each component are described in the text below.

Hydrophobic proteins of the outer membrane need to be arrested in the outer membrane whereas hydrophobic proteins belonging to the inner membrane should escape the outer membrane and reach the inner membrane via dedicated internal signals. Hydrophilic proteins should pass via two hydrophobic membranes and either be retained in the inner membrane space or move on to the matrix. Protein Translocases of the Outer and Inner membrane (TOM/TIM) work in conjunction with various proteins and facilitate mitochondrial protein import. The mitochondria import machinery has been well characterized in the model organism *S. cerevisiae* [160-162].

The fact that *Giardia* mitosomes have completely lost their organellar genome requires a fully functional protein import machinery allowing nuclear encoded proteins to be imported via distinct import pathways. Despite the variation in the number and types of proteins imported into mitosomes, the *Giardia* mitosome import machinery has remained fairly conserved functionally [131]. In this section, I will briefly explain the various protein complexes required for post-translational insertion of mitochondrial proteins in *S. cerevisiae* and later provide an overview of the machinery present in MRO harboring organisms including *G. lamblia*.

### 3.3.1 Translocase of the Outer Membrane (TOM): The gateway to mitochondria

TOM is the first translocase that an incoming protein has to pass through in order to be incorporated in mitochondria. In yeast, the complex is made up of a 40 kDa β-barrel protein Tom40, the MTS recognizing receptor protein Tom20, the carrier protein receptor Tom70 and the small proteins Tom5, Tom6 and Tom7, Fig. 7. In addition, Tom22 acts as a central receptor and accepts precursor proteins from Tom20 and Tom70, mediating their transfer to Tom40 [162].

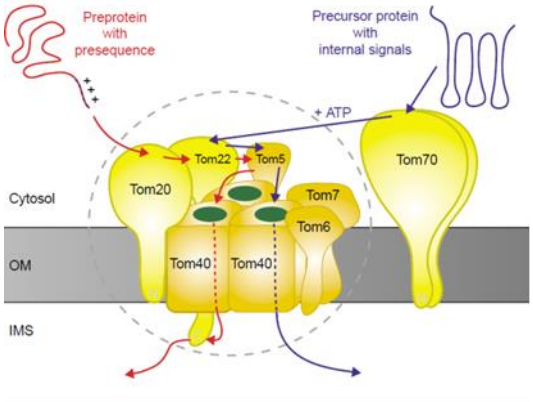


**Figure 7: Translocase of the Outer Membrane (TOM).** Tom 40 and the associated proteins are shown. 3 receptors for the translocase are Tom20, 22, and 70. Tom 5, 6 and 7 provide stability to the Tom complex. Adapted from Pfanner *et. al* 2002.

Amongst all the proteins involved in the TOM complex, Tom40 seems to be the most conserved as it has homologues in all organisms including those that harbor MROs, e.g. *Cryptosporidium parvum* [137], *Encephalitozoon cuniculi* [163], *Entamoeba histolytica* [164-166] and *Trichomonas vaginalis* [167]. Interestingly, *Trypanosoma brucei* (member of Excavate super group) lacks a direct homolog of Tom40 but rather possesses an old archeal homolog of Omp85, ATOM (Archeal TOM) [168].

The first documentation on the presence of a giardial Tom40 homologue (*Gl50803_17161*) came from co-immunoprecipitation experiments where the authors demonstrated that the TOM40 complex was considerably smaller in size (~200 kDa) compared to ~400 kDa in yeast. In line with the observed reduced size of the complex, the authors could not identify any of the other conserved protein components involved in the machinery [169]. Despite the identification of Tom40 in *Giardia*, functional evidence for translocation activity of *Gl*Tom40 is still missing till date. Furthermore, since there is no direct evidence for the presence of Tom receptors (Tom20/Tom70) in *Giardia*, it is highly intriguing how MTS harboring/ carrier proteins are correctly recognized and subsequently translocated through *Gl*Tom40.

### 3.3.2 Structure and Assembly Machinery (SAM): Integration into the outer membrane

Due to the prokaryotic origin of the modern day mitochondria, the outer membrane contains proteins that have a β-barrel conformation, for e.g. Tom40. Besides the translocase, mitochondrial division and morphology protein 10 (Mdm10) and Sam50 are proteins that also bear β-barrel conformation. Fully functional porins are very important to the cell as they form voltage-dependent anion-selective channel (VDAC), important for maintaining ionic

gradient across the membrane [170]. The SAM complex is composed of 3 proteins, Sam50 (core subunit), Sam35 (β-signal recognizer) and Sam37 (releases proteins from the SAM complex to the lipid bilayer), Fig. 8 [171, 172]. For insertion into the outer membrane, the β-barrel proteins first pass though Tom40 into the inner membrane space. Subsequently, small chaperone complexes Tim8-13 escorts these proteins and delivers them to the SAM complex for insertion into the lipid bilayer where they attain their final conformation [173].

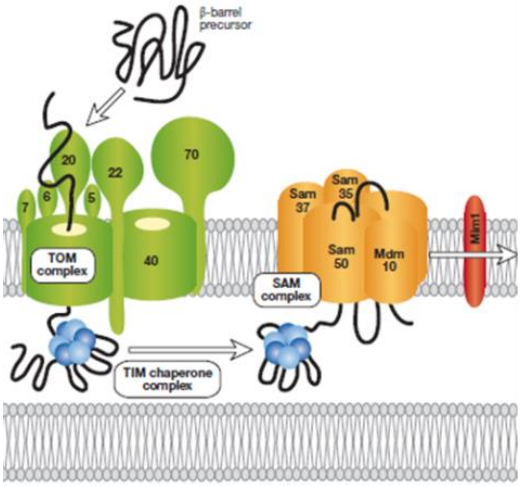


**Figure 8: Structure and Assembly Machinery (SAM).** Beta-barrel proteins are inserted into the IMS via the Tom40 and then escorted by tiny Tims 8-13 to the SAM complex where they are inserted into the outer membrane. Adapted from Bolender *et. al* 2008.

Like Tom40, Sam50 is highly conserved and has homologues in all organisms harboring mitochondria or MROs excluding *Giardia* despite the presence of β-barrel protein (Tom40) in the outer mitosomal membrane. However, homologues for Sam35 and Sam37 are absent in all MRO harboring organisms mentioned above including *Giardia* and hence the mechanisms through which these organisms integrate β-barrel proteins in the mitosomal membrane remains uncharacterized. On the contrary, insertion of α-helical membrane spanning proteins occurs via mitochondrial import 1 protein (Mim1) and is independent of the SAM complex [174]. Notably, the homologues of Mim1 are also absent in all anaerobic protists, suggesting a further reduction in the composition of the transport machinery.

### 3.3.3 Mitochondrial Intermembrane Space Import and Assembly (MIA): Integration into the inner membrane space.

Proteins harboring conserved cysteine residues are imported into the inner membrane space via the Mia40-sulfhydryl oxidase (Erv1) disulfide relay pathway [175, 176]. In short the cysteine rich proteins exit the Tom40 pore in a reduced state and are recognized by the redox activated protein Mia40. Recognition by Mia40 leads to mixed disulfide bond formation between substrate and Mia40 [177]. The substrate is finally released in an oxidized state facilitating its folding and is trapped in the IMS, leaving Mia40 in a reduced state [178]. The reduced Mia40 is reactivated (oxidized) via sulfhydryl oxidase (Erv1), Fig. 9.

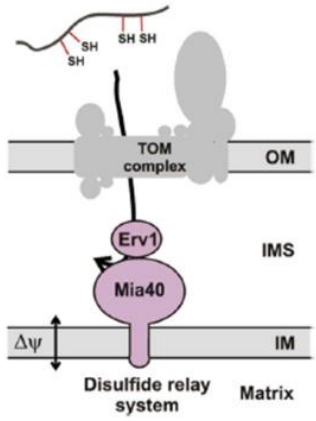


**Figure 9: Mitochondrial Intermembrane Space Import and Assembly (MIA): Integration into the inner membrane space.** Cysteine rich proteins are inserted in a reduced state through Tom40 where they interact with an oxidized (activated) Mia40 in the inner membrane. Subsequently the protein is oxidized facilitating folding and trapping in the IMS. Erv1 reactivates the reduced (inactivated) Mia40. Adapted from Mokranjac *et. al* 2009.

The characteristic cysteine motif Cx3C or Cx9C necessary for disulphide bond formation is present in many small intermembrane space proteins such as the tiny Tims 9-10 and 8-13 [140, 179]. Phylogenetic and genomic analyses have failed to identify the components involved in this pathway in other anaerobic parasitic protists. Therefore, the knowledge about their presence in *Giardia*, and how the cysteine rich proteins are localized in the inner membrane space in *Giardia* is still lacking.

### 3.3.4 Translocase of the Inner Membrane 22 (TIM22): Translocation of the metabolite carriers to the inner mitochondrial membrane

An important feature of canonical mitochondria is the presence of metabolite carrier proteins in the inner membrane. The carrier proteins are escorted by cytosolic chaperones (Hsp70 and Hsp90) to the mitochondrial outer membrane where they are recognized via their hydrophobic residues by the carrier protein receptor Tom70. Upon entering the IMS the carrier proteins are bound to the tiny Tim 9-10 complex. Finally, the membrane anchored chaperone Tim12 binds the carrier protein-Tim9-10 complex and tethers the protein to Tim22, the core component of the TIM22 complex, facilitating membrane-potential-dependent insertion into the inner membrane, Fig. 10. However, the mechanism with which carrier proteins are laterally translocated in the IM is unknown.

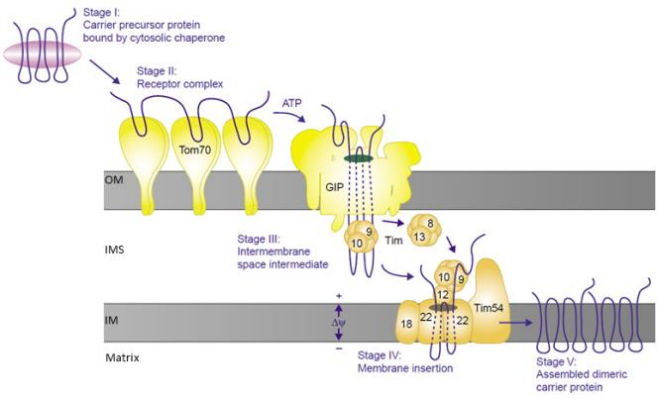


**Figure 10: Translocation of the metabolite carriers to the inner mitochondrial membrane by Translocase of the Inner Membrane 22 (TIM22).** Proteins required for insertion of carrier proteins in the inner membrane are Tom70, Tom40, tiny Tim9-10, Tim12 and Tim22. Five different stages of protein insertion are depicted. Adapted from Pfanner *et. al* 2002.

In addition, the TIM22 complex is involved in membrane insertions of Tim 23 and Tim17. TIM 22 complex also comprises of Tim 18 and Tim 54 and a Sdh3 subunit. Although there is little information regarding the function of Tim54, Tim 18 has been proposed to provide conformational stability during Tim 22 assembly [180, 181]. Tim22 homolog have been identified in *Encephalitozoon cuniculi* [163], *Cryptosporidium parvum* [137], *Trichomonas vaginalis* [167] and *Blastocystis hominis* [182]. However, a Tim22 homolog has not yet been identified in mitosome bearing *Entamoeba* and *Giardia* genome [183].

### 3.3.5 Translocase of the Inner Membrane 23 (TIM23): Translocation of proteins harboring N-terminal MTS into the matrix

As already mentioned in section 3.2.1, the mitochondrial matrix proteins harboring positively charged N-terminal MTS are translocated to their destination via the Tim 23 translocon. The TIM23 complex works in cooperation with the presequence translocase-associated motor complex of the matrix (PAM) in order to achieve synergy with the TOM40 complex during the transport of the protein. TIM23 complex is composed of 3 core subunit Tim23, Tim17 and Tim50, Fig. 11. Tim23 forms a channel across the inner membrane while Tim17 regulates the sorting of the preproteins and Tim50 regulates the closing of the Tim23 pore. The opening of the Tim23 channel is regulated by the electrochemical gradient and Tim50 prevents the diffusion of the electrochemical gradient [184-187]. The MTS harboring proteins first binds to Tom40 where the MTS is anchored thereby facilitating the mobilization of the protein to the Tim23 pore. Once the protein exits the Tim23 translocon it is processed by the PAM machinery [183]. The PAM machinery consists of mitochondria chaperone Hsp70 (mtHsp70) and several co-chaperones such as Pam18, Pam16, Mge1, Tim44 and Pam17 [188]. The ATPase activity of the mtHsp70 binds the presequence and folds the protein using the energy fueled by Mge1 (the mitochondrial-nucleotide exchange factor).

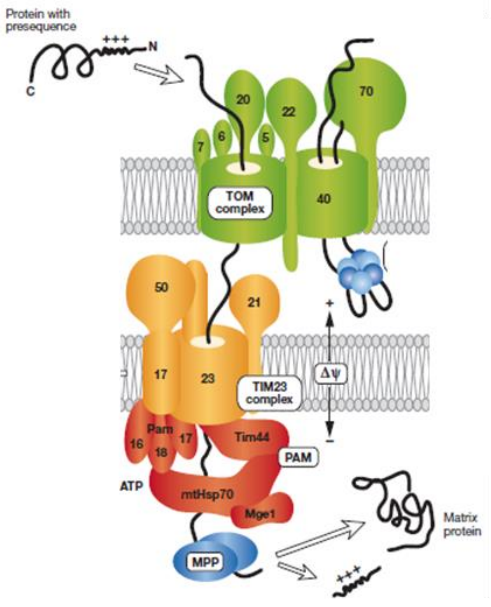


**Figure 11: Translocase of the Inner Membrane 23 (TIM23): Translocation of proteins harboring N-terminal MTS into the matrix.** Translocation of matrix proteins harboring a MTS is facilitated via the Tim23 complex. Tim23 functions with the PAM complex in conjunction to facilitate protein import into the matrix. Imported preproteins are then processed by the mitochondrial processing peptidase to giving rise to the mature protein. Adapted from Bolender *et. al* 2008.

MTS harboring proteins have been discovered in many anaerobic eukaryotes bearing MROs including *Giardia* and the machinery required for their import into the matrix is variably conserved in these eukaryotes. Many components of this machinery are found in the genera *Encephalitozoon*, *Cryptosporidium*, *Trichomonas*, *Blastocystis* and in the anaerobic amoeba *Sawyeria marylandensis* [137, 163, 167, 182, 189]. In *Giardia*, no direct homologue or paralogue for components of the TIM23 complex has been detected. However, *Giardia* possesses homologs for the components of PAM complex such as mtHsp70, Mge1, Pam18, and Pam16 [136]. Recently, a Tim44 homologue has been identified in the *Giardia* genome [190]. Therefore the identification of homologues for components of the TIM23 complex in *Giardia* underlines the fact that the protein translocation into the mitosomal matrix occurs via conserved pathways similar to their eukaryotic counterparts.

# 4. Goals of the thesis

## 4.1 Investigating the role of Arf and ARF-like small GTPases during encystation in *Giardia lamblia*

*Giardia* relies on highly regulated secretion machinery in order to form the protective extra-cellular biopolymer (the cyst wall) essential for its transmission to a new host. *De novo* generated encystation specific vesicles (ESVs) are responsible for maturation, sorting and regulated secretion of cyst wall material (CWM). ESV genesis and maturation is dependent on small GTPases such as Sar1 and Arf1 [42]. The *G. lamblia* homologue of Arf1 (*Gl50803_7789*) was shown to be recruited to ESVs during the later stages of this differentiation process. Furthermore, over-expression of a non-functional Arf1 mutant protein led to a "naked cyst" phenotype, suggestive of a block in ESV maturation which would interfere with correct CWM secretion. These cysts lacked water resistance and thus were presumably non-infective [42].

Using homology-based *in silico* searches, we identified 5 additional Arf and ARF- like protein (Arl) homologues in the *Giardia* genome database. ORFs *Gl50803_ 13930* and *Gl50803_7562* are Arf family members, ORFs *Gl50803_4192*, *Gl50803_13523* and *Gl50803_13478* are Arl family members. Moreover, together with ORF *Gl*7789 which encodes for *Gl*Arf1, ORF *Gl*7562 is the only other giardial Arf homologue known to have a predicted N-myristoylation motif. This post-translational modification is a pre-requisite for membrane recruitment of Arf family proteins to target membranes.

Since *G. lamblia* is a highly reduced eukaryote, the space for redundancy in such a parsimonious system is quite narrow. Therefore we hypothesized that these additional Arf and Arl proteins are also involved in CWM deposition and that a loss of function for these proteins would inhibit cyst wall formation. To test this hypothesis, we begin by defining the additional *G. lamblia* Arf and Arl homologues their localization within the cell and possible role(s) in ESV maturation and functionality by expression of non-functional Arf and Arl mutants exerting dominant negative effects.

A detailed investigation of the function of additional Arf and Arl homologues is pivotal in understanding the exact role of these small GTPases in *Giardia* and would provide us with novel molecular targets to prevent encystation, thereby reducing infectivity and parasite spread.

## 4.2 Induction of apoptosis in *Giardia lamblia*

*Giardia* mitosomes, even though reduced are nevertheless essential and have conserved pathways for protein import [131]. In the course of an investigation of Tom/Tim-dependent protein import into giardial mitosomes we fortuitously uncovered a dramatic and rapid form of cell deterioration as a result of interference with mitosome protein import function upon treatment of trophozoites with Mitoblock (an experimental compound targeting the Tim import complex in mitochondria) (Hehl, unpublished data). Furthermore, recent reports suggest that mitosomes not only play a role in Fe-S protein maturation but might be also involved in a form of programmed cell death (PCD) [128].

Based on the following observations i.e., absence of a significant inflammatory response in the gut epithelium upon infection, the possible control of parasite population density in the intestine, and sensitivity of parasites to interference with mitosomal protein import functions, we hypothesized that mitosomes not only fulfill essential metabolic functions but also act as a highly sensitive central switch for monitoring cell health and for integrating possible cell death signals in a simple/primitive form of PCD. PCD as a strategy to avoid large scale necrosis and exposure of strong antigen to immune cells in the small intestine might be an explanation for the surprisingly mild inflammatory response recorded even during chronic infection.

Therefore, to test this hypothesis we aim to: 1) elicit cell death in culture and provide a catalog of quantifiable changes which accompany this event and 2) provide criteria to discriminate PCD-like phenomena and cell necrosis.

Characterization of PCD especially in basal protozoan parasite *Giardia* that does not possess a mitochondrion would hint towards the existence of an antique cell death pathway related to mitosomes and would shed light on the evolution of programmed cell death.

### 4.3 Optimization of a co-immunoprecipitation assay to identify organelle specific sub proteomes

Mitochondrion-related organelles in *Giardia* (mitosomes) contain no DNA, thus all remaining endosymbiont-derived genes are localized in the nuclear genome. Their products are translated on cytoplasmic ribosomes and subsequently imported into the organelle. However, due to massive albeit selective sequence divergence in *G. lamblia*, traditional strategies for identification of mitosome proteins based on homology-based *in silico* searches fall short. Until now only 20 mitosomal proteins have been identified including only one component of the conventional protein import machinery of the outer membrane (*Gl*Tom40), although there is unambiguous experimental evidence for the presence of pre-sequence dependent and independent protein import pathways in *Giardia* mitosomes [131].

Since *Giardia* mitosomes are positioned at the very extreme on the spectrum of reductive evolution we hypothesized that these minimized organelles harbor not more than 100-150 proteins functioning in the matrix or present at the membrane facilitating protein import, or establishing contact with the cellular compartments. To test our hypothesis we aim to generate a comprehensive list of mitosome proteins and to analyze the molecular basis for protein import. This would enable us to determine the functional range of these reduced organelles and possibly to expand on the mechanisms for their maintenance and distribution.

Specifically, we aim to 1) establish an organelle centered co-immunoprecipitation (co-IP) assay for efficient pull down of membrane and soluble complexes. 2) Perform a series of *ad hoc* co-IP assays with validated *Giardia* proteins to identify components of the import machinery and other non-conserved proteins which would enable us to create a *Gl*Tom40-centered interactome that expands inwards towards the matrix and outwards towards the cytosol.

A detailed proteome analysis of *Giardia* mitosomes is a must for careful speculation on the vast array of functions that can be assigned to these reduced organelles. Furthermore, comprehensive identification of mitosome proteins and characterization of protein import dynamics are a prerequisite for uncovering a postulated link with PCD and/or cell proliferation.

## 5. Bibliography


1. Adam, R.D., *Biology of Giardia lamblia*. Clinical microbiology reviews, 2001. **14**(3): p. 447-75.
2. Ankarklev, J., et al., *Behind the smile: cell biology and disease mechanisms of Giardia species*. Nat Rev Microbiol, 2010. **8**(6): p. 413-22.
3. Savioli, L., H. Smith, and A. Thompson, *Giardia and Cryptosporidium join the 'Neglected Diseases Initiative'*. Trends in parasitology, 2006. **22**(5): p. 203-8.
4. Fletcher, S.M., et al., *Enteric protozoa in the developed world: a public health perspective*. Clinical microbiology reviews, 2012. **25**(3): p. 420-49.
5. Huang, D.B. and A.C. White, *An updated review on Cryptosporidium and Giardia*. Gastroenterol Clin North Am, 2006. **35**(2): p. 291-314, viii.
6. Sullivan, P.B., et al., *Prevalence and treatment of giardiasis in chronic diarrhoea and malnutrition*. Arch Dis Child, 1991. **66**(3): p. 304-6.
7. Touz, M.C., *The Unique Endosomal/Lysosomal System of Giardia lamblia*. 2012.
8. Bernander, R., J.E. Palm, and S.G. Svard, *Genome ploidy in different stages of the Giardia lamblia life cycle*. Cellular microbiology, 2001. **3**(1): p. 55-62.
9. Keister, D.B., *Axenic culture of Giardia lamblia in TYI-S-33 medium supplemented with bile*. Transactions of the Royal Society of Tropical Medicine and Hygiene, 1983. **77**(4): p. 487-8.
10. Sogin, M.L., *Early evolution and the origin of eukaryotes*. Current opinion in genetics & development, 1991. **1**(4): p. 457-63.
11. Sogin, M.L. and J.D. Silberman, *Evolution of the protists and protistan parasites from the perspective of molecular systematics*. International journal for parasitology, 1998. **28**(1): p. 11-20.
12. Dacks, J.B., G. Walker, and M.C. Field, *Implications of the new eukaryotic systematics for parasitologists*. Parasitology international, 2008. **57**(2): p. 97-104.
13. Cavalier-Smith, T., *The simultaneous symbiotic origin of mitochondria, chloroplasts, and microbodies*. Ann N Y Acad Sci, 1987. **503**: p. 55-71.
14. van der Giezen, M., *Hydrogenosomes and mitosomes: conservation and evolution of functions*. J Eukaryot Microbiol, 2009. **56**(3): p. 221-31.
15. Adl, S.M., et al., *The revised classification of eukaryotes*. J Eukaryot Microbiol, 2012. **59**(5): p. 429-93.
16. Elmendorf, H.G., S.C. Dawson, and J.M. McCaffery, *The cytoskeleton of Giardia lamblia*. International journal for parasitology, 2003. **33**(1): p. 3-28.
17. Goldberg, A.V., et al., *Localization and functionality of microsporidian iron-sulphur cluster assembly proteins*. Nature, 2008. **452**(7187): p. 624-8.
18. Marti, M., et al., *The secretory apparatus of an ancient eukaryote: protein sorting to separate export pathways occurs before formation of transient Golgi-like compartments*. Mol Biol Cell, 2003. **14**(4): p. 1433-47.
19. Lujan, H.D., et al., *Developmental induction of Golgi structure and function in the primitive eukaryote Giardia lamblia*. J Biol Chem, 1995. **270**(9): p. 4612-8.
20. Soltys, B.J., M. Falah, and R.S. Gupta, *Identification of endoplasmic reticulum in the primitive eukaryote Giardia lamblia using cryoelectron microscopy and antibody to Bip*. J Cell Sci, 1996. **109 ( Pt 7)**: p. 1909-17.
21. Faso, C. and A.B. Hehl, *Membrane trafficking and organelle biogenesis in Giardia lamblia: use it or lose it*. International journal for parasitology, 2011. **41**(5): p. 471-80.
22. Knodler, L.A., et al., *Novel protein-disulfide isomerases from the early-diverging protist Giardia lamblia*. J Biol Chem, 1999. **274**(42): p. 29805-11.
23. McArthur, A.G., et al., *The evolutionary origins of eukaryotic protein disulfide isomerase domains: new evidence from the Amitochondriate protist Giardia lamblia*. Mol Biol Evol, 2001. **18**(8): p. 1455-63.
24. Feely, D.E. and J.K. Dyer, *Localization of acid phosphatase activity in Giardia lamblia and Giardia muris trophozoites*. J Protozool, 1987. **34**(1): p. 80-3.

25. Lanfredi-Rangel, A., et al., *The peripheral vesicles of trophozoites of the primitive protozoan Giardia lamblia may correspond to early and late endosomes and to lysosomes*. J Struct Biol, 1998. **123**(3): p. 225-35.
26. Morrison, H.G., et al., *Genomic minimalism in the early diverging intestinal parasite Giardia lamblia*. Science, 2007. **317**(5846): p. 1921-6.
27. Samuelson, J., et al., *The diversity of dolichol-linked precursors to Asn-linked glycans likely results from secondary loss of sets of glycosyltransferases*. Proc Natl Acad Sci U S A, 2005. **102**(5): p. 1548-53.
28. Robbins, P.W. and J. Samuelson, *Asparagine linked glycosylation in Giardia*. Glycobiology, 2005. **15**(6): p. 15G-16G.
29. Abodeely, M., et al., *A contiguous compartment functions as endoplasmic reticulum and endosome/lysosome in Giardia lamblia*. Eukaryot Cell, 2009. **8**(11): p. 1665-76.
30. Rivero, M.R., et al., *Adaptor protein 2 regulates receptor-mediated endocytosis and cyst formation in Giardia lamblia*. Biochem J, 2010. **428**(1): p. 33-45.
31. Touz, M.C., L. Kulakova, and T.E. Nash, *Adaptor protein complex 1 mediates the transport of lysosomal proteins from a Golgi-like organelle to peripheral vacuoles in the primitive eukaryote Giardia lamblia*. Mol Biol Cell, 2004. **15**(7): p. 3053-60.
32. Gaechter, V., et al., *The single dynamin family protein in the primitive protozoan Giardia lamblia is essential for stage conversion and endocytic transport*. Traffic, 2008. **9**(1): p. 57-71.
33. Reiner, D.S., M. McCaffery, and F.D. Gillin, *Sorting of cyst wall proteins to a regulated secretory pathway during differentiation of the primitive eukaryote, Giardia lamblia*. Eur J Cell Biol, 1990. **53**(1): p. 142-53.
34. Slavin, I., et al., *Dephosphorylation of cyst wall proteins by a secreted lysosomal acid phosphatase is essential for excystation of Giardia lamblia*. Mol Biochem Parasitol, 2002. **122**(1): p. 95-8.
35. Lujan, H.D., et al., *Identification of a novel Giardia lamblia cyst wall protein with leucine-rich repeats. Implications for secretory granule formation and protein assembly into the cyst wall*. J Biol Chem, 1995. **270**(49): p. 29307-13.
36. Mowatt, M.R., et al., *Developmentally regulated expression of a Giardia lamblia cyst wall protein gene*. Mol Microbiol, 1995. **15**(5): p. 955-63.
37. Sun, C.H., et al., *Mining the Giardia lamblia genome for new cyst wall proteins*. J Biol Chem, 2003. **278**(24): p. 21701-8.
38. Lauwaet, T., et al., *Encystation of Giardia lamblia: a model for other parasites*. Curr Opin Microbiol, 2007. **10**(6): p. 554-9.
39. Svard, S.G., P. Hagblom, and J.E. Palm, *Giardia lamblia -- a model organism for eukaryotic cell differentiation*. FEMS Microbiol Lett, 2003. **218**(1): p. 3-7.
40. Chatterjee, A., et al., *Giardia cyst wall protein 1 is a lectin that binds to curled fibrils of the GalNAc homopolymer*. PLoS Pathog, 2010. **6**(8): p. e1001059.
41. Faso, C., et al., *Export of cyst wall material and Golgi organelle neogenesis in Giardia lamblia depend on endoplasmic reticulum exit sites*. Cellular microbiology, 2013. **15**(4): p. 537-53.
42. Stefanic, S., et al., *Neogenesis and maturation of transient Golgi-like cisternae in a simple eukaryote*. J Cell Sci, 2009. **122**(Pt 16): p. 2846-56.
43. Konrad, C., C. Spycher, and A.B. Hehl, *Selective condensation drives partitioning and sequential secretion of cyst wall proteins in differentiating Giardia lamblia*. PLoS Pathog, 2010. **6**(4): p. e1000835.
44. Marti, M., et al., *An ancestral secretory apparatus in the protozoan parasite Giardia intestinalis*. J Biol Chem, 2003. **278**(27): p. 24837-48.
45. Losev, E., et al., *Golgi maturation visualized in living yeast*. Nature, 2006. **441**(7096): p. 1002-6.
46. Marti, M. and A.B. Hehl, *Encystation-specific vesicles in Giardia: a primordial Golgi or just another secretory compartment?* Trends in parasitology, 2003. **19**(10): p. 440-6.
47. Hehl, A.B. and M. Marti, *Secretory protein trafficking in Giardia intestinalis*. Mol Microbiol, 2004. **53**(1): p. 19-28.

48. Touz, M.C., et al., *Sorting of encystation-specific cysteine protease to lysosome-like peripheral vacuoles in Giardia lamblia requires a conserved tyrosine-based motif*. J Biol Chem, 2003. **278**(8): p. 6420-6.
49. Pimenta, P.F., P.P. da Silva, and T. Nash, *Variant surface antigens of Giardia lamblia are associated with the presence of a thick cell coat: thin section and label fracture immunocytochemistry survey*. Infect Immun, 1991. **59**(11): p. 3989-96.
50. Singer, S.M., et al., *Biological selection of variant-specific surface proteins in Giardia lamblia*. J Infect Dis, 2001. **183**(1): p. 119-24.
51. Nash, T.E., *Surface antigenic variation in Giardia lamblia*. Mol Microbiol, 2002. **45**(3): p. 585-90.
52. Aggarwal, A., J.W. Merritt, Jr., and T.E. Nash, *Cysteine-rich variant surface proteins of Giardia lamblia*. Mol Biochem Parasitol, 1989. **32**(1): p. 39-47.
53. Nash, T.E., *Antigenic variation in Giardia lamblia*. Exp Parasitol, 1989. **68**(2): p. 238-41.
54. Papanastasiou, P., et al., *The release of the variant surface protein of Giardia to its soluble isoform is mediated by the selective cleavage of the conserved carboxy-terminal domain*. Biochemistry, 1996. **35**(31): p. 10143-8.
55. Nash, T.E., et al., *Variant-specific surface protein switching in Giardia lamblia*. Infect Immun, 2001. **69**(3): p. 1922-3.
56. Mowatt, M.R., A. Aggarwal, and T.E. Nash, *Carboxy-terminal sequence conservation among variant-specific surface proteins of Giardia lamblia*. Mol Biochem Parasitol, 1991. **49**(2): p. 215-27.
57. Prucca, C.G., et al., *Antigenic variation in Giardia lamblia is regulated by RNA interference*. Nature, 2008. **456**(7223): p. 750-4.
58. Davids, B.J., et al., *A new family of giardial cysteine-rich non-VSP protein genes and a novel cyst protein*. PLoS One, 2006. **1**: p. e44.
59. Morf, L., et al., *The transcriptional response to encystation stimuli in Giardia lamblia is restricted to a small set of genes*. Eukaryot Cell, 2010. **9**(10): p. 1566-76.
60. Boucher, S.E. and F.D. Gillin, *Excystation of in vitro-derived Giardia lamblia cysts*. Infect Immun, 1990. **58**(11): p. 3516-22.
61. Murtagh, J.J., Jr., et al., *Guanine nucleotide-binding proteins in the intestinal parasite Giardia lamblia. Isolation of a gene encoding an approximately 20-kDa ADP-ribosylation factor*. J Biol Chem, 1992. **267**(14): p. 9654-62.
62. Lee, F.J., J. Moss, and M. Vaughan, *Human and Giardia ADP-ribosylation factors (ARFs) complement ARF function in Saccharomyces cerevisiae*. J Biol Chem, 1992. **267**(34): p. 24441-5.
63. Castillo-Romero, A., et al., *Rab11 and actin cytoskeleton participate in Giardia lamblia encystation, guiding the specific vesicles to the cyst wall*. PLoS Negl Trop Dis, 2010. **4**(6): p. e697.
64. Stefanic, S., et al., *Organelle proteomics reveals cargo maturation mechanisms associated with Golgi-like encystation vesicles in the early-diverged protozoan Giardia lamblia*. J Biol Chem, 2006. **281**(11): p. 7595-604.
65. McBride, H.M., M. Neuspiel, and S. Wasiak, *Mitochondria: more than just a powerhouse*. Current biology : CB, 2006. **16**(14): p. R551-60.
66. Newmeyer, D.D. and S. Ferguson-Miller, *Mitochondria: releasing power for life and unleashing the machineries of death*. Cell, 2003. **112**(4): p. 481-90.
67. Schatz, G., *The magic garden*. Annual review of biochemistry, 2007. **76**: p. 673-8.
68. Kroemer, G., et al., *The biochemistry of programmed cell death*. FASEB J, 1995. **9**(13): p. 1277-87.
69. Lill, R., et al., *The essential role of mitochondria in the biogenesis of cellular iron-sulfur proteins*. Biol Chem, 1999. **380**(10): p. 1157-66.
70. John, P. and F.R. Whatley, *Paracoccus denitrificans and the evolutionary origin of the mitochondrion*. Nature, 1975. **254**(5500): p. 495-8.
71. Andersson, S.G., et al., *On the origin of mitochondria: a genomics perspective*. Philos Trans R Soc Lond B Biol Sci, 2003. **358**(1429): p. 165-77; discussion 177-9.
72. Andersson, S.G. and C.G. Kurland, *Origins of mitochondria and hydrogenosomes*. Curr Opin Microbiol, 1999. **2**(5): p. 535-41.

73. Burger, G., M.W. Gray, and B.F. Lang, *Mitochondrial genomes: anything goes.* Trends Genet, 2003. **19**(12): p. 709-16.
74. Lang, B.F., M.W. Gray, and G. Burger, *Mitochondrial genome evolution and the origin of eukaryotes.* Annu Rev Genet, 1999. **33**: p. 351-97.
75. Gray, M.W., *The evolutionary origins of organelles.* Trends Genet, 1989. **5**(9): p. 294-9.
76. Gray, M.W., *Origin and evolution of mitochondrial DNA.* Annu Rev Cell Biol, 1989. **5**: p. 25-50.
77. Gray, M.W., et al., *On the evolutionary origin of the plant mitochondrion and its genome.* Proc Natl Acad Sci U S A, 1989. **86**(7): p. 2267-71.
78. Martin, W. and M. Muller, *The hydrogen hypothesis for the first eukaryote.* Nature, 1998. **392**(6671): p. 37-41.
79. Loytynoja, A. and M.C. Milinkovitch, *Molecular phylogenetic analyses of the mitochondrial ADP-ATP carriers: the Plantae/Fungi/Metazoa trichotomy revisited.* Proc Natl Acad Sci U S A, 2001. **98**(18): p. 10202-7.
80. LóPez-García, P., Moreira, D *The Syntrophy Hypothesis for the Origin of Eukaryotes.* 2002.
81. van der Giezen, M., *Endosymbiosis: past and present.* Heredity (Edinb), 2005. **95**(5): p. 335-6.
82. Gray, M.W., *Mitochondrial evolution.* Cold Spring Harb Perspect Biol, 2012. **4**(9): p. a011403.
83. Thrash, J.C., et al., *Phylogenomic evidence for a common ancestor of mitochondria and the SAR11 clade.* Sci Rep, 2011. **1**: p. 13.
84. van der Giezen, M. and J. Tovar, *Degenerate mitochondria.* EMBO Rep, 2005. **6**(6): p. 525-30.
85. van der Giezen, M., S. Cox, and J. Tovar, *The iron-sulfur cluster assembly genes iscS and iscU of Entamoeba histolytica were acquired by horizontal gene transfer.* BMC Evol Biol, 2004. **4**: p. 7.
86. Muller, M., et al., *Biochemistry and evolution of anaerobic energy metabolism in eukaryotes.* Microbiol Mol Biol Rev, 2012. **76**(2): p. 444-95.
87. van der Giezen, M., J. Tovar, and C.G. Clark, *Mitochondrion-derived organelles in protists and fungi.* Int Rev Cytol, 2005. **244**: p. 175-225.
88. Lindmark, D.G. and M. Muller, *Hydrogenosome, a cytoplasmic organelle of the anaerobic flagellate Tritrichomonas foetus, and its role in pyruvate metabolism.* J Biol Chem, 1973. **248**(22): p. 7724-8.
89. Mai, Z., et al., *Hsp60 is targeted to a cryptic mitochondrion-derived organelle ("crypton") in the microaerophilic protozoan parasite Entamoeba histolytica.* Mol Cell Biol, 1999. **19**(3): p. 2198-205.
90. Tovar, J., A. Fischer, and C.G. Clark, *The mitosome, a novel organelle related to mitochondria in the amitochondrial parasite Entamoeba histolytica.* Mol Microbiol, 1999. **32**(5): p. 1013-21.
91. Embley, T.M. and R.P. Hirt, *Early branching eukaryotes?* Current opinion in genetics & development, 1998. **8**(6): p. 624-9.
92. Embley, T.M., et al., *Hydrogenosomes, mitochondria and early eukaryotic evolution.* IUBMB Life, 2003. **55**(7): p. 387-95.
93. Embley, T.M., et al., *Mitochondria and hydrogenosomes are two forms of the same fundamental organelle.* Philos Trans R Soc Lond B Biol Sci, 2003. **358**(1429): p. 191-201; discussion 201-2.
94. Riordan, C.E., et al., *Cryptosporidium parvum Cpn60 targets a relict organelle.* Curr Genet, 2003. **44**(3): p. 138-47.
95. Cerkasovová A, et al., *Biochemical characterization of large granule fraction of Tritrichomonas foetus (strain KV1).* Journal of Protozoology, 1973. **20**(525).
96. Whatley, J.M., P. John, and F.R. Whatley, *From extracellular to intracellular: the establishment of mitochondria and chloroplasts.* Proc R Soc Lond B Biol Sci, 1979. **204**(1155): p. 165-87.
97. Boxma, B., et al., *An anaerobic mitochondrion that produces hydrogen.* Nature, 2005. **434**(7029): p. 74-9.

98. Shiflett, A.M. and P.J. Johnson, *Mitochondrion-related organelles in eukaryotic protists*. Annu Rev Microbiol, 2010. **64**: p. 409-29.
99. Williams, B.A., et al., *A mitochondrial remnant in the microsporidian Trachipleistophora hominis*. Nature, 2002. **418**(6900): p. 865-9.
100. Williams, B.A., et al., *Distinct localization patterns of two putative mitochondrial proteins in the microsporidian Encephalitozoon cuniculi*. J Eukaryot Microbiol, 2008. **55**(2): p. 131-3.
101. Tovar, J., et al., *Mitochondrial remnant organelles of Giardia function in iron-sulphur protein maturation*. Nature, 2003. **426**(6963): p. 172-6.
102. Brown, J.R. and W.F. Doolittle, *Root of the universal tree of life based on ancient aminoacyl-tRNA synthetase gene duplications*. Proc Natl Acad Sci U S A, 1995. **92**(7): p. 2441-5.
103. Hashimoto, T., et al., *Secondary absence of mitochondria in Giardia lamblia and Trichomonas vaginalis revealed by valyl-tRNA synthetase phylogeny*. Proc Natl Acad Sci U S A, 1998. **95**(12): p. 6860-5.
104. Soltys, B.J. and R.S. Gupta, *Presence and cellular distribution of a 60-kDa protein related to mitochondrial hsp60 in Giardia lamblia*. J Parasitol, 1994. **80**(4): p. 580-90.
105. Arisue, N., et al., *Mitochondrial-type hsp70 genes of the amitochondriate protists, Giardia intestinalis, Entamoeba histolytica and two microsporidians*. Parasitology international, 2002. **51**(1): p. 9-16.
106. Morrison, H.G., et al., *Giardia lamblia expresses a proteobacterial-like DnaK homolog*. Mol Biol Evol, 2001. **18**(4): p. 530-41.
107. Millet, C.O., et al., *Mitochondria-derived organelles in the diplomonad fish parasite Spironucleus vortens*. Exp Parasitol, 2013. **135**(2): p. 262-73.
108. Williams, C.F., et al., *Diversity in mitochondrion-derived organelles of the parasitic diplomonads Spironucleus and Giardia*. Trends in parasitology, 2013. **29**(7): p. 311-2.
109. Jerlstrom-Hultqvist, J., et al., *Hydrogenosomes in the diplomonad Spironucleus salmonicida*. Nat Commun, 2013. **4**: p. 2493.
110. Martin, W., *The missing link between hydrogenosomes and mitochondria*. Trends Microbiol, 2005. **13**(10): p. 457-9.
111. Jacobson, M.D., M. Weil, and M.C. Raff, *Programmed cell death in animal development*. Cell, 1997. **88**(3): p. 347-54.
112. Wyllie, A.H., J.F. Kerr, and A.R. Currie, *Cell death: the significance of apoptosis*. International review of cytology, 1980. **68**: p. 251-306.
113. Yuan, J. and H.R. Horvitz, *A first insight into the molecular mechanisms of apoptosis*. Cell, 2004. **116**(2 Suppl): p. S53-6, 1 p following S59.
114. Welburn, S.C., M.A. Barcinski, and G.T. Williams, *Programmed cell death in trypanosomatids*. Parasitology today, 1997. **13**(1): p. 22-6.
115. Fiers, W., et al., *More than one way to die: apoptosis, necrosis and reactive oxygen damage*. Oncogene, 1999. **18**(54): p. 7719-30.
116. Sperandio, S., I. de Belle, and D.E. Bredesen, *An alternative, nonapoptotic form of programmed cell death*. Proceedings of the National Academy of Sciences of the United States of America, 2000. **97**(26): p. 14376-81.
117. Elmore, S., *Apoptosis: a review of programmed cell death*. Toxicologic pathology, 2007. **35**(4): p. 495-516.
118. Bortner, C.D., N.B. Oldenburg, and J.A. Cidlowski, *The role of DNA fragmentation in apoptosis*. Trends in cell biology, 1995. **5**(1): p. 21-6.
119. Fadok, V.A. and P.M. Henson, *Apoptosis: getting rid of the bodies*. Current biology : CB, 1998. **8**(19): p. R693-5.
120. Bratton, D.L., et al., *Appearance of phosphatidylserine on apoptotic cells requires calcium-mediated nonspecific flip-flop and is enhanced by loss of the aminophospholipid translocase*. The Journal of biological chemistry, 1997. **272**(42): p. 26159-65.
121. Zamzami, N. and G. Kroemer, *The mitochondrion in apoptosis: how Pandora's box opens*. Nat Rev Mol Cell Biol, 2001. **2**(1): p. 67-71.

122. Brenner, C. and G. Kroemer, *Apoptosis. Mitochondria--the death signal integrators.* Science, 2000. **289**(5482): p. 1150-1.
123. van Loo, G., et al., *The role of mitochondrial factors in apoptosis: a Russian roulette with more than one bullet.* Cell death and differentiation, 2002. **9**(10): p. 1031-42.
124. Chose, O., et al., *A form of cell death with some features resembling apoptosis in the amitochondrial unicellular organism Trichomonas vaginalis.* Experimental cell research, 2002. **276**(1): p. 32-9.
125. Mariante, R.M., et al., *Hydrogen peroxide induces caspase activation and programmed cell death in the amitochondrial Tritrichomonas foetus.* Histochemistry and cell biology, 2003. **120**(2): p. 129-41.
126. Chose, O., et al., *Cell death in protists without mitochondria.* Annals of the New York Academy of Sciences, 2003. **1010**: p. 121-5.
127. Ghosh, E., et al., *Oxidative stress-induced cell cycle blockage and a protease-independent programmed cell death in microaerophilic Giardia lamblia.* Drug design, development and therapy, 2009. **3**: p. 103-10.
128. Correa, G., et al., *Cell death induction in Giardia lamblia: effect of beta-lapachone and starvation.* Parasitology international, 2009. **58**(4): p. 424-37.
129. Bagchi, S., et al., *Programmed cell death in Giardia.* Parasitology, 2012. **139**(7): p. 894-903.
130. Embley, T.M. and W. Martin, *Eukaryotic evolution, changes and challenges.* Nature, 2006. **440**(7084): p. 623-30.
131. Regoes, A., et al., *Protein import, replication, and inheritance of a vestigial mitochondrion.* J Biol Chem, 2005. **280**(34): p. 30557-63.
132. Dolezal, P., et al., *Giardia mitosomes and trichomonad hydrogenosomes share a common mode of protein targeting.* Proc Natl Acad Sci U S A, 2005. **102**(31): p. 10924-9.
133. Nasirudeen, A.M. and K.S. Tan, *Isolation and characterization of the mitochondrion-like organelle from Blastocystis hominis.* J Microbiol Methods, 2004. **58**(1): p. 101-9.
134. Hehl, A.B., et al., *Bax function in the absence of mitochondria in the primitive protozoan Giardia lamblia.* PLoS One, 2007. **2**(5): p. e488.
135. Lill, R. and G. Kispal, *Maturation of cellular Fe-S proteins: an essential function of mitochondria.* Trends Biochem Sci, 2000. **25**(8): p. 352-6.
136. Jedelsky, P.L., et al., *The minimal proteome in the reduced mitochondrion of the parasitic protist Giardia intestinalis.* PLoS One, 2011. **6**(2): p. e17285.
137. Abrahamsen, M.S., et al., *Complete genome sequence of the apicomplexan, Cryptosporidium parvum.* Science, 2004. **304**(5669): p. 441-5.
138. Franzen, O., et al., *Draft genome sequencing of giardia intestinalis assemblage B isolate GS: is human giardiasis caused by two different species?* PLoS Pathog, 2009. **5**(8): p. e1000560.
139. Chan, K.W., et al., *A novel ADP/ATP transporter in the mitosome of the microaerophilic human parasite Entamoeba histolytica.* Current biology : CB, 2005. **15**(8): p. 737-42.
140. Chacinska, A., et al., *Importing mitochondrial proteins: machineries and mechanisms.* Cell, 2009. **138**(4): p. 628-44.
141. Clements, A., et al., *The reducible complexity of a mitochondrial molecular machine.* Proc Natl Acad Sci U S A, 2009. **106**(37): p. 15791-5.
142. Neupert, W. and J.M. Herrmann, *Translocation of proteins into mitochondria.* Annual review of biochemistry, 2007. **76**: p. 723-49.
143. Schatz, G. and B. Dobberstein, *Common principles of protein translocation across membranes.* Science, 1996. **271**(5255): p. 1519-26.
144. Pfanner, N. and A. Geissler, *Versatility of the mitochondrial protein import machinery.* Nat Rev Mol Cell Biol, 2001. **2**(5): p. 339-49.
145. Brix, J., K. Dietmeier, and N. Pfanner, *Differential recognition of preproteins by the purified cytosolic domains of the mitochondrial import receptors Tom20, Tom22, and Tom70.* J Biol Chem, 1997. **272**(33): p. 20730-5.

146. Meisinger, C., et al., *Protein import channel of the outer mitochondrial membrane: a highly stable Tom40-Tom22 core structure differentially interacts with preproteins, small tom proteins, and import receptors*. Mol Cell Biol, 2001. **21**(7): p. 2337-48.
147. von Heijne, G., J. Steppuhn, and R.G. Herrmann, *Domain structure of mitochondrial and chloroplast targeting peptides*. Eur J Biochem, 1989. **180**(3): p. 535-45.
148. Gakh, O., P. Cavadini, and G. Isaya, *Mitochondrial processing peptidases*. Biochim Biophys Acta, 2002. **1592**(1): p. 63-77.
149. Smid, O., et al., *Reductive evolution of the mitochondrial processing peptidases of the unicellular parasites trichomonas vaginalis and giardia intestinalis*. PLoS Pathog, 2008. **4**(12): p. e1000243.
150. Dolezal, P., et al., *Evolution of the molecular machines for protein import into mitochondria*. Science, 2006. **313**(5785): p. 314-8.
151. Smutna, T., et al., *Flavodiiron protein from Trichomonas vaginalis hydrogenosomes: the terminal oxygen reductase*. Eukaryot Cell, 2009. **8**(1): p. 47-55.
152. Bradley, P.J., et al., *Targeting and translocation of proteins into the hydrogenosome of the protist Trichomonas: similarities with mitochondrial protein import*. EMBO J, 1997. **16**(12): p. 3484-93.
153. Gerber, J., et al., *The yeast scaffold proteins Isu1p and Isu2p are required inside mitochondria for maturation of cytosolic Fe/S proteins*. Mol Cell Biol, 2004. **24**(11): p. 4848-57.
154. Mukhopadhyay, A., et al., *Precursor protein is readily degraded in mitochondrial matrix space if the leader is not processed by mitochondrial processing peptidase*. J Biol Chem, 2007. **282**(51): p. 37266-75.
155. Saavedra-Alanis, V.M., et al., *Rat liver mitochondrial processing peptidase. Both alpha- and beta-subunits are required for activity*. J Biol Chem, 1994. **269**(12): p. 9284-8.
156. Kitada, S., et al., *A protein from a parasitic microorganism, Rickettsia prowazekii, can cleave the signal sequences of proteins targeting mitochondria*. J Bacteriol, 2007. **189**(3): p. 844-50.
157. Brown, M.T., et al., *A functionally divergent hydrogenosomal peptidase with protomitochondrial ancestry*. Mol Microbiol, 2007. **64**(5): p. 1154-63.
158. Westermann, B. and W. Neupert, *'Omics' of the mitochondrion*. Nat Biotechnol, 2003. **21**(3): p. 239-40.
159. Mokranjac, D. and W. Neupert, *Thirty years of protein translocation into mitochondria: unexpectedly complex and still puzzling*. Biochim Biophys Acta, 2009. **1793**(1): p. 33-41.
160. Chacinska, A., N. Pfanner, and C. Meisinger, *How mitochondria import hydrophilic and hydrophobic proteins*. Trends Cell Biol, 2002. **12**(7): p. 299-303.
161. Pfanner, N. and K.N. Truscott, *Powering mitochondrial protein import*. Nat Struct Biol, 2002. **9**(4): p. 234-6.
162. Pfanner, N. and N. Wiedemann, *Mitochondrial protein import: two membranes, three translocases*. Current opinion in cell biology, 2002. **14**(4): p. 400-11.
163. Katinka, M.D., et al., *Genome sequence and gene compaction of the eukaryote parasite Encephalitozoon cuniculi*. Nature, 2001. **414**(6862): p. 450-3.
164. Loftus, B., et al., *The genome of the protist parasite Entamoeba histolytica*. Nature, 2005. **433**(7028): p. 865-8.
165. Loftus, B.J. and N. Hall, *Entamoeba: still more to be learned from the genome*. Trends in parasitology, 2005. **21**(10): p. 453.
166. Makiuchi, T., et al., *Novel TPR-containing subunit of TOM complex functions as cytosolic receptor for Entamoeba mitosomal transport*. Sci Rep, 2013. **3**: p. 1129.
167. Carlton, J.M., et al., *Draft genome sequence of the sexually transmitted pathogen Trichomonas vaginalis*. Science, 2007. **315**(5809): p. 207-12.
168. Pusnik, M., et al., *An essential novel component of the noncanonical mitochondrial outer membrane protein import system of trypanosomatids*. Mol Biol Cell, 2012. **23**(17): p. 3420-8.

169. Dagley, M.J., et al., *The protein import channel in the outer mitosomal membrane of Giardia intestinalis*. Mol Biol Evol, 2009. **26**(9): p. 1941-7.
170. Dukanovic, J. and D. Rapaport, *Multiple pathways in the integration of proteins into the mitochondrial outer membrane*. Biochim Biophys Acta, 2011. **1808**(3): p. 971-80.
171. Lithgow, T. and A. Schneider, *Evolution of macromolecular import pathways in mitochondria, hydrogenosomes and mitosomes*. Philosophical Transactions of the Royal Society B-Biological Sciences, 2010. **365**(1541): p. 799-817.
172. Kutik, S., et al., *Dissecting membrane insertion of mitochondrial beta-barrel proteins*. Cell, 2008. **132**(6): p. 1011-24.
173. Habib, S.J., et al., *Assembly of the TOB complex of mitochondria*. J Biol Chem, 2005. **280**(8): p. 6434-40.
174. Becker, T., et al., *Biogenesis of the mitochondrial TOM complex: Mim1 promotes insertion and assembly of signal-anchored receptors*. J Biol Chem, 2008. **283**(1): p. 120-7.
175. Hell, K., *The Erv1-Mia40 disulfide relay system in the intermembrane space of mitochondria*. Biochim Biophys Acta, 2008. **1783**(4): p. 601-9.
176. Stojanovski, D., et al., *The MIA system for protein import into the mitochondrial intermembrane space*. Biochim Biophys Acta, 2008. **1783**(4): p. 610-7.
177. Mesecke, N., et al., *A disulfide relay system in the intermembrane space of mitochondria that mediates protein import*. Cell, 2005. **121**(7): p. 1059-69.
178. Grumbt, B., et al., *Functional characterization of Mia40p, the central component of the disulfide relay system of the mitochondrial intermembrane space*. J Biol Chem, 2007. **282**(52): p. 37461-70.
179. Milenkovic, D., et al., *Identification of the signal directing Tim9 and Tim10 into the intermembrane space of mitochondria*. Mol Biol Cell, 2009. **20**(10): p. 2530-9.
180. Hwang, D.K., et al., *Tim54p connects inner membrane assembly and proteolytic pathways in the mitochondrion*. J Cell Biol, 2007. **178**(7): p. 1161-75.
181. Gebert, N., et al., *Dual function of Sdh3 in the respiratory chain and TIM22 protein translocase of the mitochondrial inner membrane*. Mol Cell, 2011. **44**(5): p. 811-8.
182. Denoeud, F., et al., *Genome sequence of the stramenopile Blastocystis, a human anaerobic parasite*. Genome Biol, 2011. **12**(3): p. R29.
183. Makiuchi, T. and T. Nozaki, *Highly divergent mitochondrion-related organelles in anaerobic parasitic protozoa*. Biochimie, 2014. **100**: p. 3-17.
184. Chacinska, A., et al., *Mitochondrial presequence translocase: switching between TOM tethering and motor recruitment involves Tim21 and Tim17*. Cell, 2005. **120**(6): p. 817-29.
185. van der Laan, M., et al., *Pam17 is required for architecture and translocation activity of the mitochondrial protein import motor*. Mol Cell Biol, 2005. **25**(17): p. 7449-58.
186. Meier, S., W. Neupert, and J.M. Herrmann, *Conserved N-terminal negative charges in the Tim17 subunit of the TIM23 translocase play a critical role in the import of preproteins into mitochondria*. J Biol Chem, 2005. **280**(9): p. 7777-85.
187. Bauer, M.F., et al., *Role of Tim23 as voltage sensor and presequence receptor in protein import into mitochondria*. Cell, 1996. **87**(1): p. 33-41.
188. Dudek, J., P. Rehling, and M. van der Laan, *Mitochondrial protein import: common principles and physiological networks*. Biochim Biophys Acta, 2013. **1833**(2): p. 274-85.
189. Barbera, M.J., et al., *Sawyeria marylandensis (Heterolobosea) has a hydrogenosome with novel metabolic properties*. Eukaryot Cell, 2010. **9**(12): p. 1913-24.
190. Martincova, E., et al., *Probing the biology of Giardia intestinalis mitosomes using in vivo enzymatic tagging*. Mol Cell Biol, 2015.

# PART IV RESULTS

## Characterization of ARF and ARL homologs in *Giardia lamblia*

### 1. Introduction

*Giardia lamblia* is an excellent model organism to study relic organelles and/or minimized cellular mechanisms [1-3]. A case in point is the absence of a steady-state Golgi apparatus at the center of the constitutive and regulated protein secretion pathway [4]. However, in absence of a canonical Golgi, stage specifically regulated, *de novo* generated encystation specific vesicles (ESVs) function as Golgi analogs accumulating, maturing and depositing cyst wall material (CWM) on the plasma membrane to form the protective cyst wall. Despite the lack of essential components of the secretory pathway *Giardia* harbors a minimal set of conserved proteins and depends on small Ras-family GTPases such as Sar1, Rab1 and Arf1 for successful transmission suggesting that the basic principles of protein transport are conserved [4, 5]. For example, the *G. lamblia* homologue for Arf1 was recruited to ESVs during later stages of differentiation process and over-expression of a non-functional *Gl*Arf1 mutant protein led to a "naked cyst" phenotype which lacked infectivity. Homology based *in silico* searches identified 5 additional Arf and Arl homologues in *Giardia*, Fig. 1. We hypothesize that the additional Arf and Arl proteins are involved cyst wall deposition in *Giardia* and a loss of function would interfere with cyst wall formation. Immunofluorescence microscopy suggests that *Gl*Arf1 is the only member of the Arf family in *Giardia* involved in cyst maturation. The other homologues tested do not interfere with either ESV genesis or cyst formation.

```
GlARF1_7789       MGQGASKIFGKLFSKKEVRILMVGLDAAGKTTILYKLMLG-EVVTTVPTIGFNVETVE—
GlARF3_13930      MGIALGRLIQSLFGSRQARVVMVGLDAAGKTTILHQMAYG-MTVETIPTMGFTLQTVK—
GlARL1_13478      MGL-FDLIRRHRKGKKEIRVLILGLDNSGKTTILRKLCEE-DTSVIMPTQGFNAKTIK—
GlARL_13523       ----------------MARLIFIGLEATGKTAAFHNITGQRNYMTTRETVGINTSTFSVR
GlARF2_7562       ----MGAASSRPARHKTAKLLILGRQFSGKSTLINYLKTN-SFTVVNPTINFTAEKYN—
GlARL2_4192       MGF-LSVLRAIKASENEARVLVVGLDCSGKTTIVSSLLGK-PLTEIAPTLGFKISTWR--

GlARF1_7789        -----YKNINFTVWDVGGQDSIRPLWRHYYQNTDALIYVIDSADLEPKRIEDARNELHTL
GlARF3_13930       -----KGKLELDVWDIGGQSEFRNIWVHYYVDKHAAIFVVDAADHSKARMEEARTALEGV
GlARL1_13478       ----GPKGVSLNCWDVGGQKAIRTYWQNYYAGTTCLIWVVDAAD—VKRMDEVALEVSLA
GlARL_13523        GTGCRSQDISITLVDLGGSEKIRDLWSSQFFDTSGALYFI-------RDPDTLDLAVQLL
GlARF2_7562        ---------RYEVIDVGGSAEMMQLWSEHYSGTQTCLFVVDGT----SPLDQARDLIKD
GlARL2_4192        ---PQNTSMAVALWDVGGQQTIRTYWRNYFSSTDALIWVVDSTD--RRRMDTCRKALSEV
```

**Fig 1: Multiple alignment of the 6 Arf and Arl homologues in *Giardia*:** Conserved threonine at position 31 (for GDP release) and conserved glutamine at position 71 (for GTP hydrolysis) are highlighted.

# 2. Methods

## 2.1 Oligonucleotides used in this study are listed in the table below.

Table 1: Oligonucleotides used for amplification of full length Arf and Arl homologues.

| ORF number | Forward | Reverse |
|---|---|---|
| Gl50803_7789 (ARF1) | 5'gcatgcat atgggccaaggcgc | 5'gcttaattaa tta cgcgtagtctgggacatcgtatgggta tctcttcttccc |
| Gl50803_13930 (ARF3) | 5'gcatgcat atgggcatcgccct | 5'gcttaattaa tta cgcgtagtctgggacatcgtatgggta gctagtctccttccagcgccg |
| Gl50803_13478 (ARL1) | 5'gcatgcat atggggttatttga | 5'gcttaattaa cta cgcgtagtctgggacatcgtatgggta cttgtcagtcttactgaccat |
| Gl50803_13523 (ARL) | 5'gcatgcat atggcgcgtttaat | 5'gcttaattaa tta cgcgtagtctgggacatcgtatgggta cacagacgttgtaaacat |
| Gl50803_7562 (ARF2) | 5'gcatgcat atgggtgcagccagct | 5'gcttaattaa tca cgcgtagtctgggacatcgtatgggta aggctgctttggcacatcga |
| Gl50803_4192 (ARL2) | 5'gcatgcat atgggctttctct | 5'gcttaattaa tca cgcgtagtctgggacatcgtatgggta ccaaatagcagtctccaggtt |

Table 2: Oligonucleotides used for amplification of GTP/GDP locked mutants.

| ORF number | Q71L forward | Q71L reverse | T31N forward | T31N reverse |
|---|---|---|---|---|
| Gl50803_7789 (ARF1) | 5'gttggaggcct cgattcgatc | 5'gatcgaatcgaggcc tccaac | tgccgggaaaaataccat tcttt | aaagaatggtatttttt cccggca |
| Gl50803_13930 (ARF3) | 5'acatcggtggcc tttccgagttc | 5'gaactcggaa aggccaccgatgt | cgctgggaagaatacgat cctcc | ggaggatcgtattctt cccagcg |
| Gl50803_13478 (ARL1) | 5'atgtgggcgggc ttaaggcgatt | 5'aatcgcctta agcccgcccacat | ctctggcaagaataccat tttac | gtaaaatggtattctt gccagag |
| Gl50803_13523 (ARL) | Not done | Not done | cactgggaaaaatgctgc ttttc | gaaaagcagcattttt cccagtg |
| Gl50803_7562 (ARF2) | Not done | Not done | ttctctgggaaa aataatctgatcaattac | gtaattgatcag attatttttcccagag aa |
| Gl50803_4192 (ARL2) | 5'atgttggtggac ttcagaccatca | 5'tgatggtctgaagt ccaccaacat | 5'ctctggcaagaatact atcgtca | 5'tgacgatagtattc ttgccagac |

## 2.2 Immunofluorescence assay and image analysis

Preparation of chemically fixed cells for immunofluorescence and analysis of subcellular distribution of proteins by wide-field microscopy were done as described previously [6]. Nuclear labelling was performed with 4', 6-diamidino-2-phenylindole (DAPI).

# 3. Results

## 3.1 *Giardia* Arf1 is necessary for correct cyst wall formation.

Small GTPase Arf1 is responsible for generation of COP I and clathrin coated vesicles at the trans-Golgi network. Indeed it has been previously documented that β-COP is associated to early ESVs in *Giardia* [6]. Interesting *Gl*Arf1 also localizes to ESVs around 7-14 hours post induction of encystation (hpie). Furthermore, the effect of *Gl*Arf1 in correct cyst wall formation has been proven unequivocally [7]. Since small GTPases cycle between an active GTP-bound (membrane associated) and an inactive GDP-bound (cytosolic) form, we wanted to investigate if the GDP-locked *Gl*Arf1 mutant would also elicit an effect as documented for its GTP-locked counterpart [7]. In order to test this we used a functional knockdown approach by conditional over-expression of a dominant negative (GDP-locked) Arf1 mutant in encysting trophozoites. As shown in Fig. 1, the giardial homologues for Arf and Arls harbor a conserved threonine at position 31. Using overlap PCR reaction we generated a cyst wall protein promoter driven T31N GDP-locked Arf1 mutant (*Gl*Arf1T31N-HA). Un-transfected and transgenic parasites expressing a GTP-locked Arf1 variant were included in the analysis as a control for encystation and a reference for the "naked cyst" phenotype respectively. As shown in Fig. 2, wild-type un-transfected parasites encysted properly with complete secretion of CWM on the cell periphery after 24 hpie (top panel).

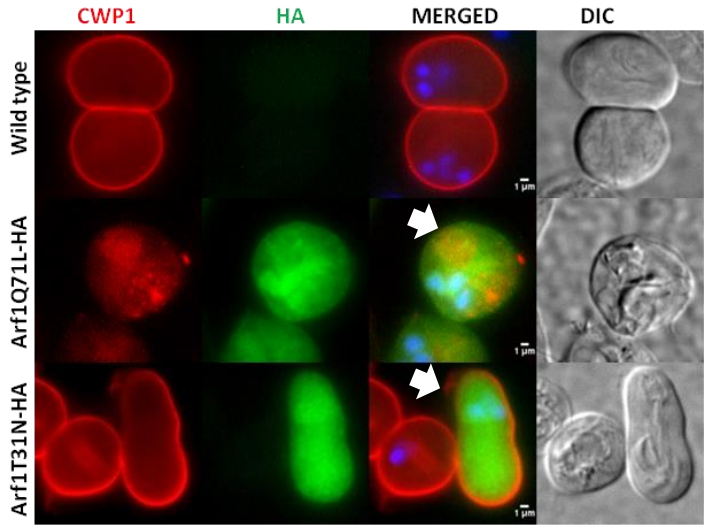


**Figure 2: *Giardia* Arf1 is essential for correct cyst formation.** Wild type, *Gl*Arf1Q71L and *Gl*Arf1T31N expressing parasites were encysted for 24hours and the effect of the transgene on correct cyst formation was determined by IFA. Non-transgenic parasites (wild-type) form perfect cysts with a prominent cyst wall (top panel). *Gl*Arf1Q71L expressing parasites display "naked cyst" phenotype (middle panel). Interestingly *Gl*Arf1T31N expression doesn't affect cyst formation (bottom panel). Nuclear DNA is stained with DAPI (blue). Scale bar 1μM.

Consistent with the previous publication, transgenic parasites expressing the GTP-locked Arf1 mutant displayed the "naked cyst phenotype" characterized by the distribution of CWM in the cytosol and an absence of a prominent cyst wall after 24 hpie (middle panel, white arrow). Interestingly, parasites expressing the GDP-locked Arf1 mutant formed proper cyst wall (bottom panel, white arrow) and did not recapitulate the GTP-locked *Gl*Arf1 phenotype.

### 3.2 *Giardia* Arl1Q71L localizes to peri-nuclear ER during early stages of encystation.

The localization of *Gl*Arf1 to ESVs has been previously documented [7]. We synthesized constructs for inducible expression of 3 additional *Giardia* Arf and Arl homologues (*Gl*13930, *Gl*13478, *Gl*4192) during encystation in order to localize their epitope-tagged products and to understand if and when they are recruited to ESVs. Localization in almost all cases was exclusively cytosolic throughout encystation. However, we detected a unique localization for the dominant-negative (GTP-locked) *Gl*Arl1 homologue (*Gl*13478Q71L). During early stages of encystation process (4-5 hpie), *Gl*13478-HA was mostly cytosolic, Fig. 3a (top panel) and ESVs morphology appeared to be normal. In contrast, the GTP-locked *Gl*13478Q71L-HA protein had a distinct peri-nuclear localization, Fig. 3a (bottom panel, white arrow). The significance of this unusual localization is unknown, however ESV genesis and morphology seems unhindered albeit this peculiar localization of the dominant negative GTPase. Furthermore, in order to confirm the peri-nuclear localization of *Gl*13478Q71L, we performed co-localization experiments using an ER marker (PDI 1). As shown in Fig. 3b (top and middle panel), at early stages of encystation we detected significant co-localization of *Gl*13478Q71L-HA with the *Giardia* PDI 1 antibody. However during later stages of encystation the peri-nuclear localization is lost and the protein is mainly cytosolic.

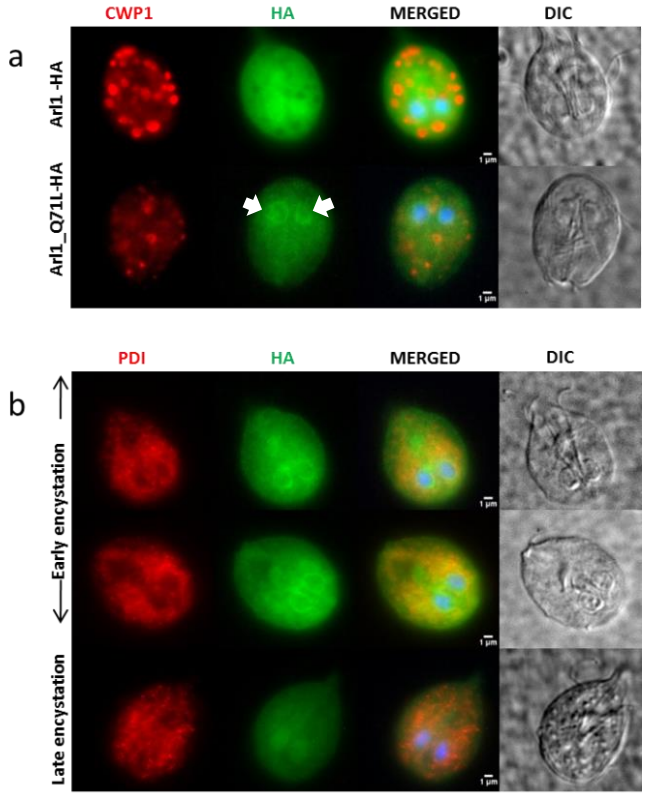


**Figure 3: Unique peri-nuclear localization for *Gl*Arl1Q71L:** Transgenic parasites expressing HA tagged *Gl*Arl1 and *Gl*Arl1Q71L were analyzed by IFA for their sub-cellular localization in encysting trophozoites. **(a)** IFA analysis demonstrates how the sub-cellular localization (green) changes from cytoplasmic for *Gl*Arl1-HA (top panel) to peri-nuclear for *Gl*Arl1Q71L-HA (bottom panel). However, ESVs (red) appear to be normal in both *Gl*Arl1-HA and *Gl*Arl1Q71L-HA expressing parasite. **(b)** Significant co-localization is observed between *Gl*Arl1Q71L-HA (green) and *Gl*PDI 1 (red) confirming the peri-nuclear localization of the GTP locked *Gl*Arl3. Nuclear DNA is stained with DAPI. Scale bar: 1 µM.

### 3.3 Conditional over-expression of *Gl*13939Q71L, *Gl*13478Q71L and *Gl*4192Q71L does not affect cyst wall formation and encystation efficiency in *Giardia lamblia.*

Since over-expression of GTP-locked Arf1 generated the naked cyst phenotype, we wanted to characterize 3 additional Arf and Arl homologues for their effect on correct cyst wall formation. For this purpose, we first generated C-terminally HA tagged GTP-locked (Q71L) variants of *Gl*13939 (*Gl*Arf3), *Gl*13478 (*Gl*Arl1) and *Gl*4192 (*Gl*Arl2) under an inducible CWP1 promoter. Transgenic trophozoites expressing the wild type protein and the GTP-locked variant protein were encysted for 24 hours and the effect of over-expression of the mutant protein on correct cyst wall formation was determined by IFA. Un-transfected trophozoites were also included in the IFA and served as positive control for correct cyst formation. Un-transfected trophozoites encysted properly displaying normal cyst morphology after 24 hpie, Fig 4a. Furthermore, no significant differences in cyst wall formation were observed in transgenic parasites expressing either the wild type GTPases or the dominant negative mutant version of the GTPases. Representative images for *Gl*13939, *Gl*13939Q71L are shown in Fig. 4- b, c; for *Gl*13478, *Gl*13478Q71L are shown in Fig. 4- d, e and for *Gl*4192, *Gl*4192Q71L are shown in Fig. 4- f, g.

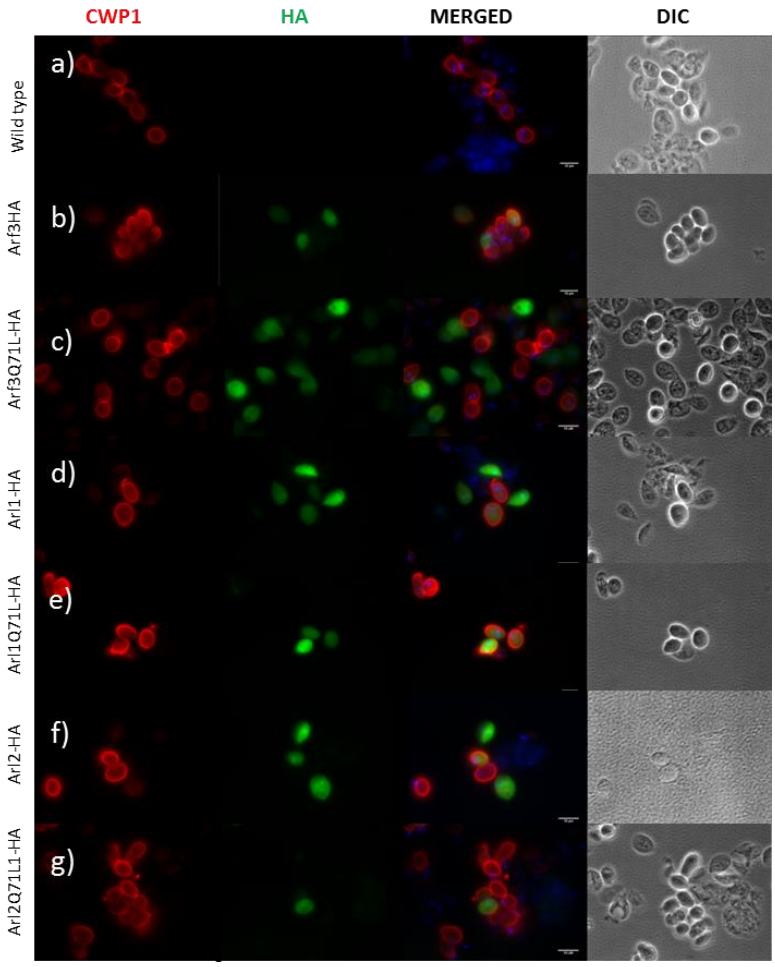


**Figure 4: Over-expression of *Gl*13939Q71L, *Gl*13478Q71L and *Gl*4192Q71L has no effect on cyst wall formation.** Representative IFA images showing the effect of conditional over-expression of *Gl*13939-HA, *Gl*13478-HA and *Gl*4192-HA and their corresponding GTP-locked versions (green) on cyst wall formation (red). Nuclear DNA is stained is stained with DAPI (blue). Scale bar 10 µM. **(a)** Wild type cells show correct cyst wall formation. **(b-c)** parasites expressing *Gl*13939 or *Gl*13939Q71L. **(d-e)** parasites expressing *Gl*13478 or *Gl*13478Q71L and **(f-g)** parasites expressing *Gl*4192 or *Gl*4192Q71L.

Furthermore, we tested the effect of the *Gl*Arf1Q71L, *Gl*Arf1T31N, *Gl*Arl1Q71L, *Gl*Arl2 and *Gl*Arl2Q71L on encystation efficiency. Wild-type un-transfected trophozoites along with transgenic parasites expressing the GTP-locked or GDP-locked version of selected GTPases were encysted for 24 hours prior to IFA. 30 whole frame differential interface contrast images were randomly acquired and cysts were counted. Encystation efficiency of the un-transfected control parasites was normalized to 100% and the encystation of transgenic parasites were compared against it. Significant reduction in encystation was observed only for *Gl*Arf1Q71L. However, none of the other GTPase variants tested had an effect on encystation efficiency, Fig. 5.

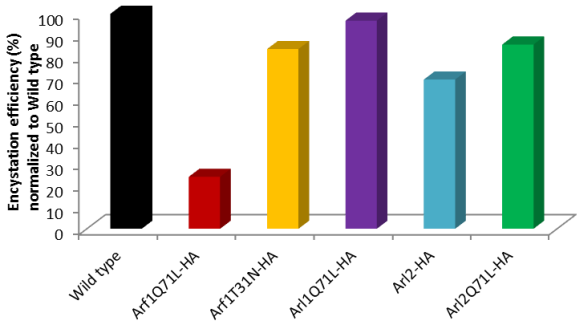


**Figure 5: Dominant negative Arf1 (*Gl*Arf1Q71L) affects encystation efficiency.** Significant reduction in encystation is seen in parasites expressing GTP-locked Arf1 (2nd column).

### 3.4 *Gl*4192 does not affect cytokinesis in *G. lamblia*.

Price *et. al* had demonstrated the role of the small GTPase Arl2 during cytokinesis in *Trypanosoma bricei* [8]. In short, knockdown by RNA interference of *Tb*Arl2 caused severe defect in cytokinesis by inhibiting the formation and ingression of cleavage furrows. Since *Giardia* possesses a homologue for Arl2 (*Gl*4192), we reasoned that *Gl*4192 might also play a role in giardial cell division. Short-lived excyzoites (quadri-nucleate tetraploid cells resulting from excysting cysts) undergo 2 rapid rounds of cell division to produce 4 binucleate diploid trophozoites. Therefore we decided to implement cell division in the eczyzoite following excystation as a read-out for the effects of *Gl*4192 overexpression. To do this we encysted strains expressing *Gl*4192 and the corresponding GTP-locked mutant version *Gl*4192Q71L and then excysted the resulting cysts produced during this period. As a control for encystation and excystation, we included a wild-type un-transfected strain. We could not detect any substantial differences in either excystation efficiency (Fig. 6) or growth dynamics in the transgenic strains compared to the wild-type strain, although the transgenic strains were capable of construct expression to the same degree as pre-excysted cells.

| Strain | Cells/ml |
|---|---|
| WB | 700.000 |
| *Gl*4192 | 687.500 |
| *Gl*4192Q71L | 635.000 |

**Figure 6: Over-expression of GTP-locked Arl2 (*Gl*4192Q71L) does not affect cytokinesis in *Giardia*.** Wild-type un-transfected and transgenic parasites expressing *Gl*4192 and *Gl*4192Q71L were encysted followed by excystation and growth in normal culture medium for 14 hours. Subsequently parasites were counted with a Neubauer counting chamber. No significant decrease in number of cells was observed upon over expression of *Gl*Arl2Q71L.

# 4 Conclusion

In summary, we have attempted to assign a role to the additional Arf and Arl homologues in *Giardia* during encystation. So far, we conclude that Arf1 is possibly the only Arf family member involved in encystation. The other homologues may either be redundant in relation to *Gl*Arf1 or be involved in other as-yet unidentified cellular processes. New insights and/or novel tools are required to obtain a more comprehensive view of Arf and Arl functions in *G. lamblia*.

# 5 Bibliography


1. Morrison, H.G., et al., *Genomic minimalism in the early diverging intestinal parasite Giardia lamblia*. Science, 2007. **317**(5846): p. 1921-6.
2. Tovar, J., et al., *Mitochondrial remnant organelles of Giardia function in iron-sulphur protein maturation*. Nature, 2003. **426**(6963): p. 172-6.
3. Lloyd, D. and J.C. Harris, *Giardia: highly evolved parasite or early branching eukaryote?* Trends in microbiology, 2002. **10**(3): p. 122-7.
4. Marti, M., et al., *An ancestral secretory apparatus in the protozoan parasite Giardia intestinalis*. J Biol Chem, 2003. **278**(27): p. 24837-48.
5. Lee, F.J., J. Moss, and M. Vaughan, *Human and Giardia ADP-ribosylation factors (ARFs) complement ARF function in Saccharomyces cerevisiae*. J Biol Chem, 1992. **267**(34): p. 24441-5.
6. Marti, M., et al., *The secretory apparatus of an ancient eukaryote: protein sorting to separate export pathways occurs before formation of transient Golgi-like compartments*. Mol Biol Cell, 2003. **14**(4): p. 1433-47.
7. Stefanic, S., et al., *Neogenesis and maturation of transient Golgi-like cisternae in a simple eukaryote*. J Cell Sci, 2009. **122**(Pt 16): p. 2846-56.
8. Price, H.P., et al., *The small GTPase ARL2 is required for cytokinesis in Trypanosoma brucei*. Molecular and biochemical parasitology, 2010. **173**(2): p. 123-31.

# PART V RESULTS

## Induction of apoptosis-like cell death in *Giardia lamblia*

### 1. Introduction

Programmed cell death (PCD) is a highly regulated cellular process that has been extensively characterized in metazoans. PCD can be triggered by external and internal factors involving several effectors and regulators [1]. Two major classes of PCD have been described; 1) Apoptosis (type I PCD) is accompanied by specific morphological and biochemical changes leading to the demise of the cell [2] and 2) Autophagy (type II PCD) which involves the autophagosomal–lysosomal system and is responsible for engulfment of vesicles during turnover of organelles [3]. PCD has also been documented in several unicellular eukaryotes namely *T. vaginalis, E. histolytica, Dictystelium, Blastocystis, Trypanosoma* and *Giardia lamblia* [4-7]. Most if not all of the above mentioned organisms do not possess canonical mitochondria but instead harbor mitochondrion-related organelles (mitosomes and hydrogenosomes). Therefore it is indeed intriguing to investigate the processes and factors involved in apoptosis in MRO harboring organisms.

*Giardia lamblia* parasites reside in millions in the gut epithelium during an acute infection but, in most cases of giardial infection, the parasites are eventually cleared by the host. However, despite being present at high concentrations, they do not elicit any significant host inflammatory response [8, 9]. We hypothesized that *Giardia* trophozoites undergo an organized form of cell death; likely apoptosis-related, to avoid excessive exposure of antigenic molecules to the host's immune system and hence proliferate incognito in the host's small intestine. Interestingly, PCD in *Giardia* has been demonstrated previously using drugs like beta-lapachone, $H_2O_2$ [10, 11]. However, since these drugs are not present under physiological conditions we wanted to use: 1) nutrient starvation by growth in EBSS medium (lacking L-cysteine and ascorbic) and 2) heat shock, as physiological insults to elicit apoptosis in *Giardia*. Using annexin-FITC apoptosis assay and immunofluorescence microscopy we could demonstrate an apoptosis-like cell death exhibiting many if not all characteristics of apoptosis upon altercation of physiological conditions.

# 2. Methods

## 2.1 Induction of PCD

PCD was induced mainly by interfering with two physiological conditions; 1) Glucose starvation and 2) heat shock.

1) For induction of PCD via glucose starvation, parasites were grown up to 75% confluency in TYI-S-33 medium. Subsequently the medium was removed eliminating non-adherent cells (dead/damaged cells) and was replaced by Earle's balanced salts solution (EBSS) medium and incubated for 12-36 hours prior to harvesting for annexin binding assay or flow cytometry analysis.

2) Heat treatment was another criterion used to elicit cell death in *Giardia*. Parasites were grown up to 75% confluency in TYI-S-33 medium followed by incubation at varying temperatures (39-42°C) in a water bath. Control parasites were incubated at 37°C and served as negative control. Parasites were then harvested and processed accordingly for annexin binding assay or flow cytometry analysis

## 2.2 Annexin- binding assay and microscopy analysis

Giardial trophozoites were induced for PCD as outlined above. Un-treated parasites were also included as negative controls. The parasites were harvested and washed once by centrifugation (900 x *g* for 10 mins and 4°C) with cold PBS. The parasites were processed as described in FITC Annexin V/Dead Cell Apoptosis Kit with FITC annexin V and PI, for Flow Cytometry, Cat no. V13242, Invitrogen. The pellet was re-suspended in 100 µl of cold 1X binding buffer to which 5 µl of annexin V-FITC (Invitrogen, UK) and 2 µl of propidium iodide (PI) (1mg/ml) was added, followed by incubation in the dark at room temperature for 15 minutes. Subsequently the cells were washed with 1X annexin binding buffer and finally analyzed either by flow cytometry (Beckman Coulter and Kaluza software) or by epifluorescence microscopy. Microscopy analysis was performed on the standard fluorescence microscopes Leica DM IRBE with MetaVue software version 5.0r1, or Nikon Eclipse 80i with Openlab Improvision software 5.5.2 for data collection. WCIF ImageJ was used for image processing.

## 2.3 DNA laddering (fragmentation)

Glucose starved and mock treated parasites were harvested followed by genomic DNA isolation to detect DNA fragmentation. Samples were then run on a 1% agarose gel stained with ethidium bromide to visualize DNA shearing and fragmentation.

## 2.4 Immunofluorescence Assay (IFA)

IFA was performed according to standard protocols [12].

# 3. Results

## 3.1 Glucose starvation leads to apoptosis-like cell death in *Giardia lamblia*

Different protocols and inhibitors such as beta-lapachone and compounds generating reactive oxygen and nitrogen species were used to elicit apoptosis-related cell death in *G. lamblia* in vitro [10, 11]. However, we decided to test our central hypothesis using parameters that could mimic stress encountered under physiological conditions such as glucose starvation and heat shock. We achieved IC 50 cell death after 36 hours of glucose starvation. In addition, we were able to demonstrate a known phenotype of apoptosis-related cell death which has been described in many cell types such as extracellular membrane exposure of phosphatidylserine (PS). In order to visualize parasites actively dying by apoptosis we starved cells for 12 hours prior to harvesting. Un-starved parasites were used as control. As depicted in Fig. 1a, majority of cells were apoptotic (green) after 12 hours of glucose starvation. Apoptotic cells (green) are labelled with FITC-conjugated annexin which binds to phosphatidylserine exposed on the outer leaflet of apoptotic cells and dead cells (red) are labelled with PI. Living cells show low levels of annexin staining. In order to quantify apoptotic cells we performed fluorescence activated cell sorting (FACS) experiments and we observed a significant increase in annexin-V positive cells in glucose-starved parasites (Fig. 1 c) as compared to non-starved control samples (Fig. 1 b) after 12 hours of starvation. Our data suggests that trophozoites indeed undergo cell death by apoptosis upon nutrient starvation.

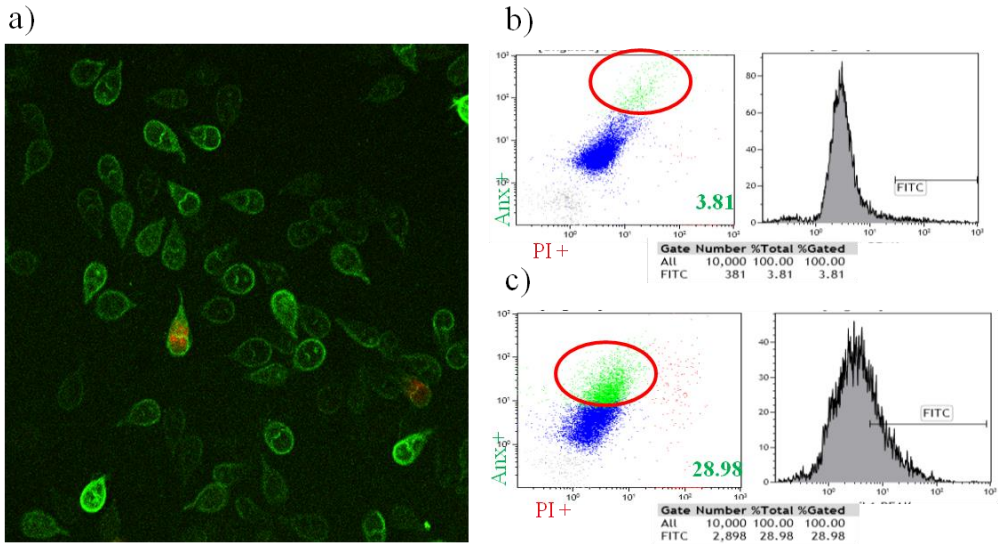


**Figure 1 Glucose starvation results in *Giardia lamblia* cell death by apoptosis (a)** IFA of glucose-starved cells labeled with annexin V-FITC (green) and PI (red). Apoptotic cells are characterized by a strong annexin V-FITC dependent green signal. Terminally dead cells are dual labeled. **(b-c)** Flow cytometry analysis of non-starved trophozoites **(b)** and glucose starved trophozoites **(c)**. A seven-fold increase in apoptotic cells in observed in the glucose starved trophozoites.

### 3.2. Apoptosis in *Giardia* is accompanied by visible morphological changes such as ER disintegration and nuclear condensation.

Apoptosis is accompanied by various physiological and morphological changes such as cell shrinkage (reduced size, condensed cytoplasm and tightly packed organelles), pyknosis (condensed chromatin) and fragmentation of genomic material into oligonucleosomal fragments of 200kb leading to a characteristic DNA laddering pattern [13]. In order to provide a catalogue of distinct sub-cellular changes accompanying apoptosis in *Giardia*, we investigated the morphology of ER and nuclei in glucose starved parasites. Untreated parasites were also included in the analysis and served as positive controls. Antibodies against resident ER protein (protein disulphide isomerase 2) and DAPI were used to detect changes in ER and nuclei respectively. As expected, ER and nuclei morphology appear to be normal in the wild-type un-transfected parasites (Fig 2, top panel). Peri-nuclear ER is visible and the ER spreads across the whole length of the parasite. However, in glucose starved parasites the peripheral ER appears to be massively disintegrated accompanied with visible signs of nuclear shrinkage (Fig 2, bottom panel) suggesting that the nuclear material might be highly condensed.

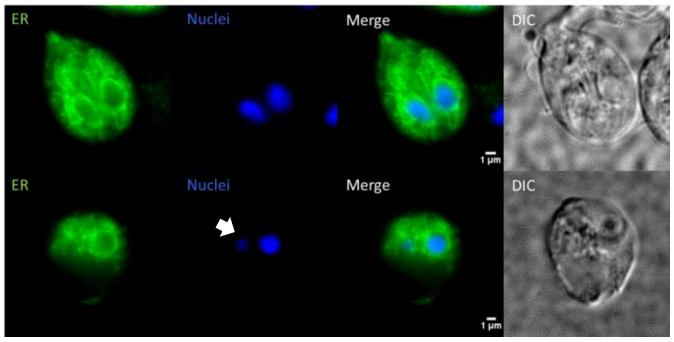


**Figure 2: ER disintegration and nuclei condensation are morphological changes in apoptotic *Giardia* parasites.** Un-starved and glucose starved parasites were harvested and processed for IFA analysis to check for organellar integrity. ER and nuclear morphology appears to be normal in un-starved parasites (top panel) than in glucose starved parasites (bottom panel).

### 3.3. Glucose starvation leads to DNA degradation in *Giardia lamblia*

DNA degradation is a hallmark characteristic of apoptosis-like cell death. After the onset of apoptosis the genetic material gets dispersed in the cell which can be labelled with PI. Fig. 3 depicts the various stages of cells undergoing apoptosis along with the nuclear material degradation. PS is generally located in the inner leaflet of the plasma membrane (PM), therefore the living cells display a faint annexin staining and no PI staining (PI is cell impermeable) Fig. 3a, as compared to apoptotic cells which exhibit a stronger annexin staining due to the flipping of PS to the outer leaflet of the PM, Fig. 3b. However because the cell membrane is still intact in these cells the nuclei are not stained with PI. On the other hand, dying cells exhibit a faint annexin signal and a bright PI signal, Fig. 3c. PI is a DNA intercalating agent and the two nuclei of *Giardia* can be easily identified after PI staining.

Terminally dead cells with completely degraded nuclear material (bold arrows) are shown in Fig. 3d. Punctate PI staining is observed and in some cases the entire cytoplasm is stained with PI since the nuclear material is completely degraded and dispersed throughout the cell. Extensive DNA degradation (cytoplasmic PI staining) marks the "point of no return" and the cells are destined to die silently.

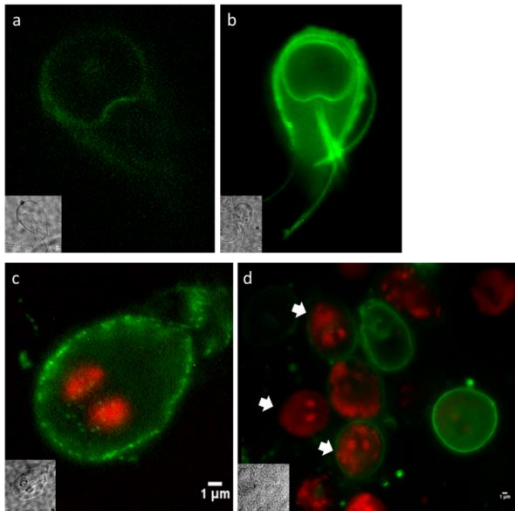


**Figure 3: Apoptosis results in nuclear material degradation.** Representative images showing varying degrees of nuclear material degradation during apoptosis **(a)** Living, **(b)** Apoptotic, **(c)** Dying and **(d)** Terminally dead.

### 3.4 DNA laddering and fragmentation

Genomic DNA fragmentation is a biochemical hallmark in apoptotic cells and is an irreversible event in PCD. This step occurs before changes in plasma membrane permeability. Glucose starved and un-starved parasites were subjected to genomic DNA analysis and were analyzed on a 1% agarose gel. The typical recursive electrophoretic laddering pattern was not seen in glucose starved parasites (Fig. 4b) as compared to unstarved parasites (Fig. 4a). However, distinct DNA band (fragmented/sheared DNA) mainly in lower molecular weight region was observed in the glucose starved parasites.

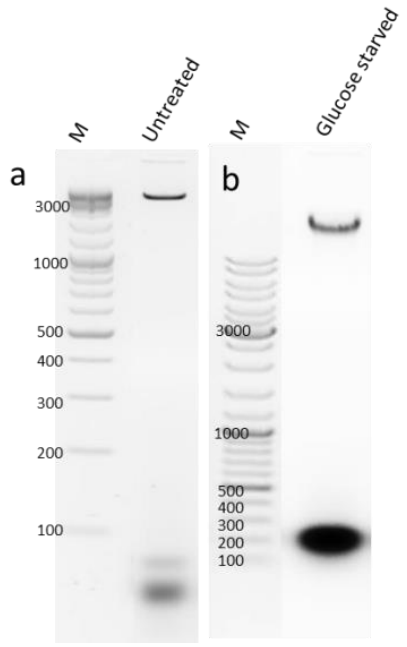


**Figure 4: Apoptotic cells display an unusual DNA banding pattern at low molecular size range.**

Electrophoretic analysis of DNA degradation shows an accumulation of fragmented DNA at 200 bps in glucose starved parasites **(b)**, whereas the un-starved have a single band for intact genomic DNA **(a)**.

### 3.5 Heat treatment can induce apoptosis in *Giardia lamblia*.

In addition to glucose starvation, heat stress was used as another physiological insult to induce apoptosis in *Giardia*. We did not see an increase in PS positive cells after treating trophozoites for 12 hours with a varying range of temperatures, starting from 39 - 41.5 °C. However, at 41.5 °C, 56% of the trophozoites were PI positive, suggesting that they were terminally dead. In order to find out whether this population of dead cells had undergone apoptosis at an early time point during our heat stress treatment, we performed a time course experiment at 42 °C and harvested trophozoites after 1 hr, 2 hrs and 3 hrs (Fig. 5 a-c). After 3 hours at 42 °C we found an inverse correlation between apoptotic cells and dead cells which was marked by a decreasing population of PS positive cells (apoptotic) and an increasing population of PI-positive cells (terminally dead), suggesting that the strong increase in PI-positive cells after 12 hours at 42 °C was the result of cell death by apoptosis (Fig. 5d).

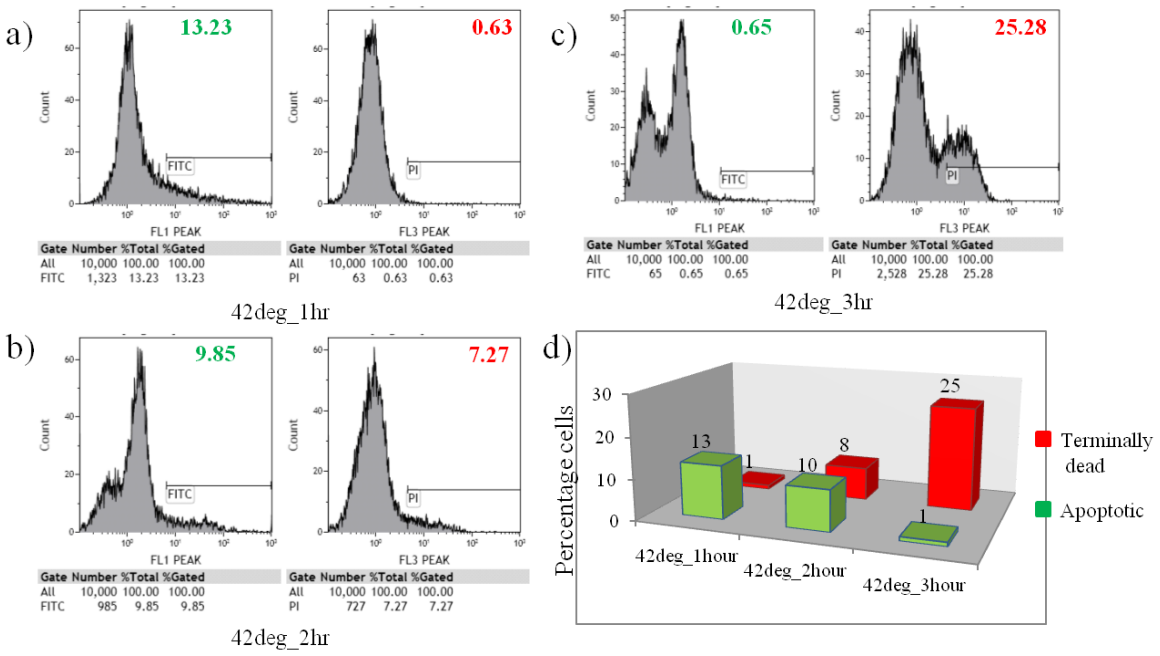


**Figure 5: Heat induces cell death by apoptosis in *Giardia*. (a)**. Flow cytometry analysis of heat stressed parasites (42 °C) harvested after 1, 2 and 3 hours **(a**, **b** and **c)**. **(d)**. A bar graph showing the inverse correlation between apoptotic cells and dead cells for the 3 time points tested at 42°C.

## 4. Discussion

We had tested several protocols to induce apoptosis in *Giardia* described in the literature (e.g. starvation conditions, exposure to chemicals and inhibitors) and found significant discrepancies. For example β-lapachone only induced cytokinesis defects but did not kill trophozoites. Therefore, we focused on conditions which might reflect those occurring in nature, e.g. starvation conditions as well as heat shock to induce apoptosis in *Giardia*. Our data confirms that alterations in physiological conditions such as glucose starvation and

incubation temperature can induce apoptosis in *Giardia lamblia* with many if not all characteristics of canonical apoptosis suggesting that programmed cell death pathway involved in *Giardia* could be parasite-specific occurring within an infected host.

## 5. Bibliography


1. Brenner, C. and G. Kroemer, *Apoptosis. Mitochondria--the death signal integrators.* Science, 2000. **289**(5482): p. 1150-1.
2. Elmore, S., *Apoptosis: a review of programmed cell death.* Toxicologic pathology, 2007. **35**(4): p. 495-516.
3. Fiers, W., et al., *More than one way to die: apoptosis, necrosis and reactive oxygen damage.* Oncogene, 1999. **18**(54): p. 7719-30.
4. Chose, O., et al., *Cell death in protists without mitochondria.* Annals of the New York Academy of Sciences, 2003. **1010**: p. 121-5.
5. Bruchhaus, I., et al., *Protozoan parasites: programmed cell death as a mechanism of parasitism.* Trends in parasitology, 2007. **23**(8): p. 376-83.
6. Nasirudeen, A.M. and K.S. Tan, *Programmed cell death in Blastocystis hominis occurs independently of caspase and mitochondrial pathways.* Biochimie, 2005. **87**(6): p. 489-97.
7. Tan, K.S. and A.M. Nasirudeen, *Protozoan programmed cell death--insights from Blastocystis deathstyles.* Trends in parasitology, 2005. **21**(12): p. 547-50.
8. Ringqvist, E., et al., *Release of metabolic enzymes by Giardia in response to interaction with intestinal epithelial cells.* Molecular and biochemical parasitology, 2008. **159**(2): p. 85-91.
9. Roxstrom-Lindquist, K., et al., *Giardia immunity--an update.* Trends in parasitology, 2006. **22**(1): p. 26-31.
10. Bagchi, S., et al., *Programmed cell death in Giardia.* Parasitology, 2012. **139**(7): p. 894-903.
11. Correa, G., et al., *Cell death induction in Giardia lamblia: effect of beta-lapachone and starvation.* Parasitology international, 2009. **58**(4): p. 424-37.
12. Marti, M. and A.B. Hehl, *Encystation-specific vesicles in Giardia: a primordial Golgi or just another secretory compartment?* Trends in parasitology, 2003. **19**(10): p. 440-6.
13. Hacker, G., *The morphology of apoptosis.* Cell and tissue research, 2000. **301**(1): p. 5-17.

# PART VI RESULTS

## 1. Development of an *ad hoc* co-immunoprecipitation protocol for efficient pull down of protein complexes from *Giardia* mitosomes

Owing to the extensive secondary reduction and massive sequence divergence, only 20 mitosomal proteins have been identified until now in *Giardia* despite of significant bioinformatics and proteomics approaches. Although there is unambiguous experimental evidence for pre-sequence dependent and independent protein import pathways into mitosomes only one component (*Gl*Tom40) of the conventional import machinery of the outer membrane has been identified till date. In order to identify additional proteins of the mitosomal import machinery we developed an *ad hoc* co-immunoprecipitation (co-IP) assay with *Gl*Tom40 as the starting point for efficient pull down of membrane bound or soluble interacting protein complexes. An overview of the workflow is depicted in Fig.1.

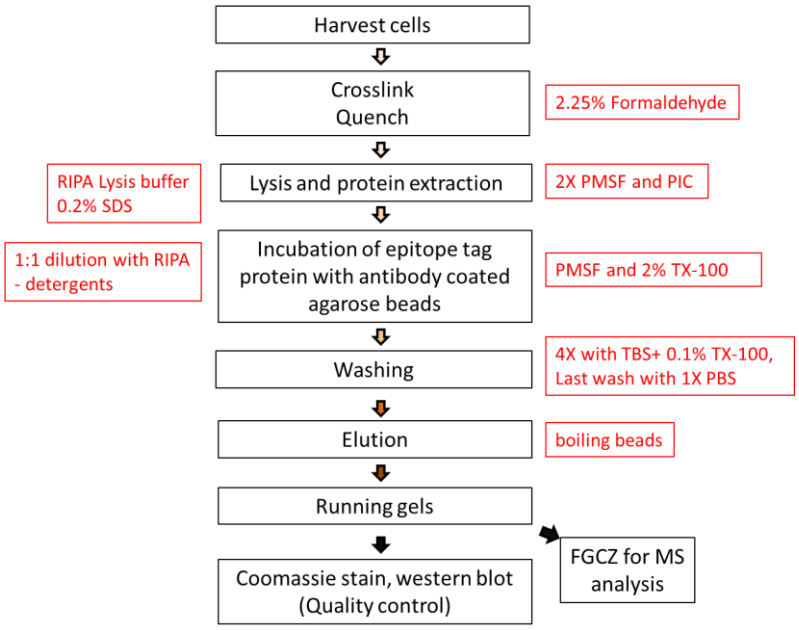


**Figure 1: Schematic representation of the major steps in a *Giardia* optimized co-immunoprecipitation experiment.**
Steps of the *Giardia* optimized co-IP assay are shown in black boxes. Major changes incorporated for efficient pull down of membrane bound protein complexes in *Giardia* are depicted in red boxes.

Initial co-IP experiments performed under non-crosslinking conditions were not successful in pulling down enough bait protein (*Gl*Tom40) and subsequently its interacting partners (data not shown). There are 2 plausible explanations; 1) protein-protein interactions could be weak or transient and hence difficult to capture. 2) Because Tom40 has a beta-barrel structure and is embedded within the lipid bilayer, protein solubilization could be challenging.

The latter can be addressed by using harsh extraction protocols (RIPA lysis buffer) facilitating efficient protein solubilization. However, this might account for the loss of interacting proteins in absence of a crosslinker. The former scenario can be addressed by using a chemical crosslinker as they "freeze" and capture transient and/or low-affinity interactions. Therefore, we tested 2 crosslinkers in our co-IP assays, 1) Formaldehyde, 2) DSP [1]. DSP, Dithiobis [succinimidyl propionate] is a cell permeable, lysine reactive crosslinker which has been successfully used to pull down weakly interacting binding partners [2, 3].

However, prior to usage of the crosslinker, the appropriate concentration had to be determined. We performed a crosslinker titration assay for both formaldehyde and DSP. The aim of this experiment was to find an optimum concentration range where the bait protein would slowly form complexes with its interacting partners and would eventually disappear from its monomeric size (43 KDa). 10 different concentrations from each crosslinker were tested, Fig. 2. In short, $4*10^6$ c-terminally HA tagged *Gl*Tom40 transgenic parasites were harvested and incubated with an appropriate crosslinker concentration for 30 mins, cells were washed and quenched with 0.1 mM glycine before sonicating the cells to release the complexes in the supernatant. Cell debris was pelleted and the supernatant was loaded onto a SDS gel without reversing the crosslinker and analyzed by immunoblotting. Immunoblot analysis shows a direct relationship between increasing percentage of the crosslinker with accumulation of high molecular weight complex formation and an inverse relationship with disappearance of the bait from its monomeric size. From this result we concluded that 0.4 mM DSP and 2.25 % formaldehyde were ideal concentration for the future co-IP assays. However, due to a gradual high molecular weight complex formation in formaldehyde crosslinked samples (Fig. 2b), we used formaldehyde as a chemical crosslinker for subsequent co-IP assays.

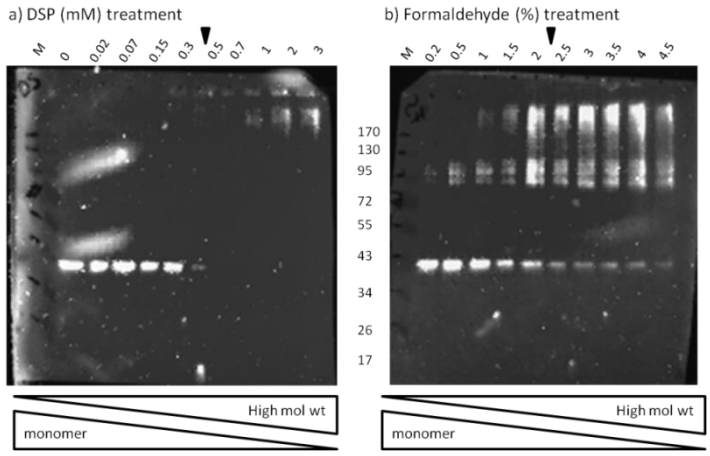


**Figure 2: Crosslinker titration experiment:** **(a)** DSP titration assay. Trophozoites were incubated with 0-3 mM DSP concentrations. 0.4 mM was determined to be ideal crosslinker concentrations indicated by the arrowhead. **(b)** Formaldehyde titration assay. Trophozoites were incubated with 0.2-4.5 % formaldehyde concentrations. 2.25 % was selected for co-IP assays.

Wild type trophozoites were subjected to the entire co-IP protocol and served as a control co-IP sample. Intersection of the bait co-IP dataset with the control co-IP dataset would eliminate potential contaminants.

Reversal of the crosslinker is the final step in a co-IP protocol. Overnight incubation at 65 °C leads to efficient reversal of the formaldehyde crosslinked protein complexes. Since elution was performed by re-suspending agarose beads in 30 µl of PBS, overnight incubation for reversal of the crosslinker resulted in drying of the loaded beads. Nevertheless, western blot analysis shows enrichment of the bait protein (*Gl*Tom40; molecular size: 43 KDa). Additionally, we observed a smear throughout the lane at high molecular weight range indicating that reversing of the crosslinker might not have worked efficiently (Fig. 3b).

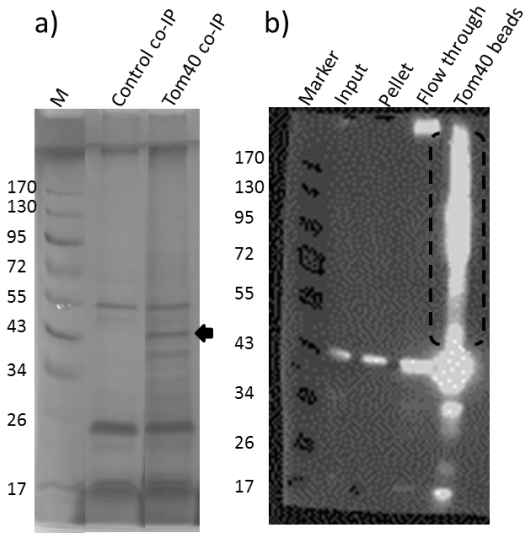


**Figure 3: Detection of high molecular weight complexes even after reversal of formaldehyde crosslinked samples. (a)** Coomassie gel showing enrichment of bait protein (*Gl*Tom40: 43 KDa, black arrow) in the *Gl*Tom40 co-IP column while it is completely absent in the wild type co-IP column. **(b)** Western blot analysis after reversal of the formaldehyde crosslinker confirms the presence of *Gl*Tom40 in the beads column. Detection of the *Gl*Tom40 signal in the high molecular weight range (dashed brackets) suggests inefficient reversal of the crosslinker.

Since reversal of formaldehyde crosslinked protein complexes was not efficient and resulted in drying of the agarose beads, we performed subsequent co-IP assays without reversing the crosslinker. This ensures that all the interacting partners are still intact and overnight reversal of crosslinker doesn't degrade the bait along with its partners due to drying of the beads. Coomassie stained gel of a co-IP assay using *Gl*Tom40 as bait protein show enrichment of bait protein in the *Gl*Tom40 co- IP column, Fig. 4a. However, as expected

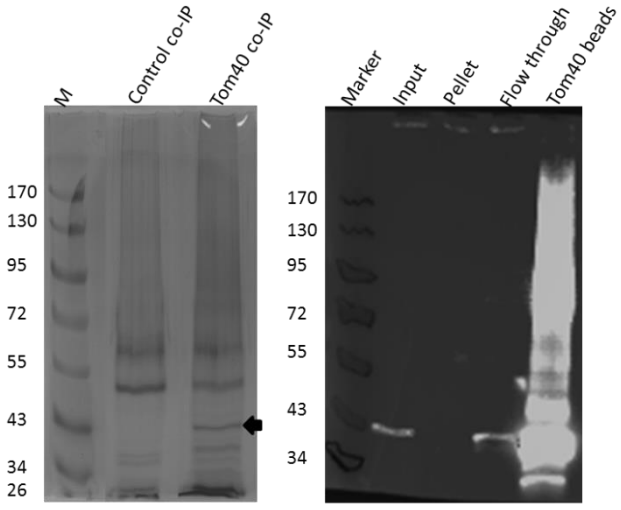


**Figure 4: Accumulation of high molecular weight complexes in non-reverse crosslinked formaldehyde samples.** Coomassie stain gel **(a)** and western blot **(b)** confirming presence of bait protein (*Gl*Tom40). Western blot confirms the presence of high molecular weight complexes ranging from 170KDa to 43KDa. This region contains the bait protein along with its crosslinked interacting partners.

western blot analysis shows a smeared signal for *Gl*Tom40 at high molecular size range due to formation of *Gl*Tom40 crosslinked protein complexes primarily due to non-reversal of the crosslinker . Regardless, boiling of agarose beads for 5 mins prior to loading resulted in reversal of the crosslinker to some extent as we detect accumulation of *Gl*Tom40 at its monomeric size (43 KDa), Fig. 4b. Furthermore, the absence of Tom40 signal in the pellet fraction suggested efficient solubilization after incubation with RIPA lysis buffer.

The generation of an *ad hoc* co-IP assay in *Giardia* was highly successful and yielded two publications;

1) **Comparative characterisation of two nitroreductases from *Giardia lamblia* as potential activators of nitro compounds** (International Journal for Parasitology: Drugs and Drug Resistance)

Joachim Müller [a], **Samuel Rout** [b], David Leitsch [a], Jathana Vaithilingam [a], Adrian Hehl [b], Norbert Müller [a],*

a Institute of Parasitology, Vetsuisse Faculty, University of Berne, Länggass-Strasse 122, CH-3012 Berne, Switzerland

b Institute of Parasitology, Eukaryotic Microbiology, University of Zürich, Winterthurerstrasse 266a, CH-8057 Zürich, Switzerland

2) **A Tom40-centered membrane interactome of the highly diverged parasite Giardia lamblia reveals functional conservation of protein import and organelle morphogenesis machinery in mitosomes** (under review in PLoS Pathogens)

**Samuel Rout**[1], Jon Paulin Zumthor[1], Elisabeth M. Schraner[2], Carmen Faso[1]* and Adrian B. Hehl[1]*

[1] Institute of Parasitology, University of Zurich (ZH), Switzerland

[2] Institute of Veterinary Anatomy, University of Zurich (ZH), Switzerland

## Bibliography

1. Smith, A.L., et al., *ReCLIP (reversible cross-link immuno-precipitation): an efficient method for interrogation of labile protein complexes*. PLoS One. **6**(1): p. e16206.
2. Humphries, J.D., et al., *Proteomic analysis of integrin-associated complexes identifies RCC2 as a dual regulator of Rac1 and Arf6*. Sci Signal, 2009. **2**(87): p. ra51.
3. Zhang, L., et al., *Successful co-immunoprecipitation of Oct4 and Nanog using cross-linking*. Biochem Biophys Res Commun, 2007. **361**(3): p. 611-4.

# PART VI RESULTS (MANUSCRIPT I)

Comparative characterisation of two nitroreductases from *Giardia lamblia* as potential activators of nitro compounds

This paper was an outcome of collaboration work together with Institute of Parasitology, Bern. My contribution to this work consisted of performing co-immunoprecipitation experiments, analysis of MS dataset (see page 5, Table 2 and 3) and writing of the manuscript.

International Journal for Parasitology: Drugs and Drug Resistance 5 (2015) 37–43

Contents lists available at ScienceDirect

International Journal for Parasitology: Drugs and Drug Resistance

journal homepage: www.elsevier.com/locate/ijpddr

# Comparative characterisation of two nitroreductases from *Giardia lamblia* as potential activators of nitro compounds

Joachim Müller [a], Samuel Rout [b], David Leitsch [a], Jathana Vaithilingam [a], Adrian Hehl [b], Norbert Müller [a,*]

[a] Institute of Parasitology, Vetsuisse Faculty, University of Berne, Länggass-Strasse 122, CH-3012 Berne, Switzerland
[b] Institute of Parasitology, Eukaryotic Microbiology, University of Zürich, Winterthurerstrasse 266a, CH-8057 Zürich, Switzerland

ARTICLE INFO

*Article history:*
Received 5 February 2015
Received in revised form 12 March 2015
Accepted 16 March 2015
Available online 25 March 2015

*Keywords:*
Mode of action of nitro compounds
Functional assays
Nitroreduction

ABSTRACT

*Giardia lamblia* is a protozoan parasite that causes giardiasis, a diarrhoeal disease affecting humans and various animal species. Nitro drugs such as the nitroimidazole metronidazole and the nitrothiazolide nitazoxanide are used for treatment of giardiasis. Nitroreductases such as GlNR1 and GlNR2 may play a role in activation or inactivation of these drugs. The aim of this work is to characterise these two enyzmes using functional assays. For respective analyses recombinant analogues from GlNR1 and GlNR2 were produced in *Escherichia coli*. *E. coli* expressing GlNR1 and GlNR2 alone or together were grown in the presence of nitro compounds. Furthermore, pull-down assays were performed using HA-tagged GlNR1 and GlNR2 as baits. As expected, *E. coli* expressing GlNR1 were more susceptible to metronidazole under aerobic and semi-aerobic and to nitazoxanide under semi-aerobic growth conditions whereas *E. coli* expressing GlNR2 were susceptible to neither drug. Interestingly, expression of both nitroreductases gave the same results as expression of GlNR2 alone. In functional assays, both nitroreductases had their strongest activities on the quinone menadione (vitamin $K_3$) and FAD, but reduction of nitro compounds including the nitro drugs metronidazole and nitazoxanide was clearly detected. Full reduction of 7-nitrocoumarin to 7-aminocoumarin was preferentially achieved with GlNR2. Pull-down assays revealed that GlNR1 and GlNR2 interacted in vivo forming a multienzyme complex. These findings suggest that both nitroreductases are multifunctional. Their main biological role may reside in the reduction of vitamin K analogues and FAD. Activation by GlNR1 or inactivation by GlNR2 of nitro drugs may be the consequence of a secondary enzymatic activity either yielding (GlNR1) or eliminating (GlNR2) toxic intermediates after reduction of these compounds.


## 1. Introduction

*Giardia lamblia* (syn. *Giardia duodenalis*; *Giardia intestinalis*), a flagellated protozoan, is the most common causative agent of persistent diarrhoea worldwide (Thompson, 2000; Robertson et al., 2010). Currently, anti-giardial chemotherapy is performed using a couple of effective drugs, namely, the nitroheterocyclic drugs tinidazole, metronidazole, furazolidone, quinacrine, the aminoglycoside paromomycin, and the benzimidazole albendazole (Wright et al., 2003; Lalle, 2010). Furthermore, the nitrothiazolide nitazoxanide has been introduced as an alternative option (Hemphill et al., 2006).

As frequently hypothesised, metronidazole and other nitro drugs are reduced to a nitro-radical. According to one of these hypotheses, electrons are provided by the enzyme pyruvate:flavodoxin/ferredoxin oxidoreductase (PFOR), representing a protein that is lacking in higher eukaryotic cells (Brown et al., 1998; Horner et al., 1999). Referring to this model, the electrons are transferred via PFOR from pyruvate to ferredoxin. The resulting reduced ferredoxin is then re-oxidised by ferredoxin:NAD-oxidoreductase transferring its electrons to NAD(P). The resulting NAD(P)H serves as a redox partner for subsequent reactions such as the reduction of $O_2$ by NAD(P)H oxidase (Brown et al., 1998). Nitro drugs may interfere in this pathway and capture electrons directly from the reduced ferredoxin or from the NAD(P)H-oxidase. This process leads to the accumulation of toxic radicals that cause irreversible damage in the parasite. Further evidence for PFOR being a major target for nitro drugs in *Giardia* comes from metronidazole-resistant isolates with lower PFOR expression levels (Upcroft and Upcroft, 2001).

Since a few years, however, evidence is emerging that PFOR may not represent the exclusive target of nitro drugs in semi-aerobic or anaerobic pathogens. In the case of *T. vaginalis*, metronidazole and other nitroimidazoles were shown to covalently bind, and thus inactivate, proteins involved in the thioredoxin reductase pathway. Resistant cells compensate this blocking by re-regulating PFORs and

* Corresponding author. Institute of Parasitology, Vetsuisse Faculty Berne, University of Berne, Länggass-Strasse 122, CH-3012 Berne, Switzerland. Tel.: +41 31 6312474; fax: +41 31 6312477.
*E-mail address:* norbert.mueller@vetsuisse.unibe.ch (N. Müller).

http://dx.doi.org/10.1016/j.ijpddr.2015.03.001

other enzymes participating in oxidoreductive processes. Accordingly, down-regulation of PFOR seems not to be a prerequisite but rather a consequence of resistance formation (Leitsch et al., 2009). Moreover, our investigations on *Giardia* cell lines resistant to nitro drugs have demonstrated that resistance is not necessarily linked to down-regulation of PFOR (Müller et al., 2007a, 2008). Although some nitro drugs are supposed to interact with PFOR in a direct manner, direct reduction of the nitro group via ferredoxin is rather unlikely. Accordingly, catalysis of this reaction by nitroreductases is a more realistic scenario (Roldán et al., 2008).

Nitroreductases belong to the enzymatic repertoire of many archaebacteria and eubacteria (Nixon et al., 2002), where they contribute to the assimilation of nitro compounds as carbon sources (Johnson and Spain, 2003; Luque-Almagro et al., 2006). From a mechanistic point of view, nitroreductases are divided into two classes, namely oxygen-sensitive and oxygen-insensitive nitroreductases (Roldán et al., 2008). Oxygen-sensitive nitroreductases transfer electrons one by one from NAD(P)H to the nitro group. In presence of oxygen, the intermediate radicals are re-oxydised. Thus, there is NAD(P)H consumption without nitroreduction, and the reaction looks most like the one catalysed by a NAD(P)H oxydase. Oxygen-insensitive nitroreductases catalyse the full reduction of nitro compounds into the corresponding amines by two-electron transfers. Also this type of reaction produces toxic intermediates, namely, nitroso or hydroxylamine intermediates (Moreno and Docampo, 1985).

In anaerobic or microaerophilic pathogens, nitroreductases are also well documented as resistance factors. In *Helicobacter pylori*, resistance to metronidazole is associated with loss-of-function mutations of the gene rdxA encoding an oxygen-insensitive nitroreductase (Goodwin et al., 1998), which reduces metronidazole under anaerobic conditions (Olekhnovich et al., 2009). Other nitroreductases are found in enteric bacteria including *Escherichia coli* (Lee et al., 1994; Zenno et al., 1996a, 1996b, 1996c; Guillén et al., 2009; Tavares et al., 2009; Yanto et al., 2010).

Nitroreductases have also been identified in microaerophilic or anaerobic eukaryotic parasites such as *Entamoeba histolytica* and *G. lamblia*. These organisms may have acquired the respective genes from prokaryotes by lateral transfer (Nixon et al., 2002). *G. lamblia* (clone WB C6) harbours two genes encoding nitroreductases GlNR1 (accession N° EDO80257; Gl50803-22677, referred to as Fd-NR2 in the *Giardia* database) and GlNR2 (accession N° XM_764091.1; Gl50803-6175, referred to as Fd-NR1 in the *Giardia* database). The polypeptide sequence of GlNR2 is rather similar to that one of GlNR1. Both proteins contain a ferredoxin domain with four Fe-S-clusters at their N-terminus and a nitro-FMN-reductase domain at their C-terminus. Our previous results suggest that both enzymes have a different action on nitro drugs: GlNR1 behaving as an activator (Müller et al., 2007b; Nillius et al., 2011), GlNR2 more as an inactivator (Müller et al., 2013). The biological role of these enzymes is, however, completely unclear.

Here, we present results from functional assays showing that both nitroreductases are multifunctional with strong quinone reductase activities. Moreover, we show that both nitroreductases interact in vivo forming a multienzyme complex.

## 2. Materials and methods

### 2.1. Tissue culture media, biochemicals and drugs

If not otherwise stated, all biochemical reagents were from Sigma (St Louis, MO, USA). 7-Nitrocoumarin was purchased from Santa Cruz Biotechnology (Dallas, Texas, USA). Nitazoxanide was synthesised at the Department of Chemistry and Biochemistry, University of Berne (kindly provided by Ch. Leumann). The nitroimidazole C17 was kindly provided by J. A. Upcroft (Molecular Genetics Laboratory, Queensland Institute of Medical Research, Brisbane, Australia). CB1954 was purchased from Santa Cruz Biotechnology. The compounds were kept as 100 mM stock solutions in DMSO at –20 °C.

### 2.2. Overexpression of recombinant GlNR1 and 2 in E. coli and His-Tag-purification

Overexpression of recombinant GlNR1 and GlNR2 in *E. coli* BL21 (DE3) and their purification by His-Tag-affinity-chromatography was performed as previously described (Müller et al., 2007b, 2013).

### 2.3. Overexpression of recombinant HA-tagged GlNR1 and 2 in G. lamblia

Cloning of PCR-amplified GlNR1 and GlNR2 open reading frames into the XbaI and PacI sites from vector pPacV-Integ (Jiménez-García et al., 2008) was essentially done as previously described (Müller et al., 2007b, 2009). Briefly, GlNR1 and GlNR2-specific forward primer contained the XbaI site followed by the constitutive glutamate dehydrogenase (GDH) promoter sequence (Davis-Hayman and Nash, 2002) (Table S1). In the reverse primer, a sequence encoding three consecutive human influenza haemagglutinin (HA) tags was introduced 5′ of the PacI site (Table S1). PCRs for amplification of GlNR1 and GlNR2 open reading frames, insertion of amplification products into XbaI and PacI sites from pPacV thus yielding pPacV-GlNR1-3xHA or pPacV-GlNR2-3xHA, and transfection of *G. lamblia* WBC6 with Swa1-linearised recombinant plasmids were performed as previously described (Müller et al., 2007b, 2009).

### 2.4. Co-immunoprecipitation assay with HA-tagged nitroreductases

*G. lamblia* WBC6 GlNR1-3xHA and GlNR2-3xHA transgenic trophozoites were grown under anaerobic condition in triple flasks (Nunc, cat. 132867). The parasites were harvested by chilling in ice water for an hour followed by centrifugation (900 × *g*, 10 min, 4 °C), washed in 50 ml ice cold PBS, and counted in a Neubauer chamber. For co-immunoprecipitation assays, $10^9$ parasites were then re-suspended in a 15-ml-Falcon-tube containing 5 ml of lysis buffer (RIPA) consisting of 50 mM Tris pH 7.4, 150 mM NaCl, 1% IGEPAL, 0.5% sodium deoxycholate, 0.1% SDS, 10 mM EDTA supplemented with 2 mM phenylmethylsulfonyl fluoride, PMSF and 1X Protease Inhibitor cocktail, PIC (cat. No. 539131, Calbiochem USA), and sonicated twice (60 pulses, 2 output control, 30% duty cycle and 60 pulses, 4 output control, 40% duty cycle). To solubilise the proteins, the Falcon tube was incubated on a rotating wheel (1 h, 4 °C). Cell lysate was transferred into 1.5 ml microtubes and the supernatant containing the solubilised protein was collected after high-speed centrifugation (14,000 × *g*, 10 min, 4 °C). The solubilised protein fraction was diluted 1:1 with detergent-free RIPA lysis buffer supplemented with 2% Triton-X-100. To this diluted protein lysate, 40 µl anti-HA agarose bead slurry from the Pierce HA Tag IP/Co-IP Kit (Thermo Fisher Scientific, Rockford, Il.) were added and incubated at 4 °C for 2 h on a rotating wheel in order to allow the HA-tagged proteins to bind to the agarose beads. Samples were pulse-centrifuged at 3500 *g* at 4 °C and 100 µl was stored as flow though control. Samples were washed 4 times with 3 ml of Tris-Buffered Saline (TBS) supplemented with 0.1% Triton-X-100 and once with 3 ml PBS. The agarose slurry was re-suspended in 350 µl PBS and transferred into the spin column provided in the kit and pulse-fuged at 14,000 × *g* for 10 s at 4 °C. The agarose beads (boiled beads) were then re-suspended in 30 µl PBS and transferred into a 1.5 ml microtubes and stored at –20 °C overnight for further analysis.

### 2.5. Protein analysis and sample preparation for mass spectrometry

For SDS-PAGE according to (Laemmli (1970), the samples collected as described above were suspended in one volume of SDS-PAGE sample buffer containing 100 mM dithiothreitol, and boiled for 5 min followed by high speed centrifugation (14,000 × *g*, 10 min, RT). For MS analysis, 25 µl of boiled bead sample were loaded on a 12% polyacrylamide gel under reducing conditions. The gel (see Fig. S1) was then stained with Instant blue (Expedeon, San Diego, CA), de-stained with sterile water, and subsequently sent to the Functional Genomics Center Zürich for mass spectrometry. For immunoblot analysis, approximately $10^7$ trophozoites were processed and samples were collected as described above. Immunoblots were performed with rabbit anti-GlNR1 (Nillius et al., 2011) and mouse-anti-HA (Roche Diagnostics, Rotkreuz, Switzerland) antibodies as described before (Nillius et al., 2011).

### 2.6. Mass spectrometry

Gel lanes (see Fig. S1) were cut in 8 equal sections. Each section was further diced into smaller pieces and washed twice with 100 µl of 100 mM ammonium bicarbonate/50% acetonitrile for 15 min at 50 °C. The sections were dehydrated with 50 µl of acetonitrile. The supernatants of the washing and de-hydration steps were discarded. The gel pieces were re-hydrated with 20 µl trypsin solution (5 ng/ µl in 10 mM Tris/2 mM $CaCl_2$ at pH 8.2) and 40 µl buffer (10 mM Tris/2 mM $CaCl_2$ at pH 8.2). Microwave-assisted digestion was performed for 30 min at 60 °C with the microwave power set to 5 W (CEM Discover, CEM Corp., USA). Supernatants were collected in fresh tubes and the gel pieces were extracted with 150 µl of 0.1% trifluoroacetic acid/50% acetonitrile. Supernatants were combined, dried, and the samples were dissolved in 20 µl of 0.1% formic acid before being transferred to the autosampler vials for liquid chromatography-tandem mass spectrometry, 7 to 9 µl were injected. Samples were measured on a Q-exactive mass spectrometer (Thermo Fisher Scientific) equipped with a nanoAcquity UPLC (Waters Corporation, Milford, MA). Peptides were trapped on a trap column (Symmetry C18, 5 µm, 180 µm × 20 mm, Waters Corporation) before they were separated on a BEH300 C18, 1.7 µm, 75 µm × 150 mm column (Waters Corporation) by applying a gradient formed between solvent A (0.1% formic acid in water) and solvent B (0.1% formic acid in acetonitrile). On the mass spectrometer, a gradient starting at 1% solvent B and increasing to 40% within 60 min was established. Database searches were performed using the MASCOT search program against the *Giardia* database (http://giardiadb.org/giardiadb/) with a concatenated decoy database supplemented with commonly observed contaminants and the Swissprot database to increase size of the database. The identified hits were then loaded onto the Scaffold Viewer version 4 (Proteome Software, Portland, USA) and the hits were filtered based on high stringency parameters, namely, minimal mascot score of 95 for peptide probability, a protein probability of 95% and a minimum of 2 unique peptides per protein.

### 2.7. Quantification of nitroreductase activity

For enzymatic quantification, the nitroreductase activity was measured in 96-well microtiter plates containing 100 µl of a reaction mix containing buffer (50 mM Tris-$Cl^-$, pH 7.0), 0.1 mM of the compounds to be tested, 0.5 mM thiazolyl blue tetrazolium (MTT), 0.5 mM NADH or NADPH and 0.1 to 0.2 µg of the recombinant enzymes. The plates were incubated at 37 °C under aerobic conditions or in an anaerobic growth chamber. Substrate and enzyme blanks were included. After different time points, the reaction was stopped by adding 100 µl of pure ethanol thus solubilising the product formed by the reduction of MTT, formazan. The absorbance at 590 nm was read on a 96-well plate spectrophotometer (Versamax; Molecular Devices, Sunnyvale, CA). After subtraction of substrate and enzyme blanks, nitroreductase activity was expressed as $\Delta A_{590}$/min/mg (Prochaska and Santamaria, 1988).

The reduction of 7-nitrocoumarin to 7-aminocoumarin was quantified using the reaction mix as described above, but without MTT, with the same volumes and under the same conditions of incubation. Enzyme and substrate blanks were included. The reaction was stopped by adding 100 µl of 50 mM HCl. The resulting solution had pH 2 resulting in full protonation of 7-aminocoumarin which was quantified by fluorimetry with excitation at 365 nm and emission at 455 nm (Wagner, 2009) using a 96-well-multimode plate reader (Enspire; Perkin-Elmer, Waltham, MA).

### 2.8. Determination of drug susceptibility in E. coli

Drug susceptibility of recombinant *E. coli* BL21 (DE3) lines (Invitrogen, Carlsbad, CA, USA) expressing either GlNR1 (recombinant plasmid pGlNR1), GlNR2 (pGlNR2), glucuronidase A (pGusA) alone (Nillius et al., 2011; Müller et al., 2013) or both nitroreductases (this study, see below) were tested as described (Müller et al., 2013). Single gene expression was achieved in vector system pET151 Directional TOPO® (Invitrogen) containing the ampicillin resistance marker for selection of transformants and allowing IPTG-inducible overexpression of recombinant proteins (see pET151 Directional TOPO® manual provided by the manufacturer) as described (Müller et al., 2013). In order to achieve double transfectants expressing both nitroreductases, the following cloning strategies were chosen: (i) the entire pET151 Directional TOPO® expression cassettes carrying GlNR1 and GusA open reading frames were amplified by PCR using T7 forward (5′-TAATACGACTCACTATAGGG-3′) and T7 reverse (5′-TAGTTATTGCTCAGCGGTGG-3′) primers (annealing to regions flanking the expression cassette of pET151 Directional TOPO®) and pGlNR1 and pGusA as DNA templates. (ii) PCR products were used for re-cloning of GlNR1 and GusA into pCR-Blunt II-TOPO® (Invitrogen) containing a kanamycin resistance marker. (iii) This re-cloning step provided plasmid constructs, pGlNR1-$Kan^R$ and pGusA-$Kan^R$, suitable for subsequent transformation of ampicillin-resistant BL21 (DE3)/pGlNR2, and BL21 (DE3)/pGusA strains by selection for ampicillin (100 µg/ml)/kanamycin (50 µg/ml) double-resistant clones. *E. coli* BL21 (DE3) carrying pGlNR1, pGlNR2, pGusA, pNR1-$Kan^R$/pGlNR2 and pGusA-$Kan^R$/pGusA were tested under aerobic or microaerobic (5% $O_2$, 10% $CO_2$, 85% $N_2$) conditions by a conventional disc diffusion agar procedure as described (Müller et al., 2013). Growth inhibition zone diameters were determined and the inhibition zone around the disc was calculated (in $mm^2$).

### 2.9. Statistical methods

Statistical analysis of the results was done based on the tools from the open source software package R (R Core Team, 2012) Differences exhibiting $p$ values < 0.01 were considered significant.

## 3. Results

### 3.1. E. coli expressing recombinant GlNR1 and GlNR2 have different susceptibilities to nitro drugs

We generated recombinant *E. coli* lines producing GlNR1 or GlNR2 alone (Müller et al., 2013) or both (this study). As a control, we have created recombinant lines expressing glucuronidase A (Gus) alone (Müller et al., 2013) or double (Gus/Gus) (this study). In a pilot experiment, overproduction of proteins induced by IPTG strongly reduced growth of *E. coli*. Accordingly, non-induced, recombinant *E. coli* cultures were chosen for growth inhibition assays as described earlier (Nillius et al., 2011). With these five strains, disc diffusion assays were performed with metronidazole, nitazoxanide

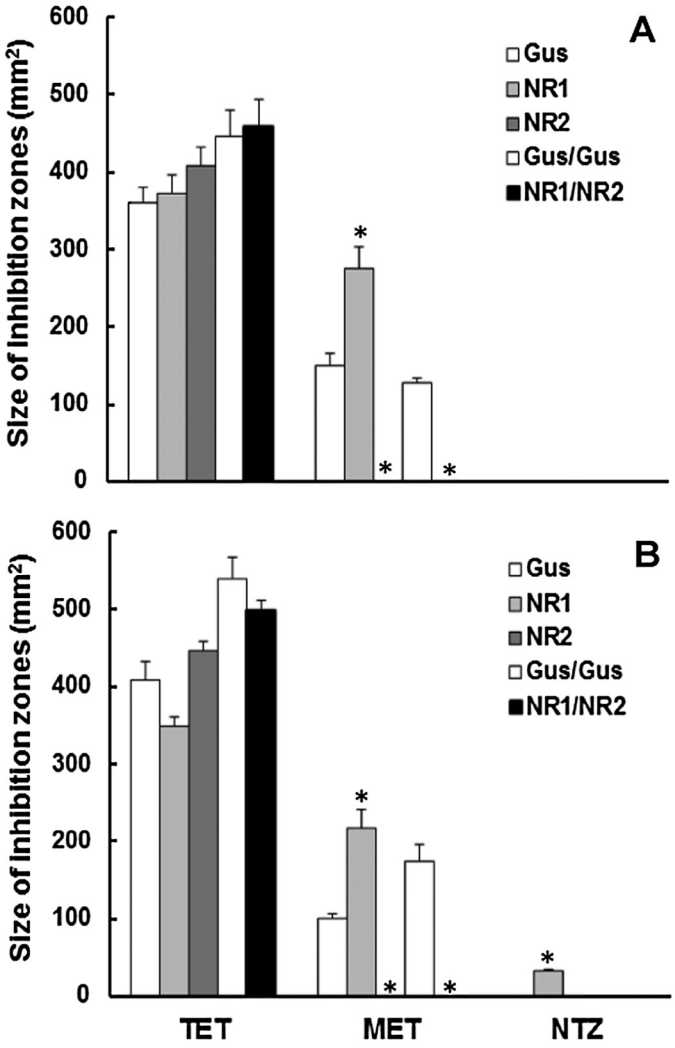


**Fig. 1.** Susceptibility of *E. coli* BL21 (DE3) expressing GusA as a control (Gus), GlNR1 (NR1), and GlNR2 (NR2), two GusA (Gus/Gus), or both nitroreductases (NR1/NR2) to metronidazole (MET) and to nitazoxanide (NTZ). Tetracycline (TET) was included as a positive control. Plates with different cell lines exposed to discs containing the drugs were incubated under aerobic (A) or semi-aerobic (B) conditions. After 24 h, diameters of inhibition zones were determined. Mean values ± SE are given for 3 replicates. Values marked by asterisks are significantly different from the controls, i.e. to Gus for the single transformants and to Gus/Gus for the double transformant (paired *t*-test, two-sided, $^{*}p < 0.01$).

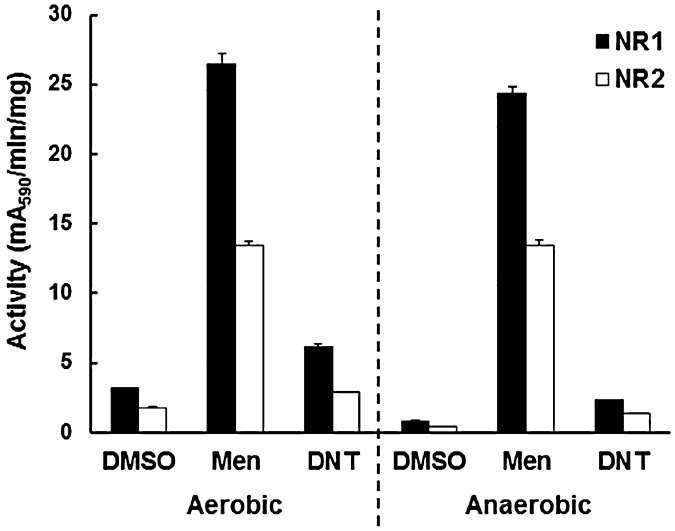


**Fig. 2.** Activity of recombinant *G. lamblia* nitroreductases GlNR1 (NR1) and GlNR2 (NR2) with menadione (Men) or dinitrotoluene (DNT) as substrates (0.1 mM). DMSO was included as a solvent control, thus as a substrate blank. Functional assays were performed with NADH as an electron donor and MTT as chromogenic electron acceptor. The reaction was performed at 37 °C under normal atmosphere (aerobic) or in an anaerobic chamber (100% $N_2$; anaerobic) and stopped after 2 h addition of one volume pure ethanol. Mean values (±SE) are given for three replicates.

or tetracyclin as a positive control under aerobic or semi-aerobic conditions. Under aerobic as well as semi-aerobic growth conditions, metronidazole clearly inhibited growth of control strains transformed with Gus or Gus/Gus. In the presence of GlNR1 alone, this susceptibility was significantly enhanced. Bacteria transformed with GlNR2 alone or with both nitroreductases were completely resistant to metronidazole. Under aerobic conditions, nitazoxanide did not affect growth of bacteria. Under semi-aerobic conditions, however, bacteria expressing GlNR1 exhibited a significantly higher susceptibility to nitazoxanide than control bacteria. Other inserts than GlNR1 had no effects. There were no significant effects in nitroreductase-transformed strains vs. control strains in the presence of tetracycline (Fig. 1).

### 3.2. Recombinant GlNR1 and GlNR2 are quinone reductases

The results obtained with metronidazole clearly suggested a role of both nitroreductases under aerobic conditions. Was their role thus restricted to the reduction of nitro compounds? To answer this question we implemented a functional assay based on the reduction of MTT to formazan by reduced nitrocompounds or quinones. In a first experiment, we incubated the assays in a 37 °C incubator under normal atmosphere or in an anaerobic culture chamber (100% $N_2$). We offered NADH as electron donor, the quinone menadion and dinitrotoluene as electron acceptors or DMSO as a solvent control. Interestingly, both nitroreductases reduced menadione, and this even to much higher extents than dinitrotoluene. Both enzymes worked evenly well under anaerobic and under aerobic conditions (Fig. 2).

### 3.3. Both nitroreductases are NADH dependent and have a preference for menadione

We tested the preference for NADH or NADPH as electron donors with menadione or dinitrotoluene as a substrate. Both nitroreductases had clearly a preference for NADH with both substrates (Table 1). In a next step, we determined the activities of both enzymes on a series of compounds including FAD, dicoumarol, quinacrine and various nitro compounds including the antigiardial drugs metronidazole and nitazoxanide as well as C17 and CB1954. Furthermore, we included 7-nitrocoumarin, a compound yielding the highly fluorescent 7-aminocoumarin upon complete reduction.

The highest activities were observed for both enzymes with menadione as a substrate. Dicoumarol, a typical inhibitor of mammalian quinone reductases (Müller and Hemphill, 2011), had no effects. The second best substrate in our series was FAD. Ubiquinone (coenzyme Q10) was also reduced by both enzymes but with lower specific activities than meandione (Table 1).

With respect to nitro compounds as substrates, 7-nitrocoumarin was clearly the best. Interestingly, we could detect a reduction of all nitrocompounds with antigiardial activity, i.e. metronidazole, nitazoxanide, and C17. Dinitrophenol was only reduced by GlNR1. GlNR1 had a higher specific activity with all substrates (Table 1).

**Table 1**
Activity of recombinant *G. lamblia* nitroreductases (GlNR1 and GlNR2) with various nitro- and non-nitro compounds (0.1 mM) as substrates. Functional assays were performed with MTT as chromogenic electron acceptor. Electron donor was NADH or NADPH if specified. The reaction was performed at 37 °C and stopped after various time points by addition of one volume pure ethanol. Mean values (±SE) are given for three replicates after subtraction of enzyme and substrate blanks.

| Substrate | GlNR1 | GlNR2 |
|---|---|---|
| | ($\Delta A_{590}$ $min^{-1}$ mg $prot^{-1}$) | |
| Menadione | 22.9 ± 0.4 | 16.2 ± 0.2 |
| Menadione NADPH | 1.8 ± 0.2 | 0.2 ± 0.1 |
| Dicoumarol | 3.1 ± 0.2 | 0.8 ± 0.1 |
| Menadione + dicoumarol | 27.2 ± 0.3 | 14.5 ± 0.1 |
| Ubiquinone (coenzyme $Q_{10}$) | 2.8 ± 0.1 | 1.8 ± 0.2 |
| FAD | 11.8 ± 0.4 | 8.9 ± 0.9 |
| Dinitrotoluene | 5.2 ± 0.3 | 2.8 ± 0.2 |
| Dinitrotoluene NADPH | 0.9 ± 0.3 | 0.3 ± 0.1 |
| 7-Nitrocoumarine | 10.6 ± 0.3 | 6.5 ± 0.5 |
| Dinitrophenol | 5.9 ± 0.4 | 0.2 ± 0.1 |
| Nitrophenol | 2.9 ± 0.1 | 2.6 ± 0.1 |
| Metronidazole | 2.8 ± 0.2 | 1.7 ± 0.1 |
| Nitazoxanide | 2.7 ± 0.2 | 1.9 ± 0.1 |
| CB1954 | 3.0 ± 0.1 | 1.7 ± 0.1 |
| C17 | 2.1 ± 0.2 | 0.9 ± 0.1 |

**Table 2**
Proteins interacting with HA-tagged GlNR1 in vivo. *G. lamblia* WBC6 was transformed with GlNR1-3xHA. Crude extracts were affinity-purified using anti-HA-antibodies immobilised on beads followed by mass spectrometry. A control experiment was performed with crude extract from WBC6 expressing no recombinant protein. Only hits with highest stringency, namely, minimal mascot score of 95 for peptide probability, a protein probability of 95% and a minimum of 2 unique peptides per protein, are shown.

| Name | Accession-N° | Molecular weight (kDa) | Unique peptides (N°) |
|---|---|---|---|
| Axoneme-associated protein GASP-180 | GL50803_137716 | 175 | 4 |
| Fructose-bisphosphate aldolase | GL50803_11043 | 35 | 3 |
| GlNR2 (Fd-NR1) | GL50803_6175 | 31 | 2 |
| Hypothetical protein | GL50803_9183 | 214 | 2 |
| TCP1-chaperon-subunit gamma | GL50803_17411 | 62 | 2 |
| Phosphoglycerate kinase | GL50803_90872 | 44 | 2 |
| Arginyl-tRNA-synthetase | GL50803_10521 | 70 | 2 |
| Vacuolar ATP-synthase catalytic subunit A | GL50803_7532 | 72 | 2 |
| Malate dehydrogenase | GL50803_3331 | 35 | 2 |

### 3.4. 7-nitrocoumarin is fully reduced preferentially by GlNR2

These results prompted us to investigate whether 7-aminocoumarin was fully reduced by both nitroreductases thus yielding the fluorescent 7-aminocoumarin. For this purpose, we performed the same assay as above without MTT, and quantified the fluorescent product. Although GlNR2 had a lower specific activity in the assay as described above, it was twice as active as GlNR1 in fully reducing 7-aminocoumarin. When added together, both enzymes were more active than the sum of the single activities (Fig. 3).

### 3.5. GlNR1 and GlNR2 interact in vivo

The synergistic effect of the two nitroreductases (see Fig. 3) suggested a physical interaction of the two enzymes prompting us to perform pull-down assays using HA-tagged GlNR1 and GlNR2 as baits. These pull-down assays were used for the identification of proteins which specifically bind to these nitroreductases in *G. lamblia*. Crude extracts from *G. lamblia* WBC6 expressing the corresponding constructs were affinity-purified using anti-HA-antibodies immobilised on beads followed by mass spectrometry. Under high stringency conditions, HA-tagged nitroreductase GlNR1 co-purified with GlNR2 and with a couple of other proteins including fructose-bisphosphate aldolase (Table 2). Conversely, HA-tagged GlNR2 co-purified with GlNR1 and with two other proteins, namely, fructose-bisphosphate aldolase and ornithine carbamoyl-transferase (Table 3). Immunoblot analysis using an antibody specific for GlNR1 and an anti-HA antibody showed the presence of GlNR1 in the immunoprecipitate of GlNR2-3xHA. GlNR2 was not cross reactive with GlNR1. (Fig. 4).

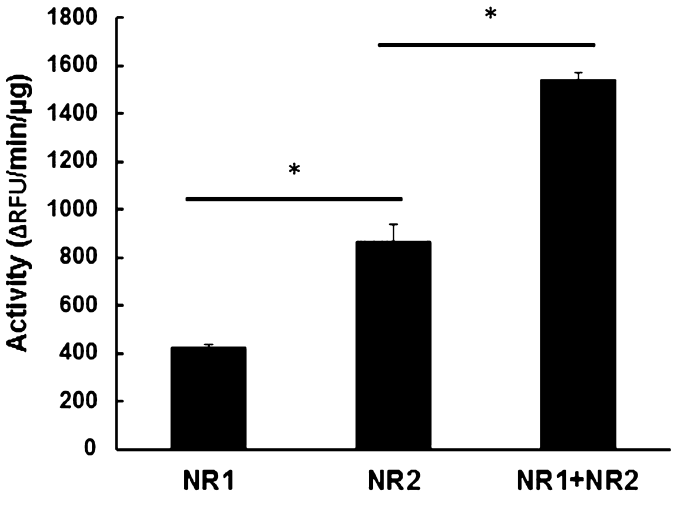


**Fig. 3.** Activity of recombinant *G. lamblia* nitroreductases GlNR1 (NR1) and GlNR2 (NR2) with 7-nitrocoumarine as a substrate (0.1 mM) and with NADH as an electron donor. The reaction was performed at 37 °C with GlNR1, GlNR2 alone (125 ng each) or together (62.5 ng each) and stopped after various time points by addition of one volume HCl 0.05 M. Formation of 7-aminocoumarin was quantified by fluorimetry (excitation at 365 nm, emission at 455 nm). Mean values (±SE) are given for three replicates. Values marked by asterisks are significantly different from each other (paired *t*-test, two-sided, $^{*}p < 0.01$).

## 4. Discussion

Like some other antiparasitic nitro drugs, metronidazole is considered as a prodrug that is activated by partial reduction. This reaction is supposed to form a toxic radical (Docampo and Moreno, 1984), or partially reduced nitroso- or hydroxylamine-intermediates (Moreno and Docampo, 1985), causing DNA damage (Sisson et al., 2000). Conversely, complete reduction results in detoxification of nitro compounds thus allowing various bacteria to use toxic compounds such as trinitrotoluene as carbon sources (Kutty and Bennett, 2005). Our results obtained with MTT as a final electron acceptor suggest that both nitroreductases are multifunctional and able to

**Table 3**
Proteins interacting with HA-tagged GlNR2 in vivo. *G. lamblia* WBC6 was transformed with GlNR2-3xHA. Crude extracts were affinity-purified using anti-HA-antibodies immobilised on beads followed by mass spectrometry. A control experiment was performed with crude extract from WBC6 expressing no recombinant protein. Only hits with highest stringency, namely, minimal mascot score of 95 for peptide probability, a protein probability of 95% and a minimum of 2 unique peptides per protein, are shown.

| Name | Accession-N° | Molecular weight (kDa) | unique peptides (N°) |
|---|---|---|---|
| GlNR1 (Fd-NR2) | GL50803_22677 | 29 | 15 |
| Fructose-bisphosphate aldolase | GL50803_11043 | 35 | 2 |
| Ornithine carbamoyl-transferase | GL50803_10311 | 36 | 2 |

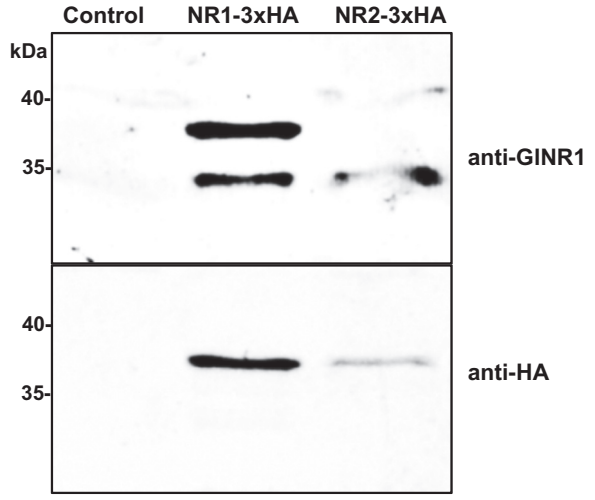


**Fig. 4.** Immunoblot with anti-GlNR1 and anti HA-antibodies of immunoprecipitates from untransformed WBC6 (control), WBC6 transformed with GlNR1-3xHA as a bait, and WBC6 transformed with GlNR2-3xHA as a bait. Trophozoites were processed as described. The position of molecular weight markers is indicated in kDa.

use a variety of nitro compounds as substrates. With 7-nitrocoumarin as a substrate, full reduction to the corresponding 7-aminocoumarin can be investigated (Wagner, 2009). In our hands, GlNR2 is twice as effective as GlNR1 in this reaction indicating that it performs the full reduction rather than a partial reduction. When mixed, both enzymes act synergistically.

In *E. coli*, expression of GlNR1 increases the susceptibility to nitazoxanide exclusively under semi-aerobic growth conditions whereas susceptibility to metronidazole is increased under semi-aerobic and aerobic conditions. In contrast, GlNR2 decreases the susceptibility to metronidazole under both growth conditions confirming previous results (Nillius et al., 2011; Müller et al., 2013). Interestingly, expression of both enzymes has the same effects as expression of GlNR2 alone suggesting that *E. coli* BL21(DE3) is able to express endogenous nitroreductases even under aerobic growth conditions what is fully in frame with previously published results (Zenno et al., 1996a, 1996c; Valle et al., 2012). While these endogenous nitroreductases reduce metronidazole to toxic intermediates, GlNR2 acts antagonistically and eliminates metronidazole toxicity in *E. coli*. Susceptibility of *E. coli* to metronidazole has been reported earlier (Olekhnovich et al., 2009; Nillius et al., 2011). The results with nitroreductase-expressing *E. coli* and the results obtained with 7-nitrocoumarin in functional assays suggest that GlNR1 preferentially performs a partial reduction of nitro compounds yielding toxic intermediates. Conversely, GlNR2 is able to entirely reduce a nitro compound thus generating a non-toxic end product, e.g. the corresponding amine.

Our experiments show, however, that nitro compounds are not the best substrates for both enzymes having highest activities on menadione as substrate. This quinone reductase activity is not inhibited by dicoumarol as it is the case for typical mammalian nitroreductases such as the human quinone reductase NQO1 (Müller and Hemphill, 2011). Moreover, both enzymes reduce free FAD. Similar multifunctional nitroreductases have been identified in various bacteria including *E. coli* (Zenno et al., 1996a, 1996b, 1996c), *Lactobacillus plantarum* (Guillén et al., 2009), *Salmonella typhimurium* (Yanto et al., 2010) and in eukaryotes such as *Trypanosoma cruzi* (Hall et al., 2012), The genome of *G. lamblia* WBC6 contains three putative NADPH dependent quinone reductases, namely, Gl50803_15004 (18.6 kDa), Gl50803_17150 (18.5 kDa), and Gl50803_17151 (19.5 kDa). Only one, Gl50803_15004, has been previously characterised in detail. This enzyme reduces menadione using NADPH as preferred electron donor (Sanchez et al., 2001).

The biological function of GlNR1 and GlNR2 could be the reduction of quinones and other heterocyclic compounds in essential steps of intermediate metabolism. Menadione is not a quinone present in *Giardia* and is even toxic (Paget et al., 2004). This toxicity may be due to a partial reduction of menadione to the corresponding semiquinone. Other potential substrates such as FAD and ubiquinone (Ellis et al., 1994) are, however, present in *Giardia* and play an important role in intermediate metabolism.

This could explain why knock-down approaches have failed, so far in our hands, and why a nitroreductase is essential for *Leishmania donovani* (Voak et al., 2013). From an evolutionary point of view, the reduction of nitro compounds could be a side effect without negative selective pressure until a nitro compound yielding toxic intermediates after reduction comes into play. Then, the presence of an otherwise beneficial activity turns into a disaster for the cell. In the presence of sublethal concentrations of the nitro compound, resistance formation is then achieved not by a mere down-regulation of the nitroreductase responsible for the toxic intermediate formation, but rather by a complete re-organisation of cellular metabolism as exemplified by the resistance formation of WBC6 against nitazoxanide (Müller et al., 2008).

Pull-down assays with both nitroreductases as baits and immunoblot analysis show that both enzymes interact with each other. Moreover, they may also interact with fructose-bisphosphate aldolase, a key enzyme of glycolysis. The significance of this finding is unclear and will be studied in further immunoprecipitation experiments using fructose-bis-phosphate aldolase as a bait.

Novel promising techniques like conditional knock-outs (Wampfler et al., 2014) could open the way to understand the biological function of nitroreductases in *G. lamblia*.

## Acknowledgements

We would like to thank The Functional Genomics Center Zürich (FGCZ) for highly valuable technical support. We also wish to thank A. Hemphill (Institute of Parasitology, University of Berne, Berne, Switzerland) for proofreading of the manuscript and C. Huber as well as V. Balmer (Institute of Parasitology, University of Berne, Berne, Switzerland) for technical assistance. This study was supported by grants from the Swiss National Science Foundation (grants No. 31003A_138353 [NM, JM] and No. 31-140803/1 [AH]) and the Austrian Science Fund (project J3492 1 [DL].

## Conflict of interest

The authors declared that there is no conflict of interest.

## AppendixSupplementary material

Supplementary data to this article can be found online at doi:10.1016/j.ijpddr.2015.03.001.

## References

Brown, D.M., Upcroft, J.A., Edwards, M.R., Upcroft, P., 1998. Anaerobic bacterial metabolism in the ancient eukaryote *Giardia duodenalis*. Int. J. Parasitol. 28, 149–164.
Davis-Hayman, S.R., Nash, T.E., 2002. Genetic manipulation of *Giardia lamblia*. Mol. Biochem. Parasitol. 122, 1–7.
Docampo, R., Moreno, S.N., 1984. Free radical metabolites in the mode of action of chemotherapeutic agents and phagocytic cells on *Trypanosoma cruzi*. Rev. Infect. Dis. 6, 223–238.
Ellis, J.E., Setchell, K.D., Kaneshiro, E.S., 1994. Detection of ubiquinone in parasitic and free-living protozoa, including species devoid of mitochondria. Mol. Biochem. Parasitol. 65, 213–224.

Goodwin, A., Kersulyte, D., Sisson, G., Veldhuyzen van Zanten, S.J., Berg, D.E., Hoffman, P.S., 1998. Metronidazole resistance in *Helicobacter pylori* is due to null mutations in a gene (*rdxA*) that encodes an oxygen-insensitive NADPH nitroreductase. Mol. Microbiol. 28, 383–393.

Guillén, H., Curiel, J.A., Landete, J.M., Muñoz, R., Herraiz, T., 2009. Characterization of a nitroreductase with selective nitroreduction properties in the food and intestinal lactic acid bacterium *Lactobacillus plantarum* WCFS1. J. Agric. Food Chem. 57, 10457–10465.

Hall, B.S., Meredith, E.L., Wilkinson, S.R., 2012. Targeting the substrate preference of a type I nitroreductase to develop antitrypanosomal quinone-based prodrugs. Antimicrob. Agents Chemother. 56, 5821–5830.

Hemphill, A., Müller, J., Esposito, M., 2006. Nitazoxanide, a broad-spectrum thiazolide anti-infective agent for the treatment of gastrointestinal infections. Expert Opin. Pharmacother. 7, 953–964.

Horner, D.S., Hirt, R.P., Embley, T.M., 1999. A single eubacterial origin of eukaryotic pyruvate: ferredoxin oxidoreductase genes: implications for the evolution of anaerobic eukaryotes. Mol. Biol. Evol. 16, 1280–1291.

Jiménez-García, L.F., Zavala, G., Chávez-Munguía, B., Ramos-Godínez Mdel, P., López-Velázquez, G., Segura-Valdez Mde, L., et al., 2008. Identification of nucleoli in the early branching protist *Giardia duodenalis*. Int. J. Parasitol. 1297–1304.

Johnson, G.R., Spain, J.C., 2003. Evolution of catabolic pathways for synthetic compounds: bacterial pathways for degradation of 2,4-dinitrotoluene and nitrobenzene. Appl. Microbiol. Biotechnol. 62, 110–123.

Kutty, R., Bennett, G.N., 2005. Biochemical characterization of trinitrotoluene transforming oxygen-insensitive nitroreductases from *Clostridium acetobutylicum* ATCC 824. Arch. Microbiol. 184, 158–167.

Laemmli, U.K., 1970. Cleavage of structural proteins during the assembly of the head of bacteriophage T4. Nature 227, 680–685.

Lalle, M., 2010. Giardiasis in the post genomic era: treatment, drug resistance and novel therapeutic perspectives. Infect. Disord. Drug Targets 10, 283–294.

Lee, H., Cherng, S.H., Liu, T.Y., 1994. Bacterial mutagenicity, metabolism, and DNA adduct formation by binary mixtures of benzo[a]pyrene and 1-nitropyrene. Environ. Mol. Mutagen. 24, 229–234.

Leitsch, D., Kolarich, D., Binder, M., Stadlmann, J., Altmann, F., Duchêne, M., 2009. Trichomonas vaginalis: metronidazole and other nitroimidazole drugs are reduced by the flavin enzyme thioredoxin reductase and disrupt the cellular redox system. Implications for nitroimidazole toxicity and resistance. Mol. Microbiol. 72, 518–536.

Luque-Almagro, V.M., Blasco, R., Paloma Sáez, L., Roldán, M.D., Moreno-Vivián, C., Castello, F., et al., 2006. Interactions between nitrate assimilation and 2,4-dinitrophenol cometabolism in *Rhodobacter capsulatus* E1F1. Curr. Microbiol. 53, 37–42.

Moreno, S.N., Docampo, R., 1985. Mechanism of toxicity of nitro compounds used in the chemotherapy of trichomoniasis. Environ. Health Perspect. 64, 199–208.

Müller, J., Hemphill, A., 2011. Identification of a host cell target for the thiazolide class of broad-spectrum anti-parasitic drugs. Exp. Parasitol. 128, 145–150.

Müller, J., Sterk, M., Hemphill, A., Müller, N., 2007a. Characterization of *Giardia lamblia* WB C6 clones resistant to nitazoxanide and to metronidazole. J. Antimicrob. Chemother. 60, 280–287.

Müller, J., Wastling, J., Sanderson, S., Müller, N., Hemphill, A., 2007b. A novel *Giardia lamblia* nitroreductase, GlNR1, interacts with nitazoxanide and other thiazolides. Antimicrob. Agents Chemother. 51, 1979–1986.

Müller, J., Ley, S., Felger, I., Hemphill, A., Müller, N., 2008. Identification of differentially expressed genes in a *Giardia lamblia* WB C6 clone resistant to nitazoxanide and metronidazole. J. Antimicrob. Chemother. 62, 72–82.

Müller, J., Nillius, D., Hehl, A., Hemphill, A., Müller, N., 2009. Stable expression of Escherichia coli β-glucuronidase A (GusA) in *Giardia lamblia*: application to high-throughput drug susceptibility testing. J. Antimicrob. Chemother. 64, 1187–1191.

Müller, J., Schildknecht, P., Müller, N., 2013. Metabolism of nitro drugs metronidazole and nitazoxanide in *Giardia lamblia*: characterization of a novel nitroreductase (GlNR2). J. Antimicrob. Chemother. 68, 1781–1789.

Nillius, D., Müller, J., Müller, N., 2011. Nitroreductase (GlNR1) increases susceptibility of *Giardia lamblia* and *Escherichia coli* to nitro drugs. J. Antimicrob. Chemother. 66, 1029–1035.

Nixon, J.E., Wang, A., Field, J., Morrison, H., McArthur, A.G., Sogin, M.L., et al., 2002. Evidence for lateral transfer of genes encoding ferredoxins, nitroreductases, NADH oxidase, and alcohol dehydrogenase 3 from anaerobic prokaryotes to *Giardia lamblia* and *Entamoeba histolytica*. Eukaryot. Cell 1, 181–190.

Olekhnovich, I.N., Goodwin, A., Hoffman, P.S., 2009. Characterization of the NAD(P)H oxidase and metronidazole reductase activities of the RdxA nitroreductase of *Helicobacter pylori*. FEBS J. 276, 3354–3364.

Paget, T., Maroulis, S., Mitchell, A., Edwards, M.R., Jarroll, E.L., Lloyd, D., 2004. Menadione kills trophozoites and cysts of *Giardia intestinalis*. Microbiology 150, 1231–1236.

Prochaska, H.J., Santamaria, A.B., 1988. Direct measurement of NAD(P)H:quinone reductase from cells cultured in microtiter wells: a screening assay for anticarcinogenic enzyme inducers. Anal. Biochem. 169, 328–336.

R Core Team, 2012. R: A language and environment for statistical computing.

Robertson, L.J., Hanevik, K., Escobedo, A.A., Mørch, K., Langeland, N., 2010. Giardiasis – why do the symptoms sometimes never stop? Trends Parasitol. 26, 75–82.

Roldán, M.D., Pérez-Reinado, E., Castillo, F., Moreno-Vivián, C., 2008. Reduction of polynitroaromatic compounds: the bacterial nitroreductases. FEMS Microbiol. Rev. 32, 474–500.

Sanchez, L.B., Elmendorf, H., Nash, T.E., Müller, M., 2001. NAD(P)H:menadione oxidoreductase of the amitochondriate eukaryote *Giardia lamblia*: a simpler homologue of the vertebrate enzyme. Microbiology 147, 561–570.

Sisson, G., Jeong, J.Y., Goodwin, A., Bryden, L., Rossler, N., Lim-Morrison, S., et al., 2000. Metronidazole activation is mutagenic and causes DNA fragmentation in *Helicobacter pylori* and in *Escherichia coli* containing a cloned H. pylori RdxA(+) (Nitroreductase) gene. J. Bacteriol. 182, 5091–5096.

Tavares, A.F., Nobre, L.S., Melo, A.M., Saraiva, L.M., 2009. A novel nitroreductase of *Staphylococcus aureus* with S-nitrosoglutathione reductase activity. J. Bacteriol. 191, 3403–3406.

Thompson, R.C.A., 2000. Giardiasis as a re-emerging infectious disease and its zoonotic potential. Int. J. Parasitol. 30, 1259–1267.

Upcroft, P., Upcroft, J.A., 2001. Drug targets and mechanisms of resistance in the anaerobic protozoa. Clin. Microbiol. Rev. 14, 150–164.

Valle, A., Le Borgne, S., Bolívar, J., Cabrera, G., Cantero, D., 2012. Study of the role played by NfsA, NfsB nitroreductase and NemA flavin reductase from *Escherichia coli* in the conversion of ethyl 2-(2′-nitrophenoxy)acetate to 4-hydroxy-(2H)-1,4-benzoxazin-3(4H)-one (D-DIBOA), a benzohydroxamic acid with interesting biological properties. Appl. Microbiol. Biotechnol. 94, 163–171.

Voak, A.A., Gobalakrishnapillai, V., Seifert, K., Balczo, E., Hu, L., Hall, B.S., et al., 2013. An essential type I nitroreductase from *Leishmania major* can be used to activate leishmanicidal prodrugs. J. Biol. Chem. 288, 28466–28476.

Wagner, B.D., 2009. The use of coumarins as environmentally-sensitive fluorescent probes of heterogeneous inclusion systems. Molecules 14, 210–237.

Wampfler, P.B., Faso, C., Hehl, A.B., 2014. The Cre/loxP system in *Giardia lamblia*: genetic manipulations in a binucleate tetraploid protozoan. Int. J. Parasitol. 44, 497–506.

Wright, J.M., Dunn, L.A., Upcroft, P., Upcroft, J.A., 2003. Efficacy of antigiardial drugs. Expert Opin. Drug Saf. 2, 529–541.

Yanto, Y., Hall, M., Bommarius, A.S., 2010. Nitroreductase from *Salmonella typhimurium*: characterization and catalytic activity. Org. Biomol. Chem. 8, 1826–1832.

Zenno, S., Koike, H., Kumar, A.N., Jayaraman, R., Tanokura, M., Saigo, K., 1996a. Biochemical characterization of NfsA, the *Escherichia coli* major nitroreductase exhibiting a high amino acid sequence homology to Frp, a Vibrio harveyi flavin oxidoreductase. J. Bacteriol. 178, 4508–4514.

Zenno, S., Koike, H., Tanokura, M., Saigo, K., 1996b. Conversion of NfsB, a minor *Escherichia coli* nitroreductase, to a flavin reductase similar in biochemical properties to FRase I, the major flavin reductase in *Vibrio fischeri*, by a single amino acid substitution. J. Bacteriol. 178, 4731–4733.

Zenno, S., Koike, H., Tanokura, M., Saigo, K., 1996c. Gene cloning, purification, and characterization of NfsB, a minor oxygen-insensitive nitroreductase from *Escherichia coli*, similar in biochemical properties to FRase I, the major flavin reductase in *Vibrio fischeri*. J. Biochem. 120, 736–744.

# PART VI RESULTS (MANUSCRIPT II)

A Tom40-centered membrane interactome of the highly diverged parasite *Giardia lamblia* reveals functional conservation of protein import and organelle morphogenesis machinery in mitosomes

This paper summarizes the main part of my PhD thesis. I started working on this project since the beginning of 2012 for 2 years. The concept of *Giardia* based co-immunoprecipitation using *G. lamblia* Tom40 as a point of origin and (re)constructing a *Gl*Tom40 centered interactome inwards towards the mitosomal matrix and outwards towards the cytosol was developed together with my direct supervisor Prof. Dr. Adrian B. Hehl and co-supervisor Dr. carmen Faso who supported me during all stages of the project including writing of the manuscript.

My contribution to this work includes developing the co-IP protocol for membrane anchored *G. lamblia* proteins, *in silico* analysis of the MS dataset and localization studies. I was assisted in light and electron microscopy by Dr. Carmen Faso (Fig 5A-B), Prof. Dr. Adrian B. Hehl (Fig 7), and Elisabeth M. Schraner (Fig 6I-J). Compilation of all the figures for the manuscript was done by me.

Tandem mass spectrometry was performed in collaboration with the functional genomics center Zurich (FGCZ).

# A Tom40-centered membrane interactome of the highly diverged parasite *Giardia lamblia* reveals functional conservation of protein import and organelle morphogenesis machinery in mitosomes

Samuel Rout[1], Jon Paulin Zumthor[1], Elisabeth M. Schraner[2], Carmen Faso[1]* and Adrian B. Hehl[1]*

[1] Institute of Parasitology, University of Zurich (ZH), Switzerland

[2] Institute of Veterinary Anatomy, University of Zurich (ZH), Switzerland

*Corresponding authors

Email: adrian.hehl@access.uzh.ch (AH)

carmen.faso@access.uzh.ch (CF)

## Abstract

Protozoan parasites of the genus *Giardia* are highly prevalent globally and infect a wide range of vertebrate hosts including humans, but proliferation and pathology is restricted to the small intestine. This narrow ecological specialization entailed extensive structural and functional adaptations during host-parasite co-evolution. *G. lamblia* mitochondria-related organelles (mitosomes) are at the farthest extreme on the spectrum of mitochondrial reductive evolution with iron-sulphur protein maturation as the only identifiable biochemical pathway. We describe construction of the extensively diverged mitosome-specific proteome based entirely on protein-protein interactions, using the only identifiable component of a predicted TOM/TIM protein import complex (Tom40) as a starting point. Using serial co-immunoprecipitation assays and validation steps we extended a robust Tom40 core interactome network outwards, revealing additional outer membrane proteins and candidate links to membranes of the endoplasmic reticulum (ER), as well as inwards, identifying many novel imported proteins in addition to the few annotated conserved metabolic factors and chaperones. Live cell imaging revealed that the 30-40 organelles in a cell are highly immobilized and do not form dynamic networks, which is also consistent with interactome data suggesting physical links with the cytoskeleton, in particular with the basal body complex. On the other hand, identification of small GTPases and factors with dual mitosome and ER localization in the interactome suggested intimate connections with the ER. Functional analysis of mitosomes showed conceptual conservation of protein import although the machinery for translocation is diverged beyond recognition, as well as association of the single *G. lamblia* dynamin-related protein with mitosomes and direct evidence for its involvement in organelle morphogenesis. This study underscores the

potential of this strategy for identification of proteins and machinery *ab initio* in a highly diverged but clearly delimited organelle system.

## Author Summary

Organelles with endosymbiotic origin are present in all extant eukaryotes and have undergone considerable remodeling during > 1 billion years of evolution. Highly diverged organelles such as mitosomes or plastids in some parasitic protozoa are the product of extensive secondary reduction. They are sufficiently unique to generate interest as targets for pharmacological intervention, in addition to providing a rich ground for evolutionary cell biologists. The so-called mitochondria-related organelles (MROs) comprise mitosomes and hydrogenosomes, with the former having lost any role in energy metabolism along with the organelle genome. The mitosomes of the intestinal pathogen *Giardia lamblia* are the most highly reduced MROs known and have proven difficult to investigate because of their extreme divergence and their unique physical properties. Here, we implemented a novel strategy aimed at systematic analysis of the organelle proteome by iterative expansion of a protein-protein interaction network. We demonstrated the effectiveness of serial co-immunoprecipitations combined with mass spectrometry analysis and *in vivo* validation for generating an interactome network centered on a giardial Tom40 homolog. This iterative *ab initio* proteome reconstruction provided protein-protein interaction data in addition to identifying novel organelle proteins and functions. Building on this information we investigated mitosome morphogenesis and organelle dynamics in living cells, and showed that the single giardial dynamin plays a role in organelle replication.

## Introduction

Since the single endosymbiotic event leading to establishment of mitochondria approximately 2 billion years ago [1,2,3] these organelles have undergone massive changes and have evolved into highly specialized and essential subcellular compartments in all eukaryotes [4,5]. These changes comprise a dramatic size reduction, nuclear transfer of organelle genomes, and a renewal of the proteome, which is synthesized almost entirely as precursor proteins on cytosolic ribosomes [6,7,8,9,10,11,12,13] and imported from the cytoplasm [14]. Mitochondria have been remodeled and/or restructured to very different degrees in different species. Mitochondria-related organelles (MROs), *i.e.* hydrogenosomes and mitosomes [15,16,17,18,19] in some protists lacking canonical mitochondria represent extreme forms of reduction and/or divergence. The potential of highly diverged organelle-specific pathways as targets for intervention has sparked research into the evolution of MROs in single-celled organisms of all five eukaryotic supergroups [20,21]. Notably, the microaerophilic protozoan pathogens *Entamoeba histolytica* [19], *Giardia lamblia* [22,23],

*Blastocystis hominis* [24] as well as obligate intracellular parasites such as *Cryptosporidium parvum* [25] and *Encephalitozoon cuniculi* [26] harbor highly reduced mitosomes. Interestingly, recent investigation of MROs in *Spironucleus salmonicida*, a diplomonad and the closest relative of *G. lamblia* belonging to the Excavata super-group, revealed that these organelles are in fact hydrogenosomes [27]. Although it has been demonstrated that *G. lamblia* mitosomes don't produce hydrogen, this sheds a completely new light on the evolution of MRO's in diplomonads.

Proliferating *G. lamblia* trophozoites contain 20-50 double membrane-bounded 100 nm spherical mitosomes [22,23] devoid of an organellar genome [28,29,30,31]. Although not proven experimentally, *G. lamblia* mitosomes are likely essential due to a subset of conserved mitochondrial proteins required for iron- sulphur (Fe-S) protein maturation [22,32,33,34,35]. Yeast genetic experiments suggested that Fe-S protein maturation, the only function currently ascribable to *G. lamblia* mitosomes, is in fact the minimal essential function of mitochondria [36]. Hence, these organelles have also generated considerable interest as cell biological models to study extreme reductive evolution of MROs [22,37,38,39,40,41,42]. However, due to massive, albeit selective sequence divergence in *G. lamblia*, conventional strategies for identification of mitosome proteins based on homology-based *in silico* searches fall short [26,28,32,43,44,45,46,47]. Moreover, proteome analyses approaches have had very limited success due to the small size of the organelles and the omnipresence of contaminating endoplasmic reticulum (ER) and cytoskeleton elements in enriched mitosome fractions [33,48].

Nevertheless, there is unambiguous experimental evidence for the functional conservation of the mitosomal protein import machinery [19,22,23]. The small subset of structurally conserved mitosome proteins such as *G. lamblia* IscU, ferredoxin, Cpn60, IscS and mtHsp70 are imported by transit peptide-dependent and -independent mechanisms [22]. However, the predicted components of the TOM/TIM import apparatus are diverged beyond recognition by state-of-the-art homology search tools or have been lost. Only one subunit of the translocon in the outer mitochondrial (TOM) complex, a highly diverged Tom40 homologue (*Gl*Tom40), has been identified [49].

Because most *G. lamblia* mitosome components have undergone extreme sequence divergence or have been lost altogether, the vast knowledge about the molecular biology and biochemistry of mitochondria cannot be directly applied to investigations into evolution, morphogenesis, and function of these organelles. Hence, exploration of the range of *G. lamblia* mitosome functions requires alternative strategies aimed at comprehensive identification of their proteome and of essential *Giardia*-specific factors. We hypothesized that the diminutive organelles harbored no more than 100-150 different proteins inside or

associated with a clearly delineated cellular compartment. Thus, it should be possible to use a putative *Gl*TOM40 [22,33] as a starting point for identifying a core membrane interactome and extend this in an iterative process to eventually encompass the whole organelle proteome. The rationale for using *Gl*Tom40 as a starting point is the fact that it is the only, albeit poorly, conserved outer membrane protein and plays a key role for the import of organelle proteins. Using a series of co-immunoprecipitation assays we obtained a robust *Gl*Tom40 interactome and extend this network in both directions, *i.e.* outwards onto the cytoplasmic face of mitosomes, including peripheral membrane proteins such as a diverged putative TOM receptor (*Gl*Tom40R), and inwards, encompassing the few known and many novel imported organelle proteins. We used this information to probe mitosome morphogenesis and function and to test constraints for import of nuclear encoded mitosome proteins.

## Materials and Methods

*Giardia cell culture, induction of encystation, pulse-empty chase set-up and transfection*

*G. lamblia* WBC6 (ATCC catalog number 50803) trophozoites were grown and harvested using standard protocols [50]. Encystation was induced with the two-step method as described previously [40,51]. Transgenic parasites were generated according to established protocols by electroporation of linearized pPacV-Integ-based plasmid vectors prepared from *E. coli* as described in [42]. After selection for puromycin resistance, transgenic *G. lamblia* cell lines were cultured and analyzed without antibiotic.

*Construction of expression vectors*

All sequences of oligonucleotide primers for PCR used in this work are listed in S1 Table.

For cloning of C-terminally hemagglutinin (HA)-tagged proteins in *Giardia*, a vector PAC-CHA was designed on the basis of the previously described vector pPacV-Integ [42], where additional restriction sites were inserted. A detailed vector map can be found in S1 Fig.

A cyst wall protein 1 promoter (pCWP1)-driven *G. lamblia* ferredoxin (fd)-human dihydrofolate reductase (DHFR) chimeric gene was generated by fusing two genes by overlapping PCR: i) an intron-less fd mitosomal targeting signal (MTS) (MTSfd$\Delta_{int}$) open reading frame (ORF) was generated using primer pair 33 (S1 Table) with *G. lamblia* cDNA as template, ii) a DHFR_HA minigene was generated using primer pair 34 (S1 Table) with a cloned human DHFR cDNA as template. The fused product was digested with *Spe*I and *Pac*I and inserted in a PAC vector to yield construct pCWP1_MTSfd$\Delta_{int}$-DHFR_HA.

A pCwp1_ MTSfd$\Delta_{int}$-DHFR_Neomycin resistance construct (without HA tag) was generated for protein import block assays. Primer pair 35 (S1 Table) was used on pCwp1_ MTSfd$\Delta_{int}$-DHFR_HA as a template. The amplified product was digested with *Nsi*I and *Pac*I and ligated into a vector containing a neomycin resistance cassette [52].

*Co-immunoprecipitation with limited cross-linking*

*G. lamblia* WBC6 and transgenic trophozoites expressing C-terminally HA tagged bait proteins were harvested and subjected to immunofluorescence assay to confirm correct subcellular distribution of bait proteins. Parasites were collected by centrifugation (900 x *g*, 10 minutes, 4 °C), washed in 50 ml of cold phosphate buffer saline solution (PBS) and adjusted to 2 *$10^7$ cells $\cdot ml^{-1}$ in PBS (VWR Prolabo). The appropriate formaldehyde concentration for cross-linking (2.25%) was determined by a titration assay (S2 Fig). For the co-immunoprecipitation (co-IP) assays, $10^9$ parasites were resuspended in 10 ml 2.25% formaldehyde (in PBS) supplemented with 1 mM phenylmethylsulfonyl fluoride (PMSF; SIGMA, Cat. No. P7626) and incubated for 30 minutes at room temperature (RT). Cells were pelleted, washed once with 10 ml PBS, and quenched in 10 ml 100 mM glycine in PBS for 15 minutes at RT. The collected cells were then resuspended in 5 ml RIPA lysis buffer (50 mM Tris pH 7.4, 150 mM NaCl, 1% IGEPAL, 0.5% sodium deoxycholate, 0.1% SDS, 10 mM EDTA) supplemented with 2 mM PMSF and 1 x Protease Inhibitor cocktail (PIC, Cat. No. 539131, Calbiochem USA) and sonicated twice using a Branson Sonifier with microtip (Branson Sonifier 250, Branson Ultrasonics Corporation) with the following settings: 60 pulses, 2 output control, 30% duty cycle and 60 pulses, 4 output control, 40% duty cycle. The sonicate was incubated on a rotating wheel for 1 h at 4 °C, aliquoted into 1.5 ml tubes and centrifuged (14,000 x *g*, 10 minutes, 4 °C). The soluble protein fraction was mixed with an equal volume detergent-free RIPA lysis buffer supplemented with 2% TritonX (TX)-100 (Fluka Chemicals) and 40 µl anti-HA agarose bead slurry (Pierce, product # 26181). After binding of tagged proteins to the beads at 4 °C for 2 h on a rotating wheel, beads were pulse-centrifuged and washed 4 times with 3 ml Tris-Buffered Saline (TBS) supplemented with 0.1% TX-100 at 4 °C. After a final wash with 3 ml PBS the loaded beads were resuspended in 350 µl PBS, transferred to a spin column (Pierce spin column screw cap, product # 69705, Thermo Scientific) and centrifuged for 10 s at 4 °C. Elution was performed by resuspending beads in 30 µl of PBS. Dithiothreitol (DTT; 100mM; Thermo Scientific, Cat. # RO861) was added and samples were boiled for 5 min followed by centrifugation (14,000 x *g*, 10 minutes, RT).

*Protein analysis and sample preparation for mass spectrometry-based protein identification*

SDS-PAGE and immunoblotting analysis of input, flow-through, and eluate fractions was performed on 4%-12% polyacrylamide gels under reducing conditions, (molecular weight

marker Cat. No. 26616, Thermo Scientific, Lithuania). Transfer to nitrocellulose membranes and antibody probing were done as described previously [53]. Gels for mass spectrometry (MS) analysis were stained using Instant blue (Expedeon, Prod. # ISB1L) and de-stained with sterile water.

*Mass Spectrometry and protein identification*

Stained gel lanes were cut into 8 equal sections. Each section was further diced into smaller pieces and washed twice with 100 µl of 100 mM ammonium bicarbonate/ 50 % acetonitrile for 15 min at 50 °C. The sections were dehydrated with 50 µl of acetonitrile. The gel pieces were rehydrated with 20 µl trypsin solution (5 ng/µl in 10 mM Tris-HCl/ 2 mM $CaCl_2$ at pH 8.2) and 40 µl buffer (10 mM Tris-HCl/ 2 mM $CaCl_2$ at pH 8.2). Microwave-assisted digestion was performed for 30 minutes at 60 °C with the microwave power set to 5 W (CEM Discover, CEM corp., USA). Supernatants were collected in fresh tubes and the gel pieces were extracted with 150 µl of 0.1% trifluoroacetic acid/ 50% acetonitrile. Supernatants were combined, dried, and the samples were dissolved in 20 µl 0.1% formic acid before being transferred to the autosampler vials for liquid chromatography-tandem MS (injection volume 7 to 9 µl). Samples were measured on a Q-exactive mass spectrometer (Thermo Scientific) equipped with a nanoAcquity UPLC (Waters Corporation). Peptides were trapped on a Symmetry C18, 5 µm, 180 µm x 20 mm column (Waters Corporation) and separated on a BEH300 C18, 1.7 um, 75 µm x 150 mm column (Waters Corporation) using a gradient formed between solvent A (0.1% formic acid in water) and solvent B (0.1% formic acid in acetonitrile). The gradient started at 1% solvent B and the concentration of solvent B was increased to 40% within 60 minutes. Following peptide data acquisition, database searches were performed using the MASCOT search program against the *G. lamblia* database (http://tinyurl.com/37z5zqp) with a concatenated decoy database supplemented with commonly observed contaminants and the Swissprot database to increase database size. The identified hits were then loaded onto the Scaffold Viewer version 4 (Proteome Software, Portland, US) and filtered based on high stringency parameters (minimal mascot score of 95% for peptide probability, a protein probability of 95%, and a minimum of 2 unique peptides per protein). For a description of relaxed conditions see “Results”.

*In silico co-immunoprecipitation dataset analysis*

Analysis of primary structure and domain architecture of putative mitosomal hypothetical proteins was performed using the following tools and databases: MITOPROT (http://ihg.gsf.de/ihg/mitoprot.html) and PSORTII (http://psort.hgc.jp/form2.html) for subcellular localization prediction, TMHMM (http://www.cbs.dtu.dk/services/TMHMM/) for transmembrane helix prediction, SMART (http://smart.embl-heidelberg.de/) for prediction of patterns and functional domains, pBLAST for protein homology detection

(http://blast.ncbi.nlm.nih.gov/Blast.cgi?PAGE=Proteins), HHPred (http://toolkit.tuebingen.mpg.de/hhpred) for protein homology detection based on Hidden Markov Model (HMM-HMM) comparison, and the Giardia Genome Database (http://giardiadb.org/giardiadb/) to extract other/organism-specific information, e.g. expression levels of the protein, predicted molecular size and nucleotide/protein sequence. For functional domains predicted by SMART we used an e-value of $10e^{-5}$ as cutoff, and for protein homologies predicted by pBLAST we accepted alignment scores above 80. However, since G. *lamblia* homologs for eukaryotic proteins are highly diverged, we also considered functional domain predictions associated to a lower e-value. Alignment scores between 50 and 80 were accepted only when pBLAST predictions were consistent with HHPred output.

*Immunofluorescence analysis (IFA) and microscopy*

Preparation of chemically fixed cells for immunofluorescence and analysis of subcellular distribution of reporter proteins by wide-field and confocal microscopy were done as described previously [42,53]. Nuclear labelling was performed with 4',6-diamidino-2-phenylindole (DAPI).

*Live-cell microscopy and fluorescence recovery after photobleaching (FRAP)*

Transgenic *G. lamblia* trophozoites expressing GFP-*Gl*Tom40 or *Gl*29147-GFP were harvested and prepared for imaging in PBS supplemented with 5 mM glucose (Cat. No. 49139, Fluka), 5 mM L-cysteine (Cat. No. C6852, Sigma) and 0.1 mM ascorbic acid (Cat. No. 95209, Fluka) at pH 7.1. FRAP and time-lapse series were performed as described previously [53,54] .

*Sample preparation for transmission electron microscopy*

Transgenic trophozoites ectopically expressing wild type *G. lamblia* dynamin related protein (*Gl*DRP) (ORF *Gl50803_14373*) or the constitutively active (GTP-locked) *Gl*DRP-K43E variant under the control of the CWP1 promoter [54] were harvested 3 h post induction and analyzed by transmission electron microscopy (TEM) as described previously [54].

*Sub-cellular fractionation analysis*

For sub-cellular fraction experiments, $4{\cdot}10^6$ *Gl*DRP-HA and *Gl*DRP-K43E-HA- expressing transgenic cells were lysed by freeze-thawing and supernatant (soluble fraction) and pellet (membrane fraction) were prepared by centrifugation at 14'000 x *g* for 10 minutes at 4 °C. The HA-tagged proteins were detected by SDS-PAGE and Western blot using a rat anti-HA mAb (clone 3F10, Roche) as described previously [53].

*DHFR-MTX protein import block assay*

The MTSfd$\Delta_{int}$-DHFR fusion (see also above under "Constructs") was expressed under the control of the inducible CWP1 promoter in a background transgenic line constitutively expressing HA- tagged 17030 (cell line Cwp1_MTSfd$\Delta_{int}$-DHFR/*Gl*17030HA). DHFR expression was induced using the 2-step method [40] for 4 h and "chased" for 24 h by placing the cells again in standard growth medium in the presence or absence of 1 μM methotrexate (MTX). Total cell lysates were separated by SDS-PAGE and Western blot to detect processed and unprocessed forms of the *Gl*17030HA reporter. Subcellular distribution was analyzed by immunofluorescence assay (IFA) using wide field microscopy.

## Results

### Co-IP with the *G. lamblia* Tom40 homolog identifies novel interacting proteins of the mitosome outer membrane

Despite efforts aimed at defining the protein content of mitosomes [49] in *Giardia*, the composition of this organelle's membrane proteome and specifically the predicted import machinery in the outer and inner membranes remained unknown, with the exception of a highly diverged putative Tom40 homologue (*Gl*Tom40; ORF *Gl50803_17161*) [49]. To generate the first mitosome outer membrane proteome we focused on *Gl*Tom40 as a point of origin and developed a customized co-IP protocol with an HA-tagged variant as "bait". A transgenic line *Gl*Tom40-HA constitutively expressing the epitope-tagged bait protein was generated; exclusive mitosome localization of the bait protein in transgenic cells was confirmed by IFA (Fig. 1A). However, a broad range of conditions and detergents that are standard for purifying mitochondrial membrane proteins [55] yielded not a single protein associated to the *Gl*Tom40-HA bait in initial co-IP experiments (data not shown). Because conditions necessary for solubilizing the strongly curved double membranes of these tiny organelles apparently also dispersed all *Gl*Tom40-interacting proteins, we used carefully titrated, formaldehyde-based cross-linking [56] to stabilize predicted protein-protein interactions for co-IP experiments (S2 Fig; see also in Materials and Methods). Co-IP and tandem MS analyses yielded a first Tom40 interactome dataset (*Gl*Tom40 co-IP); a control dataset obtained from un-transfected cells (ctrl co-IP) was generated under identical conditions for data filtration, i.e. identification and elimination of hits in *Gl*Tom40 co-IP generated by non-specific interactions (e.g. physical trapping). Data processing was done in Scaffold4 viewer (http://www.proteomesoftware.com/products/free-viewer/) initially with high stringency parameters (95_2_95), yielding a total of 78 hits with a false discovery rate (FDR) of 0% (S2 Table). Data filtering showed 46 hits exclusively in the *Gl*Tom40 co-IP dataset, whereas 31 proteins were identified in both datasets and 1 protein was exclusive to the ctrl co-IP dataset (Fig. 1B). The 46 *Gl*Tom40-specific hits and an additional 6 candidates from the *Gl*Tom40/ctrl co-IP intersection that had peptide ratios >5 (S3 Table) were parsed

and subdivided into different metabolic and/or functional categories (Fig. 1C). Four previously identified mitosome proteins were detected: mitochondrial HSP70 (ORF *Gl50803_14581*), oxidoreductase 1 (*Gl*OR1; ORF *Gl50803_91252*) and hypothetical proteins *Gl50803_9296* and *Gl50803_14939* [33]. Based on the topology of *Gl*Tom40 in the outer membrane and the conditions used in these co-IP experiments, it was not surprising to find 20 hits for annotated metabolic enzymes and other cytosolic components which could be eliminated from the candidate pool. We extracted additional information from the *Gl*Tom40 co-IP data by relaxing stringency parameters to (95_1_95), obtaining a total of 150 proteins (FDR 3.4%; S4 Table). Of these, 109 hits were exclusive to the expanded *Gl*Tom40 co-IP dataset, whereas 40 proteins were identified in both datasets and 1 protein was exclusive to the ctrl co-IP dataset. Of note, the expanded dataset contained three additional annotated mitosome proteins namely, chaperonin 60 (Cpn60; ORF *Gl50803_103891*), *Gl*Qb-SNARE 3 (putative Sec20, ORF *Gl50803_5161*) and NifU-like protein (ORF *Gl50803_15196*). Pending validation of the remaining non-annotated hits strongly suggests that the expanded dataset contains additional as yet unidentified mitosome proteins.

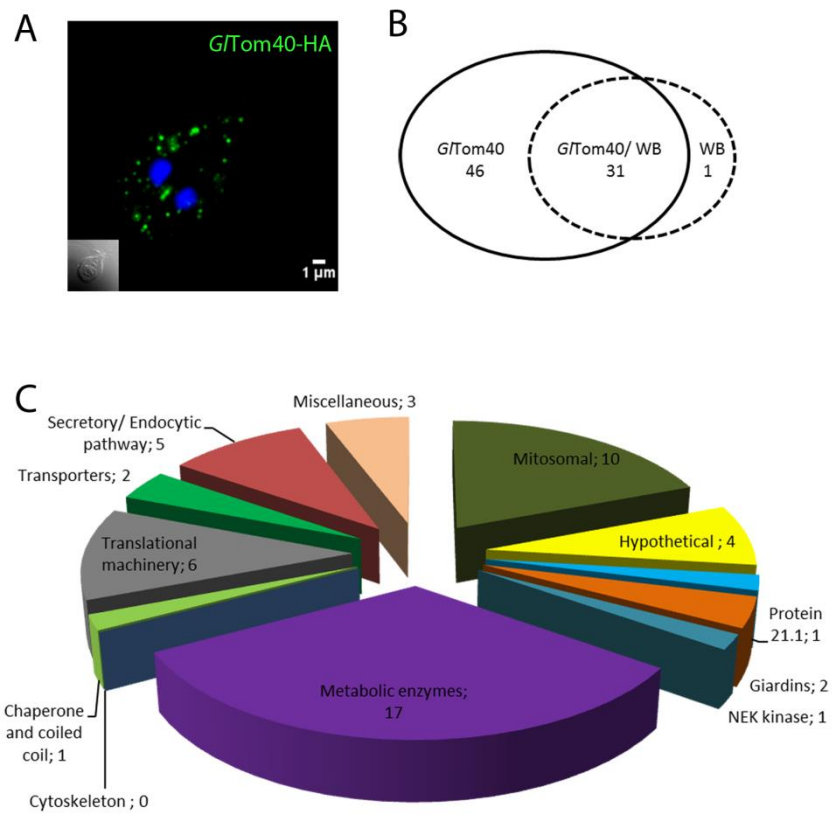


**Fig 1. Co-IP with G. lamblia Tom40 yields numerous candidate interacting proteins.** (A) Immunofluorescence microscopy: C-terminally HA-tagged *Gl*Tom40 (*Gl*Tom40-HA) is an exclusive marker for mitosomes (green). Nuclear DNA is stained with DAPI (blue). Inset: DIC image. (B) Venn diagram indicating 46 *Gl*Tom40 specific hits. (C) Parsing of 46 *Gl*Tom40-specific proteins and an additional 6 candidates from the *Gl*Tom40/ctrl co-IP overlap that had peptide ratios >5 (metabolic and/or functional categories are indicated in the pie chart).

### Validation of the *Gl*Tom40 co-IP data

Because of the non-targeted nature of limited chemical cross-linking in co-IP assays we performed careful validation of the datasets generated in these experiments based on two criteria: i) subcellular localization of ectopically expressed, epitope-tagged candidates to mitosomes, and ii) successful retrieval of the endogenous protein previously used as bait in reverse co-IP experiments.

To test subcellular localization we selected 13 of the 109 candidate Tom40 interacting proteins based on MASCOT scores or protein domains identified in HHPred. The 9 hypothetical proteins with the highest MASCOT scores and four additional candidates with domains predicted to be involved in mitochondrial functions (S5 Table) were cloned as endogenous promoter-driven C-terminally HA-tagged variants into a *G. lamblia* expression vector and used to generate transgenic lines [57]. Using IFA of chemically fixed transgenic cells, we confirmed mitosomal localization for 8 out of 9 candidates (Figs. 2A-2N).

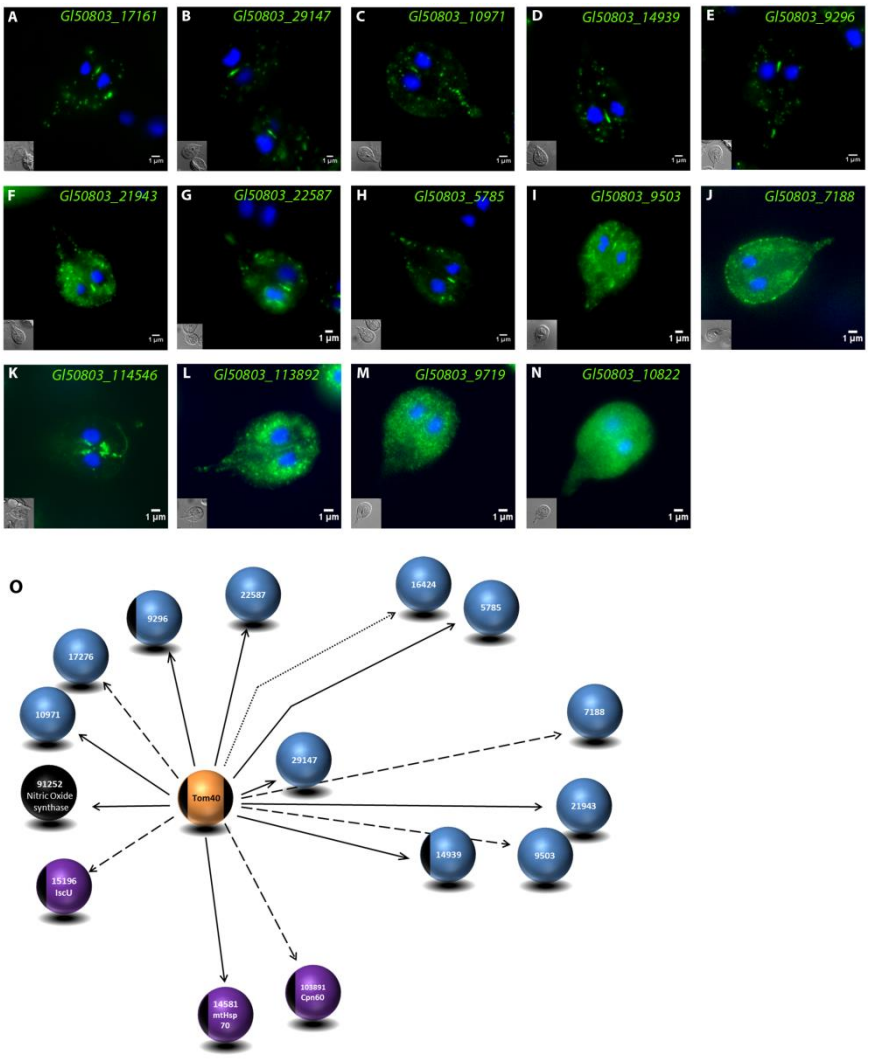


**Fig 2. Subcellular localization of candidate GlTom40 interaction partners.** (A-N) Immunofluorescence microscopy: subcellular localization of C-terminally HA-tagged *Gl*Tom40 and 13 putative interaction partners (green) falls into 3 categories: Typical mitosome localization (A-E); dual localization to mitosomes and ER (F-I); no or ambiguous mitosome localization (J-N). Nuclear DNA is stained with DAPI (blue). Insets: DIC image. (O) Partially validated *Gl*Tom40 interactome showing the bait protein (orange sphere), matrix proteins (purple), previously identified and mitosome-localized proteins (black), and mitosome-localized hypothetical proteins (blue). The stringency parameters used for detection (high, medium, and relaxed) are represented by bold, dashed, and dotted arrows, respectively.

This high proportion underscores the quality of the *Gl*Tom40 co-IP dataset. Interestingly, 4 proteins without annotation (ORFs *Gl50803_ 21943, 22587, 5785 and 9503)* presented dual localization (mitosome and ER) (Figs. 2F-2I). The cartoon in Fig. 2O shows a consolidated depiction of a first *Gl*Tom40 interactome, which includes the 8 proteins localized to mitosomes described above, as well as 4 previously identified matrix proteins and 3 newly validated hypothetical proteins comprised in the list of *Gl*Tom40 interacting proteins.

To test the second validation criterion, we performed reverse co-IP experiments, using the *Gl*Tom40 interaction partner with the highest MASCOT score (*Gl50803_29147*) as a first bait. The gene codes for a predicted single-pass transmembrane protein of 133 amino acids with mitosomal localization of an HA-tagged variant confirmed by fluorescence microscopy (Fig. 2B). Its domain structure is reminiscent of Tom40 receptors found in mitochondria of higher eukaryotes, i.e. a transmembrane helix in the N-terminal part of the protein followed by a cytoplasmically exposed C-terminal domain as predicted by TMHMM (http://www.cbs.dtu.dk/services/TMHMM/). Although experimental confirmation of a receptor function is pending, we henceforth refer to the *Gl50803_29147* product as *Gl*Tom40R. A cell line, constitutively expressing HA-tagged *Gl*Tom40R as a mitosome-localized co-IP bait protein produced a dataset of 221 *Gl*Tom40R co-IP exclusive proteins after filtering and elimination of all hits intersecting with the ctrl co- IP fraction at high stringency parameters (Fig. 3A; S6 Table). Importantly, the *Gl*Tom40R-HA bait protein and endogenous *Gl*Tom40 were detected with high MASCOT values, confirming the *Gl*Tom40 – *Gl*Tom40R interaction. The 221 *Gl*Tom40R co-IP specific hits and an additional 20 candidates from the *Gl*Tom40R/ctrl co-IP intersection that had peptide ratios >5 were parsed according to different metabolic and/or functional categories (Fig. 3B; S7 Table). In addition to *Gl*Tom40, the dataset contained several known mitosomal proteins, including matrix proteins HSP70 and GiOR1, cysteine desulfurase (IscS; *Gl50803_14519*), Cpn60, [2Fe-2S] ferredoxin (*Gl50803_27266*) and NifU-like protein. Using high stringency criteria, we retrieved all 8 hypothetical proteins previously identified in the *Gl*Tom40 co-IP dataset and 4 additional non-annotated candidate mitosome proteins listed in S8 Table (Fig. 3C-3F). Taken together, combined subcellular localization experiments and a first reverse co-IP dataset using the single-pass transmembrane *Gl*Tom40-interacting protein *Gl*Tom40R provided robust validation of the experimental approach used to identify mitosome membrane proteins, and has expanded the predicted mitosomal membrane and import machinery interactome to 22 proteins (Fig. 3G). Interestingly, this dataset contained two axoneme-associated GASP-180 proteins (*Gl50803_137716* and *Gl50803_16745*) [58]with high MASCOT scores.

The two high-stringency co-IP datasets suggests a strong interaction between *Gl*Tom40 and *Gl*Tom40R. Thus, hits appearing in the intersection of the two are considered to be particularly informative (Fig. 3H). The curated list of hits after elimination of obvious

cytoplasmic contaminants (S9 Table) contains 27 candidates, 10 of which have now been confirmed as mitosome proteins.

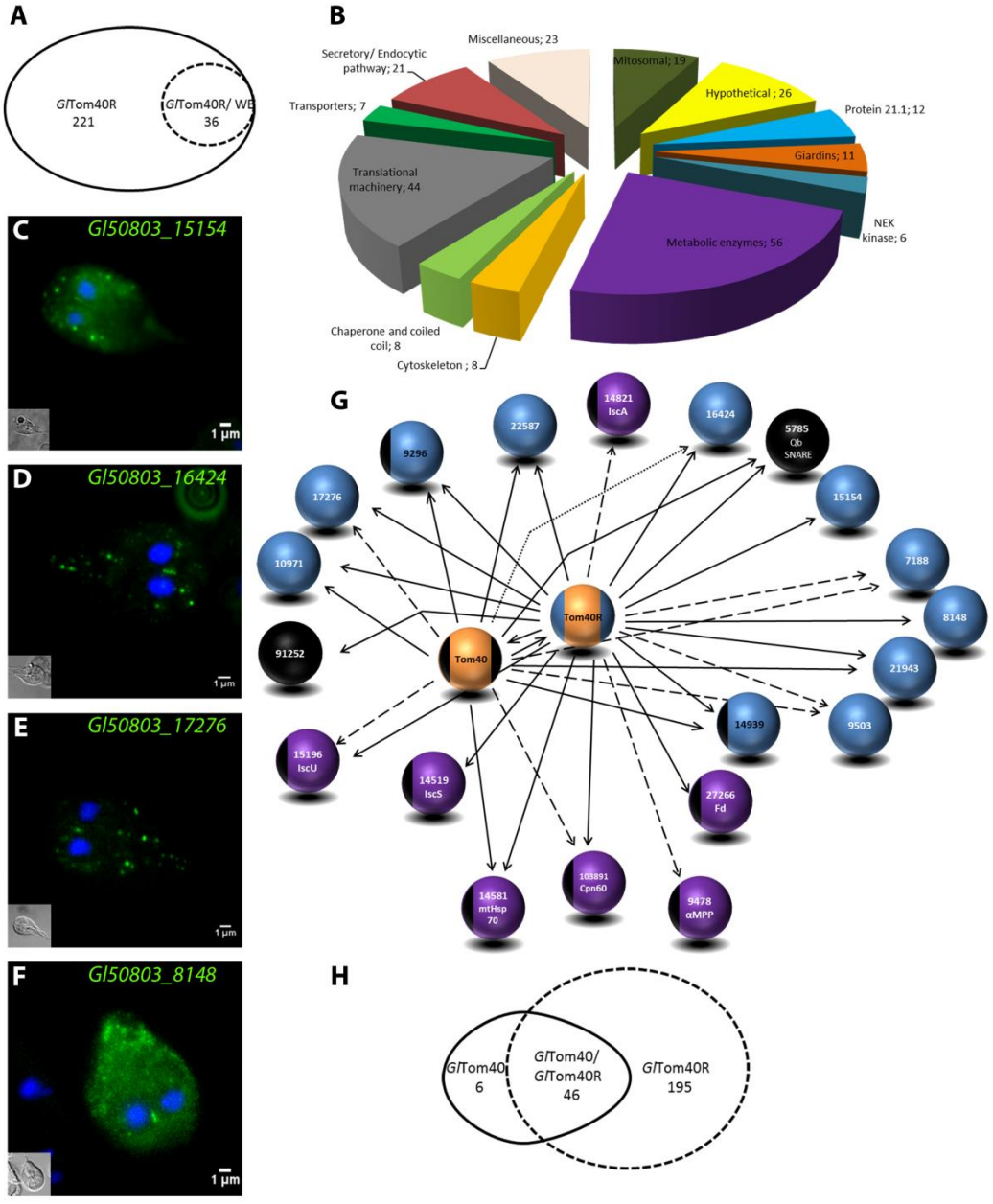


**Fig 3. Expansion and validation of the interactome by reverse co-IP with GlTom40R.**
(A) Venn diagram showing *Gl*Tom40R-specific proteins identified after filtering the dataset. (B) Parsing of 221 bait-specific and an additional 20 candidates from the *Gl*Tom40R/ctrl co-IP overlap that had peptide ratios >5 (metabolic and/or functional categories are indicated in the pie chart). (C-F) Subcellular localization of selected C-terminally HA-tagged novel hypothetical proteins by IFA (green). Nuclear DNA is stained with DAPI (blue). Insets: DIC images. (G) Preliminary interactome of *Gl*Tom40 and *Gl*Tom40R showing validated hits. Bait proteins (orange spheres), matrix proteins (purple), previously identified and localized proteins (black), and localized hypothetical proteins (blue). The stringency parameters used for detection (high, medium, and relaxed) are represented by bold, dashed, and dotted arrows, respectively. (H) Venn diagram showing the intersection of *Gl*Tom40 and *Gl*Tom40R datasets.

**Co-IP experiments confirm *Gl*Tom40-specific protein-protein interactions and reveal strong links with four additional mitosome proteins**

In the absence of an absolute measure for strength/affinity of the physical interaction between proteins in these interactomes we used MASCOT peptide scores as a non-exclusive qualitative criterion for "interaction" in a preliminary manner. To determine a robust *Gl*Tom40- and *Gl*Tom40R-centered core interactome consisting of the most frequently detected interaction partners and, more importantly, to explore the boundaries of the growing interaction network (Fig. 3G), we performed a series of additional co-IP experiments using HA-tagged Qb-SNARE 4 (*Gl50803_5785*), *Gl*IscS, and hypothetical proteins *Gl50803_9296* and *Gl50803_14939* as baits. These proteins were chosen because they were identified, in some cases exclusively, in both the *Gl*Tom40- and *Gl*Tom40R co-IP datasets (S2 and S6 Tables), suggesting they may be most proximal to *Gl*Tom40. Furthermore, mitosomal localization of all four HA-tagged bait proteins was confirmed by IFA (Fig. 2). As was done previously, all bait-specific datasets were processed by filtering with a ctrl co-IP dataset generated from un-transfected trophozoites and analyzed in MASCOT using high stringency (95_2_95) and more relaxed (95_1_95) parameters.

*Co-IP with the mitosome transmembrane protein Gl50803_14939*

*Gl50803_14939*, which contains two transmembrane domains (TMD), was analyzed because of its potential role as a component of the import complex. Using high stringency parameters (95_2_95) 129 proteins with a FDR of 10% were detected with 93 candidates specific for the *Gl*14939 co-IP dataset (S10 Table). Both *Gl*Tom40 and *G. lamblia* oxidoreductase 1 (GiOR1; ORF *Gl50803_91252*) were detected with these parameters, in addition to several previously identified hypothetical mitosome proteins (e.g. *Gl*Tom40R, *Gl50803_10971* and *Gl50803_7188)* (Fig. 4A). This further supports the idea that *Gl50803_14939* is a significant interacting partner of *Gl*Tom40 and *Gl*Tom40R.

*Co-IP with the predicted outer membrane protein Qb-SNARE 4 (Gl50803_5785)*

Qb-SNARE 4 has dual localization, (mitosome and ER; Fig. 2H) and was identified in both the *Gl*Tom40 co-IP and the *Gl*Tom40R reverse co-IP datasets. This suggests that Qb-SNARE 4 may have a role in inter-organelle communication between mitosomes and the ER, and potentially in protein/lipid transport [59,60]. We reasoned that identifying interaction partners could shed light on the nature of physical contacts between mitosomes and other membrane-bounded compartments. MS analysis of the *Gl*5785 co-IP dataset with medium stringency parameters (95_1_95) yielded a total of 260 proteins with a FDR of 0% of which 157 were bait-specific after filtering with ctrl co-IP (S11 Table). The bait protein itself along with *Gl*14939 were the only 2 proteins detected with high MASCOT values (≥ 5 peptide score). Several non- annotated proteins, e.g., *Gl50803_10971*, *Gl*Tom40R, *Gl50803_7188, Gl*Tom40 as well as Type III DnaJ protein *Gl50803_9751* were detected with lower MASCOT values (>1 but <5). Interestingly, another hypothetical protein in this dataset,

*Gl50803_9503*, was also shown to have a dual localization (Fig. 2I). This protein was present in the *Gl*Tom40 co-IP and *Gl*Tom40R co-IP datasets with medium stringency parameters (95_1_95). Identification of *Gl50803_9503* by the SNARE proteins and bait proteins harboring trans-membrane domains combined with dual localization to mitosomes and ER suggests that this protein might be involved in the organization of physical contact points, establishing direct links between mitosomes and ER. All known or previously identified proteins interacting with *Gl*5785 are depicted in Fig. 4B.

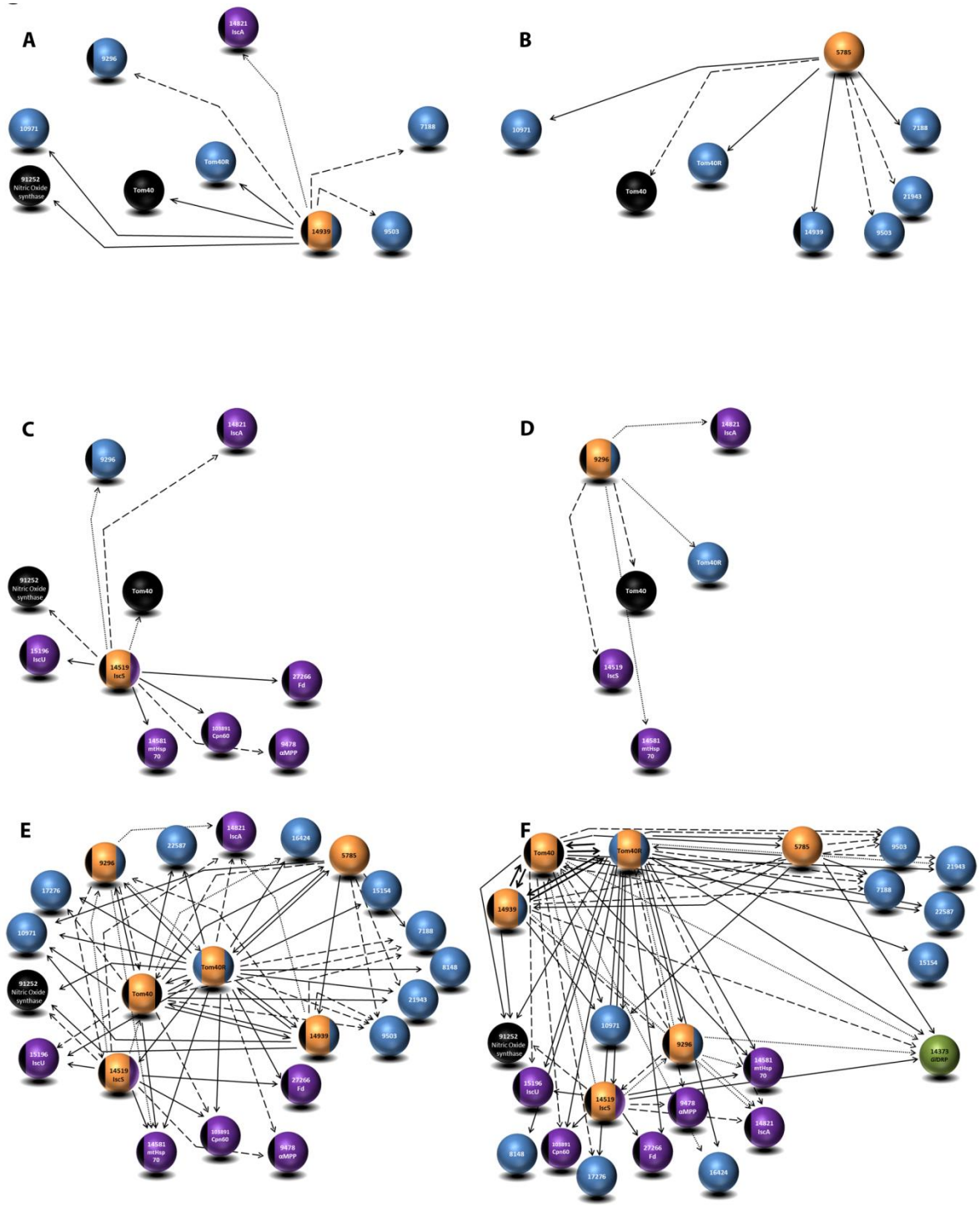

**Fig 4. Validation of the GlTom40 interactome by reverse co-IP using four additional mitosome proteins as bait.**

(A) *Gl*14939, (B) *Gl*5785, (C) *Gl*IscS and (D) *Gl*9296 –derived interactomes. (E, F) Alternative depictions of the cumulative interactome of proteins localizing to mitosomes generated with 6 bait proteins. Note the tight association of *Gl*Tom40 with *Gl*Tom40R and *Gl*14939. (F) Matrix and soluble proteins are grouped at the bottom left, proteins with dual localization (ER and mitosomes) and possibly involved in inter-organelle communication are grouped at the top right. *Gl*DRP is pulled down with all 6 bait proteins used in the co-IP assay and is also included (green sphere). Bait proteins (orange spheres), matrix proteins (purple), previously identified and localized proteins (black), and localized hypothetical proteins (blue). The stringency parameters used for detection (high, medium, and relaxed) are represented by bold, dashed, and dotted arrows, respectively.

*Co-IP with the matrix protein cysteine desulfurase (Gl*IscS*)*

Cysteine desulfurase (*Gl50803_14519*) is a mitosomal matrix protein and the central component of the Fe-S assembly machinery [61]. All mitosomal matrix proteins including *Gl*IscS are translated in the cytoplasm and reach their final destination after unfolding and translocation across the mitosome double membrane. Thus, this trafficking route (cytoplasm – translocon – matrix) should be reflected in the protein-protein interactions of a co-IP dataset with *Gl*14519-HA as bait. The MS dataset contained a total of 208 proteins using high stringency parameters (95_2_95), with a FDR of 1.5%. After filtering with ctrl co-IP, 177 bait-specific hits remained (S12 Table). Among those, we identified 5 known matrix proteins namely, NifU-like protein, HSP70, [2Fe-2S] ferredoxin, Cpn60, and GiOR1. *Gl*Tom40 as the sentinel protein for the translocon was detected only with relaxed stringency (50_1_50, FDR of 30%). Seventy out of 177 hits were highly specific for *Gl*IscS with ≥ 5 peptide counts. Eighteen of those (25%) belong to the Protein 21.1 family. The biological function of this cytoplasmic protein family in *G. lamblia* and the significant association to *Gl*IscS is not known [62]. The frequency of hits for 21.1 family members in the dataset might be relevant in the context of stabilization of *Gl*IscS in the cytoplasm before translocation and merits further investigation. No additional candidate components of the import machinery (i.e. novel proteins harboring TMDs) and/or novel or previously identified soluble proteins were identified using *Gl*14519 as bait protein. However, 43 additional hypothetical proteins still remain to be investigated for their localization and putative function. Fourteen out of 43 hypothetical proteins have high MASCOT values (peptide score of >5). Interestingly, MITOPROT analysis suggests that six out of these fourteen proteins harbor an identifiable MTS (S13 Table) and thus merit further investigation. All known/ previously identified proteins interacting with *Gl*5785 at varying stringency parameters are depicted in Fig. 4C.

*Co-IP with a hypothetical imported mitosome protein Gl50803_9296*

*Gl50803_9296* is a predicted soluble protein of unknown function localizing exclusively to mitosomes (Fig. 2E). Despite this, MS data analysis performed at high stringency parameters (95_2_95) yielded only 22 proteins with a FDR of 0% with 12 bait-specific hits. The bait protein itself was by far the most significant hit in the dataset and under stringent analysis

conditions the dataset contained no known mitosome proteins. Analysis with more relaxed stringency parameters (90_1_90) yielded 85 proteins with a FDR of 6.2% with 47 bait-specific identifications (S14 Table). Aside from the bait, 2 known mitosome proteins namely, *Gl*IscS and *Gl*Tom40 were identified. Taken together, the *Gl*9296 co-IP dataset suggests that this mitosome protein doesn't have an interactome enriched in matrix or membrane proteins despite its clear-cut localization and considerable expression levels judged by the signal obtained in Fig. 2E. Its localization might be in the intermembrane space, but remains to be determined. The fact that the putative *Gl*Tom40R was identified once with a very low stringency of 20_1_20 with a FDR of 51% suggested that *Gl9296* and *Gl*Tom40R don't interact directly, but could be connected *via* bridging proteins. All identified *Gl*9296-interacting proteins are depicted in Fig. 4D.

In summary, we have generated an extensive protein interaction network (Fig. 4E) from 6 independent co-IP assays using *Gl*Tom40 and 5 interaction partners (*Gl*Tom40R, *Gl50803_14939*, *Gl50803_5785*, *Gl50803_14519* and *Gl50803_9296*) selected as baits based on i) number of peptide hits in the *Gl*Tom40 co-IP dataset and ii) confirmed localization of epitope-tagged variants to mitosomes by IFA. Pending final validation of the >200 novel candidate matrix-, outer membrane, and membrane-associated mitosome components, the validated information from this series of co-IP experiments will be instrumental to refine and complete the current map of the mitosome protein repertoire shown in (Fig. 4E and 4F).

**Pharmacological induction of a mitosome matrix-targeted DHFR complex generates a protein import block and inhibits processing of an endogenous reporter in mitosomes**

The highly diverged *Gl*Tom40 orthologue in the *G. lamblia* genome is considered the translocase across the outer mitosomal membrane. However, there are currently no reports on the organelle-specific effects of interference on protein import into mitosomes. We tested to what degree mitosome protein import is functionally conserved with respect to the corresponding process in *bona fide* mitochondria by adapting the DHFR-folate analogue system [63] to *G. lamblia*. Pre-sequence directed DHFR is a classical substrate used in protein translocation studies due to its ability to fold irreversibly upon binding a folate analog, e.g. MTX. Complexed with MTX, DHFR becomes unsuitable as a substrate for import and blocks translocons, which results in a general blockage of organelle protein import [63]. Transfection of MTSfd$\Delta_{int}$-DHFR into a *Gl*17030-HA background, i.e. a line expressing a HA-tagged MTS-directed mitosomal reporter, allowed testing of the general effects of MTX-induced import block. Importantly, *G. lamblia* lacks a DHFR homologue, and heterologous over-expression of human DHFR did not result in any detectable phenotypic aberration or change in growth rate (data not shown). We reasoned that the presence of MTX in MTSfdΔint-DHFR expressing cells would lead to an import block with cytosolic accumulation

of the unprocessed form of *Gl*17030-HA due to jamming of the translocase. IFA indeed showed an increased cytosolic *Gl*17030-HA signal after addition of 1 µM MTX (Fig. 5B) compared to parasites exposed to the solvent alone (Fig. 5A). To test whether this was due to a generalized import block we measured the ratio of the slightly larger *Gl*17030-HA reporter precursor protein (+MTS) and the imported and therefore processed form (-MTS) by SDS-PAGE and Western blot using anti-HA antibodies. We detected accumulation of unprocessed *Gl*17030-HA in the MTX treated sample, whilst in the absence of MTX, only the processed form was present (Fig. 5C). Taken together the data strongly supported functional conservation of the structurally highly diverged protein import machinery of *G. lamblia* mitosomes.

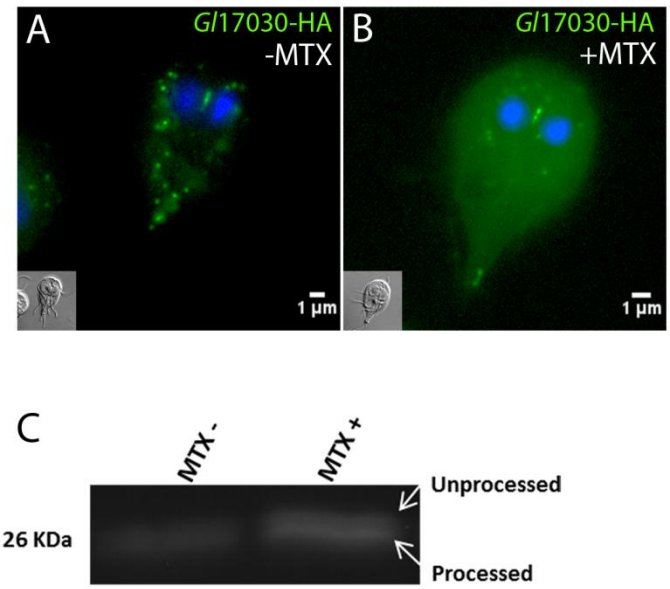


**Fig 5. Mitosome-targeted DHFR protein blocks import and processing of a reporter in transgenic cells treated with MTX.**

Subcellular distribution of a matrix targeted reporter (*Gl*17030-HA) without MTX (A) or after addition of 1µM MTX for 24 h (B) in transgenic cells expressing mitosome-targeted DHFR. Note the accumulation of HA-signal in the cytoplasm. Nuclear DNA is stained with DAPI (blue). Insets: DIC images. (C) Immunoblot analysis detects accumulation of unprocessed *Gl*17030-HA in the presence of MTX.

## Conditional ectopic expression of a dominant-negative GTP-locked DRP variant elicits a mitosome morphogenesis phenotype

Despite intensive research in the field of MROs, little is known regarding factors required for their division. Dynamin-related proteins (DRPs) are implicated in mitochondrial and hydrogenosome division in higher eukaryotes and in protozoa such as *Trypanosoma brucei* [64,65] and *Trichomonas vaginalis* [66]. *G. lamblia* harbors a single DRP (ORF *Gl50803_14373*) [54] with a previously documented role in trafficking of cyst wall material, and endocytic and exocytic organelle homeostasis [54]. Interestingly, *Gl*DRP was strongly overrepresented in 3 high-stringency co-IP datasets where mitosome membrane proteins were used as bait. Moreover, with relaxed stringency parameters *Gl*DRP was detected in all 6 co-IP datasets (Fig. 6H). To test for a hitherto unrecognized role of *Gl*DRP in determining mitosome morphology and/number, we used a dual cassette expression vector [53] to express constitutive C-terminally myc-tagged *Gl*Tom40 and inducible C-terminally HA-tagged wild-type (*Gl*DRP) or GTP-locked (*Gl*DRP-K43E) variants in trophozoites. IFA

analyses (Fig. 6A- 6F) demonstrate how the subcellular distribution for *Gl*Tom40-myc changed from "dispersed" in cells expressing *Gl*DRP-HA (Fig. 6A-6C) to "clustered" (Fig. 6D-6F), indicative of enlarged organelles in cells expressing *Gl*DRP-K43E-HA.

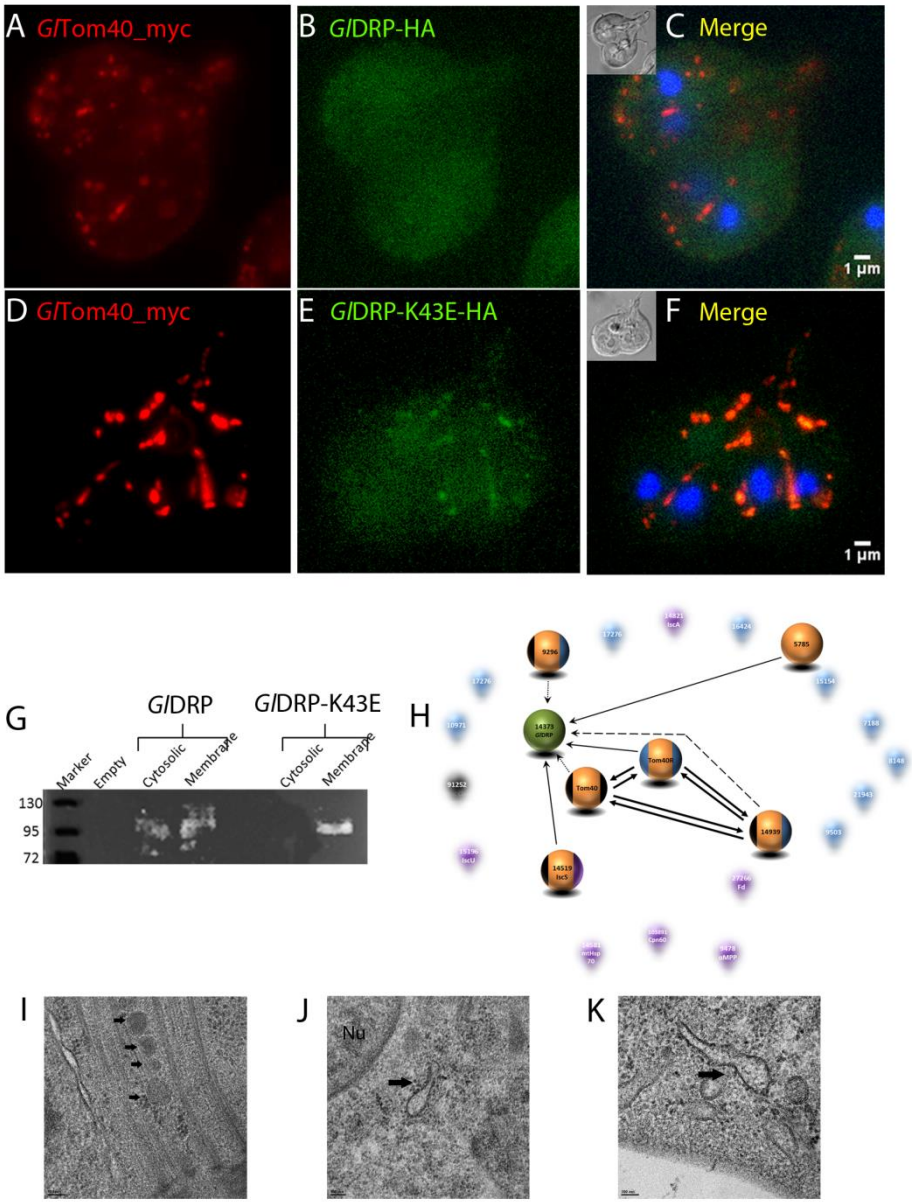


**Fig 6. Conditional expression of GlDRP-K43E elicits a mitosome morphogenesis phenotype.** (A-C) Subcellular localization of a C-myc tagged *Gl*Tom40 (red) by IFA in cells induced to express a wild type *Gl*DRP (green) or *Gl*DRP-K43E (D-F). Note the altered size and distribution of organelles labeled with Tom40-myc in *Gl*DRP-K43E expressing lines. Nuclear DNA is stained with DAPI (blue). Insets: DIC images (G) - Cell fractionation experiments confirm fixed membrane localization of *Gl*DRP-K43E. (H) *Gl*DRP (green) is associated to 6 bait proteins and identified at different stringency parameters as depicted in the *Gl*Tom40-centered interactome. Bait proteins (orange spheres), matrix proteins (purple), previously identified proteins (black), and localized hypothetical proteins (blue). The stringency parameters used for detection (high, medium, and relaxed) are represented by bold, dashed, and dotted arrows, respectively. (I) TEM: normal morphology of mitosomes (black arrows) in the CMC in cells expressing wild type *Gl*DRP whilst cells expressing *Gl*DRP-K43E show enlarged dumbbell-shaped mitosomes (black arrow in J, K) indicative of defective organelle division. Nu: nucleus. Scale bars: 100 nm.

Consistent with this phenotype and in line with previous reports [54], the subcellular distribution of HA-tagged *Gl*DRP remained mostly cytosolic (Fig. 6B). Conversely, *Gl*DRP-K43E-HA showed a punctate distribution (Fig. 6E) and significant signal overlap with *Gl*Tom40-myc (Fig. 6F), suggesting selective accumulation of *Gl*DRP-K43E-HA on mitosome membranes. We tested whether this marked association of ectopically expressed *Gl*DRP-K43E with organelle membranes compared to the wild type DRP variant in IFA could be corroborated in cell fractionation experiments. Separation by SDS-PAGE and immunoblot analysis revealed that epitope-tagged *Gl*DRP-HA was almost equally distributed between the "cytosolic" and "membrane" fraction, whereas the mutated variant *Gl*DRP-K43E-HA was detected only in the "membrane" fraction (Fig. 6G). This data was consistent with the microscopical analysis in Fig. 6E and a strongly increased association with organelle membranes compared to wild-type *Gl*DRP-HA. To characterize the nature of the *Gl*DRP-K43E phenotype in more detail, we performed transmission electron microscopy of induced transgenic cells. Cells expressing the GTP-locked *Gl*DRP-K43E-HA variant frequently presented elongated and tubular mitosome structures (Fig. 6J and 6K) compared to cells expressing wild type *Gl*DRP (Fig. 6I). This was consistent with IFA data in Fig. 6D and 6A and suggestive of an organelle morphogenesis phenotype. Taken together, these data provide an explanation for the frequent detection of *Gl*DRP in co-IP datasets and strongly support a transient association of *Gl*DRP to these organelles. The phenotype elicited by expression of GTP-locked *Gl*DRP-K43E-HA suggests a previously unappreciated role for this GTPase in the maintenance of mitosome integrity and organelle morphogenesis.

### *G. lamblia* mitosomes are immobilized and do not form dynamic networks

Mitochondria in higher eukaryotes are highly dynamic organelle networks that move in the cell via microtubules and microfilaments and undergo constant fission and fusion to meet the energy requirements of the cell [67,68]. IFA and TEM analyses suggest that *G. lamblia* mitosomes are very small spherical organelles with no evidence of network formation. In addition, the mitosome population in each cell can be divided into peripheral mitosomes (PM) distributed randomly in the cytoplasm and what has been dubbed the central mitosome complex (CMC) [22]. The latter appear to form a grape-like cluster of individual organelles of the size and shape of peripheral mitosomes that is closely and permanently associated to the basal body complex between the two nuclei [22]. Interestingly, these organelles remain separate despite their close proximity. The motility of this central cluster is restricted to segregation with the duplicated basal body complex during cell division [22]. However, no information is available on the spatial dynamics of peripheral mitosomes in the cytoplasm. We investigated organelle dynamics in living cells by performing time lapse microscopy of cells expressing GFP-tagged mitosome reporters. Conditional expression of N-

terminally GFP-tagged *Gl*Tom40 with 3 h of induction followed by "chasing" newly-synthesized GFP-Tom40 into mitosomes over 2-3 h in normal conditions can be used to label organelles for imaging (Fig. 7A and 7B). Tracking of individual organelles over a period of >30 min showed no significant cytoplasmic movement or changes in morphology (Fig. 7C), suggesting that organelles neither move randomly nor are they transported directionally in the cytoplasm along cytoskeleton structures. This is consistent with the lack of motor proteins in any of the interactomes, suggesting that peripheral organelles do not undergo frequent fusion and fission and may have lost the ability for fusion altogether. To test whether mitosome outer membrane proteins are exchanged between organelles we performed FRAP experiments on cells conditionally expressing *Gl*Tom40-GFP. Since *Gl*Tom40-GFP is membrane-anchored, FRAP addresses the question how isolated mitosome organelles are and whether they form membrane continuities. No recovery of fluorescence in bleached CMC or PM organelles was detected (Fig. 7D- 7G), even when re-imaging bleached areas after 20 min. Identical outcomes were observed in cells constitutively expressing GFP-tagged *Gl*Tom40R (data not shown). GFP-tagged *Gl*Tom40R was expressed constitutively from episomal (circular) expression vectors. The reporter localized exclusively to mitosome organelles in all cases, but many cells showed a mitosome morphology dubbed "string" phenotype suggestive of extensive elongation of organelles to large tubules (Fig. 7H). In many cases, virtually all PMs had been replaced by a single long organelle with a diameter that corresponded to that of an individual mitosome. FRAP analysis confirmed that these tubular mitosomes were made from a single contiguous membrane (data not shown). Although the "string" mitosome phenotype was compatible with survival of the parasites, many trophozoites appeared to be delayed or even arrested in cytokinesis and had a typical heart-shaped appearance (Fig. 7I) previously observed in cells which cannot complete cytokinesis [69]. Because the tubular organelles ran through the non-divided part connecting both daughter cells, we postulated that inability to divide mitosomes impairs completion of cytokinesis.

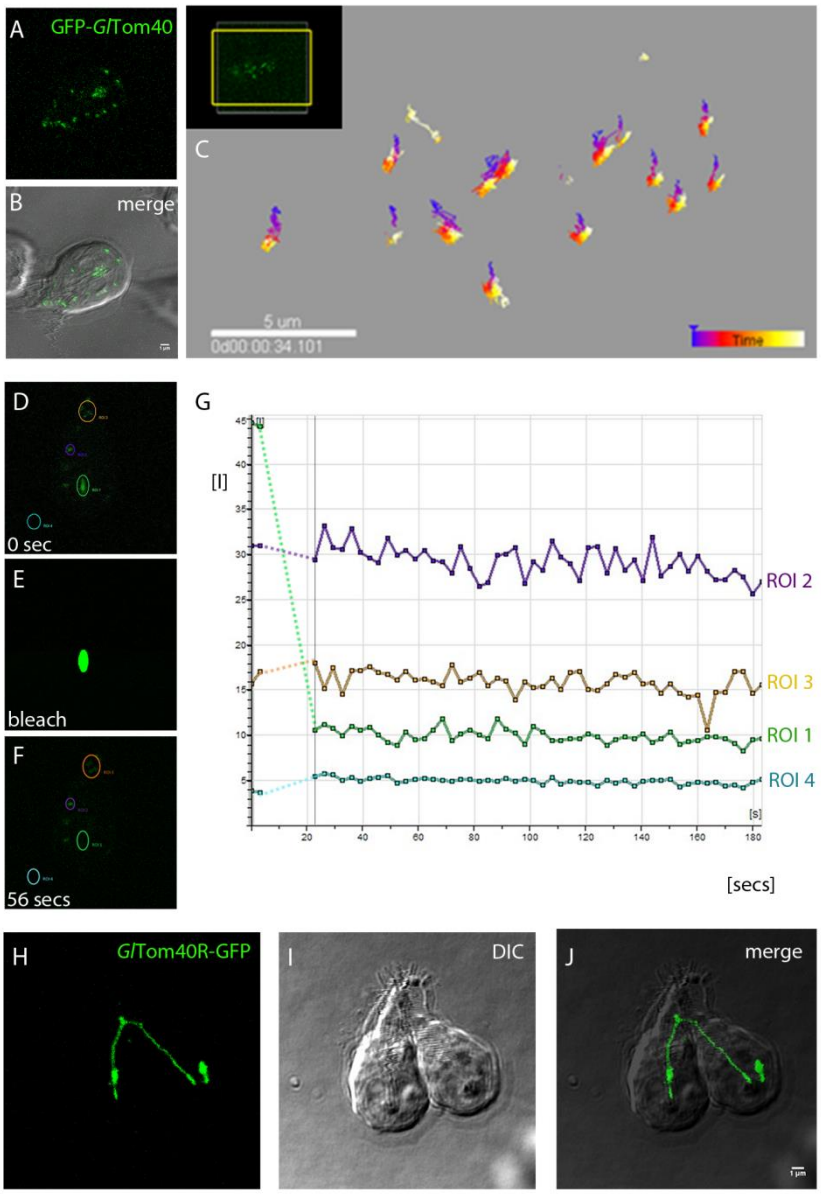


**Fig 7. G. lamblia mitosomes are immobilized and do not form dynamic networks**

(A-B) Detection of typical organelle distribution of GFP-tagged *Gl*Tom40 (green) in time-lapse microscopy. (B) Overlay showing the CMC in between the two nuclei and PMs dispersed throughout the cell. (C) Tracking of organelles during a period of 30 min shows no significant movement of mitosomes in the cytosol. (D-G) FRAP experiments performed on cells conditionally expressing GFP-tagged *Gl*Tom40 suggest that outer membrane proteins are not able to move amongst/in between organelles. (E) Photobleaching of a single mitosome (region of interest 1 (ROI 1)) in a living cell is shown. (F-G) Fluorescence in a bleached organelle (green line in the graph) does not recover even after several minutes (>20 min). Purple and brown lines in the graph represent fluorescence in unbleached areas (ROIs 2 and 3). (G) Fluorescence micrographs from the image series at the start (0 sec) of the experiment, during bleaching, and at the beginning of the recovery phase (20 sec). Arbitrary units of fluorescence are indicated [I]. Broken lines connect pre- and post-bleaching values in the graph. (H-J) "String" mitosome phenotype observed upon constitutive expression of GFP- tagged *Gl50803_29147* (*Gl*Tom40R- GFP). (H) *Gl*Tom40R-GFP localized exclusively to mitosomes and in some cases virtually all of the peripheral organelles have been replaced by a single long tubular mitosome spanning both daughter cells length-wise. (I) DIC image. (J) Overlay of the two channels. Scale bar: 1 μM.

## Discussion

Eukaryotes that were previously considered to be amitochondriate are now known to contain MROs such as hydrogenosomes and mitosomes [70,71]. Although there is a consensus that MROs are evolutionarily derived from mitochondria, there is extensive structural and functional divergence among organelles in different species. Bioinformatics analyses show clearly that constraints for sequence divergence vary greatly, i.e. components of the universal enzymatic machinery for the Fe-S protein maturation in MROs can be detected in the nuclear genome using straightforward homology searches, whereas most MRO membrane proteins have diverged beyond recognition if they were not lost altogether. Three groups of membrane proteins are of particular interest in terms of organelle function and propagation: the TOM/TIM complex and other protein import machinery, factors that mediate interaction with the ER and the cytoskeleton, and transporters for ADP/ATP and other building blocks. Attempts to discern the contribution of MROs to the cell's metabolism and catabolism and to understand why these organelles have been preserved even after they lost their role in energy metabolism are confronted with two obstacles. Firstly, extensive sequence divergence prevents identification of organelle proteins *via* homology-based searches and secondly, the function of candidate factors identified by other means and localized to organelle membranes can usually not be deduced based on existing structural information from well-characterized mitochondrial homologs. In addition, the divergence between orthologues of MRO proteins even in closely related species is very high. A case in point is *Gl*TOM40 whose sequence degeneration is so extensive that the identification of orthologues in *Giardia*, *Entamoeba* or *Spironucleus* remains tentative despite the constraints imposed by the beta barrel structure of these mitochondrial porins [44]. Unambiguous identification is even more difficult for highly diverged proteins that lack clearly identifiable structural domains (e.g. a putative *Gl*Tim44 homolog, a component of the TIM complex) [72].

*G. lamblia* mitosomes remain the smallest known and least characterized MROs. Systematic identification of protein components using proteome analysis of enriched mitosome preparations has proven challenging primarily due to extensive contamination and difficulty to isolate organelles in sufficient amounts [33,48]

Here, we accounted for the paucity of data which may inform strategies for the systematic identification of *Giardia* mitosome proteins by implementing an approach based on MS analysis of chemically stabilized protein-protein interactions. Our starting premise was that the diminutive mitosomes harbored no more than 100-150 different proteins inside or associated with a clearly delineated cellular compartment. Using a putative *Gl*TOM40 [22,33] as a starting point, this study focused on organelle membrane components, in particular the

mitosome protein import machinery whose function has been demonstrated but whose composition remains unknown.

With only six bait proteins, the strategy based on iterative co-IP experiments allowed for building a core membrane interactome and a complex interactome network extending inwards to the organelle matrix as well as outwards to components of the ER membrane, the axoneme cytoskeleton and the cytoplasm. The rationale is that with sufficient numbers of reverse co-IP experiments using validated organelle proteins as baits, a comprehensive organelle proteome can be built.

Co-IP with *Gl*Tom40 as bait and reverse co-IP performed with 5 subsequent new bait proteins resulted in identification of 22 mitosomal proteins (annotated and hypothetical) out of which 16 proteins were localized to mitosomes; 5 proteins displayed dual localization to mitosomes and ER and one protein (*Gl*7188) showed a ER and PV pattern even though it was pulled down exclusively with mitosome-localized bait proteins harboring TMDs. Based on their localization pattern, we grouped these mitosome proteins into 2 categories (Fig. 4F). The group at the bottom left with *Gl*IscS at the center depict proteins with exclusive mitosome localization suggesting that these proteins are mitosome residents (soluble or membrane-anchored) whereas the group at the top right (Fig. 4F) includes all proteins with dual localization, suggesting they might be at the junction between ER and mitosomes with a potential role in establishing inter-organelle communication, e.g. for lipid transport.

### *Gl*Tom40 and interaction partners *Gl*Tom40R and *Gl*14939: a minimized mitosome protein import apparatus?

Following its identification as a prominent *Gl*Tom40 interaction partner, the single pass membrane protein *Gl*Tom40R was the first bait protein selected for reverse co-IP in order to validate the experimental procedure and to expand the *Gl*Tom40 interactome. Importantly, the protein has a predicted N-terminal TMD similar to mitochondrial Tom40 receptors (Tom20 and Tom70) in *Saccharomyces cerevisiae*. Furthermore, this TMD is preceded by a short N-terminal region and followed by a large C-terminal stretch. Ectopic expression of the C-terminal portion of *Gl*Tom40R alone showed a distinct cytosolic localization by IFA (data not shown), without a detectable phenotype. However, several *in silico* analysis tools failed to predict a MTS at the protein's N-terminus. Nevertheless, a C-terminally GFP-tagged full-length variant determines the specific topology of this protein. We have shown previously that GFP only fluoresces if exposed to the cytoplasm and never after import into mitosomes ([22] and unpublished data). Therefore, the brightly fluorescing and mitosome-localized *Gl*Tom40R-GFP fusion provided conclusive data and is a direct proof for the proposed topology of *Gl*Tom40R. This transgenic line also provided an additional tool for time lapse microscopy of mitosomes in trophozoites.

Reverse co-IP using *Gl*Tom40R as bait pulled down *Gl*Tom40 with the most abundant peptide counts and 220 additional specific proteins (annotated and hypothetical). So far 20 proteins have been validated by localization to mitosomes, allowing for a significant expansion of the *Gl*Tom40/*Gl*Tom40R interactome. The topology of *Gl*Tom40R, its exclusive mitosomal localization, and the repertoire of pulled down proteins further supports that *Gl*Tom40R is a Tom40 accessory protein with a potential receptor function for protein import. Specifically, the long cytoplasmically exposed C-terminal stretch interacts with several imported matrix proteins independently of the presence of a predicted transit peptide (S6 Table). To test this idea, we performed co-IP using the HA-tagged C-terminal part of *Gl*Tom40R (amino acid 31-133), which has a cytoplasmic localization, under non-crosslinking conditions. The resulting data is difficult to interpret, given that out of a total of 232 proteins detected at high stringency (95_2_95), 171 were specific to the C-terminal *Gl*Tom40R with none of the previously known mitosomal resident proteins in the dataset. However, upon analysis with medium stringency parameters (95_1_95), we identified only 2 novel hypothetical mitosomal proteins (*Gl*16424, *Gl*9503) in the C-terminal *Gl*Tom40R specific dataset. This suggests that the cytoplasmic *Gl*Tom40R fragment does not recapitulate the interaction properties of the full-length membrane anchored variant. Taken together, the co-IP data suggest that i) capture of imported matrix proteins is context-dependent, i.e. likely requires incorporation of the receptor domain into a TOM complex, and ii) interaction with *Gl*Tom40 requires the domains on either side of the membrane anchor and possibly additional accessory membrane proteins. Hence, the hypothesis of a receptor function for *Gl*Tom40R remains to be tested directly to evaluate its exact role in proteins import. Interestingly, although BLASTp yielded no strong homologs for *Gl*Tom40R, profile sequence comparisons with HHpred showed homology to a “high potential iron sulfur protein” (p-value 0.007). “High potential iron sulfur protein” in higher eukaryotes, also known as mitoNEET, is an integral membrane protein localized at the outer membrane of mitochondria and is responsible for transport of iron into mitochondria [73]. If we consider that Fe-S protein maturation is the only metabolic pathway currently associated to *G. lamblia* mitosomes, *Gl*Tom40R might also function as a mitoNEET homolog in *G. lamblia*.

Another *Gl*Tom40 interaction partner of special interest is *Gl*14939. This protein was exclusively identified in the *Gl*Tom40 and the *Gl*Tom40R co-IP datasets, suggesting that *Gl*14939 and *Gl*Tom40R may function as part of a complex. TMHMM predicts two TMDs at its N-terminus, followed by a large C-terminal domain in *Gl*14939. Powerful HMMER-based searches across several eukaryotic lineages, including the closely related diplomonad *Spironucleus salmonicida* [74], yielded no orthologues for this protein (data not shown). To date, there is no further information available indicating a function for *Gl*14939. However, a recent study showed that *Gl*14939 (dubbed GiMOMP35) localizes at the outer mitosome

membrane with its C- terminus in the cytosol [72]. Nonetheless, given that *Gl*Tom40 (the translocon), *Gl*Tom40R, and *Gl*14939 (putative accessory protein) are outer membrane-associated proteins and part of the same interactome, the data is consistent with a minimized import apparatus whose core import machinery is composed of only these three proteins. Likewise, a function in protein import of several other novel hypothetical proteins without TMD, e.g. *Gl*10971, *Gl*9296, *Gl*8148, *Gl*17276, and *Gl*16424, remains to be elucidated. Reverse co-IP using *Gl*9296 as bait protein pulled down *Gl*IscS, *Gl*IscA, *Gl*Hsp70, and outer membrane proteins including *Gl*Tom40 and *Gl*Tom40R, indicating close association to the import machinery and imported matrix proteins. Furthermore, *Gl*9296 has a predicted MTS but protein sequence analysis using the SMART prediction tool identified no functional domain of significance. Similarly, *Gl9296* appears specific to the *Giardia* lineage. Given its interaction profile, predicted import signal, and lack of homology to metabolic enzymes, we hypothesize that *Gl*9296 is a matrix protein interacting with the import pore in mitosomes. Recent developments in gene knockout strategies in *G. lamblia* [75] will facilitate the definition of the role of these novel hypothetical proteins.

All 24 localized mitosome proteins (previously known and newly identified hypotheticals) were parsed according to molecular function and biological process (S3A and S3B Figs) using Blast2go (https://www.blast2go.com/). Metal ion, Fe-S, ATP, and protein binding were the major molecular functions associated with these proteins. Interestingly, other biological processes involving response to lipid and transmembrane transport were also identified with significant p-values. An additional 93 candidates annotated as hypothetical proteins (from all the 6 co-IP assays) were analyzed using Blast2go (S4A and S4B Figs). Binding and catalytic activities were the 2 major GO terms associated to this group. Their potential involvement in binding of lipids, flavin mono-nucleotide co-factor, metal ion, Fe-S cluster, calcium ion, nucleotide, Fe and protein kinase will have to be tested experimentally. The number of combined candidate mitosome proteins after elimination of obvious contaminants such as cytoplasmic proteins is sufficiently large to suggest that mitosomes may have a role beyond Fe-S protein maturation. Only recently the major function of *E. histolytica* mitosomes was shown to be sulfate activation, and not Fe-S protein maturation as previously thought [44]. Although genes involved in this pathway are missing in other MRO-containing organisms such as *G. lamblia*, *T. vaginalis*, and *C. parvum*, the *Entamoeba* example points to a wider range of functions ascribable to mitosomes. This may even include general functions in stage-differentiation as recently shown in *E. histolytica* whose mitosomes are essential for the encystation process [76].

**Mitosome-ER contact sites**

Co-IP data identified proteins with dual localization at mitosomes and ER. Contact between these organelles mediates at least two major functions, i.e. replication of mitosomes

and transport associated to lipid biosynthesis. Thus far, we have identified five mitosome proteins with dual localization potentially involved in inter-organelle communication (Fig. 4F). One of them is a transmembrane Qb-SNARE 4 (*Gl50803_5785)* [77] identified in *Gl*Tom40 and *Gl*Tom40R co-IP datasets. IFA analysis localized a tagged variant to mitosomes and parts of the ER.

For their biogenesis, mitochondria and MROs rely on lipid transfer from the ER, the central site for phospholipid synthesis in the cell [78,79]. SNAREs are best known for mediating membrane fusion in vesicular transport [80] In the context of mitochondria and the ER, they function as components of so called ER-mitochondria encounter structures (ERMES). In addition to being associated to mitochondrial protein import [81,82], ERMES fulfills an essential function in inter-organelle lipid transport [81]. Phosphatidylserine is shuttled from the ER to mitochondria through the ERMES complex where it is converted to phosphatidylethanolamine (PE) by a decarboxylation reaction that generates most if not all PE in mitochondria [81,83]. Whether this function is preserved in Giardia mitosomes is not known, however, organelle biogenesis necessarily depends on ER-derived lipids which are transported to mitosomes either by carrier proteins or *via* membrane contact sites. The latter requires a tethering complex to facilitate phospholipid exchange between the two organelles. We explored the idea that Qb-SNARE 4 is part of a larger complex mediating ER-mitosome interaction by generating co-IP data. Indeed, in addition to outer membrane proteins such as *Gl*Tom40, *Gl*Tom40R and *Gl*14939, 3 hypothetical proteins were identified in the dataset, two of which, *Gl*9503 (3 TMDs) and *Gl*21943 (soluble), localized both to the ER and to mitosomes. In addition, data mining identified a domain in *Gl9503* with similarity to a yeast "Maintenance of mitochondrial morphology" protein 1 (Mmm1) of the ERMES complex as well as a predicted anhydrolase domain involved in lipid synthesis. HHpred analysis revealed a link between *Gl*21943 and a beta barrel lipid binding protein MLN64 (e-value 0.0006) in *H. sapiens* which facilitates cholesterol transport to mitochondria [84]. This preliminary data points to an outer mitosomal membrane-associated complex in *G. lamblia* mitosomes involved in generating ER-mitosome membrane contact sites analogous to ERMES. However, unlike in the hydrogenosome-containing *T. vaginalis* [85], ERMES homologs have not been identified in *G. lamblia* possibly due to extensive sequence divergence. Further experiments are necessary to test whether the dually-localized proteins *Gl*21943, *Gl*22587, *Gl*5785, *Gl*9503 and *Gl*15154 (Figs. 2F-2I and Fig. 3C) are indeed components of bona fide ER-mitosome membrane contact sites.

**Functional analysis of protein import into the mitosome matrix**

Using transgenic lines co-expressing MTSfd$\Delta_{int}$-DHFR and *Gl*17030-HA we induced a protein import block by addition of the folate analog MTX. Accumulation of the reporter in the cytoplasm upon MTX treatment shown in IFA (Fig. 5A and 5B) suggested blocked import

of the reporter presumably as a result of clogging of the import pore. Consistent with this, cells exposed to MTX presented accumulation of the unprocessed form of the reporter *Gl*17030-HA in a Western blot analysis (Fig. 5C). Based on the interaction of MTX with the mitosome targeted DHFR this is evidence for a blockage of the import pore analogous to established assays in bona fide mitochondria [63]. The data also confirms the previously tested notion that membrane translocation requires pre-proteins to remain in an unfolded state [72]. Furthermore, it provides direct experimental evidence for the functional conservation of the mitosome protein import pathway and the presence of a canonical general insertion pore (GIP)/translocon in *G. lamblia* mitosomes. Given that *Gl*Tom40 localizes exclusively to mitosomes and is the only predicted beta barrel protein in *G. lamblia*, this highly diverged protein is currently the only candidate for the mitosomal translocon. Interestingly, recent reports on mitochondrial protein import in *T. brucei* (Excavata super-group) identified an archaic TOM (ATOM) as the functional translocase at the outer mitochondrial membrane [86]. ATOM is not phylogenetically related to canonical Tom40 proteins, suggesting there is more than one kind of eukaryotic translocase that can function as an import pore. Whether this is also the case in *G. lamblia* remains to be investigated.

**Mitosome dynamics and a novel role for *Gl*DRP in mitosome morphogenesis**

We had previously shown that replication and inheritance of the CMC is coordinated in a cell cycle-dependent manner, whereas PMs divided stochastically [22]. The lack of a system to track organelles in living trophozoites precluded addressing the question whether mitosomes were motile and constituted a dynamic network of organelles. Development of two GFP-tagged reporters GFP-*Gl*Tom40 and *Gl*Tom40R-GFP (this study) allowed for time-lapse experiments to follow individual organelles in a cell. However, we found no evidence for motility of organelles, neither in the CMC nor in PMs, even after prolonged observation (1.5 h). Moreover, FRAP experiments revealed no exchange of GFP-tagged membrane proteins between organelles during the period of observation (Fig. 7F and 7G), which further corroborated the relative isolation of mitosomes within the cytosol. The lack of motility, inter-organelle contact and -interaction in *Giardia* mitosomes complicates investigation of their replication and morphogenesis. The two most plausible scenarios for this are currently the following: i) PMs are released from the CMC, which continuously produces new organelles by elongation and fission to maintain a constant number of organelles in a cell-cycle independent manner; ii) PMs and the CMC organelles replicate independently in a cell-cycle independent and -dependent manner, respectively [22]. Although time-lapse microscopy experiments did not provide evidence for either scenario, conditional expression of a dominant-negative, constitutively active *Gl*DRP-K43E revealed a distinct morphogenesis phenotype (see also below) indicative of an organelle replication defect. Moreover, the distinctive “string” mitosome phenotype in cells expressing *Gl*Tom40R-GFP clearly demonstrated that mitosomes can assume an elongated, tubular morphology, which is a

prerequisite for organelle division and replication. The implication is that *G. lamblia* mitosomes retain at least the machinery for fission in which the mechanoenzyme DRP plays a central role. Without the capability for fusion, this organelle "network" remains in a maximally fragmented state. The "string" mitosome phenotype therefore reflects a lack of fission, for example because the presence of the GFP-tagged protein on the surface interferes with recruitment of DRP to the mitosome membrane.

As one of the key players in the regulation of mitochondrial fission, dynamin related protein (DRP) is a mechanoenzyme conserved from yeast to vertebrates [87,88,89,90]. *G. lamblia* harbors a single dynamin homologue (*Gl*DRP) encoded by ORF *Gl50803_14373*; this protein has been shown to play a major role in this parasite's endocytic pathway and stage conversion [54,91,92]. Transgenic parasites expressing the mutant *Gl*DRP-K43E protein exhibited larger and fewer mitosomes, compared to cells overexpressing wild type *Gl*DRP (Fig. 6). This is in line with the dominant-negative effect on mitochondrial fission elicited by the corresponding mutation in DRPs in other organisms. To our knowledge, this is the first report on the involvement of *Gl*DRP in mitosome homeostasis, supporting the (at least partial) functional conservation of mitochondrial and MRO fission [93,94,95,96]. The notion that *G. lamblia* mitosome fission is functionally conserved is further substantiated by the identification of ORF *Gl*22587 in the mitosome-specific co-IP datasets. This protein presents dual localization to mitosomes and the ER. Interestingly, HMMER-based predictions relate *Gl*22587 to human mitochondrial fission protein (Fis1, e-value 6.3E-05) which, along with mitochondrial fission factor (Mff) and mitochondrial dynamics proteins (MiD 49 and MiD51), acts as a receptor to recruit dynamin-related protein 1 (Drp1) to the mitochondrial surface [97,98]. The isolation of *Gl*22587-interaction partners might lead to the identification of regulators and recruiting factors for *Gl*DRP, thereby shedding light on the composition of the mitosome fission machinery and replication mechanism in *Giardia*.

## Conclusion

Starting from the premise that mitosomes represent distinct cellular compartments with a very limited number of components in close physical proximity, we used an iterative approach based on co-IP experiments to generate a *Gl*Tom40-centered interactome network. The ultimate purpose of this strategy is to build a full proteome, which delineates the full complement of organelle proteins, peripherally associated factors, as well as interfaces with the ER and the cytoskeleton. Although this strategy requires numerous rounds of sequential co-IP and validation, it is highly informative because it produces interaction data in addition to identifying novel proteins. Combined with testing of epitope-tagged variants of candidate proteins for organelle localization as a straightforward validation criterion, serial co-IPs allow unambiguous definition of the organelle-specific proteome, as well as interfaces with other

cellular structures. A case in point is the complete lack of false-negative hits in the *Gl*IscS co-IP dataset, which contained all previously identified factors in addition to numerous novel candidate matrix and inner membrane proteins. Due to the extreme sequence divergence in nuclear-encoded genes for mitosome proteins, functional models for most components and pathways cannot simply be replicated based on a mitochondrial blueprint, but require almost complete *ab initio* (re)construction. Consequently, an exact and comprehensive delineation of the organelle proteome is an indispensable prerequisite for any attempt at defining the functional range of mitosome metabolism, as well as the organelle's machinery for replication and morphogenesis.

## Acknowledgements

We thank Therese Michel for technical assistance. Dr. Peter Hunziker and his team at the proteomics service facility of the Functional Genomics Center-Zürich are gratefully acknowledged for their support in tandem mass spectrometry performance and analysis. Prof. Robert Sinden at Imperial College, London (UK) is gratefully acknowledged for providing the human DHFR-encoding plasmid. Dr. Chandra Ramakrishnan is gratefully acknowledged for critical revision of the manuscript.

## References

**1. Gray MW, Burger G, Lang BF (1999) Mitochondrial evolution. Science 283: 1476-1481.**

**2. Hedges SB, Blair JE, Venturi ML, Shoe JL (2004) A molecular timescale of eukaryote evolution and the rise of complex multicellular life. BMC Evol Biol 4: 2.**

**3. Yang D, Oyaizu Y, Oyaizu H, Olsen GJ, Woese CR (1985) Mitochondrial origins. Proc Natl Acad Sci U S A 82: 4443-4447.**

**4. Olsen GJ, Woese CR, Overbeek R (1994) The winds of (evolutionary) change: breathing new life into microbiology. J Bacteriol 176: 1-6.**

**5. Viale AM, Arakaki AK (1994) The chaperone connection to the origins of the eukaryotic organelles. FEBS Lett 341: 146-151.**

**6. Bauer MF, Hofmann S, Neupert W, Brunner M (2000) Protein translocation into mitochondria: the role of TIM complexes. Trends Cell Biol 10: 25-31.**

**7. Jensen RE, Johnson AE (2001) Opening the door to mitochondrial protein import. Nat Struct Biol 8: 1008-1010.**

**8. Koehler CM, Merchant S, Schatz G (1999) How membrane proteins travel across the mitochondrial intermembrane space. Trends Biochem Sci 24: 428-432.**

**9. Matouschek A, Pfanner N, Voos W (2000) Protein unfolding by mitochondria. The Hsp70 import motor. EMBO Rep 1: 404-410.**

**10. Prokisch H, Scharfe C, Camp DG, 2nd, Xiao W, David L, et al. (2004) Integrative analysis of the mitochondrial proteome in yeast. PLoS Biol 2: e160.**

**11. Reinders J, Zahedi RP, Pfanner N, Meisinger C, Sickmann A (2006) Toward the complete yeast mitochondrial proteome: multidimensional separation techniques for mitochondrial proteomics. J Proteome Res 5: 1543-1554.**

**12. Sickmann A, Reinders J, Wagner Y, Joppich C, Zahedi R, et al. (2003) The proteome of Saccharomyces cerevisiae mitochondria. Proc Natl Acad Sci U S A 100: 13207-13212.**

**13. Pfanner N, Truscott KN (2002) Powering mitochondrial protein import. Nat Struct Biol 9: 234-236.**

**14. Gabaldon T, Huynen MA (2004) Shaping the mitochondrial proteome. Biochim Biophys Acta 1659: 212-220.**

**15. Cerkasovová A, Lukasová G, Cerkasòv J, J K (1973) Biochemical characterization of large granule fraction of Tritrichomonas foetus (strain KV1). Journal of Protozoology 20.**

**16. Lindmark DG, Muller M (1973) Hydrogenosome, a cytoplasmic organelle of the anaerobic flagellate Tritrichomonas foetus, and its role in pyruvate metabolism. J Biol Chem 248: 7724-7728.**

**17. Mai Z, Ghosh S, Frisardi M, Rosenthal B, Rogers R, et al. (1999) Hsp60 is targeted to a cryptic mitochondrion-derived organelle ("crypton") in the microaerophilic protozoan parasite Entamoeba histolytica. Mol Cell Biol 19: 2198-2205.**

**18. Muller M (1993) The hydrogenosome. J Gen Microbiol 139: 2879-2889.**

**19. Tovar J, Fischer A, Clark CG (1999) The mitosome, a novel organelle related to mitochondria in the amitochondrial parasite Entamoeba histolytica. Mol Microbiol 32: 1013-1021.**

**20. Shiflett AM, Johnson PJ (2010) Mitochondrion-related organelles in eukaryotic protists. Annu Rev Microbiol 64: 409-429.**

**21. Adl SM, Simpson AG, Lane CE, Lukes J, Bass D, et al. (2012) The revised classification of eukaryotes. J Eukaryot Microbiol 59: 429-493.**

**22. Regoes A, Zourmpanou D, Leon-Avila G, van der Giezen M, Tovar J, et al. (2005) Protein import, replication, and inheritance of a vestigial mitochondrion. J Biol Chem 280: 30557-30563.**

**23. Tovar J, Leon-Avila G, Sanchez LB, Sutak R, Tachezy J, et al. (2003) Mitochondrial remnant organelles of Giardia function in iron-sulphur protein maturation. Nature 426: 172-176.**

**24. Makiuchi T, Nozaki T (2014) Highly divergent mitochondrion-related organelles in anaerobic parasitic protozoa. Biochimie 100: 3-17.**

**25. Riordan CE, Ault JG, Langreth SG, Keithly JS (2003) Cryptosporidium parvum Cpn60 targets a relict organelle. Curr Genet 44: 138-147.**

**26. Katinka MD, Duprat S, Cornillot E, Metenier G, Thomarat F, et al. (2001) Genome sequence and gene compaction of the eukaryote parasite Encephalitozoon cuniculi. Nature 414: 450-453.**

**27. Jerlstrom-Hultqvist J, Einarsson E, Xu F, Hjort K, Ek B, et al. (2013) Hydrogenosomes in the diplomonad Spironucleus salmonicida. Nature communications 4: 2493.**

**28. Abrahamsen MS, Templeton TJ, Enomoto S, Abrahante JE, Zhu G, et al. (2004) Complete genome sequence of the apicomplexan, Cryptosporidium parvum. Science 304: 441-445.**

**29. Leon-Avila G, Tovar J (2004) Mitosomes of Entamoeba histolytica are abundant mitochondrion-related remnant organelles that lack a detectable organellar genome. Microbiology 150: 1245-1250.**

**30. Turner G, Muller M (1983) Failure to detect extranuclear DNA in Trichomonas vaginalis and Tritrichomonas foetus. J Parasitol 69: 234-236.**

**31. van der Giezen M, Sjollema KA, Artz RR, Alkema W, Prins RA (1997) Hydrogenosomes in the anaerobic fungus Neocallimastix frontalis have a double membrane but lack an associated organelle genome. FEBS Lett 408: 147-150.**

**32. Dolezal P, Smid O, Rada P, Zubacova Z, Bursac D, et al. (2005) Giardia mitosomes and trichomonad hydrogenosomes share a common mode of protein targeting. Proc Natl Acad Sci U S A 102: 10924-10929.**

**33. Jedelsky PL, Dolezal P, Rada P, Pyrih J, Smid O, et al. (2011) The minimal proteome in the reduced mitochondrion of the parasitic protist Giardia intestinalis. PLoS One 6: e17285.**

**34. Lill R (2009) Function and biogenesis of iron-sulphur proteins. Nature 460: 831-838.**

**35. Craig EA, Voisine C, Schilke B (1999) Mitochondrial iron metabolism in the yeast Saccharomyces cerevisiae. Biol Chem 380: 1167-1173.**

**36. Schilke B, Voisine C, Beinert H, Craig E (1999) Evidence for a conserved system for iron metabolism in the mitochondria of Saccharomyces cerevisiae. Proc Natl Acad Sci U S A 96: 10206-10211.**

**37. Ankarklev J, Jerlstrom-Hultqvist J, Ringqvist E, Troell K, Svard SG (2010) Behind the smile: cell biology and disease mechanisms of Giardia species. Nat Rev Microbiol 8: 413-422.**

**38. Morrison HG, McArthur AG, Gillin FD, Aley SB, Adam RD, et al. (2007) Genomic minimalism in the early diverging intestinal parasite Giardia lamblia. Science 317: 1921-1926.**

**39. Davis-Hayman SR, Nash TE (2002) Genetic manipulation of Giardia lamblia. Molecular and biochemical parasitology 122: 1-7.**

**40. Boucher SE, Gillin FD (1990) Excystation of in vitro-derived Giardia lamblia cysts. Infect Immun 58: 3516-3522.**

**41. Abodeely M, DuBois KN, Hehl A, Stefanic S, Sajid M, et al. (2009) A contiguous compartment functions as endoplasmic reticulum and endosome/lysosome in Giardia lamblia. Eukaryot Cell 8: 1665-1676.**

**42. Stefanic S, Morf L, Kulangara C, Regos A, Sonda S, et al. (2009) Neogenesis and maturation of transient Golgi-like cisternae in a simple eukaryote. J Cell Sci 122: 2846-2856.**

**43. Goldberg AV, Molik S, Tsaousis AD, Neumann K, Kuhnke G, et al. (2008) Localization and functionality of microsporidian iron-sulphur cluster assembly proteins. Nature 452: 624-628.**

**44. Mi-ichi F, Abu Yousuf M, Nakada-Tsukui K, Nozaki T (2009) Mitosomes in Entamoeba histolytica contain a sulfate activation pathway. Proc Natl Acad Sci U S A 106: 21731-21736.**

**45. Putignani L, Tait A, Smith HV, Horner D, Tovar J, et al. (2004) Characterization of a mitochondrion-like organelle in Cryptosporidium parvum. Parasitology 129: 1-18.**

**46. Sanderson SJ, Xia D, Prieto H, Yates J, Heiges M, et al. (2008) Determining the protein repertoire of Cryptosporidium parvum sporozoites. Proteomics 8: 1398-1414.**

**47. Tsaousis AD, Kunji ER, Goldberg AV, Lucocq JM, Hirt RP, et al. (2008) A novel route for ATP acquisition by the remnant mitochondria of Encephalitozoon cuniculi. Nature 453: 553-556.**

**48. Wampfler PB, Tosevski V, Nanni P, Spycher C, Hehl AB (2014) Proteomics of secretory and endocytic organelles in Giardia lamblia. PLoS One 9: e94089.**

**49. Dagley MJ, Dolezal P, Likic VA, Smid O, Purcell AW, et al. (2009) The protein import channel in the outer mitosomal membrane of Giardia intestinalis. Mol Biol Evol 26: 1941-1947.**

**50. Hehl AB, Marti M, Kohler P (2000) Stage-specific expression and targeting of cyst wall protein-green fluorescent protein chimeras in Giardia. Mol Biol Cell 11: 1789-1800.**

**51. Morf L, Spycher C, Rehrauer H, Fournier CA, Morrison HG, et al. (2010) The transcriptional response to encystation stimuli in Giardia lamblia is restricted to a small set of genes. Eukaryot Cell 9: 1566-1576.**

**52. Hehl AB, Marti M, Kohler P (2000) Stage-specific expression and targeting of cyst wall protein-green fluorescent protein chimeras in Giardia. Molecular biology of the cell 11: 1789-1800.**

**53. Konrad C, Spycher C, Hehl AB (2010) Selective condensation drives partitioning and sequential secretion of cyst wall proteins in differentiating Giardia lamblia. PLoS Pathog 6: e1000835.**

**54. Gaechter V, Schraner E, Wild P, Hehl AB (2008) The single dynamin family protein in the primitive protozoan Giardia lamblia is essential for stage conversion and endocytic transport. Traffic 9: 57-71.**

**55. Pusnik M, Mani J, Schmidt O, Niemann M, Oeljeklaus S, et al. (2012) An essential novel component of the noncanonical mitochondrial outer membrane protein import system of trypanosomatids. Molecular biology of the cell 23: 3420-3428.**

**56. Rajala N, Hensen F, Wessels HJ, Ives D, Gloerich J, et al. (2015) Whole cell formaldehyde cross-linking simplifies purification of mitochondrial nucleoids and associated proteins involved in mitochondrial gene expression. PLoS One 10: e0116726.**

**57. Jimenez-Garcia LF, Zavala G, Chavez-Munguia B, Ramos-Godinez Mdel P, Lopez-Velazquez G, et al. (2008) Identification of nucleoli in the early branching protist Giardia duodenalis. International journal for parasitology 38: 1297-1304.**

**58. Elmendorf HG, Rohrer SC, Khoury RS, Bouttenot RE, Nash TE (2005) Examination of a novel head-stalk protein family in Giardia lamblia characterised by the pairing of ankyrin repeats and coiled-coil domains. International journal for parasitology 35: 1001-1011.**

**59. Isenmann S, Khew-Goodall Y, Gamble J, Vadas M, Wattenberg BW (1998) A splice-isoform of vesicle-associated membrane protein-1 (VAMP-1) contains a mitochondrial targeting signal. Mol Biol Cell 9: 1649-1660.**

**60. Duman JG, Forte JG (2003) What is the role of SNARE proteins in membrane fusion? Am J Physiol Cell Physiol 285: C237-249.**

**61. Bandyopadhyay S, Chandramouli K, Johnson MK (2008) Iron-sulfur cluster biosynthesis. Biochemical Society transactions 36: 1112-1119.**

**62. Manning G, Reiner DS, Lauwaet T, Dacre M, Smith A, et al. (2011) The minimal kinome of Giardia lamblia illuminates early kinase evolution and unique parasite biology. Genome biology 12: R66.**

**63. Eilers M, Schatz G (1986) Binding of a specific ligand inhibits import of a purified precursor protein into mitochondria. Nature 322: 228-232.**

**64. Morgan GW, Goulding D, Field MC (2004) The single dynamin-like protein of Trypanosoma brucei regulates mitochondrial division and is not required for endocytosis. J Biol Chem 279: 10692-10701.**

**65. Chanez AL, Hehl AB, Engstler M, Schneider A (2006) Ablation of the single dynamin of T. brucei blocks mitochondrial fission and endocytosis and leads to a precise cytokinesis arrest. Journal of cell science 119: 2968-2974.**

**66. Wexler-Cohen Y, Stevens GC, Barnoy E, van der Bliek AM, Johnson PJ (2014) A dynamin-related protein contributes to Trichomonas vaginalis hydrogenosomal fission. Faseb J 28: 1113-1121.**

**67. Chan DC (2006) Mitochondria: dynamic organelles in disease, aging, and development. Cell 125: 1241-1252.**

**68. Chen H, Chan DC (2009) Mitochondrial dynamics--fusion, fission, movement, and mitophagy--in neurodegenerative diseases. Human molecular genetics 18: R169-176.**

**69. Sonda S, Stefanic S, Hehl AB (2008) A sphingolipid inhibitor induces a cytokinesis arrest and blocks stage differentiation in Giardia lamblia. Antimicrobial agents and chemotherapy 52: 563-569.**

**70. van der Giezen M (2009) Hydrogenosomes and mitosomes: conservation and evolution of functions. J Eukaryot Microbiol 56: 221-231.**

**71. Aguilera P, Barry T, Tovar J (2008) Entamoeba histolytica mitosomes: organelles in search of a function. Experimental parasitology 118: 10-16.**

**72. Martincova E, Voleman L, Pyrih J, Zarsky V, Vondrackova P, et al. (2015) Probing the biology of Giardia intestinalis mitosomes using in vivo enzymatic tagging. Mol Cell Biol.**

**73. Paddock ML, Wiley SE, Axelrod HL, Cohen AE, Roy M, et al. (2007) MitoNEET is a uniquely folded 2Fe 2S outer mitochondrial membrane protein stabilized by pioglitazone. Proc Natl Acad Sci U S A 104: 14342-14347.**

**74. Xu F, Jerlstrom-Hultqvist J, Einarsson E, Astvaldsson A, Svard SG, et al. (2014) The genome of Spironucleus salmonicida highlights a fish pathogen adapted to fluctuating environments. PLoS genetics 10: e1004053.**

**75. Wampfler PB, Faso C, Hehl AB (2014) The Cre/loxP system in Giardia lamblia: genetic manipulations in a binucleate tetraploid protozoan. International journal for parasitology 44: 497-506.**

**76. Mi-Ichi F, Miyamoto T, Takao S, Jeelani G, Hashimoto T, et al. (2015) Entamoeba mitosomes play an important role in encystation by association with cholesteryl sulfate synthesis. Proc Natl Acad Sci U S A.**

**77. Elias EV, Quiroga R, Gottig N, Nakanishi H, Nash TE, et al. (2008) Characterization of SNAREs determines the absence of a typical Golgi apparatus in the ancient eukaryote Giardia lamblia. J Biol Chem 283: 35996-36010.**

**78. de Kroon AI, Dolis D, Mayer A, Lill R, de Kruijff B (1997) Phospholipid composition of highly purified mitochondrial outer membranes of rat liver and Neurospora crassa. Is cardiolipin present in the mitochondrial outer membrane? Biochim Biophys Acta 1325: 108-116.**

**79. Zinser E, Sperka-Gottlieb CD, Fasch EV, Kohlwein SD, Paltauf F, et al. (1991) Phospholipid synthesis and lipid composition of subcellular membranes in the unicellular eukaryote Saccharomyces cerevisiae. J Bacteriol 173: 2026-2034.**

**80. Kumar P, Guha S, Diederichsen U (2015) SNARE protein analog-mediated membrane fusion. Journal of peptide science : an official publication of the European Peptide Society 21: 621-629.**

**81. Tamura Y, Sesaki H, Endo T (2014) Phospholipid transport via mitochondria. Traffic 15: 933-945.**

**82. Yamano K, Tanaka-Yamano S, Endo T (2010) Tom7 regulates Mdm10-mediated assembly of the mitochondrial import channel protein Tom40. J Biol Chem 285: 41222-41231.**

**83. Tatsuta T, Scharwey M, Langer T (2014) Mitochondrial lipid trafficking. Trends Cell Biol 24: 44-52.**

**84. Rigotti A, Cohen DE, Zanlungo S (2010) STARTing to understand MLN64 function in cholesterol transport. Journal of lipid research 51: 2015-2017.**

**85. Wideman JG, Gawryluk RM, Gray MW, Dacks JB (2013) The ancient and widespread nature of the ER-mitochondria encounter structure. Mol Biol Evol 30: 2044-2049.**

**86. Mani J, Desy S, Niemann M, Chanfon A, Oeljeklaus S, et al. (2015) Mitochondrial protein import receptors in Kinetoplastids reveal convergent evolution over large phylogenetic distances. Nature communications 6: 6646.**

**87. Zhao J, Lendahl U, Nister M (2013) Regulation of mitochondrial dynamics: convergences and divergences between yeast and vertebrates. Cell Mol Life Sci 70: 951-976.**

**88. van der Bliek AM, Shen Q, Kawajiri S (2013) Mechanisms of mitochondrial fission and fusion. Cold Spring Harb Perspect Biol 5.**

**89. Okamoto K, Shaw JM (2005) Mitochondrial morphology and dynamics in yeast and multicellular eukaryotes. Annu Rev Genet 39: 503-536.**

**90. Elgass K, Pakay J, Ryan MT, Palmer CS (2013) Recent advances into the understanding of mitochondrial fission. Biochim Biophys Acta 1833: 150-161.**

**91. Marti M, Li Y, Schraner EM, Wild P, Kohler P, et al. (2003) The secretory apparatus of an ancient eukaryote: protein sorting to separate export pathways occurs before formation of transient Golgi-like compartments. Mol Biol Cell 14: 1433-1447.**

**92. McArthur AG, Morrison HG, Nixon JE, Passamaneck NQ, Kim U, et al. (2000) The Giardia genome project database. FEMS Microbiol Lett 189: 271-273.**

**93. Smirnova E, Shurland DL, Ryazantsev SN, van der Bliek AM (1998) A human dynamin-related protein controls the distribution of mitochondria. The Journal of cell biology 143: 351-358.**

**94. Miyagishima SY, Nishida K, Mori T, Matsuzaki M, Higashiyama T, et al. (2003) A plant-specific dynamin-related protein forms a ring at the chloroplast division site. Plant Cell 15: 655-665.**

**95. Nishida K, Takahara M, Miyagishima SY, Kuroiwa H, Matsuzaki M, et al. (2003) Dynamic recruitment of dynamin for final mitochondrial severance in a primitive red alga. Proc Natl Acad Sci U S A 100: 2146-2151.**

**96. Pan R, Hu J (2011) The conserved fission complex on peroxisomes and mitochondria. Plant Signal Behav 6: 870-872.**

**97. Otera H, Mihara K (2011) Discovery of the membrane receptor for mitochondrial fission GTPase Drp1. Small GTPases 2: 167-172.**

**98. Lee H, Yoon Y (2014) Mitochondrial fission: regulation and ER connection. Molecules and cells 37: 89-94.**

## Supporting information

S1 Fig. A modified pPacV-integrated vector used for cloning of putative mitosomal candidates.

S1 Fig.

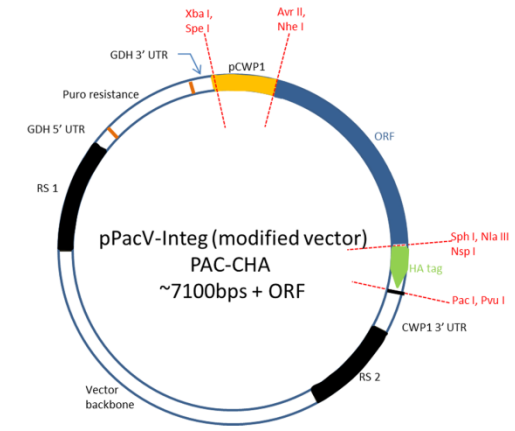


S2 Fig. Titration assay to determine optimum crosslinker concentration.

S2 Fig.

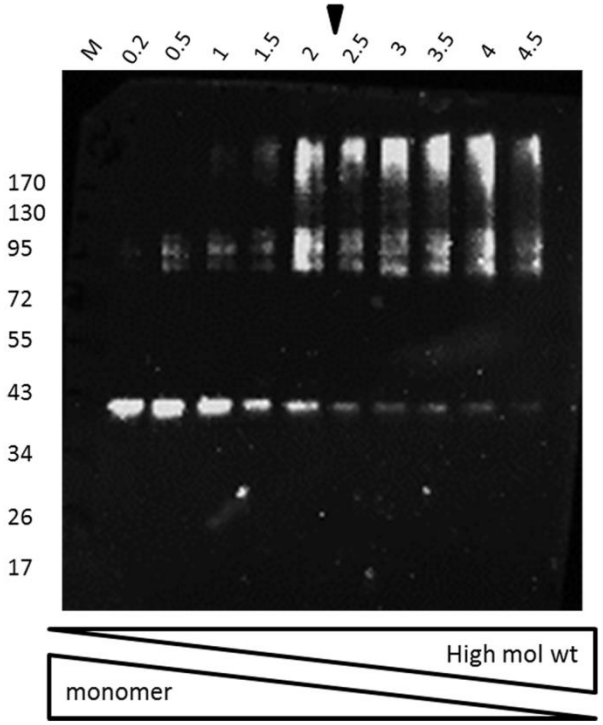

S3A- 3D Figs. Blast2Go analysis for 26 mitosome localized proteins.

S3A Fig.

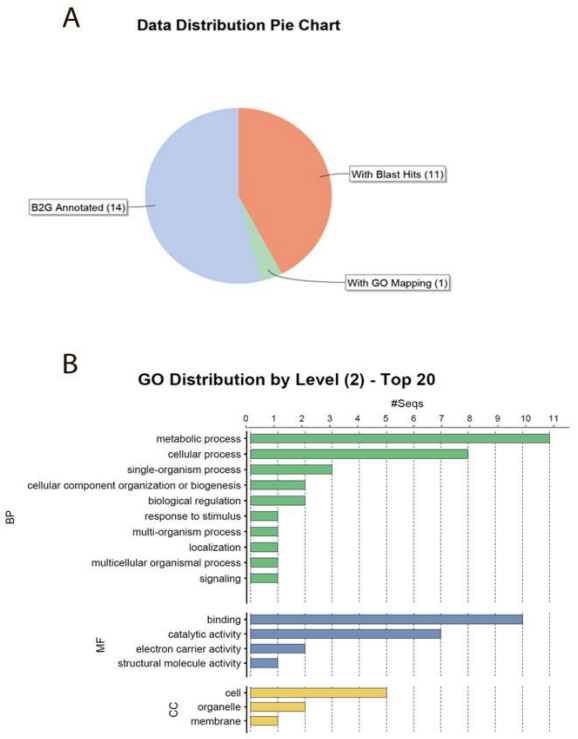


S3B Fig.

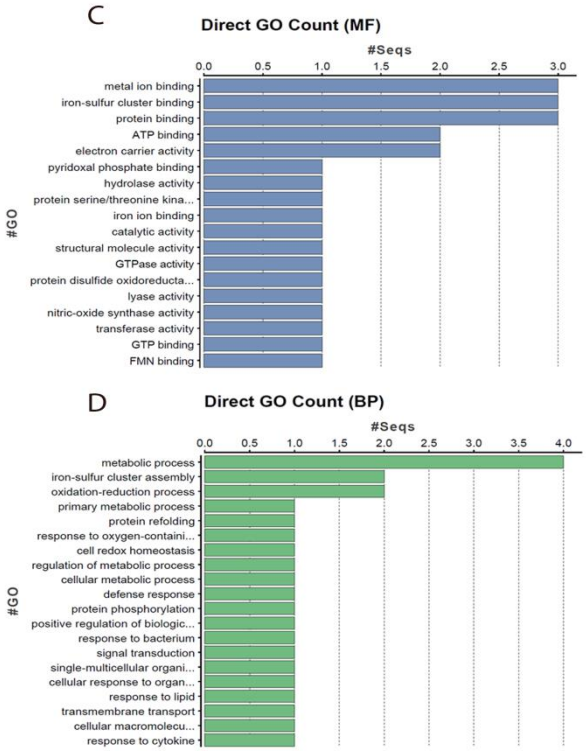


S4A- 4D Figs. Blast2Go analysis for 93 hypothetical mitosomal proteins from 6 co-IP assays.

S4A Fig.

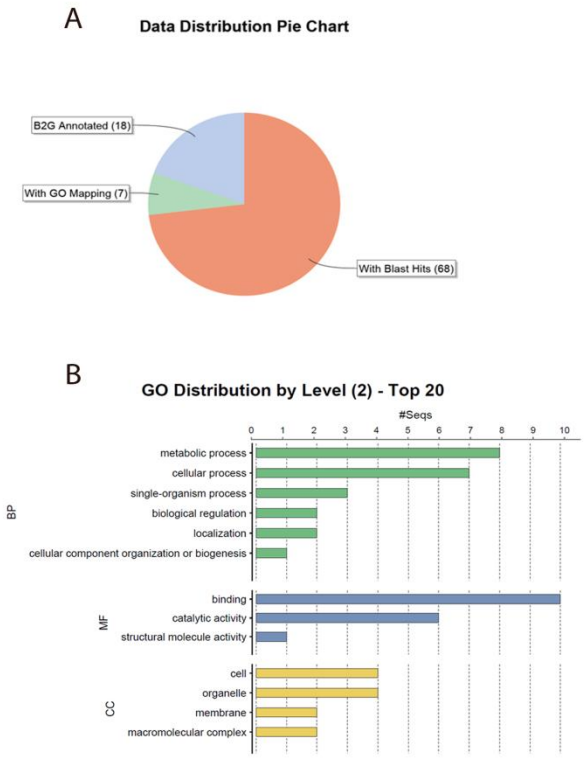


S4B Fig.

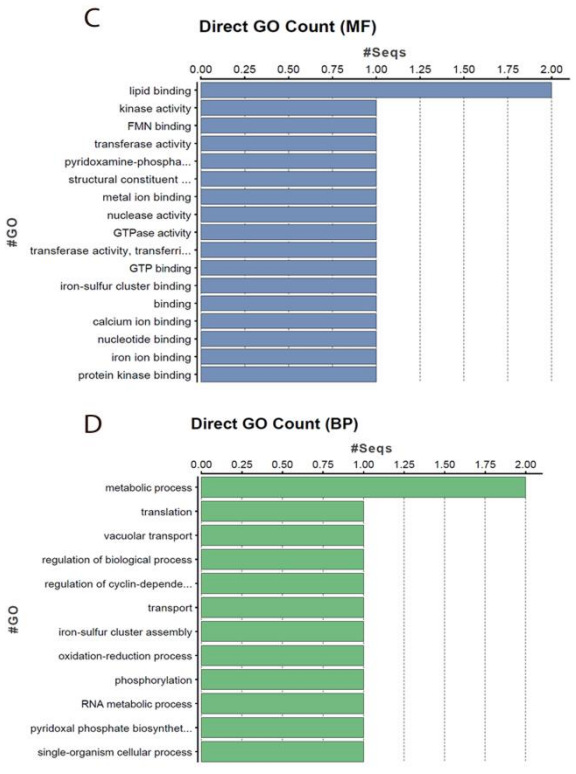

S1 Table. Oligonucleotides used in the study.

S2 Table. 95_2_95 analysis for *Gl*Tom40 co-IP dataset.

S3 Table. Parsing of 52 *Gl*Tom40 co-IP proteins.

S4 Table. 95_1_95 analysis for *Gl*Tom40 co-IP dataset.

S5 Table. Selected candidates for subcellular localization.

S6 Table. 95_2_95 analysis for *Gl*Tom40R co-IP dataset.

S7 Table. Parsing of 241 *Gl*Tom40R co-IP proteins.

S8 Table. List of mitosome localized proteins.

S9 Table. Overlap between *Gl*Tom40 and *Gl*Tom40R co-IP datasets.

S10 Table. 95_2_95 analysis for *Gl*14939 co-IP dataset.

S11 Table. 95_1_95 analysis for *Gl*5785 co-IP dataset.

S12 Table. 95_2_95 analysis for *Gl*IscS co-IP dataset.

S13 Table. MITOPROT analysis for 14 hypothetical proteins in the *Gl*IscS co-IP dataset.

S14 Table. 90_1_90 analysis for *Gl*9296 co-IP dataset.

# PART VII DISCUSSION AND FUTURE DIRECTIONS

## 1. Discussion

### 1.1 General

Unicellular protozoan parasites are responsible for worldwide health problems. *Giardia lamblia* is one of the leading causative agents for water borne non-bacterial diarrhea. *G. lamblia* has a broad host range and not only affects humans but also causes severe morbidity and economic loss in the livestock industry. Along with other parasitic protists such as *Trichomonas vaginalis* and *Entamoeba histolytica*, *Giardia* has undergone reductive evolution, frequently a hallmark of transition from free-living to parasitic lifestyle. These adaptation and diverse biological processes are the results of the outcome due to long term co-evolution with the host and are flaunted in the dramatic simplification of almost all cellular systems and machineries. For e.g. the absence of a steady state Golgi apparatus and the presence of mitochondrion-related organelles (mitosomes) (see below). Nevertheless, the simplified cellular compartmentalization of *Giardia* makes for a useful platform to investigate basic cellular functions and pathways which are challenging to dissect in complex eukaryotes. Furthermore, it is also a practical model system to investigate principles of reductive evolution, i.e. why and how adoption of a parasitic life-style leads to the loss of even archetypical organelles, and which minimal machinery is maintained for fundamental cellular functions.

During my doctoral thesis, I worked on two organelles in *Giardia*; the stage specifically induced ESVs and the mitochondrion-related organelles mitosomes. I started with a project to analyze the function of different homologues of small GTPase on ESV genesis and cyst formation during the complex differentiation process. In my second project, I wanted to characterize program cell death in *Giardia*. The main aim of this study was to assign giardial mitosomes a novel function in program cell death by inducing apoptosis upon altering conditions encountered by the parasite in physiological conditions such as nutrient starvation and heat. The last part of my doctoral thesis was dedicated to optimizing a co-immunoprecipitation assay (co-IP) enabling efficient pull down of organelle specific sub-proteomes. The main aim of this part of my thesis was to characterize the mitosomal protein import machinery and to identify other non-conserved proteins or factors responsible for maintaining inter-organellar communication.

## 1.2 Project 1: Arfs and Arls

### 1.2.1 Aside from *Gl*Arf1, none of the additional Arf and Arl homologues tested effect ESV genesis or cyst maturation.

Stage differentiation from a trophozoite to a cyst is a pre-requisite for *Giardia* to infect a new host and depends on a functional secretory pathway. The entire exocytic secretory system in *Giardia* comprises of ER along with ESVs (*de novo* generated Golgi analogs in encysting trophozoites). Despite having a secondary loss of major compartments associated with membrane transport, *Giardia* harbors key components of the secretory pathway such as coat complexes (COPI, COPII and clathrin) and adaptor proteins (AP1 and AP2/3) and depends on small GTPases such as the Sar1, Rab1 and Arf1 for genesis and maturation of ESVs respectively [1]. Since both the machinery and the cargo of the single regulated protein secretion pathway appear to the uniquely simple in *Giardia*, it is a promising model to study minimal requirements for Golgi genesis and maturation.

The role of small GTPases as molecular switches during protein secretion from ER to ESV has been extensively studied in our laboratory. It has been demonstrated unequivocally that ESV genesis, maturation and cargo secretion depends on Sar1, Rab1 and Arf1 GTPases [1] strengthening the cisternal progression model [2] for ESV maturation in *Giardia*. Briefly conditional overexpression of dominant-negative mutant variant of *Gl*Sar1 resulted in complete block of ESV formation suggesting that the Golgi-like ESV formation happens via Sar1-COPII dependent fashion [3]. Furthermore, conditional expression of dominant-negative mutant variant of *Gl*Arf1 resulted in complete blockage of cyst material prior to secretion yielding a naked cyst phenotype.

*In silico* analysis revealed the presence of 5 additional Arf and Arf-like (Arl) homologues in the *Giardia* genome. Therefore in the first part of my doctoral thesis work I focused on characterizing these additional Arf and Arl homologues in *Giardia* and deciphering their possible involvement in ESV maturation and cyst formation.

We began by synthesizing constructs for the inducible overexpression of the corresponding genes (*Gl*13930, *Gl*13478, *and Gl4192*) during encystation to localize their epitope-tagged products. In all cases, localization was almost exclusively cytosolic throughout encystation, in marked contrast to *Gl*Arf1 which shows recruitment to ESVs in the later stages of encystation. We also synthesized mutant versions of these ORFs in either their GDP-(T31N) or GTP (Q71L)-locked conformations, in the attempt to perturb membrane trafficking during encystation by saturating the system with non-functional Arfs and Arls. In our conditions, none of the mutants tested produced significant effects on either ESV maintenance or encystation efficiency. Importantly, a wild-type un-transfected cell line encysted properly and we were able to reproduce the “naked cyst” phenotype in the strain transfected with a construct for the inducible expression of GTP-locked *Gl*Arf1 (*Gl*Arf1Q71L). Based on this

data, we conclude that Arf1 is probably the only Arf family member playing a key role in ESV maintenance and trafficking. The other homologues may either be redundant/ complementary in relation to Arf1 or be involved in other as-yet novel unidentified cellular processes.

A recent report highlighted the role of Arl2 during the cell cycle in *T. brucei* [4]. We tested whether *Gl*Arl2 may play a similar role in *G. lamblia* cytokinesis. We did not record any significant differences in cytokinesis in parasites expressing GTP-locked *Gl*4192 as compared to untransfected parasites. We could not assign to giardial Arl2 a function in cytokinesis, as seen in other protozoan species. Therefore, the only characterized Arf protein to date remains *Gl*Arf1.

### 1.2.2 A case of redundancy or a scope for novelty for small GTPases in *Giardia*?

*G. lamblia* possesses 8 Rab proteins, 4 of which are well-conserved, a single Sar1 and 6 Arf and Arl homologs [5, 6] (Rout, Faso and Hehl, unpublished data). Since the cellular localization and molecular function of these GTPases are well conserved, they serve as tools for characterizing compartment organization in the secretory pathway. Although distinct phenotypes ranging from failure to undergo stage conversion to inability to secrete cyst wall have been observed in *Giardia* upon over-expression of dominant negative Rab1, Sar1 and Arf1, additional information regarding the localization and function of other homologs is still missing. Since major molecular machineries and pathways have been streamlined in *Giardia*, the scope of redundancy in such a parsimonious system is quite low.

Small GTPases are divided into 5 classes based on primary sequences, Ras, Rho/Rac, Rab, Sar/ Arf and Ran [7]. The Rab GTPases constitute the largest group amongst all and are implicated in vesicular traffic [8]. Multicellular organisms harboring a steady state Golgi apparatus possess a larger repertoire of Rab GTPases compared to unicellular eukaryotes. A case in point is the presence of 60 Rab genes in *H. sapiens* and 29 in both *A. thaliana* and *D. melanogaster*, compared to 11 Rab genes identified in yeast harboring either stacked Golgi (*P. pastoris* and *S. pombe*) or dispersed cisternae (*S. cerevisiae*) [9, 10]. Surprisingly, basal eukaryotes such as *E. histolytica* and *T. vaginalis* that do not harbor a canonical Golgi possess a large repertoire of Rab GTPases [11, 12]. Although a specific set of these GTPases (Rab1, Rab5, Rab6, Rab7, Rab11) are highly conserved [13], not every GTPase has been assigned a unique function in these species. However, the presence of unusual C-terminal domain structure in *E. histolytica* Rab proteins points towards novel modification and function [12].

Therefore, whether the presence of additional Arf and Rab homologs in *Giardia* is a case of redundancy or if there are novel functions associated to these GTPases is yet to be determined.

### 1.2.3 Are small GTPases in *Giardia* involved in additional functions beyond their involvement in the secretory system?

Beyond their documented role in vesicular trafficking, small GTPases including Arfs and Rabs have been implicated in at least 3 functions in higher eukaryotes; establishment of ER/mitochondria contact sites, mitophagy and maintenance of mitochondrial homeostasis and dynamics [14-16].

Arf1 GTPase in yeast and metazoans associates with mitochondria and ER-mitochondria contact sites respectively [17] (novel localization for a Golgi GTPase) and interacts genetically with Gem 1 (Rho-like GTPases negatively regulating ER-Mitochondria Encounter Structures (ERMES in yeast)) [18]. The mitochondrial phenotype (hyper-connected mitochondria) obtained in the Arf1/2 mutants are similar to those observed in Gem1 mutants in yeast [17]. Furthermore, the mitochondrial morphology in double mutants (Arf1/2 and Gem1) is severely compromised than in individual mutants suggesting the presence of a novel Arf dependent ER-mitochondria contact site besides the canonical ERMES in yeast. In addition, Arf1 GTPase also recruits AAA-ATPase Cdc48 to yeast mitochondria for efficient removal of Fzo1 (fusion GTPases) and other mitochondrial proteins. Cdc48 was shown to be involved in quality control of mitochondrial outer membrane proteins. Likewise over-expression of Arf1/2 mutants leads to impaired recruitment of Cdc48, leading to aberrant mitochondrial phenotype [17]. On the other hand, Rab32 is shown to associate with mitochondria and over-expression of GDP-locked variant resulted in collapse of mitochondria suggesting its role in mitochondrial fission machinery [19].

The growing body of evidence points towards the involvement of the endomembrane system (small GTPases) in mitochondrial dynamics [20]. Due to the above mentioned novel function of the small GTPases (Arf1 and Rab32), the presence of five additional Arf and Arl homologs and 8 Rab proteins in *Giardia* merits further investigation. Therefore, we hypothesize that the additional small GTPases present in *Giardia* might be performing a novel function at mitosomes or possess a *Giardia* specific function. This is supported by co-IP data showing mitosomal bait specific enrichment for *Gl*Arf1, *Gl*Rab32 (*Gl50803_16979*) and an AAA-ATPases (*Gl50803_16867*) homologs at high stringency parameters (95_2_95). Although *Gl*Arf1 and AAA-ATPases do not localize to *Giardia* mitosomes in IFA studies (data not shown), identification of these proteins in curated MS dataset suggests that a small fraction of these proteins are in close association with mitosome membranes and/or hints towards a putative novel role in establishing ER-mitosome contact sites or maintaining mitosomal dynamics. Furthermore, although the role of *Gl*Arf1 has been established in cyst maturation, little is known regarding its involvement in mitosome morphology and maintenance.

In order to address this question we propose to,

(1) Perform a thorough IFA analysis to determine the shape and morphology of mitosomes using endogenous antibody (against *Gl*IscU) in cell lines expressing the GTP- and GDP-locked Arf and Arl homologues. In depth analysis will provide novel insights (if/any) into the function of these homologues in *Giardia*. Availability of all the transgenic cell lines makes this approach less time consuming.

(2) Previous experiments to determine the role of additional Arf and Arl homologs in cyst maturation were performed using cell line expressing the dominant-negative mutants under an inducible cyst wall protein (CWP) promoter. The cytoplasmic localization observed might be a result of mistargeting of excess protein due to over-expression. Therefore, generation of HA epitope-tagged variants under the control of their respective endogenous promoters is necessary to access their correct localization within the cell.

(3) Apart from the function of *Gl*Rab1 in ESV development and cyst formation, little is known regarding the role of *Gl*Rab32 in *Giardia*. Localization studies using epitope tagged *Gl*Rab32 and IFA analysis of transgenic parasites expressing GDP and GTP locked variants is essential to determine if *Gl*Rab32 has any effect on mitosome morphology and/or distribution.

(4) Volpicelli-Daley *et. al* 2005, demonstrated that single knockdown of Arf1, 3, 4 and 5 were not required at any step of membrane traffic in HeLa cells, however, every combination of double knockdown elicited distinct defects along the secretory pathway demonstrating specificity of Arf-couples at multiple steps [21]. Furthermore, Arf1/2 double mutants' also elicited a mitochondrial phenotype in yeast. Since *Giardia* harbors an additional Arf homolog (*Gl*7562) with a predicted N-myristoylation motif, it is important to investigate the mitosome phenotype upon over-expression of both Arf mutants in *Giardia*. Availability of vectors allowing dual expression of both constructs makes this approach highly feasible.

(5) Lastly, involvement of these additional GTPase homologs in completely new *Giardia* specific pathways cannot be excluded. Therefore, established assays to determine ER morphology, PV morphology, clathrin recruitment and fluid phase uptake must be performed in cell lines expressing the GTP- and GDP- locked mutants.

The result of these proposed experiments would answer the question if the additional homologues for small GTPases present in *Giardia* are redundant or have a *Giardia* specific novel function.

### 1.3 Project 2: Apoptosis in *Giardia lamblia*

#### 1.3.1 Apoptotic like cell death can be induced in *Giardia* by altering its physiological conditions.

PCD (apoptosis) has been best characterized in multicellular life forms based on the obvious benefits it renders such as maintaining cell population, elimination of damaged cells or giving

shape to an organism [22, 23]. However, mounting evidences suggests that unicellular organisms have developed an unusual cell death pathway and undergo PCD under certain condition which is similar to their multicellular counterparts [24-26]. Based on the "original sin hypothesis" for the evolution of PCD, key molecules and factors involved in the pathway are located within the mitochondrion: the cornerstone organelle for PCD by apoptosis [27]. Therefore studies on unicellular organisms that do not harbor canonical mitochondria but demonstrate apoptosis related phenomenon would help unravel conserved factors and proteins involved in the process and will shed light on the evolution of PCD.

*G. lamblia* has undergone reductive evolution after changing from a free-living to a parasitic life style and harbors mitosomes making it a useful model to study apoptosis related processes. Despite present at high concentration during a chronic infection *Giardia* trophozoites do not elicit any host inflammatory response [28, 29]. Therefore, we hypothesized that *Giardia* trophozoites undergo an apoptosis-like cell death, which limits the stimulation of the immune system by deteriorating the parasites. By altering physiological conditions such as nutrient starvation and heat shock to trigger apoptosis, we demonstrate unambiguously that *Giardia* exhibit many, if not all morphological and biochemical characteristics of apoptosis-like cell death. Significant increase in phosphatidylserine (PS) positive cells was observed in nutrient starved and heat shocked parasites as compared to control parasites. PS exposure on the outer leaflet of the plasma membrane is a hallmark of apoptotic cells [30]. PS exposure as an excellent strategy for immune silencing has been demonstrated in protozoan parasites *L. major*, *T. gondii* and *T. brucei* [31] where exposure of PS on apoptotic cells leads to recruitment of phagocytes which recognize the signals leading to engulfment of apoptotic cells. However since apoptotic cells do not pose any danger, their engulfment does not provoke any anti-microbial effector function of phagocytes. Rather this step is accompanied by down regulation of pro-inflammatory and release of anti-inflammatory cytokines leading to silent clearing [32-34].

In addition to PS exposure, our data clearly demonstrate ER disintegration and nuclear material condensation in parasites induced to undergo apoptosis. However, analysis of the electrophoretic profile of DNA from nutrient starved parasites did not show the typical recursive DNA laddering pattern (caspase-dependent apoptosis) or high-molecular weight banding (caspase-independent apoptosis). Rather we obtained sheared DNA in the low molecular weight region. Atypical DNA fragmentation is seen in yeast cells undergoing apoptosis and many other lower eukaryotes including dinoflagellate *P. gatunense* and is linked to difference in chromatin arrangement [35, 36]. However, our data is in line with hydrogenosome-bearing *T. vaginalis* where a low molecular weight DNA smear was observed upon induction of apoptosis pointing towards the existence of an alternative DNA fragmentation mechanism in these protozoan parasites [37].

The cell death pathway involved in MRO harboring organisms is still unclear; however the end results are very much similar to studied pathways found in many unicellular organisms and metazoans. Since mitosomes are mitochondrial relic organelles and derived from endosymbiotic α-proteobacteria, we hypothesize that they might have some implications in cell death by releasing harmful proteins in the cytosol upon exposure to damaging stimuli like their eukaryotic counterpart. Although no *bona fide* effector homologs for any branch of PCD have been detected in the *Giardia* genome due of strong sequence divergence, it does not imply that such proteins do not exist since such analysis might be biased towards those proteins which have significant homology. Therefore we propose to:

(1) Perform a whole proteome analysis of apoptosis induced and non-induced parasites. Subtractive analysis of the proteome dataset would help discover *Giardia* specific abundant proteins or factors which might be involved in apoptosis. In a more targeted approach we would isolate nuclei from induced and non-induced trophozoites either by exploiting the organelle purification system optimized in our laboratory [38] or by density gradient centrifugation followed by differential proteomics analysis to identify novel *Giardia* specific regulators or transcription factor that might be upregulated upon induction of apoptosis in *Giardia*.

(2) We have shown that *Giardia* trophozoites undergo a form of apoptosis-related cell death upon nutrient starvation and heat shock. Furthermore, a dramatic and rapid form of cell deterioration was observed as a result of interference with mitosome protein import function upon treatment of trophozoites with Mitoblock (an experimental compound targeting the TIM import complex in mitochondria) (Hehl, unpublished data). Although there is indirect evidence for the role of mitosomes in apoptosis in *Giardia*, direct evidence for its involvement in the pathway is still missing. Therefore, we would exploit the DHFR-methotrexate import block assay recently implemented in our laboratory (Rout, *et.al* 2015, under review) to investigate whether a direct link is present between mitosomal protein import and apoptosis in *Giardia*. Preliminary experiments show a marginal increase of PS-positive cells in MTX-treated transgenic parasites expressing a mitosomal targeted DHFR fusion construct compared to equivalent untreated parasites (data not shown). However, large-scale quantification experiments using fluorescence activated cell sorting (FACS) will determine to what extent this phenomenon is consistent and reproducible.

3) In addition, we would develop another strategy independent of the ligand-induced block (DHFR- methotrexate) since this block is easily released upon dilution [39] and excess ligand in the solution might account for off-target effect. Therefore we would generate a chimeric construct harboring 1) a MTS at the N-terminus, 2) GST tag in the middle 3) a portion of staphylococcal protein A (as a C-terminal block) [40, 41]. The ability of the C-terminal

staphylococcal protein A as an import blocking agent has been demonstrated [42]. Characterization of apoptosis related phenotype in transgenic parasites over-expressing such a chimeric construct might also provide evidence to link mitosomes function and apoptosis in *Giardia*.

Furthermore, because this chimeric construct blocks the completion of import due to a translocation block, it spans the 4 different sub-cellular compartments in mitochondria (OM, IMS, IM, and matrix). Such a scenario would provide identification of components of the translocation machinery by affinity chromatography on IgG-Sepharose beads as an alternative for the iterative co-IP assay (Rout, et. al 2015, under review).

Such endeavors will not only help us to decipher PCD in amitochondriate organisms but also lead to an appreciation of the diversity of PCD across the eukaryotic spectrum.

## 1.4 Project 3: Optimization of a co-immunoprecipitation assay to identify organelle specific sub- proteome.

### 1.4.1 A minimized mitosomal import machinery in *Giardia*: reductionism at its best?

Mitochondrion is one of the defining organelle of an eukaryotic cell. It is not only involved in energy production by aerobic respiration, lipid synthesis but is also involved in several biosynthetic pathways. However, a number of organisms (mostly anaerobic eukaryotes) scattered throughout the 5 super-groups do not possess a canonical mitochondria but instead harbor mitochondrial related organelles (MROs) such as hydrogenosomes and mitosomes [43]. Although MROs are evolutionarily derived from mitochondria, there is extensive structural and functional divergence among organelles in different species. Bioinformatics analyses clearly demonstrate that the constraints for sequence divergence vary greatly amongst the super-groups, for e.g. enzymes of the universal Fe-S protein maturation machinery in MROs can be detected in the nuclear genome using straightforward *in silico* homology searches, whereas most MRO membrane proteins have diverged beyond recognition if they were not lost altogether. Additionally, despite unambiguous evidence for conserved mitosomal protein import pathways in *Giardia*, the composition of the import machinery remains unknowns. A case in point is *Gl*Tom40 (the only identified component of the mitosome import machinery in *Giardia*) whose sequence degeneration is so extensive that the identification of orthologues in *Giardia*, *Entamoeba* or *Spironucleus* still remains tentative. This high divergence between orthologues of MRO proteins even in closely related species makes systematic identification of protein components using proteome analysis very challenging.

We hypothesized that the reduced *Giardia* mitosomes harbored no more than 100-150 different proteins, either involved in protein import or associated with a clearly delineated cellular compartment facilitating inter-organellar communication. We accounted for the

paucity of mitosomal proteins by optimizing and implementing an approach based on iterative co-IP experiments using *Gl*Tom40 as a starting point followed by mass spectrometry (MS) analysis of chemically stabilized protein-protein interactions. This robust iterative approach lead to identification of 22 mitosomal proteins (annotated and hypothetical) out of which 16 proteins were localized to mitosomes; 5 proteins displayed dual localization to mitosomes and ER and one protein showed a ER and PV pattern even though it was pulled down exclusively with mitosome-localized bait proteins harboring TMDs (discussed below). The two proteins of the proposed minimized mitosomal import machinery are discussed below;

*Gl*29147, a single pass membrane protein was identified as a prominent *Gl*Tom40 interacting protein. The protein has a predicted N-terminal TMD similar to mitochondrial Tom40 receptors (Tom 20 and Tom 70) in *S. cerevisiae*. Although several *in silico* analysis tools have failed to identify a MTS at the protein's N-terminus, ectopic expression of the C-terminal portion of *Gl*21947 alone showed a distinct cytosolic localization by IFA (data not shown) without a detectable phenotype suggesting that targeting signals are present in the N-terminus of the protein. Additionally, C-terminally GFP-tagged full-length variant *Gl*29147-GFP enabled us to perform time lapse microscopy of mitosomes in trophozoites for the first time suggesting that *Gl*29147 is inserted in the mitosomal outer membrane in the type I orientation, extruding the C-terminal domain to the cytosol similar to Tom 20 and Tom 70 [44]. Interestingly, reverse co-IP using *Gl*29147 as bait protein pulled down *Gl*Tom40 as the most abundant membrane associated protein along with 220 additional specific proteins (annotated and hypothetical) out of which 20 proteins have been validated by localization to mitosomes, allowing for a significant expansion of the *Gl*Tom40-centered interactome. Therefore, topology of G*l*21947, its exclusive mitosomal localization, and the repertoire of pulled down proteins indicate that *Gl*21947 is a *Gl*Tom40 accessory protein with a potential receptor function for protein import (*Gl*Tom40R). However, the cytoplasmic *Gl*Tom40R fragment alone does not recapitulate the interaction properties of the full-length membrane anchored variant suggesting that the capture of imported matrix proteins requires incorporation of the receptor domain into a TOM complex and requires additional factors or domains on either side of the membrane anchor for proper functionality. However, the hypothesis of a receptor function for *Gl*Tom40R remains to be tested directly to evaluate its exact role in mitosomal protein import in *Giardia*.

Interestingly, although BLASTp yielded no strong homologues for *Gl*Tom40R, profile sequence comparisons with HHpred showed homology to a "high potential iron sulfur protein" (p-value 0.007). "High potential iron sulfur protein" in higher eukaryotes, also known as mitoNEET, is an integral membrane protein localized at the outer membrane of mitochondria and is responsible for transport of iron into mitochondria [45, 46]. If we

consider that Fe-S protein maturation is the only metabolic pathway currently associated to *G. lamblia* mitosomes, *Gl*Tom40R might also function as a mitoNEET homolog in *G. lamblia*. Alternatively, it wouldn't be surprising if *Gl*Tom40R could be performing both functions of a Tom receptor and mitoNEET simultaneously in this parasite. However, further experiments needs to be performed in order to accurately assign a function to *Gl*Tom40R in the mitosomal import machinery of *G. lamblia*.

*Gl*14939, a two TMD harboring protein was identified using *Gl*Tom40 and *Gl*Tom40R as baits in co-IP and reverse co-IP experiments respectively. Exclusive detection of the protein in both the datasets suggests that the three proteins (*Gl*Tom40, *Gl*Tom40R and *Gl*14939) might function as part of a complex. Furthermore, HMMER-based searches across several eukaryotic lineages fail to identify any orthologues for this protein. Consistent with this, there is no functional information available on this protein until now. A recent study however showed that *Gl*14939 (dubbed GiMOMP35) localizes at the outer mitosome membrane with its C-terminus in the cytosol [47]. Nonetheless, given that *Gl*Tom40 (the translocon), *Gl*29147 (*Gl*Tom40R), and *Gl*14939 (putative accessory protein) are outer membrane-associated proteins and part of the same interactome, we conclude that *Giardia* possesses a reduced mitosomal import machinery composed of the above three proteins.

Our conclusion is in line with the protein import machinery identified in other mitosome bearing organisms such as *E. histolytica* and microsporidian *E. cuniculi* [48, 49]. The presence of a single putative Tom receptor in *Giardia* is not an uncommon scenario in mitosome bearing organisms. A case in point is the presence of a sole Tom 70 receptor in the microsporidian *E. cuniculi* efficient enough for recognition and translocation of mitosomal proteins through the *E. cuniculi* Tom 40 channel [50]. Another case of massive reduction is seen in *Trypanosoma* mitochondria where only one translocon in the inner membrane performs a "jack of all trades" function substituting Tim 17/22/ and 23 [50, 51]. In these organisms however, extensive stripping of the protein import machinery to the essential is explained by the apparent paucity of proteins imported into mitosomes. Nevertheless, the most extreme case of reduction however is seen in anaerobic amoeba *Mastigamoeba balamuthi,* where despite the identification of 21 mitochondrial proteins, no components of the TOM, TIM or SAM complexes are found in the genome [52]. Based on the above information, the absence of other conserved components of the mitosome import machinery in *Giardia* can be explained in two possible ways: 1) extensive sequence divergence prevents identification of organelle proteins *via* homology-based searches; 2) *G. lamblia* lacks additional proteins of the import machinery simply due to overall mitochondrial reduction.

Nevertheless, our robust iterative co-IP approach for mitosomal protein identification also yielded five novel hypothetical proteins without a predicted TMD (*Gl*10971, *Gl*9296, *Gl*8148,

*Gl*17276, and *Gl*16424). However their function and possible involvement in the import machinery remains to be investigated. *Gl*9296 is of particular interest since it harbors an identifiable MTS. Co-IP using *Gl*9296 as bait protein identified *Gl*IscS, *Gl*IscA, *Gl*Hsp70, *Gl*Tom40 and *Gl*Tom40R suggesting close association of *Gl*9296 with few imported matrix proteins and most importantly with the import machinery. Furthermore, *Gl*9296 appears to be *Giardia* lineage specific as no other orthologues could be identified. Given its interaction profile, predicted import signal, and lack of homology to metabolic enzymes, we hypothesize that *Gl*9296 is a matrix protein and might be interacting at the trans-side for stabilization of the import pore in *Giardia* mitosomes. However, this remains to be investigated.

In addition our serial co-IP strategy identified another 93 hypothetical proteins that remain to be investigated for their localization and putative function. Interestingly, the major function associated with *E. histolytica* mitosomes was shown to be sulfate activation rather than Fe-S protein maturation [53]. Furthermore, *Entamoeba* mitosomes have been also implicated in the encystation process [54]. Although genes involved in sulfate activation pathway are absent in other MRO-containing organisms such as *Giardia*, *Trichomonas* and *Cryptosporidium*, the *Entamoeba* example points to a wider range of functions ascribable to mitosomes.

Based on the newly identified and novel validated mitosomal proteins we acquired so far from our serial co-IP approach we hypothesize that giardial mitosome might be implicated in other functions beyond Fe-S protein maturation. To test this hypothesis we propose to;

1) Perform expression and localization studies of epitope-tagged novel mitosomal candidates after careful *in silico* analysis. Proteins with an identifiable MTS would be priority candidates for this approach. We can make use of our proprietary expression system to integrate an epitope-tagged variant of each candidate into the *Giardia* genome. Open reading frames and ~200 base pairs of upstream sequence including the endogenous promoter would be cloned in frame in front of the HA-epitope tag sequence and ligated into the expression vector. Usage of the endogenous promoter avoids problems of over expression since only a single extra copy is introduced into the cells. However, if epitope tagging or ectopic expression should lead to a lethal effect, we will use conditional expression under the control of a stage-specific promoter which can be induced by changing culture medium conditions as a backup strategy. Localization studies would be done by IFA analysis on chemically fixed cells using monoclonal antibody which is specific for the HA epitope on the recombinant protein. Furthermore, co-localization studies to confirm correct mitosomal localization for candidate proteins can be done using a confirmed mitosome protein, i.e. *Gl*IscU or *Gl*IscS, to which a polyclonal antibody is available (Rout, Hehl 2015, unpublished data).

2) Perform carbonate extraction assay to determine if the novel mitosome localized TMD harboring proteins are indeed integral membrane proteins or peripheral membrane proteins. Additionally, we would perform protease protection assay in order to determine the topology of novel mitosome localized TMD harboring hypothetical protein candidates obtained from the serial co-IP assays.

3) Analyze the function of selected candidates by exploiting the recent developments in gene knockout strategy in *Giardia* based on the Cre/LoxP system [55]. Alternative strategies such as CRISPR/CAS9 or knockdown by morpholinos can be used to analyze the effect of loss of function of these proteins on mitosome (structural or functional). At present the CRISPR/ CAS9 method for genome editing in *Giardia* is being established in our laboratory. However, knockdown by morpholino oligonucleotides is already established in *Giardia* [56]. Morpholinos role as translation-blocking nucleotides has been unambiguously proven in *Trypanosoma brucei* [57]. A major advantage of this method is that morpholinos can be electroporated into cells using a standard protocol where they remain stable and highly active for days, although their concentration diminishes with each successive cell division. Furthermore, the specificity of the suppression by the experimental morpholino can be controlled in a concentration-dependent manner with a control morpholino which contains five mispaired bases.

Additionally,

3) We would perform sufficient number of reverse co-IP assays with validated mitosomal proteins as bait which would enable us to build a comprehensive *Giardia* mitosome organelle proteome.

4) We have successfully GFP-tagged mitosomes using either *Gl*Tom40 or *Gl*Tom40R. The type I topology of *Gl*Tom40R enables us to generate an organelle specific glutathione S-transferase (GST) marker for organelle purification by affinity chromatography on glutathione–Sepharose 4B beads as an alternative for our serial co-IP assay.

5) Establish a direct link between loss of mitosome function (import) and apoptosis in *Giardia*. (Discussion, Section 1.3). Uncovering a possible link between PCD and the highly degenerate mitochondrial remnants in this basal protozoan will reveal key information on the evolution of mitosomes and PCD, and would provide a unique opportunity to explore the breadth of eukaryotic diversity.

### 1.4.2 Diverged mitosome-ER contacts sites in *Giardia*?

Co-IP data identified five proteins (*Gl*5785, *Gl*9503, *Gl*21943, *Gl*22587, and *Gl*15154) with dual localization suggesting that these proteins might be present at the junction between ER and mitosomes and could be playing a role in establishing inter-organellar communication between the two organelles. In yeast, the ER-mitochondria encounter structure (ERMES) is responsible for bringing the two organelles in close proximity thereby facilitating lipid transfer. Phosphatidylserine (PS) synthesized in the ER is shuttled to mitochondria through the ERMES complex where it is converted to phosphotidylethanolamine (PE) by PS decarboxylase (Psd1) located in the inner membrane. PE is then shuttled back to the ER where is converted to phosphatidylcholine (PC) by different enzymes.

Because ERMES homologs are absent in metazoans [58], we hypothesized that there should be a tethering complex establishing organelle contact site for lipid transfer since division of mitosomes and maintenance of organelle membrane architecture require membrane lipids from ER [59, 60]. SNAREs proteins are generally involved in mediating membrane fusion in vesicular transport [61]. However the *Giardia* SNARE protein (*Gl*5785) particularly due to its dual localization might be a part of such a tethering complex facilitating phospholipid exchange between the two organelles by establishing membrane contact sites. Co-IP data generated using *Gl*5785 as bait protein partially supported our hypothesis by identifying 3 novel hypothetical proteins *Gl*9503 (3 TMDs), *Gl*21943 and *Gl*10971. *Gl*9503 and *Gl*21943 had dual localization (ER and mitosome) and data mining for both proteins identified domains with similarity to the yeast protein Mmm 1 of the ERMES complex and a beta barrel lipid binding protein MLN64 (e-value 0.0006) in *H. sapiens* involved in cholesterol transport to mitochondria [62] respectively. Additionally, *Gl*9503 also harbors an abhydrolase domain implicated in lipid synthesis. Furthermore, *Gl*5785 also pulled down the putative core import machinery in *Giardia* mitosomes (*Gl*Tom40, *Gl*Tom40R and *Gl*14939) which is in line with the association of ERMES with components of the protein import machinery in yeast mitochondria [63, 64]. Given the sub-cellular localization of the bait protein *Gl*5785, it is not surprising that we might have pulled down additional proteins working at the interface between these organelles facilitating either direct connection or working as bridging factors between the two organelles.

In addition, identification and dual localization of *Gl*22587 further supports our hypothesis for existence of a *Giardia* specific molecular tether between mitosomes and ER. HHpred identified an F-GTPase activating protein with an e-value of 1.8E-05. Based on this data, we can carefully speculate that *Gl*22587 might be a regulator of the putative contact site in *Giardia* like the yeast GTPase (Gem 1) which functions as the master regulator of the ERMES complex. Over-expression of a dominant negative variant of the *Gl*22587 would shed more light on its molecular function and likely association with mitosomes.

Interestingly, ERMES beyond their dedicated involvement in lipid trafficking are also implicated in regulation of mitochondrial fission, calcium signaling, mitophagy and inflammasome activation [65]. Nonetheless, to this date, components of the ERMES complex are not identified in metazoans and mitosome harboring organisms, however, ERMES homologues have been identified in hydrogenosome containing organism such as *T. vaginalis* [66]. However, identification of the SNARE protein (*Gl*5785) and several other proteins such as *Gl*9503, *Gl*21943, *Gl*22587, *and Gl15154* with dual localization suggest that these proteins might be components of a *Giardia* specific highly diverged molecular tether analogous to the ERMES in yeast.

Novel findings in the field of inter-organellar communication have revealed alternative pathways for lipid exchange between ER and mitochondria [67, 68]. Authors demonstrated that in the absence of an active ERMES, lipids are delivered to mitochondria via contact sites between mitochondria and vacuoles in yeast model. The identification of *Gl*7188 in our co-IP dataset and its atypical localization gives us an indication of a highly probable/alternative scenario in *G. lamblia* despite the absence of vacuoles. *Gl*7188 is a TMD harboring protein pulled down by baits present in the outer membrane in mitosomes (*Gl*Tom40, *Gl*Tom40R, *Gl*14939 and *Gl*5785) and IFA analysis revealed that this protein is localized to ER and peripheral vesicles prompting that these three organelles are in close proximity. In absence of a canonical ERMES machinery and the need for membrane lipids for mitosomal homeostasis it is tempting to speculate that membrane lipids might be exchanged between ER and mitosomes via peripheral vesicles at the basal body complex where these three organelles are in close association with each other. *Gl*7188 might be a bridging protein in-between mitosomes and ER/PVs. Close association of ER and PVs in *G. lamblia* has been previously documented [69]. Co-IP experiment using *Gl*7188 as bait protein and lipid binding assays needs to be performed to determine its interaction partners and lipid binding ability. However, the atypical localization of *Gl*7188 might also be an artefact of the epitope tag at the C-terminus of the protein. Therefore, N-terminally epitope tagged variant needs to be generated to check for its sub-cellular localizaiton .

### 1.4.3 Mitosome dynamics and a novel role for *Giardia* dynamin related protein in mitosome morphogenesis

We have previously demonstrated the existence of two morphologically distinct classes of mitosomes: 1) ~30 peripheral mitosomes (PMs) which are distributed in the cytoplasm without a particular pattern, and 2) a central mitosome complex which looks like an elongated organelle in fluorescence microscopy, but in fact is a tight bundle of spherical organelles [70]. Furthermore, the CMC has a fixed localization at the basal body complex between the two nuclei of *Giardia* and divides and segregates with the replicated basal body

complex during mitosis. The PMs on the other hand are distributed between the daughter cells in a stochastic fashion [71]. Based on this a "mother ship" hypothesis for mitosome division and morphogenesis was formulated which states that only organelles organized in the CM complex (mother ship) actively replicate and partition during mitosis, whilst PMs (satellites) are released into the cytoplasm from the CM complex by loss of attachment to the cytoskeleton, Fig. 1.

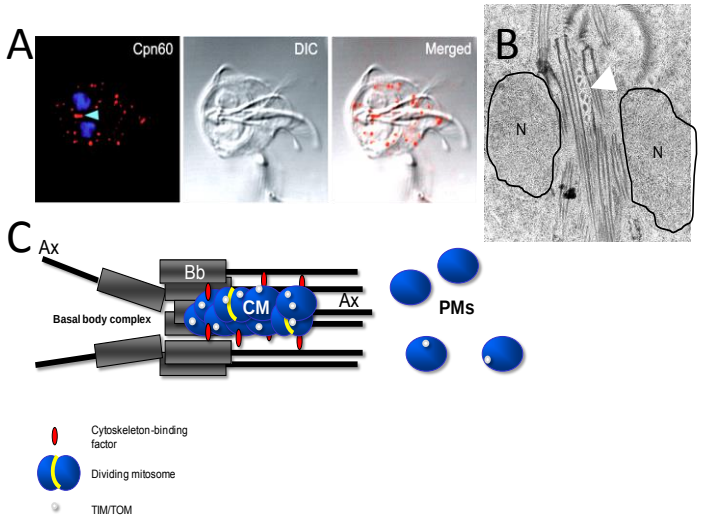


**Figure1. Two types of mitosomes in *Giardia*.**(A) IFA of Cpn60 in mitosomes (red). Nuclear DNA, blue. Arrow-head: central mitosome complex (CMC); peripheral mitosomes (PMs) are dispersed in the cytoplasm [71]. (B) Electron micrograph of the CMC (arrow-head) embedded in the basal body complex. N: nuclei [70]. (C) Model of mitosome organization. Ax: flagellar axoneme; Bb: basal body. Surface factors which mediate association with the cytoskeleton, protein import and organelle division are indicated. Scale bar: 5 μm.

This would be a completely novel and unique way of assuring both the faithful replication and the partitioning of mitochondrial functions to daughter cells, and the distribution of organelles and their function in the cell. However, the paucity of candidate proteins facilitating tracking of organelles in living trophozoites precluded addressing this hypothesis. Development of two GFP-tagged reporters GFP-*Gl*Tom40 and *Gl*Tom40R-GFP (Rout *et. al* 2015, under review) allowed us to perform time-lapse experiments to follow individual organelles in a cell. Surprisingly enough, we found no evidence for motility of organelles, neither in the CMC nor in PMs, even after prolonged observation (1.5 hrs) although co-IP data suggests close association of mitosome outer membrane proteins with cytoskeletal elements such as axoneme-associated GASP-180 proteins (*Gl50803_137716* and *Gl50803_16745*) [72] and tubulin proteins (*Gl50803_101291* , *Gl50803_103676*) hinting towards motility of mitosomes along cytoskeletal elements. The relative isolation of mitosomes was further corroborated by FRAP experiments that showed no exchange of GFP-tagged membrane proteins between organelles during the acquisition period. Therefore, the lack of motility and inter-organellar exchange indicate two plausible scenarios: 1) the PMs and CMC might be dividing independently in a cell-cycle independent and -dependent manner, respectively, and 2) CMC organelles possess surface determinants which allow them to interact specifically with the cytoskeleton elements at the basal body complex. In contrast,

the surface of PMs does not appear to associate with the cytoskeleton, and they are randomly distributed within the cytoplasm. Time lapse microscopy of synchronized transgenic *Giardia* cultures expressing either GFP-*Gl*Tom40 or *Gl*Tom40R-GFP would address the first scenario. Whereas development of an organelle purification strategy to selectively enrich CMCs and PMs and analysis of whole organelle proteome would help identify novel surface determinants for CMC that enables them to be closely associated to the basal body complex.

Interestingly, over-expression of a dominant-negative giardial dynamin mutant elicited an organellar morphogenesis phenotype indicative of organelle replication defect (discussed below). In addition, the occurrence of the "string" mitosome phenotype upon over-expression of *Gl*Tom40R-GFP (Rout *et. al* 2015, under review) clearly suggested that mitosomes assume an elongated, tubular morphology, which is a prerequisite for organelle division and replication and that the "string" phenotype reflects a lack of fission.

Tight regulation of mitochondrial division is essential as survival of the cell depends on the preservation of an adequate number of mitochondria after cytokinesis [73]. It has been extensively documented that dynamin related protein (DRP) is a crucial mechanoenzyme which is conserved from yeast to vertebrates and carries out mitochondrial fission [74-77]. *G. lamblia* harbors a single dynamin homologue (*Gl*Drp) encoded by ORF (*Gl50803_14373*) and has been shown to play a major role in the endocytic pathway and stage conversion [78-80]. However, little was known regarding the role of the single *Gl*DRP in mitosomal division and morphology. We have demonstrated for the first time the role of *Gl*DRP in division and maintenance of mitosome morphology in addition to its role in endocytosis and stage conversion (Rout *et. al* 2015, under review). Transgenic parasites expressing *Gl*DRP-K43E (dominant-negative mutant) protein exhibited larger and fewer mitosomes as compared to parasites expressing wild type *Gl*DRP, supporting the role of single *Gl*DRP in mitosomal fission.

Our results are in line with the aberrant mitochondrial phenotype (long elongated interconnected tubular networks) observed in higher eukaryotes upon over-expression of dominant negative DRP [74, 81]. Interestingly, DRPs role in mitochondrial and hydrogenosomal division has also been demonstrated in the protozoan parasites *Trypanosoma brucei* [82, 83] and *Trichomonas vaginalis* [84], respectively. Therefore, our data partially corroborates the mechanistic conservation of mitochondrial and MRO fission [85-88].

Identification and mitosomal localization of a protein candidate (*Gl50803_22587*) further substantiates the functional conservation of mitosomal fission machinery. HMMER-based predictions relate this protein to a mitochondrial fission protein (Fis1, e value 6.3E-05) in *H. sapiens*. Fis1, together with mitochondrial fission factor (Mff) and mitochondrial dynamic

proteins (MiD 49 and MiD 51) act as receptors that recruit Drp1 to the mitochondrial surface, thus regulating fission mechanisms in eukaryotes [87, 89]. Therefore based on the association of *Gl*22587 to mitosomal outer membrane proteins we hypothesize that it might be involved in recruiting proteins together with *Gl*Drp onto the mitosomal surface eliciting the same function seen in higher eukaryotes. Co-IP assays using *Gl*22587 as bait protein are a prerequisite for identification of regulating, recruiting and interacting partners for *Gl*Drp. Data obtained from these experiments would not only shed light on the composition of the mitosome fission machinery and replication in *Giardia* but would also provide new targets for development of therapeutic tools to prevent parasite transmission and hence giardiasis.

## 2. Bibliography


1. Stefanic, S., et al., *Neogenesis and maturation of transient Golgi-like cisternae in a simple eukaryote*. J Cell Sci, 2009. **122**(Pt 16): p. 2846-56.
2. Losev, E., et al., *Golgi maturation visualized in living yeast*. Nature, 2006. **441**(7096): p. 1002-6.
3. Faso, C., et al., *Export of cyst wall material and Golgi organelle neogenesis in Giardia lamblia depend on endoplasmic reticulum exit sites*. Cellular microbiology, 2013. **15**(4): p. 537-53.
4. Price, H.P., et al., *The small GTPase ARL2 is required for cytokinesis in Trypanosoma brucei*. Molecular and biochemical parasitology, 2010. **173**(2): p. 123-31.
5. Marti, M. and A.B. Hehl, *Encystation-specific vesicles in Giardia: a primordial Golgi or just another secretory compartment?* Trends in parasitology, 2003. **19**(10): p. 440-6.
6. Stefanic, S., et al., *Organelle proteomics reveals cargo maturation mechanisms associated with Golgi-like encystation vesicles in the early-diverged protozoan Giardia lamblia*. J Biol Chem, 2006. **281**(11): p. 7595-604.
7. Bourne, H.R., D.A. Sanders, and F. McCormick, *The GTPase superfamily: a conserved switch for diverse cell functions*. Nature, 1990. **348**(6297): p. 125-32.
8. Stenmark, H., *Rab GTPases as coordinators of vesicle traffic*. Nature reviews. Molecular cell biology, 2009. **10**(8): p. 513-25.
9. Suda, Y. and A. Nakano, *The yeast Golgi apparatus*. Traffic, 2012. **13**(4): p. 505-10.
10. Pereira-Leal, J.B. and M.C. Seabra, *The mammalian Rab family of small GTPases: definition of family and subfamily sequence motifs suggests a mechanism for functional specificity in the Ras superfamily*. Journal of molecular biology, 2000. **301**(4): p. 1077-87.
11. Carlton, J.M., et al., *Draft genome sequence of the sexually transmitted pathogen Trichomonas vaginalis*. Science, 2007. **315**(5809): p. 207-12.
12. Saito-Nakano, Y., et al., *The diversity of Rab GTPases in Entamoeba histolytica*. Experimental parasitology, 2005. **110**(3): p. 244-52.
13. Lal, K., et al., *Identification of a very large Rab GTPase family in the parasitic protozoan Trichomonas vaginalis*. Molecular and biochemical parasitology, 2005. **143**(2): p. 226-35.
14. Ackema, K.B., et al., *The small GTPase Arf1 modulates mitochondrial morphology and function*. The EMBO journal, 2014. **33**(22): p. 2659-75.
15. Rabouille, C., *Old dog, new tricks: Arf1 required for mitochondria homeostasis*. The EMBO journal, 2014. **33**(22): p. 2604-5.
16. Hamasaki, M., et al., *Autophagosomes form at ER-mitochondria contact sites*. Nature, 2013. **495**(7441): p. 389-93.

17. Ackema, K.B., et al., *The small GTPase Arf1 modulates mitochondrial morphology and function.* EMBO J, 2014. **33**(22): p. 2659-75.
18. Kornmann, B., C. Osman, and P. Walter, *The conserved GTPase Gem1 regulates endoplasmic reticulum-mitochondria connections.* Proceedings of the National Academy of Sciences of the United States of America, 2011. **108**(34): p. 14151-6.
19. Alto, N.M., J. Soderling, and J.D. Scott, *Rab32 is an A-kinase anchoring protein and participates in mitochondrial dynamics.* The Journal of cell biology, 2002. **158**(4): p. 659-68.
20. Altmann, K. and B. Westermann, *Role of essential genes in mitochondrial morphogenesis in Saccharomyces cerevisiae.* Mol Biol Cell, 2005. **16**(11): p. 5410-7.
21. Volpicelli-Daley, L.A., et al., *Isoform-selective effects of the depletion of ADP-ribosylation factors 1-5 on membrane traffic.* Molecular biology of the cell, 2005. **16**(10): p. 4495-508.
22. Jacobson, M.D., M. Weil, and M.C. Raff, *Programmed cell death in animal development.* Cell, 1997. **88**(3): p. 347-54.
23. Evan, G. and T. Littlewood, *A matter of life and cell death.* Science, 1998. **281**(5381): p. 1317-22.
24. Welburn, S.C., M.A. Barcinski, and G.T. Williams, *Programmed cell death in trypanosomatids.* Parasitology today, 1997. **13**(1): p. 22-6.
25. Christensen, S.T., et al., *Staurosporine-induced cell death in Tetrahymena thermophila has mixed characteristics of both apoptotic and autophagic degeneration.* Cell biology international, 1998. **22**(7-8): p. 591-8.
26. Christensen, S.T., et al., *Signaling in unicellular eukaryotes.* International review of cytology, 1998. **177**: p. 181-253.
27. Ameisen, J.C., *On the origin, evolution, and nature of programmed cell death: a timeline of four billion years.* Cell death and differentiation, 2002. **9**(4): p. 367-93.
28. Ringqvist, E., et al., *Release of metabolic enzymes by Giardia in response to interaction with intestinal epithelial cells.* Molecular and biochemical parasitology, 2008. **159**(2): p. 85-91.
29. Roxstrom-Lindquist, K., et al., *Giardia immunity--an update.* Trends in parasitology, 2006. **22**(1): p. 26-31.
30. Bratton, D.L., et al., *Appearance of phosphatidylserine on apoptotic cells requires calcium-mediated nonspecific flip-flop and is enhanced by loss of the aminophospholipid translocase.* The Journal of biological chemistry, 1997. **272**(42): p. 26159-65.
31. Luder, C.G., et al., *Impact of protozoan cell death on parasite-host interactions and pathogenesis.* Parasites & vectors, 2010. **3**: p. 116.
32. Meagher, L.C., et al., *Phagocytosis of apoptotic neutrophils does not induce macrophage release of thromboxane B2.* Journal of leukocyte biology, 1992. **52**(3): p. 269-73.
33. Savill, J.S., et al., *Macrophage phagocytosis of aging neutrophils in inflammation. Programmed cell death in the neutrophil leads to its recognition by macrophages.* The Journal of clinical investigation, 1989. **83**(3): p. 865-75.
34. Freire-de-Lima, C.G., et al., *Apoptotic cells, through transforming growth factor-beta, coordinately induce anti-inflammatory and suppress pro-inflammatory eicosanoid and NO synthesis in murine macrophages.* The Journal of biological chemistry, 2006. **281**(50): p. 38376-84.
35. Vardi, A., et al., *Programmed cell death of the dinoflagellate Peridinium gatunense is mediated by CO(2) limitation and oxidative stress.* Current biology : CB, 1999. **9**(18): p. 1061-4.
36. Madeo, F., et al., *Oxygen stress: a regulator of apoptosis in yeast.* The Journal of cell biology, 1999. **145**(4): p. 757-67.
37. Chose, O., et al., *Cell death in protists without mitochondria.* Annals of the New York Academy of Sciences, 2003. **1010**: p. 121-5.
38. Wampfler, P.B., et al., *Proteomics of secretory and endocytic organelles in Giardia lamblia.* PLoS One, 2014. **9**(4): p. e94089.

39. Rassow, J., et al., *Translocation arrest by reversible folding of a precursor protein imported into mitochondria. A means to quantitate translocation contact sites*. The Journal of cell biology, 1989. **109**(4 Pt 1): p. 1421-8.
40. Schnell, D.J. and G. Blobel, *Identification of intermediates in the pathway of protein import into chloroplasts and their localization to envelope contact sites*. The Journal of cell biology, 1993. **120**(1): p. 103-15.
41. Schnell, D.J., F. Kessler, and G. Blobel, *Isolation of components of the chloroplast protein import machinery*. Science, 1994. **266**(5187): p. 1007-12.
42. Schulke, N., N.B. Sepuri, and D. Pain, *In vivo zippering of inner and outer mitochondrial membranes by a stable translocation intermediate*. Proceedings of the National Academy of Sciences of the United States of America, 1997. **94**(14): p. 7314-9.
43. van der Giezen, M., *Hydrogenosomes and mitosomes: conservation and evolution of functions*. J Eukaryot Microbiol, 2009. **56**(3): p. 221-31.
44. Kanaji, S., et al., *Characterization of the signal that directs Tom20 to the mitochondrial outer membrane*. The Journal of cell biology, 2000. **151**(2): p. 277-88.
45. Wiley, S.E., et al., *The outer mitochondrial membrane protein mitoNEET contains a novel redox-active 2Fe-2S cluster*. The Journal of biological chemistry, 2007. **282**(33): p. 23745-9.
46. Wiley, S.E., et al., *MitoNEET is an iron-containing outer mitochondrial membrane protein that regulates oxidative capacity*. Proceedings of the National Academy of Sciences of the United States of America, 2007. **104**(13): p. 5318-23.
47. Martincova, E., et al., *Probing the biology of Giardia intestinalis mitosomes using in vivo enzymatic tagging*. Mol Cell Biol, 2015.
48. Dolezal, P., et al., *The essentials of protein import in the degenerate mitochondrion of Entamoeba histolytica*. PLoS pathogens, 2010. **6**(3): p. e1000812.
49. Waller, R.F., et al., *Evidence of a reduced and modified mitochondrial protein import apparatus in microsporidian mitosomes*. Eukaryotic cell, 2009. **8**(1): p. 19-26.
50. Burri, L. and P.J. Keeling, *Protein targeting in parasites with cryptic mitochondria*. International journal for parasitology, 2007. **37**(3-4): p. 265-72.
51. Schneider, A., D. Bursac, and T. Lithgow, *The direct route: a simplified pathway for protein import into the mitochondrion of trypanosomes*. Trends in cell biology, 2008. **18**(1): p. 12-8.
52. Gill, E.E., et al., *Novel mitochondrion-related organelles in the anaerobic amoeba Mastigamoeba balamuthi*. Molecular microbiology, 2007. **66**(6): p. 1306-20.
53. Mi-ichi, F., et al., *Mitosomes in Entamoeba histolytica contain a sulfate activation pathway*. Proc Natl Acad Sci U S A, 2009. **106**(51): p. 21731-6.
54. Mi-Ichi, F., et al., *Entamoeba mitosomes play an important role in encystation by association with cholesteryl sulfate synthesis*. Proc Natl Acad Sci U S A, 2015.
55. Wampfler, P.B., C. Faso, and A.B. Hehl, *The Cre/loxP system in Giardia lamblia: genetic manipulations in a binucleate tetraploid protozoan*. International journal for parasitology, 2014. **44**(8): p. 497-506.
56. Carpenter, M.L. and W.Z. Cande, *Using morpholinos for gene knockdown in Giardia intestinalis*. Eukaryotic cell, 2009. **8**(6): p. 916-9.
57. Shi, H., C. Tschudi, and E. Ullu, *Depletion of newly synthesized Argonaute1 impairs the RNAi response in Trypanosoma brucei*. RNA, 2007. **13**(7): p. 1132-9.
58. Wideman, J.G., et al., *The ancient and widespread nature of the ER-mitochondria encounter structure*. Molecular biology and evolution, 2013. **30**(9): p. 2044-9.
59. de Kroon, A.I., et al., *Phospholipid composition of highly purified mitochondrial outer membranes of rat liver and Neurospora crassa. Is cardiolipin present in the mitochondrial outer membrane?* Biochim Biophys Acta, 1997. **1325**(1): p. 108-16.
60. Zinser, E., et al., *Phospholipid synthesis and lipid composition of subcellular membranes in the unicellular eukaryote Saccharomyces cerevisiae*. J Bacteriol, 1991. **173**(6): p. 2026-34.
61. Kumar, P., S. Guha, and U. Diederichsen, *SNARE protein analog-mediated membrane fusion*. Journal of peptide science : an official publication of the European Peptide Society, 2015. **21**(8): p. 621-9.

62. Rigotti, A., D.E. Cohen, and S. Zanlungo, *STARTing to understand MLN64 function in cholesterol transport*. Journal of lipid research, 2010. **51**(8): p. 2015-7.
63. Tamura, Y., H. Sesaki, and T. Endo, *Phospholipid transport via mitochondria*. Traffic, 2014. **15**(9): p. 933-45.
64. Yamano, K., S. Tanaka-Yamano, and T. Endo, *Tom7 regulates Mdm10-mediated assembly of the mitochondrial import channel protein Tom40*. J Biol Chem, 2010. **285**(53): p. 41222-31.
65. Marchi, S., S. Patergnani, and P. Pinton, *The endoplasmic reticulum-mitochondria connection: one touch, multiple functions*. Biochimica et biophysica acta, 2014. **1837**(4): p. 461-9.
66. Wideman, J.G., et al., *The ancient and widespread nature of the ER-mitochondria encounter structure*. Mol Biol Evol, 2013. **30**(9): p. 2044-9.
67. Lang, A., A.T. John Peter, and B. Kornmann, *ER-mitochondria contact sites in yeast: beyond the myths of ERMES*. Curr Opin Cell Biol, 2015. **35**: p. 7-12.
68. Elbaz-Alon, Y., et al., *A dynamic interface between vacuoles and mitochondria in yeast*. Developmental cell, 2014. **30**(1): p. 95-102.
69. Abodeely, M., et al., *A contiguous compartment functions as endoplasmic reticulum and endosome/lysosome in Giardia lamblia*. Eukaryot Cell, 2009. **8**(11): p. 1665-76.
70. Hehl, A.B., et al., *Bax function in the absence of mitochondria in the primitive protozoan Giardia lamblia*. PLoS One, 2007. **2**(5): p. e488.
71. Regoes, A., et al., *Protein import, replication, and inheritance of a vestigial mitochondrion*. J Biol Chem, 2005. **280**(34): p. 30557-63.
72. Elmendorf, H.G., et al., *Examination of a novel head-stalk protein family in Giardia lamblia characterised by the pairing of ankyrin repeats and coiled-coil domains*. International journal for parasitology, 2005. **35**(9): p. 1001-11.
73. Smirnova, E., et al., *Dynamin-related protein Drp1 is required for mitochondrial division in mammalian cells*. Mol Biol Cell, 2001. **12**(8): p. 2245-56.
74. Zhao, J., U. Lendahl, and M. Nister, *Regulation of mitochondrial dynamics: convergences and divergences between yeast and vertebrates*. Cell Mol Life Sci, 2013. **70**(6): p. 951-76.
75. van der Bliek, A.M., Q. Shen, and S. Kawajiri, *Mechanisms of mitochondrial fission and fusion*. Cold Spring Harb Perspect Biol, 2013. **5**(6).
76. Okamoto, K. and J.M. Shaw, *Mitochondrial morphology and dynamics in yeast and multicellular eukaryotes*. Annu Rev Genet, 2005. **39**: p. 503-36.
77. Elgass, K., et al., *Recent advances into the understanding of mitochondrial fission*. Biochim Biophys Acta, 2013. **1833**(1): p. 150-61.
78. Gaechter, V., et al., *The single dynamin family protein in the primitive protozoan Giardia lamblia is essential for stage conversion and endocytic transport*. Traffic, 2008. **9**(1): p. 57-71.
79. Marti, M., et al., *The secretory apparatus of an ancient eukaryote: protein sorting to separate export pathways occurs before formation of transient Golgi-like compartments*. Mol Biol Cell, 2003. **14**(4): p. 1433-47.
80. McArthur, A.G., et al., *The Giardia genome project database*. FEMS Microbiol Lett, 2000. **189**(2): p. 271-3.
81. Arimura, S., et al., *Arabidopsis ELONGATED MITOCHONDRIA1 is required for localization of DYNAMIN-RELATED PROTEIN3A to mitochondrial fission sites*. Plant Cell, 2008. **20**(6): p. 1555-66.
82. Chanez, A.L., et al., *Ablation of the single dynamin of T. brucei blocks mitochondrial fission and endocytosis and leads to a precise cytokinesis arrest*. Journal of cell science, 2006. **119**(Pt 14): p. 2968-74.
83. Morgan, G.W., D. Goulding, and M.C. Field, *The single dynamin-like protein of Trypanosoma brucei regulates mitochondrial division and is not required for endocytosis*. J Biol Chem, 2004. **279**(11): p. 10692-701.
84. Wexler-Cohen, Y., et al., *A dynamin-related protein contributes to Trichomonas vaginalis hydrogenosomal fission*. Faseb J, 2014. **28**(3): p. 1113-21.
85. Smirnova, E., et al., *A human dynamin-related protein controls the distribution of mitochondria*. The Journal of cell biology, 1998. **143**(2): p. 351-8.

86. Miyagishima, S.Y., et al., *A plant-specific dynamin-related protein forms a ring at the chloroplast division site.* Plant Cell, 2003. **15**(3): p. 655-65.
87. Nishida, K., et al., *Dynamic recruitment of dynamin for final mitochondrial severance in a primitive red alga.* Proc Natl Acad Sci U S A, 2003. **100**(4): p. 2146-51.
88. Pan, R. and J. Hu, *The conserved fission complex on peroxisomes and mitochondria.* Plant Signal Behav, 2011. **6**(6): p. 870-2.
89. Lee, H. and Y. Yoon, *Mitochondrial fission: regulation and ER connection.* Molecules and cells, 2014. **37**(2): p. 89-94.

# PART VIII CONCLUSION

Reductive evolution is intimately associated with a parasitic life style. However, data generated from my work regarding small GTPases such as Arf and Arls and from previous publication suggest that *Giardia* despite having lost major metabolic pathways and proteins have conserved the minimum machinery for organelle biogenesis and cyst formation essential for survival and propagation. This phenomenon is unambiguously demonstrated by the presence of *de novo* generated ESVs in absence of a steady state Golgi and the dependence on small GTPases for neogenesis and maturation of ESVs. In the case of the mitochondrion, reduction of the original endosymbiontic α-protobacterium which gave rise to the organelle is compounded by loss of functions or adaptation to new environmental conditions in parasitic protozoa [1]. Although this created machineries with extreme minimizations and complete transfer of organelle DNA to the nucleus of the host, giardial mitosomes are still retained. We can hypothesize that some basic functions imparted by this organelle are essential for its retention. Beyond conservation at a functional level (Fe-S protein maturation), Regoes *et. al* unambiguously demonstrated that protein import into mitosomes occurs by pre-sequence dependent and independent pathways indicating that the protein import pathway into mitosomes are conserved [2]. Furthermore, identification of novel proteins through our iterative co-IP experiments with dual localization hints towards a conservation of lipid transport machinery in *Giardia* mitosomes essential for synthesis of phospholipids. In mammalian cells, the absence of a molecular tether (ERMES complex) is compensated by the voltage dependent anion channel (VDAC) which forms stable associations with the $Ca^{2+}$ inositol trisphosphate (IP3) receptor as counterpart in the ER membranes. The presence of the only beta-barrel protein, *Gl*Tom40 in the outer membrane and its association with dually localized proteins might reflect a diverged form of contact site facilitating inter-organellar contact between mitosomes and ER. Furthermore, involvement of the only *Giardia* DRP in mitosomal division corroborates the function of DRPs in division of membrane bound organelles such as mitochondria, chloroplasts, peroxisomes [3-5] and therefore underlines the conservation at organelle morphogenesis level. Last but not the least, existence of a rudimentary apoptosis pathway in *Giardia* to 1) eliminate excess parasites without eliciting an immune response 2) as an altruistic behavior for survival of best fit individuals upon nutrient starvation, hints towards conservation at the host-parasite interaction level. In conclusion, characterization of the 2 reduced organelle systems (ESVs and mitosomes) in the basal eukaryote *Giardia* clearly demonstrates that despite having undergone secondary reduction due to the parasitic life style, essential protein factors or pathways required for organelle morphogenesis and faithful transmission to a new host are at least functionally conserved. These novel protein factors could turn out to be valuable targets for treating giardiasis, the leading cause for parasite induced diarrhea world-wide.

**Bibliography**

1. Embley, T.M. and W. Martin, *Eukaryotic evolution, changes and challenges*. Nature, 2006. **440**(7084): p. 623-30.
2. Regoes, A., et al., *Protein import, replication, and inheritance of a vestigial mitochondrion*. J Biol Chem, 2005. **280**(34): p. 30557-63.
3. Smirnova, E., et al., *A human dynamin-related protein controls the distribution of mitochondria*. The Journal of cell biology, 1998. **143**(2): p. 351-8.
4. Miyagishima, S.Y., et al., *A plant-specific dynamin-related protein forms a ring at the chloroplast division site*. The Plant cell, 2003. **15**(3): p. 655-65.
5. Pan, R. and J. Hu, *The conserved fission complex on peroxisomes and mitochondria*. Plant signaling & behavior, 2011. **6**(6): p. 870-2.

## ACKNOWLEDGEMENTS

I thank all the people who were either involved directly in the project or contributed to my work during my doctoral studies at the Institute of Parasitology in Zurich.

Firstly, I would like to thank my supervisor Prof. Dr. Adrian B. Hehl for taking me on board and giving me a possibility to explore the amazing world of parasite biology. I thank him for his patience and constant support in lab/written works and scientific discussions. I really appreciated his friendliness and open-minded attitude in and outside of the laboratory.

I also thank my co-supervisor Dr. Carmen Faso for all the scientific ideas, interesting discussions, and good advices during challenging situations and also for helping me during the thesis writing.

Many thanks to my committee members, Prof. Dr. Cornel Fraefel, Prof. Dr. Norbert Müller and Prof. Dr. Ueli Grossniklaus for supervising my thesis.

I thank Therese Michel for cloning many of my constructs for the project.

I would also like to thank the head of the institute, Prof. Dr. Peter Deplazes. Special thanks to administration team for making my life easier with all the paper works. It was great to just walk in with all the official documents and I really appreciated their helpful nature. I also thank the entire IPZ team for a wonderful time at work and funny moments outside.

I would also like to thank all ex and/or current members of the Hehl group for a wonderful time. Dr. Petra Wampfler for her systematic protocols, Dr. Paulin Zumthor for being a good office mate and for teaching me Bündner duetsch, Jacqueline Ebneter and Lenka Chirnikova for the lively environment. Furthermore, I really appreciated the fishing/biking/hiking trips organized by Dr. Sasa Stefanic and the pep talk with Dr. Chandra Ramakrishnan.

I would like to convey my special thanks to Lynn Pisan for her constant support, comforting words during stress times and for helping me with Microsoft office☺. I will cherish these moments forever. I would also like to thank Prof. Dr. Peter Lüthy and his wife for their amazing hospitality and help during the tough times with the immigration department at the start of my doctoral thesis.

Last but not the least; I would like to convey my special thanks to my family for being with me during these years away from home. Thank you for praying and supporting me throughout. I would like to specially thank my papa and ma for staying awake late at night so that I could return home and skype. I thank both my parents for patiently listening to me during the skype calls when I would get upset on small things during my stressful doctoral times and for all the love and good advices over these years.